From theory to methods and applications – for a better understanding of stem respiration and carbon dynamics in mature trees

Inauguraldissertation

zur

Erlangung der Würde eines Doktors der

Philosophie

vorgelegt der

Philosophisch-Naturwissenschaftlichen Fakultät

der Universität Basel

von

Juliane Helm

2024

Genehmigt von der Philosophisch-Naturwissenschaftlichen Fakultät
auf Antrag von

Erstbetreuer: Prof. Dr. Henrik Hartmann

Zweitbetreuer: Prof. Dr. Ansgar Kahmen

Externer Experte: Prof. Dr. John D. Marshall

Basel, den 23.05.2023

Prof. Dr. Marcel Mayor
Dekan

Table of contents

List of Abbreviations

ARD	Apparent respiratory difference (O_2 influx – CO_2 efflux)
ARQ	Apparent respiratory quotient (CO_2 efflux / O_2 influx)
CO_2	Carbon dioxide
$[CO_2]$	Concentration of CO_2
$[CO_2^*]$	Dissolved inorganic carbon (also called DIC); comprises of dissolved CO_2, carbonic acid (H_2CO_3), bicarbonate (HCO_{3-}) and carbonate (CO_3^{2-})
DOY	Day of the year
E_{CO2}	CO_2 efflux to the atmosphere
F_T	Transport flux; transport of dissolved respired C in the xylem sap
GMRP	Growth and maintenance respiration paradigm
GPP	Gross primary production
I_{O2}	O_2 influx
IRGA	Infrared gas analyzer
MBA	Mass balance approach
NSC	Non-structural carbohydrate
O_2	Oxygen
$[O_2]$	Concentration of O_2
PEPC	Phosphoenolpyruvatcarboxylase; enzyme for CO_2 fixation
PS_{cort}	Cortical photosynthesis
R_d	Dark leaf respiration
R_g	Growth respiration
R_m	Maintenance respiration
R_S	Stem respiration
ΔS	Storage flux; change in the storage of dissolved C in the stem section
V_{cmax}	Maximum carboxylation capacity of the enzyme Rubisco

Summary

Forests play an important role in the global carbon (C) cycle. As the central organ of a tree, the stem acts as an important C sink by storing substantial amounts of C in the wood. But at the same time, the respiring cells in the stem release previously assimilated C into the atmosphere via respiration. While CO_2 that is emitted from the stem can account for up to 42% of the total C loss by ecosystem respiratory fluxes in forests, our mechanistic understanding of the underlying processes of total stem respiration is still very limited. Therefore, an improved comprehension of C dynamics in mature tree stems is indispensable.

Estimating stem respiration by using only CO_2 efflux does ignore possible stem-internal transport and refixation processes that affect the fraction of CO_2 emitted locally. In the **first chapter**, I therefore provided an updated view on stem respiration estimates and their uncertainties. The review also included a research agenda to identify multiple challenges that require attention for robust predictions of woody tissue and whole-plant respiration. I underscored the need to improve upscaling procedures of stem respiration from the tree to ecosystem level by bringing together observational and experimental data with mechanistic modelling approaches.

The application of paired oxygen (O_2) and CO_2 measurements may overcome some of the challenges in stem respiration. However, simultaneous measurements have been rarely conducted as methodological limitations must first be solved. The aim of the project shown in the **second chapter** was therefore to develop a new chamber device to quantify CO_2 efflux and O_2 influx from tree stems. The utility of the device relies in its low-cost, power-autonomy (up to 10 days) and the high temporal resolution of measurements. Accordingly, it has substantial potential to facilitate research and advance knowledge on stem respiratory processes.

Until now, for practical reasons, a majority of experimental studies exploring respiratory processes have been restricted to young trees under controlled conditions. But, the fate of CO2 inside tree stems most likely depends on stem dimensions. The aim of the third chapter was to assess the different fates of CO_2 in stems of mature beech trees to gain insights on the regulation and

quantification of plant respiration. We combined CO_2 efflux, internal CO_2 flux, and O_2 influx. In contrast to CO_2, O_2 should not be affected by transport mechanisms, since it is a less soluble gas.

Additionally, we measured phosphoenolpyruvate carboxylase (PEPC) capacity in stem wood as an additional mechanism for caption of CO_2. The results of our field experiment showed that ~30% of the respired CO_2 was retained in the stem. However, the transport of respired CO_2 away from its point of production could only partially explain the difference between CO_2 efflux and O_2 influx in large trees. I provided novel evidence that PEPC-mediated CO_2 fixation can be seen as a relevant driver of the mismatch between CO_2 efflux and O_2 influx in mature trees, highlighting the potential relevance as a mechanism of local CO_2 removal to close the stem C balance.

The main focus of the **fourth chapter** was to provide novel insights into dynamics of C reserve use. The availability and usage of such C reserves during periods of limited photosynthesis are still poorly understood in mature trees. I investigated how a reduced C supply (induced via stem girdling) affected respiratory substrate use and C mobilization of storage pools in poplar. In species that do not only store C in form of carbohydrates but also lipids, storage mobilization can induce a substrate shift. However, there are very few studies addressing this in the field. The ratio of CO_2 efflux to O_2 influx (apparent respiratory quotient; ARQ) and $\delta^{13}C$ of respired CO_2 allowed inferences on respiratory substrate sources. Poplar gradually mobilized older substrates for respiration that were up to 15-yr-old. This was demonstrated by the use of the bomb-radiocarbon method (^{14}C). From our multi-year field experiment, we concluded that, after the cut-down of new photo-assimilates, a mixture of respiratory substrate (carbohydrates, lipids) with a late contribution of older reserves ensured the long-term survival of poplar trees under C starvation.

This thesis contributes to a better understanding of C fluxes in mature tree stems. The new method development of combined CO_2 and O_2 measurements allows for a more holistic approach to studying respiratory and post-respiratory processes in woody tissues. Combined with internal CO_2 flux and refixation measurements, it improves stem respiration estimates and advances our knowledge on the uncertain fate of CO_2 in stems. When addressing forest responses to more frequent and severe droughts under climate warming, C dynamics in tree stems should be an integral part of future studies.

Introduction and thesis outline

Forests, climate change and the carbon cycle

Forest ecosystems cover approximately one-third of the world's land surface (FAO, 2015). Forests exist in diverse regions from cold to temperate and tropical regions, located at high altitudes in mountains or in coastal areas. An impressive number of approximately 60,000 tree species exist worldwide (Beech *et al.*, 2017) and they have many fundamental ecological functions that support life on Earth. Trees remove carbon dioxide (CO_2) from the atmosphere and store it, produce oxygen (O_2), provide habitat for many species, protect soils against erosion and provide resources for humans, including food, fuel and timber (Myers, 1997; Pan *et al.*, 2013; Abson *et al.*, 2014; Trumbore *et al.*, 2015a; Le Quéré *et al.*, 2018). Forest ecosystems are essential for climate regulation and fulfill important functions in the water cycle (Bonan, 2008). They provide essential ecosystem services that are extremely important in the regulation of biophysical processes on Earth and understanding and protecting forest ecosystems is imperative.

Changing climate conditions are threatening forest ecosystems worldwide, as well as their accompanying ecosystem services. Trees unavoidably encounter a variety of stressors such as droughts, insect or pathogen outbreaks, windthrow or fires throughout their lifetime. However, the frequency and severity of re-current drought events and excessive heat waves has increased drastically in recent years with proceeding climate change (e.g., Reichstein *et al.*, 2013; Bastos *et al.*, 2021; Böhnisch *et al.*, 2021). Carbon dioxide, the most important anthropogenic greenhouse gas on Earth, is one of the main drivers of climate change and has increased greatly due to human activities such as fossil fuel burning and land use change, including deforestation. During the time of my PhD project, two consecutive droughts in 2018 and 2019 in Central Europe have posed a great challenge to tree survival. Especially long-living tree species were affected (Allen *et al.*, 2010; Allen *et al.*, 2015; Hartmann *et al.*, 2018; Schuldt *et al.*, 2020), due to their long reproduction period (delayed maturity) and subsequent slow adaptation (Petit & Hampe, 2006). Severe drought events lead to reduced forest productivity (Park Williams *et al.*, 2013), higher susceptibility of trees towards stress events like bark beetle attacks (Allen *et al.*, 2010) and ultimately to drought-induced tree mortality (Allen *et al.*, 2010; Adams *et al.*, 2017; Hartmann *et al.*, 2018; Hajek *et al.*, 2022).

Increased forest mortality also reduces the carbon (C) sink and impacts the C cycling of forests (Adams *et al.*, 2010; Anderegg *et al.*, 2013). Under current climate conditions, ~450 gigatons of C are stored in forests (aboveground biomass), which is about 45 times the annual CO_2 emissions deriving from human activities (10.1 Gt C per year; Friedlingstein *et al.*, 2022). In soils, this is even significantly higher with ~1500 gigatons of stored C (Friedlingstein *et al.,* 2022). As CO_2 emissions continue to increase, stressors on forests will also continue to advance with dramatic, and in some cases, not yet foreseeable consequences for all of us.

The largest C fluxes in the C cycle between the terrestrial biosphere and the atmosphere are photosynthesis and respiration (Schimel, 1995). About 120 gigatons of C are taken up by photosynthesis each year, and nearly the same amount is returned to the atmosphere by ecosystem respiration (includes plant and soil respiration). The CO_2 release by leaves and woody tissue (autotrophic respiration) represents an extremely important flux, as plant respiration releases about six times the CO_2 emissions from fossil fuel combustion globally (2010-2019; Friedlingstein *et al.*, 2020; Allan *et al.,* 2021). Understanding autotrophic respiration and its underlying drivers, as a critical and uncertain component of ecosystem and global C budgets, is of great importance for plant physiology and global-change science (King *et al.*, 2006; Houghton, 2007; Reich *et al.*, 2008; Salomón *et al.*, 2019b). A deeper understanding of regulatory mechanisms of C fluxes at the tree-level is required to improve predictions of respiration (metabolic demand) under uncertain future climatic conditions. To this date, many processes that drive and control autotrophic respiration are not fully understood, and a major concern is the role of tree stems.

Tree stem as the central organ in tree functioning

In order to better understand how forests will respond to stress, we first need to understand the processes at the individual tree-level. Tree stems are impressive organs – some of them are over 100 meters tall, and can span over 10 meters in diameter while having a variety of functions. They support and lift the crown so that leaves receive direct sunlight to perform photosynthesis. Furthermore, stems serve as long-distance transport pathway between the canopy and the root system (Furze *et al.*, 2018) by transporting water and nutrients to the canopy (via the xylem) and redistributing carbohydrates and other solutes to sink tissues for tree functioning (via the phloem) (Furze *et al.,* 2018). Carbon fixed during photosynthesis is transported in form of sugars and is used e.g., for respiration, growth or storage. Trees store water to e.g. temporarily maintain their leaf water status (Waring *et al.*, 1979; De Guzmann *et al.,* 2017). Further, tree stems represent a long-term C sink by storing structural carbohydrates and mobile, i.e. non-structural carbohydrates (NSCs),

mainly sugars and starch (Sala *et al.*, 2012; Hartmann & Trumbore, 2016). But, also neutral lipids (triacylglycerols) are considered to serve as storage compounds (Plaxton & Podestá, 2006; Hoch, 2015). The mobile C storage compounds can be accessed and metabolized by trees to buffer metabolic demand when C supply from photosynthesis is reduced (e.g., Regier *et al.*, 2009; Hartmann *et al.*, 2013; Hartmann & Trumbore, 2016). Non-structural carbohydrates act as crucial source of energy and substrates; and approximately 40% of their total amount in a tree is stored in the stem (Furze *et al.*, 2018).

Storage pools in trees play a crucial role in tree resilience to overcome periods of limited photosynthesis (e.g., caused by shade, insect defoliation, late frost-induced defoliation, prolonged drought), to maintain plant tissues, for recovery of lost tissues, or for growth and metabolism during spring when photosynthesis is lower than respiration (e.g., Kozlowski, 1992; Fischer *et al.*, 2015; Muhr *et al.*, 2016; D'Andrea *et al.,* 2019; Zohner *et al.*, 2019; Piper & Paula, 2020; Barker Plotkin *et al.*, 2021). A shift from carbohydrates, as the dominant respiratory C substrate in plants (Plaxton & Podestá, 2006), to alternative substrates, such as lipids and proteins (Sauter & van Cleve, 1994; Hoch *et al.*, 2003; O'Leary *et al.*, 2019) has been documented under C starvation in shaded herbaceous plants, during senescence and germination of seeds (Tcherkez *et al.*, 2003; Araújo *et al.*, 2011; Engqvist *et al.*, 2011; Hildebrandt *et al.*, 2015). In trees, the role of alternative respiratory substrates is still underexplored. A substrate shift to neutral lipids was shown for young scots pine under a shading treatment in climate-controlled chambers (Fischer *et al.*, 2015). Furthermore, empirical evidence of the role of neutral lipids as storage compounds is often ignored due to methodological challenges in quantifying neutral lipids in wood (e.g., Hoch *et al.,* 2003). Another strategy allowing survival during unfavorable conditions relates to the ability of trees to store NSCs over long time periods (Carbone *et al.,* 2013; Muhr *et al.,* 2013). Trees can access and use older carbohydrates for respiration or growth to withstand stress events, such as drought or insect defoliation (Carbone *et al.*, 2013; Richardson *et al.*, 2013; Trumbore *et al.*, 2015b; Muhr *et al.*, 2018; D'Andrea *et al.*, 2019). Estimating the age of NSCs helps to understand how and when trees use their C reserves. Hereby, manipulative experiments in which phloem transport for photo-assimilates from the canopy was blocked (e.g., starvation by girdling) have shown that trees can respire C that had been fixed years to decades before to ensure survival (Muhr *et al.,* 2013). Therefore, C stored for long time periods remained accessible for trees to cover metabolic C needs. Our understanding of tree storage regulation and functioning is still limited, but represents a critical aspect for the evaluation of forest resilience under changing climate conditions (Sala *et al.,* 2012).

Respiration and CO_2 efflux

The process of respiration generally requires O_2 and respiratory substrates, mainly carbohydrates (Cannell & Thornley, 2000) that are consumed while CO_2 and water are released as reaction products (O'Leary *et al.,* 2019). Respiration provides C-skeleton intermediates, reducing power and energy for plant cells (O'Leary *et al.,* 2019) which is needed in a wide array of physiological processes including growth, cellular maintenance and biosynthesis (Steppe *et al.*, 2015a; Hartmann & Trumbore, 2016; O'Leary *et al.*, 2019). The process of respiration is relevant at different biological scales – tissue and cellular scales, whole-plant or ecosystem scale (O'Leary *et al.,* 2019). Respiration plays a predominant role in the ecosystem C balance by substantially contributing to the return of photo-assimilated C to the atmosphere (Valentini *et al.*, 2000). The difference between C assimilation (gross primary production; GPP) and C loss (ecosystem respiration), which is defined as the net ecosystem production (Chapin *et al.,* 2006), serves as a proxy for the C sink and C source strength of forest ecosystems (e.g., Valentini *et al.*, 2000; Luyssaert *et al.*, 2009). For example, widely applied eddy covariance techniques quantify CO_2 fluxes from the terrestrial biosphere to the atmosphere by using tower-based sensors (reviewed by Baldocchi, 2020). Those measurements can be useful to calculate forest C sequestration rates at a local scale and helps to understand how ecosystems respond to climate variability (Baldocchi, 2020). However, eddy covariance cannot provide further insights into individual fluxes (autotrophic and heterotrophic respiration) within the ecosystem, as bulk fluxes are measured (Trumbore, 2006). In order to make a distinction between the different tree components (e.g., leaf, stem, soil respiration), chamber-based measurements are suitable. Leaf respiration has been intensively investigated (e.g., Atkin *et al.*, 2005; Vanderwel *et al.*, 2015; Heskel *et al.*, 2016; Huntingford *et al.*, 2017; Wang *et al.*, 2020) facilitated by the methodological simplicity of enclosing leaves in cuvettes for gas exchange measurements (Hunt, 2003). But, our understanding of the C release at the stem-level is much more limited (Meir *et al.*, 2017; Fatichi *et al.*, 2019). However, stems (and roots) make up most of the biomass in woody species, especially in mature trees (Poorter *et al.*, 2012) and therefore C release from the stem is an important contributor to whole plant respiration.

While respiration rates of isolated cells can easily be determined from CO_2 efflux, it becomes more complicated *in situ.* In intact stems, respired CO_2 originates from the sum of all living cells in the phloem, cambium, and parenchyma ray cells in the xylem (Teskey *et al.,* 2008; Aubrey & Teskey, 2009; Bloemen *et al.,* 2013). However, emission of CO_2 from the stem surface into the atmosphere (CO_2 efflux; E_{CO2}), measured by chamber-based approaches, does not represent the true respiration rate (Meir *et al.*, 2017; Salomón *et al.*, 2017; Teskey *et al.*, 2017). Interestingly, the crucial

differentiation between stem respiration (R_S) and E_{CO2} has been recognized already 90 years ago (Boysen-Jensen, 1933), but still today some studies incorrectly use those two terms interchangeable even though many uncertainties in quantifying the 'real' R_S remain.

Carbon dioxide can dissolve in the sap solution and be transported internally via the xylem sap flow (Teskey *et al.,* 2008). Vertical transport can result in net-import of CO_2 into a given stem segment, i.e. locally emitted CO_2 can originate from respiration within the roots or the lower stem base. Likewise, but to the opposite effect, locally respired CO_2 can dissolve and be transported further up the stem to diffuse into the atmosphere far away from the CO_2 production site (Teskey *et al.*, 2017). Other CO_2-removal processes involve the refixation of respired CO_2 by photosynthetic cells (e.g., Pfanz & Aschan, 2001; Teskey *et al.*, 2008; Ávila *et al.*, 2014), or the activity of the enzyme phosphoenlopyruvatcarboxylase (PEPC) (e.g., Chollet *et al.*, 1996; Berveiller *et al.*, 2007; Werner & Gessler, 2011; Abadie & Tcherkez, 2019) as a potentially important sink for respired CO_2 in trees. Until now, PEPC has been shown to be present in young twigs (Berveiller & Damesin 2008), but the role of this refixation mechanism remains speculative in mature trees.

Stem respiration (based on stem CO_2 efflux) is estimated to account for 5% to 42% of total ecosystem respiration, depending on season and forest type (e.g., Campioli *et al.*, 2016; Salomón *et al.*, 2017). But, the uncertain fate of respired CO_2 can lead to large uncertainties in those R_S estimates. It is therefore critical to develop a clear understanding of the respiratory physiology and the different contributors of R_S in woody tissues along the stem (Trumbore *et al.,* 2013; Teskey *et al.,* 2017). The potential uncertainties in measuring and upscaling these fluxes to the stand- or ecosystem level can have large implications for the forest C budget (e.g., Litton *et al.*, 2007).

Potential of simultaneous CO_2 and O_2 measurements at the ecosystem and stem-level

While intensive research has already been conducted on C fluxes, so far, O_2 measurements at the ecosystem and tree-level remain less studied. Combined observations of O_2 and CO_2 have the great potential to convey additional information on C fluxes that cannot be gained solely from CO_2 measurements (Seibt *et al.*, 2004). Oxygen and CO_2 are inversely coupled not only in the process of respiration, but also during photosynthesis and fossil fuel combustion (Manning & Keeling, 2006). By measuring changes in atmospheric O_2 and CO_2, the calculated terrestrial O_2:CO_2 exchange ratio can be an alternative estimate of terrestrial C sinks (Keeling & Shertz, 1992), in contrast to measuring CO_2 fluxes alone. Keeling *et al.* (1993) were the first to demonstrate a long-term decrease in O_2/N_2 concentration in the air due to the burning of fossil fuels, where O_2 is

consumed and CO_2 produced. Hereby, the burning of reduced fossil fuels leads to a different O_2:CO_2 exchange ratio than photosynthesis and subsequent respiration (Keeling, 1988). The tight coupling enables studying the natural C cycle and the effect of anthropogenic disturbances (Seibt *et al.*, 2004; Manning & Keeling, 2006; Tohjima *et al.*, 2019).

Already 50 years ago, the potential of O_2 for a better understanding of respiratory processes has been recognized at the tree level (Woodwell & Botkin, 1973). The flux of O_2 into the stem should equal the flux of CO_2 out of the stem, if we assume a carbohydrate-dominated respiration (Hoch *et al.*, 2003; Plaxton & Podestá, 2006). One (possible) advantage in using O_2 over CO_2 as proxy for respiration is related to the fact that O_2 is much less soluble compared to CO_2 (Dejours, 1981). Therefore, transport within the xylem sap should be negligible for O_2, allowing to separate transport of CO_2 from local physiological processes. Complementing measurements of CO_2 flux with simultaneous measurements of O_2 flux at the stem surface can potentially help to achieve more realistic measures of R_S and may overcome some of the challenges in R_S (Angert *et al.*, 2012; Trumbore *et al.*, 2013; Hilman & Angert, 2016; Hilman *et al.*, 2019). Furthermore, the CO_2/-O_2 ratio provides information on the substrate a tree is using for respiration, as different compounds (carbohydrates, proteins, lipids) have different ratios and thus can be distinguishable. With the combined ratio of CO_2/-O_2, storage dynamics in small trees can be better understood under controlled conditions in climate chambers (Fischer *et al.,* 2015; Hanf *et al.,* 2015). However, broader field use of O_2 and the exact interpretation of the CO_2/-O_2 ratio is yet to be resolved. Wider application of the paired O_2 and CO_2 measurements is still lacking. This is caused by the analytical challenges of detecting O_2 changes in the range caused by plant respiration (less than 0.1%) with a large O_2 background of 21% in ambient air (209,500 ppm) (Angert *et al.*, 2012). New technical innovations for combining the assessment of CO_2 and O_2 measurements would therefore make important contributions to enhance our understanding of the fate of CO_2 inside stems and C storage compounds in mature trees.

Main research questions and dissertation outline

The aim of the present thesis is to gain new insights into tree stem C dynamics of beech (*Fagus sylvatica* L.) and poplar (*Populus tremula* L.). More specifically, I will be contributing to a better understanding of R_S at the stem-level. Investigating processes that occur at smaller scales are necessary to evaluate the magnitude of R_S to the overall C balance of forest ecosystems and avoid miscalculations in the upscaling process. Further, it is essential to understand how mature trees utilize C reserves to survive under stress. For both aims, namely insights into respiratory C fluxes and C storage use, the simultaneous measurement of CO_2 and O_2 is highly beneficial. This thesis is composed of three general research questions:

i) Can we overcome challenges in stem respiration estimates by developing a field-robust method for simultaneous CO_2 and O_2 measurements at the stem-surface (*Chapter 2*)?

ii) Does the concurrent application of two different methods to estimate stem respiration in the same trees leads to similar conclusions about the fate of respired CO_2 (*Chapter 3*)?

iii) Do stressed trees shift respiration supply from carbohydrates to alternative substrates to ensure survival under field conditions (*Chapter 4*)?

The first chapter serves as literature overview (review article) and summarizes knowledge gaps in the research field of woody tissue respiration. The following three chapters of this thesis specifically address the above objectives (see also Fig. 1) and represent independent manuscripts that have been published in peer-reviewed journals.

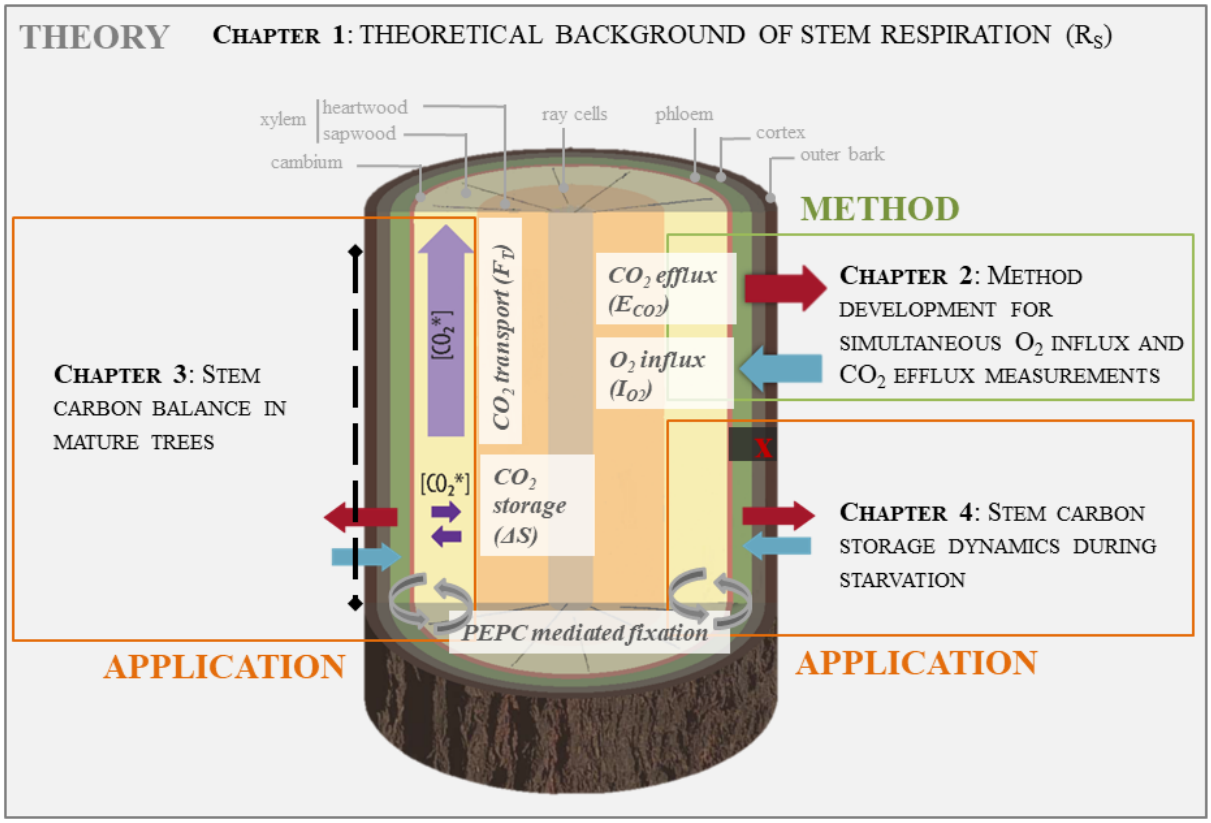

Figure 1 Overview of the four chapters of this PhD thesis to understand respiratory processes at the stem-level of a tree. The review article in Chapter 1 gives an overview of the state-of-the-art of stem respiration (R_S) measurements. Chapter 2 presents a new chamber device for simultaneous CO_2 and O_2 measurements. Chapter 3 focuses on the possible fates of CO_2 along a vertical stem gradient in beech trees. In Chapter 4, I artificially induced a lack of C supply (cross in red indicates a girdling treatment; phloem transport interrupted) to elaborate new insights into alternative respiratory substrate use as well as C remobilization pattern in poplar trees.

Chapter 1 reviews current knowledge about the state-of-the-art of R_S and the different attempts of its quantification. I underscore existing knowledge gaps concerning different fates of CO_2 and their contribution to changes in R_S as well as technical limitations. We end with pointing out persisting ambiguities that require further research.

Chapter 2 introduces a new methodology to simultaneously measure CO_2 and O_2 at the stem surface of mature trees. Including O_2-based methods when investigating stem C dynamics brings us one-step forward to better constrain local respiration and detect respiratory substrate use. This method is part of the following two experimental studies.

In **Chapter 3**, I provide a comprehensive perspective on the stem respiratory activity and different sinks of respired CO_2 in mature trees. The experiment took place in July and August 2019 in a beech forest (*Fagus sylvatica* L.) in Central Germany. European beech is one of the four dominant tree species in Germany (BMEL, 2021). Me and my collaborators quantified R_S by simultaneous measurements of O_2 influx (I_{O2}) and CO_2 efflux (E_{CO2}), as well as internal CO_2 fluxes. Our specific objectives were: (i) to use CO_2 and O_2 flux measurements simultaneously to quantify R_S and better disentangle the various contributors to R_S, and (ii) to explore the so far overlooked process of C fixation via the enzyme PEPC as a cause of CO_2 removal. Based on the objectives, the following main hypothesis was addressed:

Main hypothesis: We hypothesize that O_2 influx into the stem is greater than CO_2 efflux to the atmosphere, and that xylem CO_2 transport can explain the observed difference. The fraction of missing CO_2 not explained by xylem CO_2 transport can be attributed to CO_2 refixation via PEPC activity.

Chapter 4 deals with long-term C dynamics during C starvation of mature poplar trees (*Populus tremula* L. hybrids) during tree growing seasons (2018, 2019, 2021). Poplar is a very common and rapid growing tree species that is known to store (besides sugars and starch) substantial amounts of lipids. Within the experiment, the supply of C from the canopy was altered via stem girdling that stopped phloem flow and with them the supply of new assimilates. My particular objectives were: i) to elaborate alternative substrate use (E_{CO2}-to-I_{O2} ratio, $\delta^{13}CO_2$), in particular the use of neutral lipids as an overlooked compound in the context of reserve dynamics, and (ii) to elucidate the time trees take to tap into their long-term C reserves (radiocarbon $\Delta^{14}C$ analysis). Based on the objectives, the following main hypothesis was addressed:

Main hypothesis: After the disruption of the supply of photo-assimilates, poplar trees initially mobilize NSCs, followed by progressive mobilization and metabolization of lipids and older substrates for respiration as C starvation proceeds.

Finally, I summarize the main findings of this PhD thesis and offer new directions for future research.

CHAPTER 1

The quandary of sources and sinks of CO_2 efflux in tree stems – new insights and future directions

Juliane Helm[1,2], Arthur Gessler[3,4], Thorsten E. E. Grams[5], Boaz Hilman[1], Jan Muhr[6], Roberto L. Salomón[7,8], Kathy Steppe[8], Christiane Wittmann[9], Henrik Hartmann[1,10]

[1]Department of Biogeochemical Processes, Max Planck Institute for Biogeochemistry, Hans-Knöll-Str.10, 07743 Jena, Germany

[2]Department of Environmental Sciences–Botany, Basel University, Schönbeinstr. 6, Basel CH-4056, Switzerland

[3]Swiss Federal Institute for Forest, Snow and Landscape Research WSL, Zurcherstrasse 111, 8903Birmensdorf, Switzerland

[4]Institute of Terrestrial Ecosystems, ETH Zürich, Rämistr. 101, 8902 Zurich, Switzerland

[5]Ecophysiology of Plants, Land Surface – Atmosphere Interactions, Technical University of Munich, Von-Carlowitz-Platz 2, 85354 Freising, Germany

[6]Department of Forest Botany and Tree Physiology, Laboratory forRadioisotopes, Georg-August University Göttingen, Büsgenweg 2, 37077 Göttingen, Germany

[7]Department of Natural Systems and Resources, Technical University of Madrid (UPM), Madrid, Spain

[8]Department of Plants and Crops, Laboratory of PlantEcology, Faculty of Bioscience Engineering, Gent University, Coupure links 653, 9000 Gent, Belgium

[9]University of Duisburg-Essen, Faculty of Biology, Botanical Garden, Universitätsstr. 5, 45117 Essen, Germany

[10]Institute for Forest Protection, Federal Research Centre for Cultivated Plants, Erwin-Baur-Str. 27, 06484 Quedlinburg, Germany

Planned to re-submit to Tree Physiology.

Abstract

Plant respiration substantially contributes to the return of photo-assimilated carbon to the atmosphere, and thus to the tree carbon balance. A large component of this carbon flux, stem CO_2 efflux, is often used as a proxy for stem respiration. However, this metric has been repeatedly challenged, not only due to difficulties in identifying the spatial origin of the CO_2 released from the stem, but also because of several post-respiratory processes that may consume respired CO_2 prior to its release into the atmosphere, which causes differences between stem CO_2 efflux and local respiration. In our review article, we give an update on the state-of-the-art of the topic and develop a research agenda that aims to fill the most relevant knowledge gaps. We propose upscaling procedures and experimental approaches that can link field data with stem respiration models as means to estimate the different components that influence stem gas exchange.

Keywords

ARQ, cortical photosynthesis, O_2 influx, PEPC, sap pH, stem respiration modelling, xylem CO_2 transport

Introduction

Autotrophic respiration (defined here as respiration of autotrophic organisms and their microbiome that is directly dependent on their carbon assimilates) and its components (e.g., root, rhizosphere, stem, branch and leaf respiration) represent a major contribution to the plant and ecosystem carbon (C) balance (Luyssaert *et al.*, 2007). Globally, autotrophic respiration is the second largest CO_2 flux and releases approximately six times the amount of CO_2 (60 Pg C per year) compared to fossil fuel burning (2010–2019; Friedlingstein *et al.*, 2020). Herein, a large component is the CO_2 release from woody tissues (branch, stem, and roots), where tree stems make up most of the biomass in woody species (Poorter *et al.,* 2012). The C release through the stem into the atmosphere is estimated to be 6.7±1.1 Pg C per year (Yang *et al.,* 2016), which is in the same range as fossil fuel emissions (Friedlingstein *et al.,* 2020). Major determinants of respiration rates are environmental factors like temperature (often used as a scalar of respiration rates), nitrogen content, the availability of metabolites as respiration substrates, plant water content, growth, enzymatic activity and the energy requirement of the respiring tissue (Amthor, 1995; Atkin *et al.,* 2005; Pruyn *et al.,* 2005; Kruse *et al.,* 2011; Pruyn *et al.,* 2011).

Despite the good accessibility of tree stems, several physiological processes and factors confound R_S measurements, leading to a limited mechanistic understanding of R_S. During aerobic respiration, O_2 and CO_2 are coupled. Respiration requires respiratory substrates and O_2, while CO_2 and water are released as byproducts of this catabolic reaction (Kader & Saltveit, 2002). While respiration rates of isolated cells can easily be determined from CO_2 release, it becomes more complicated *in situ.* In intact stems, the phloem, cambium, and parenchyma ray cells in the xylem are considered as living cells and contribute to the release of CO_2 (Teskey *et al.,* 2008; Aubrey & Teskey, 2009; Bloemen *et al.,* 2013). CO_2 efflux (E_{CO2}) and O_2 influx (I_{O2}) can potentially be used as a metric of respiration rates. However, E_{CO2} from the stem surface into the atmosphere does not represent the 'real' R_S (Meir *et al.*, 2017; Salomón *et al.*, 2017; Teskey *et al.*, 2017). Different post-respiratory processes which hinder CO_2 from being locally emitted, as well as a variety of anatomical and environmental factors (like xylem anatomy and temperature) lead to a limited understanding of respiratory physiology (e.g., Bowman *et al.*, 2005; Saveyn *et al.*, 2010; Bužková *et al.*, 2015). A better understanding of the uncertain fate of respired CO_2 is needed to evaluate the magnitude of R_S to the overall C balance of forest ecosystems.

In this review, we solely focus on the stem-level of trees. We begin with an overview (section 1) of different processes (E_{CO2} and/or I_{O2} involved) that affect R_S estimations with partly unknown uncertainty. In section 2, we describe the most common R_S estimation approaches including recent

modelling approaches that integrate theory and field observational data. Based on this synthesis, section 3, proposes a detailed research agenda with observational and experimental studies, novel technical and analytical tools and modelling approaches to overcome sources of uncertainties in R_S estimates and to improve the upscaling of R_S from the tree to the ecosystem.

Processes leading to uncertainties in stem respiration estimates

A variety of processes hinder the straightforward measurement of R_S (Table 1). The following subsections will present the individual processes and potential biases of efflux (influx)-based estimates of R_S (see also Fig. 2).

Table 1 Summary of factors that may influence R_S and their effect on carbon dioxide (CO_2), oxygen (O_2) or both.

Individual contributors	Effect on CO_2	Effect on O_2
Xylem transport	Local net import (+) Local net export (-)	+/- (1/30 of the effect on CO_2)
Cortical photosynthesis	CO_2 consumption (-)	O_2 production (+)
Light-induced axial diffusion in the gas phase	Local net export (-)	(0)
Phosphoenolpyruvatcarboxylase	CO_2 refixation (-)	(0)
Oxidase enzymes	(0)	O_2 consumption (-)

Note: +, source process: positive flux; −, sink process: negative flux; +/-, no substantial flux; 0, no effect

CO_2 dissolution and transport in the xylem

Tree stems, as the linkage between the canopy and the root system, transport mainly water and nutrients in the xylem towards the canopy and redistribute carbohydrates and other solutes in the phloem towards the roots (Furze *et al.,* 2018). The vertical transport pathway is essential for understanding the fate of respired CO_2. Respired CO_2 not emitted locally into the atmosphere can dissolve in the sap solution and be transported as dissolved inorganic carbon (DIC), including carbonic acid (H_2CO_3), and two deprotonated forms, bicarbonate (HCO_3^-) and carbonate (CO_3^{2-}) via the xylem flow (Teskey *et al.,* 2008).

Locally emitted CO_2 may originate from respiration in the roots or lower stem base, resulting in a net-import of CO_2 into a given stem segment (Teskey & McGuire, 2007; Aubrey & Teskey, 2009; Bloemen *et al.*, 2013). Or, locally respired CO_2 can be transported further up the stem (net-export) and diffuses into the atmosphere far away from the CO_2 production site (Teskey *et al.*, 2017).

Importantly, vertical transport does not affect O_2 as much as CO_2, because the solubility of O_2 in water is ~30 times lower than for CO_2 (Dejours, 1981).

Cortical photosynthesis as CO_2 recycling mechanism

Cortical photosynthesis (PS_{cort}) can affect both E_{CO2} and I_{O2} by CO_2 consumption and O_2 production. Stems of woody plants can contain chlorophyll-containing tissues (present in bark, xylem parenchyma rays and the pith) (Pfanz & Aschan, 2001; Teskey *et al.*, 2008; Ávila *et al.*, 2014). Those chloroplast-containing cells are capable of photosynthesis and, when illuminated, refix some of the stem-internal CO_2 (Strain & Johnson, 1963; Pfanz *et al.*, 2002; Wittmann *et al.*, 2006). Since little light reaches the internal stem tissues/wood (0.2–5% of incident light, Pfanz *et al.*, 2002; Wittmann & Pfanz, 2016), it can be assumed that internal photosynthetic CO_2 recycling is carried out largely by the stem cortex. Therefore, we use the term cortical photosynthesis (PS_{cort}). Cortical photosynthesis mainly consumes respired CO_2 from internal sources (e.g., Sprugel, 1991; Pfanz *et al.*, 2002; Saveyn *et al.*, 2010; Ávila *et al.*, 2014; Cernusak & Cheesman, 2015). The source of respired CO_2 can be local living cells in the cortex, phloem, cambium, parenchyma cells and rays or, alternatively, distant organs (e.g. roots) from where CO_2 has been transported into the cortex chlorenchyma (e.g., by transpiration stream, Teskey *et al.*, 2008; Aubrey & Teskey, 2009; Bloemen *et al.*, 2013). In stem E_{CO2} measurements, PS_{cort} is intentionally avoided, as opaque chambers are generally used (nine out of eleven studies used opaque ones; Table 2), thereby no influence on R_S estimates is to be expected. Cortical photosynthesis can be quantified by comparing E_{CO2} under light and dark conditions (Saveyn *et al.*, 2010; Bloemen *et al.*, 2016; Tarvainen *et al.*, 2018; De Roo *et al.*, 2019; De Roo *et al.*, 2020a; De Roo *et al.*, 2020b).

Previous studies indicate that PS_{cort} can refix 72%, on average, of the respired C in young tree stems (Pfanz *et al.*, 2002; Ávila *et al.*, 2014) and varies with species, stem age (e.g., Aschan *et al.*, 2001; Damesin, 2003; Wittmann & Pfanz, 2008) and vertical position at the stem (Tarvainen *et al.*, 2018). Refixation rates decreased rapidly with ageing to around 40% in 3- to 4-year-old stems (Wittmann & Pfanz, 2008; Vick & Young, 2009). The decline is attributed to changes in structural and functional traits, such as bark optical properties (younger thinner bark is more permeable to light transmission), Chl and N content, and the area/mass ratio of the stem cortex (Cernusak & Marshall, 2000; Wittmann & Pfanz, 2008). About half of eighty-five species of angiosperms (45%) had photosynthetic cortex chlorenchyma on main stems and almost all (94%) on twigs (Rosell *et al.*, 2015). Here, it must be pointed out that most of PS_{cort} studies have been performed in young twigs or branches, while data from stems of mature trees is relatively scarce (but see Strain & Johnson, 1963; Tarvainen *et al.*, 2018).

Cortical photosynthesis also produces O_2 within woody stems (Wittmann & Pfanz, 2014; Wittmann & Pfanz, 2018), but O_2 concentration in the sapwood is usually lower than in ambient air (~1–19%) (del Hierro *et al.*, 2002; Pfanz *et al.*, 2002; Spicer & Holbrook, 2005; Teskey *et al.*, 2008; Wittmann & Pfanz, 2014). Recently, Wittmann and Pfanz (2018) revealed that PS_{cort} actively raises the cortical O_2 concentration under illumination and counteracts temporal/spatial hypoxia within woody stems. Another benefit of PS_{cort} is to provide sugars under drought conditions when photosynthetic activity in leaves is limited and the risk of C starvation increases (Sevanto *et al.*, 2014; Cernusak & Cheesman, 2015; Vandegehuchte *et al.*, 2015; Bloemen *et al.*, 2016; De Baerdemaeker *et al.*, 2017; De Roo *et al.*, 2020b).

Light-induced axial diffusion in the gas phase

A reduction of E_{CO2} can be driven by axial diffusion (light-induced) along the stem. We should therefore consider the post-respiratory (indirect) effect of photosynthesis on the local mismatch between R_S and E_{CO2} when using opaque chambers. Directly beneath the opaque chamber, photosynthesis is inhibited. However, it occurs in the stem segments above and below the cuvette, which can lead to a light-induced [CO_2] vertical gradient along the xylem resulting in vertical diffusion of respired CO_2 to distant locations with lower xylem [CO_2] (Saveyn *et al.*, 2008a; De Roo *et al.*, 2019; De Roo *et al.*, 2020a; De Roo *et al.*, 2020b; De Roo *et al.*, 2020c). For instance, in dormant 4-year-old oak (*Quercus robur* L.) trees, axial CO_2 diffusion as induced by the occurrence of PS_{cort} above the site of measurement (via illuminating stem sections) resulted in reductions in E_{CO2} up to 22% (De Roo *et al.*, 2019).

PEPC-driven dark CO_2 fixation

Bicarbonate (HCO_3^-) can also be fixed via the enzyme phosphoenolpyruvate carboxylase (PEPC) in stem tissues without chloroplasts and under dark conditions. Until now, little attention has been paid to PEPC as a potentially important post-respiratory sink for respired CO_2. This ubiquitous cytosolic enzyme (Chollet *et al.*, 1996), present in plants, green algae and cyanobacteria (O'Leary *et al.*, 2011), is involved in substrate provision (in the form of organic acids) for C assimilation in C4 and CAM plants (Nimmo, 2008; Gowik & Westhoff, 2011; O'Leary *et al.*, 2011). Moreover, it also plays a central role in CO_2 fixation for anaplerotic metabolic pathways (to replenish TCA cycle intermediates) in all tissues of plants, independent of their photosynthesis type (Chollet *et al.*, 1996; Berveiller *et al.*, 2007; Werner & Gessler, 2011; Abadie & Tcherkez, 2019). The PEPC fixation capacity was firstly evidenced in a trunk of 18-years old *Robinia pseudoacacia* with ^{14}C labelled CO_2 that was incorporated into the downstream metabolites of PEPC (Höll, 1974). Likewise, Berveiller and Damesin (2008) found high activities of PEPC in stems of 9 different trees.

Importantly, Hibberd and Quick (2002) postulated that PEPC in stems of C3 plants results in a C4 like recycling mechanisms. CO_2 binds to phosphoenolpyruvate (PEP) and the resulting oxaloacetate (OAA) is transformed to malate (and aspartate) in a following enzymatic step (Chollet *et al.*, 1996; Plaxton & Podestá, 2006; O'Leary *et al.*, 2011; Abadie & Tcherkez, 2019). The limited pH buffer capacity in cells may constrain their capacity to produce and store organic acids such as malate (Spicer & Holbrook, 2007) and thus also for CO_2 fixation via PEPC. Malate can be locally processed in the Krebs cycle in parenchymatic or stem cambial cells releasing CO_2. It can also be transported in the xylem via the transpiration stream (Schill *et al.*, 1996; Patonnier *et al.*, 1999) and increase the malate pool in leaves (Gessler *et al.*, 2009). Re-integration of this malate in the Krebs cycle during day-night transitions causes light-enhanced dark respiration (see an overview by Werner & Gessler, 2011). Alternatively, malate might be loaded into sieve tubes of the phloem and exported (Hoffland *et al.*, 1992), potentially to the root system (Touraine *et al.*, 1992), where it is released as root exudates (Shane *et al.*, 2004). Malate was observed to contribute up to 2% to the phloem C pool in several tree species (Gessler *et al.*, 2013), and thus it needs to be assumed that malate is transported in a basipetal direction via the phloem.

Oxidase enzymes

A possibility of non-respiratory O_2 uptake is given by O_2-consuming enzymes that are oxidases or hydrolases (Sweetlove *et al.*, 2013), involved in lignification. If those enzymes consume O_2 without releasing CO_2 as a by-product (Kruse & Adams, 2008; Tcherkez *et al.*, 2012; O'Leary *et al.*, 2019), I_{O2} will increase for a constant E_{CO2}. But knowledge about the actual amount is currently unknown.

Approaches for estimating stem respiration

Mass balance

The mass balance approach (MBA) from McGuire and Teskey (2004) endeavors to quantify net C emissions from respiration of the stem section by assessing the CO_2 efflux into the atmosphere (E_{CO2}), transport of dissolved respired CO_2 in the sap through the xylem (F_T), and the storage of dissolved CO_2 in the stem section (ΔS):

$$R_S = E_{CO2} + F_T + \Delta S \quad [1]$$

CO_2 efflux into the atmosphere (E_{CO2}; µmol CO_2 m^{-3} s^{-1}) is calculated as follows:

$$E_{CO2} = \frac{f_A}{v} x\, \Delta[CO_2] \quad [2]$$

where f_A is the air flow rate through the stem cuvette (mol s^{-1}), v is the sapwood volume of the stem segment (m^3) and $\Delta[CO_2]$ is the difference between CO_2 concentration at the inlet and the outlet of the cuvette (µmol mol^{-1}). Cuvettes are normally connected to an infrared gas analyzer (IRGA) in open through-flow configuration, measuring $\Delta[CO_2]$. When using a closed configuration, E_{CO2} is determined based on the CO_2 increase over time.

A compilation of studies using the MBA showed a high variation in the contribution of E_{CO2} to R_S among and within trees (45%–100%; Table 2). Two factors determine the magnitude of diffusion of xylem CO_2 into the atmosphere (according to Fick's law of diffusion) and therefore E_{CO2}. First, the radial xylem CO_2 diffusivity needs to be accounted for and can be related to conductance or (reciprocal) resistance. Second, the CO_2 concentration gradient between the stem and the atmosphere, as a consequence of substantial CO_2 diffusive barriers in xylem, cambium and bark. Build-up of respired CO_2 in the stem leads to xylem CO_2 concentrations ($[CO_2]$) between 1% and 26% (Teskey *et al.*, 2008; Stutz & Anderson, 2021), much higher than the $[CO_2]$ in the ambient atmosphere (0.04%). Lower radial CO_2 diffusivity and lower xylem $[CO_2]$ have been found in conifers with tracheid wood anatomy compared to trees with vessel-wood anatomy of broadleaf tree species (Salomón *et al.*, 2021a). Steppe *et al.* (2007) showed a six-fold difference in the resistance to radial diffusion among *Populus deltoids* tree stems, which might also be responsible for inconsistencies observed in the contribution of E_{CO2} to R_S. Differences in the (ray and axial) parenchyma tissue fraction with a greater fraction of living (and thus respiring) cells in angiosperms (26.3%) than in conifers (7.6%) (Morris *et al.*, 2016) can also determine differences in biomass- or volume-based respiration rates and CO_2 build-up among plant functional types. The contribution of E_{CO2} to R_S decreases with stem diameter and also from smaller branches to stems. This is due to a lower ratio of surface area to volume, higher diffusion barriers (thicker bark) (Cavaleri *et al.*, 2006) and a longer radial CO_2 diffusive pathway.

Transport CO_2 flux (F_T; µmol CO_2 m^{-3} s^{-1}) is the transport of dissolved, respired CO_2 in the xylem sap. F_T is calculated as follows:

$$F_T = \left(\frac{fs}{v}\right) x\, \Delta[CO_2{}^*] \qquad [3]$$

where fs is the sap flow rate (l s^{-1}), v is the sapwood volume within the stem segment (m^3) and $\Delta[CO_2{}^*]$ is the difference in total DIC concentration measured above and below the stem cuvette (µmol l^{-1}).

The relative contribution of F_T to R_S in previous studies applying the MBA has shown substantial variability (0%–55%; Table 2). According to the original formulation of the MBA, F_T is negative when CO_2 import into the stem segment under study is greater than CO_2 export. F_T is positive when CO_2 export is greater than import. One of the few studies on the effect of stem size on the contributors to R_S showed that the relative contribution of F_T to R_S increases with increasing stem diameter and sapwood area (Fan *et al.,* 2017). This is due to the higher sap flow and, therefore, greater amount of CO_2 dissolved in the sap transported upwards.

The biggest uncertainty regarding the determination of F_T in the MBA is related to sap pH. Sap pH has a major effect on the calculation of the CO_2 concentration in the liquid phase ($[CO_2^*]$) and, therefore, the fate of respired CO_2 (details see modelling exercise 1). $[CO_2^*]$ can be calculated from gaseous xylem $[CO_2]$, xylem sap temperature and xylem sap pH using Henry`s Law (Butler, 1991; McGuire & Teskey, 2004, see also Material S1 available as Supplementary Data). Given the technical challenges of continuous sap pH measurements at the stem-level, xylem sap is extracted from distant canopy twigs. Using those measurements as a proxy for stem pH might lead to over- or underestimation of $[CO_2^*]$ (Erda *et al.*, 2014), although pH values obtained from stems showed to be similar to twig pH values (Saveyn *et al.*, 2008c; Aubrey *et al.*, 2011). Values of xylem sap pH have been reported to range between 4.5 and 7.6 (for literature overview see Table 2 in Teskey *et al.*, 2017). If pH values approach 7, CO_2 solubility exponentially increases. For example, *Populus deltoides* can have a high xylem sap pH of 6.8–7.2 (Saveyn *et al.*, 2008c; Aubrey *et al.*, 2011), allowing large quantities of CO_2 to dissolve and be transported in the xylem sap. By contrast, in *Prunus domestica*, with a low sap pH between 5.1–5.6, the amount of CO_2 that can be dissolved in the sap is limited (Erda *et al.*, 2014). Most studies assume a constant pH over the study period (e.g., Saveyn *et al.*, 2008c; Aubrey & Teskey, 2009; Cerasoli *et al.*, 2009; Etzold *et al.*, 2013; Bloemen *et al.*, 2014). However, daily or seasonal pH fluctuations may be important (Erda *et al.*, 2014). Thus, the timing of collecting sap pH might introduce uncertainty in estimating xylem CO_2 transport capacity (Salomón *et al.,* 2016; see Table S1 available as Supplementary Data). In the compiled studies, seasonal variation ranged from 0.5–2.1 pH unit differences. To a lower extent, pH can also vary during the course of a day, with a 0.4 pH unit decrease from day to night in Mediterranean oak trees (Salomón *et al.,* 2016) and a 0.3 pH unit reduction at pre-dawn compared to daytime in 1-yr-old *Populus nigra* stems (Brunetti *et al.*, 2019).

Storage CO_2 flux (ΔS; μmol CO_2 m^{-3} s^{-1}) represents the change in the quantity of CO_2 stored in the xylem over time as follows:

$$\Delta S = \left(\overline{|CO_2^*|}_{t1} - \overline{|CO_2^*|}_{t0}\right) x\ L/T \qquad [4]$$

where $|CO_2^*|_{t1 \text{ and } t0}$ are the mean $[CO_2^*]$ above and below the measured stem segment at time t_1 and t_0, L is volumetric water content of sapwood (l m^{-3}) and T is the duration of the time interval between t_1 and t_0 (s).

The storage flux has been consistently observed to be the smallest contributor to R_S, commonly accounting for less than 3% of R_S on a daily basis, with sporadic values up to 8% (Table 2). However, this flux is also affected by sap pH dynamics and therefore uncertain. Positive values of ΔS imply net build-up of CO_2 dissolved in the sap ($[CO_2^*]$ increases), while negative ΔS imply net release of CO_2 dissolved in the sap ($[CO_2^*]$ decreases).

Table 2 Summary of published experimental studies on the relative contribution of CO_2 efflux (E_{CO2}), xylem CO_2 transport (F_T) and CO_2 storage (ΔS) to stem respiration (R_S). Abbreviations: DBH diameter at breast height, HRM Heat Ratio Method, IRGA Infrared Gas Analyzer, NDIR Non-dispersive infrared CO_2 sensor for xylem [CO_2], TC thermocouple, TDP thermal dissipation probe.

E_{CO2}	F_T	ΔS	Species, age (yr) or DBH (cm)	Method E_{CO2}	Method F_T	Method ΔS	References
0.77	0.15	0.08	*Fagus grandiflora Ehrh.,* 15.1 cm	PVC cuvette, IRGA, open system	CO_2 microelectrode, TC, TDP, sap pH of expressed sap from twigs	sapwood water content assumed to be 50%	McGuire and Teskey (2004)
0.45	0.55	0.00	*Platanus occidentalis L.,* 10.2 cm				
0.83	0.14	0.02	*Liquidambar styraciflua L.,* 14.5 cm				
0.88	0.11	0.01	*Dacrydium cupressinum*, 18 cm-67 cm	clear polycarbonate gas-exchange chambers, IRGA, open system	TC (1.5cm depth), TDP, F_T predicted from sap flux density	ΔS calculated as the difference between R_S and E_{CO2} ΔS negligible at night and during periods of maximum sap flux density	Bowman *et al.* (2005)
0.18 (5°C)	0.82	-	*Platanus occidentalis,* 1-3 cm branches	PVC cuvette, IRGA, open system	CO_2 microelectrode, controlled temperature 5, 20, 35°C, internal flux measured with graduated cylinder and stopwatch, Sap pH from downstream end of branch	-	McGuire *et al.* (2007)
0.44 (35°C)	0.56						
0.30 (high sap velocity)	0.70						
0.71 (low sap velocity)	0.29						

E_{CO2}	F_T	ΔS	Species, age (yr) or DBH (cm)	Method E_{CO2}	Method F_T	Method ΔS	References
0.72	0.19	0.02	*Platanus occidentalis,* mature, 19.5-24.8 cm	PVC cuvette, foil-covered, IRGA, open system	NDIR, TC, TDP at opposite sites, sap pH from stem cores	$\Delta S = \left(\overline{\lvert CO_2 * \rvert_{t1}} - \overline{\lvert CO_2 * \rvert_{t0}}\right) / \Delta T$	Teskey and McGuire (2007)
0.82	0.18	0.00	*Populus deltroides Bart.ex Marsh.,* 3-yr-old, DOY: 287	cuvette, foil-covered, IRGA, open system	NDIR, TC (0.5 cm depth), TDP, sap pH of expressed sap from twigs and stem cores after campaign	See eq. 4; sapwood water content assumed to be 50%	Saveyn *et al.* (2008c) (note: we excluded rainy days)
0.93	0.09	0.00	DOY: 296				
0.86	0.13	0.00	DOY: 299				
1.00	0.00	0.00	*Quercus pyrenaica Wild.,* 45-yr-old, DOY: 143-144	stem chamber, IRGA, closed system	NDIR, TC (2 cm depth), TDP, opposite side of each stem, sap pH of expressed sap from twigs	See eq. 4	Salomón *et al.* (2016) (note: we report results from 1.5m only, mean of n = 2)
0.95	0.05	-0.01	DOY: 183-184				
0.97	0.04	-0.02	DOY: 218-219				
0.97	0.03	-0.02	DOY: 267-268				
0.86	0.15	-0.01	*Liriodendron tulipifera L.,* 16.3 cm	cuvette, foil-covered, IRGA, open system	NDIR, TC (2 cm depth), TDP, sap pH of expressed sap from twigs	See eq. 4	Fan *et al.* (2017)
0.89	0.12	-0.01	25.2 cm				
0.73	0.26	0.01	31.4 cm				
0.54	0.41	0.05	46.2 cm				
0.46	0.55	-0.01	60.6 cm				
0.973	0.023	0.03	*Populus canadensis,* 3-yr-old	stem cuvette, IRGA, open system	NDIR, TC (1 cm depth), HRM sensors, sap pH of expressed sap from twigs	See eq. 4	Salomón *et al.* (2018)
0.82	0.19	-0.01	*Eucalyptus tereticornis*, 18.8 cm, summer season, DOY: 352–354	stem chamber, IRGA, closed system	NDIR, TC (3 cm depth), TDP two random azimuths, sap pH of expressed sap from twigs	stem water content obtained from woody samples of nearby trees	Salomón *et al.* (2019b) (note: we report results from ambient treatment only)
0.96	0.04	-0.01	DOY: 15-17				
0.94	0.06	0.00	DOY: 36-38				

E_{CO2}	F_T	ΔS	Species, age (yr) or DBH (cm)	Method E_{CO2}	Method F_T	Method ΔS	References
1.09 0.80	-0.10 0.20	0.007 -0.002	*Ash,* 13.1-16.1 cm *Birch,* 11.5-13.5 cm	chamber, IRGA, differential configuration	NDIR, TC (1 cm depth), TDP (north and south site), sap pH of expressed sap from twigs	sapwood water content assumed to be 50%	Wang *et al.* (2019)
0.97	<0.06	-	*Pinus sylvestris,* 90-yr-old	transparent acrylic plastic, IRGA, open system	NDIR, Granier-type sensors, Sap pH of expressed sap from branches (water displacement method (e.g., Glavac *et al.*, 1990)	ΔS assumed negligible	Tarvainen *et al.* (2021)
1.01 (upper stem segment) 0.65 (lower stem segment)	-0.01 0.36	0 -0.01	*Fagus sylvatica, 130-yr-old*	stem chamber, closed system	NDIR, HRM, sap pH from twigs		Helm *et al.* (2021)

Note: CO_2 microelectrodes: sensitivity to temperature changes and lower stability reduced the reliability under field conditions (Teskey & McGuire, 2007); Sap flow: installation at two (opposite) sides of a stem is useful to account for circumferential variability (Saveyn *et al.,* 2008b; Salomón *et al.,* 2016), and might be especially important for mature trees. Sap flow rate: determination by continuous heating or pulse heating (Steppe *et al.*, 2010; Vandegehuchte & Steppe, 2013; Steppe *et al.*, 2015b; Flo *et al.*, 2019). Xylem sap pH: sap is obtained from twigs with a pressure chamber or by compressing stem cores in a vice to expel the sap and measured afterwards with a pH meter and a pH electrode.

O_2 measurements

Aerobic respiration involves both CO_2 production and O_2 consumption. Simultaneous measurements of I_{O2} and E_{CO2} at the stem potentially allow to get a more robust estimate of R_S (Angert & Sherer, 2011; Angert *et al.*, 2012; Trumbore *et al.*, 2013; Hilman & Angert, 2016; Hilman *et al.*, 2019). Measuring O_2 is particularly promising because O_2 is less affected by the post-respiratory mechanisms of transport and refixation via PEPC (Section 1). Vertical transport does not affect O_2 as much as CO_2, because the solubility of O_2 in water is ~30 times lower than for CO_2 (Dejours, 1981). The enzyme PEPC, as it has no affinity for O_2, does not affect I_{O2}.

At the mitochondrial level, the CO_2-to-O_2 ratio is termed the respiratory quotient (RQ) and depends on the oxidative status of the respiration substrate. The exchange of CO_2 and O_2 in complete oxidation of a molecule is mathematically related to its stoichiometry (Masiello *et al.*, 2008). For example, in glucose ($C_6H_{12}O_6$), that is defined to have neutral C-oxidation, 6 O_2 molecules are required to release 6 CO_2 molecules, resulting in RQ of 1. For more reduced substrates like fatty acids (lipid; $C_{18}H_{34}O_2$) more O_2 molecules are required for a complete breakdown of the molecule, resulting in lower RQ ~0.7. Respiratory quotient values above 1 are associated with organic acids catabolism, as these molecules have a greater O_2 content (for an overview, see Hilman *et al.*, 2022). At the stem-level, the term 'apparent' RQ (ARQ) has been introduced by Angert and Sherer (2011) to underscore that the observed ratio may be affected by post-respiratory processes that remove CO_2 evolved in the Krebs cycle. Carbohydrates are the largest substrate pool in trees and are assumed to be the most dominant respiratory C substrate (Hoch *et al.*, 2003; Plaxton & Podestá, 2006). If solely carbohydrates are used as substrate, the ARQ is expected to be ~1 in the absence of F_T. ARQ will be lower than 1 if respired CO_2 is transported in the xylem away from the site of measurement (Teskey *et al.*, 2008; Trumbore *et al.*, 2013) and is thus anti-correlated with sap flow rate (McGuire & Teskey, 2004; Bowman *et al.*, 2005; McGuire *et al.*, 2007). However, Hilman *et al.*, 2019 found only a minor effect of sap flow rates on declines in ARQ in *Quercus ilex*. This suggests that the contribution of dissolution and transport of CO_2 in the xylem stream to the mass balance might be small. The apparent respiratory quotient will also be lower than 1 if the respiratory substrate of a tree is changing. Some tree species store substantial amounts of lipids (Sinnott, 1918; Höll, 1997; Hoch *et al.*, 2002; Hoch *et al.*, 2003) that can be used for respiration instead of carbohydrates. For example, Fischer *et al.* (2015) measured ARQ of 0.9 in pine trees, explained by a mixture of respiratory substrates. Theoretically, respiration relying solely on lipids as respiratory substrate could result in an ARQ of 0.7 and might be beneficial under C-limiting conditions, as shown for young pine trees under a shading treatment (Fischer *et al.,* 2015). However, ARQ values ranged between 0.4-0.8 in nine non-lipid tree species (Hilman *et al.*, 2019). Those low values cannot

be explained by a substrate shift alone, suggesting that non-respiratory processes (e.g., transport) retain part of the respired CO_2 in the stem (Angert & Sherer, 2011; Angert *et al.*, 2012; Hilman *et al.*, 2019; Hilman *et al.*, 2022).

In situ I_{O2} measurements are technical challenging, because of the high background of O_2 in ambient air (~21%), making the detection of [O_2] changes within continuous-flow chamber in the range caused by plant respiration (several hundred ppm, or less than 0.1%) more difficult than the detection of [CO_2] changes. While continuous-flow O_2 measurements are possible, it requires considerable infrastructure and labor (e.g., Stephens *et al.*, 2007; Battle *et al.*, 2019). Technical innovations are needed for broader field use.

Stem respiration modelling

General overview

Our limited understanding of the complex metabolic processes involved in the production and consumption of O_2 and CO_2 hinders the development of a simple biochemical respiration model (Tcherkez & Ghashghaie, 2017; O'Leary *et al.*, 2019) equivalent to that of photosynthesis (Farquhar *et al.*, 1980). Instead, the growth and maintenance respiration paradigm (GMRP) proposed in the early 70s (Thornley, 1970) constitutes the basis of how plant respiration is currently estimated by most terrestrial biosphere models (TBM, reviewed by Atkin *et al.*, 2017). Here, plant respiration is divided into growth (R_g) and maintenance (R_m) components and parameters estimated from leaf respiration measurements. Temperature-normalized leaf R_m is commonly measured during non-growing periods and can be estimated from the empirical relationship between dark leaf respiration (R_d) and foliar nitrogen (N) content (Smith & Dukes, 2013) or as a function of the maximum carboxylation capacity of the enzyme Rubisco (V_{cmax}). Once leaf R_m at a reference temperature is determined, temperature-driven variation in R_m is accounted for by the Q_{10} parameter, which reflects the relative increase of R_m for a 10°C rise in temperature according to Arrhenius kinetics (e.g., De Vries *et al.*, 1974; Cannell & Thornley, 2000; Amthor, 1989). Then, leaf R_m respiration is scaled up to the whole-plant level using tree biomass partitioning and N allocation patterns, given the well-known link between N content and protein turnover rates involved in maintenance metabolism (Ryan, 1991; Reich *et al.*, 2008). By contrast, whole-tree growth respiration is commonly estimated as a fixed fraction of the difference between gross primary production (GPP) and whole-plant R_m (see Table 2 in Atkin *et al.* (2017)). Therefore, this source-driven perspective of plant C cycling estimates stem and root respiration from leaf metabolism (GPP, V_{cmax} and R_d), likely as a consequence of our better understanding of leaf photosynthetic processes. Nevertheless,

the respiratory regulation of non-photosynthetic woody tissues, where chlorophyll-containing cells are scarce, might substantially differ from that in foliar tissues. Indeed, the coordination between photosynthetic and respiratory metabolism in foliar tissues (via a direct link between R_d and V_{cmax} parameters) to optimize net C gain under variable abiotic conditions (Wang *et al.*, 2020) is unlikely to regulate respiration in non-photosynthetic stems, as denoted by different thermal acclimation responses (Smith *et al.*, 2019) and N-R_d relations (Reich *et al.*, 2008) between organs.

Hölttä and Kolari (2009) developed a physical model integrating CO_2 diffusion and solubility processes in different stem compartments (heartwood, sapwood, phloem and outer bark) to interpret measurements of stem E_{CO2}. The CASSIA model constituted another step forward for more mechanistic modelling of stem and plant respiration (Schiestl-Aalto *et al.*, 2015; Schiestl-Aalto *et al.*, 2019). CASSIA considers the sink strength of growth and respiratory processes in different tree organs to reflect intra-annual and inter-annual growth variability, and it was successfully applied in a boreal conifer stand. More recently, a biophysical tree stem respiration model (TReSpire) was developed to determine stem respiration independent of leaf metabolism (Salomón *et al.*, 2019a). TReSpire simulates water and carbon fluxes at an hourly resolution (see also Meir *et al.*, 2020) and can estimate parameters of respiratory traits commonly used in large-scale models such as the growth yield (Y_G), the temperature-normalized R_m per unit of N, and its temperature sensitivity (Q_{10}). Importantly, TReSpire is calibrated against measurements of E_{CO2} and stem diameter variations, allowing decoupling from source-driven models, and has proven helpful in capturing the sink strength of growth and respiratory processes across species and seasons (Salomón *et al.*, 2022).

Uncertainty analysis of R_S using TReSpire

In the following modelling exercises, we use TReSpire to illustrate the potential of modelling to understand the movement of respired CO_2 in the stem. Specifically, we showcase the importance of two critical parameters involved in the solubility and transport of CO_2 through the xylem: sap pH and stem size. The first modelling exercise evaluates how uncertainty in sap pH measurements propagates through the model and informs on the uncertainty of $[CO_2^*]$ estimates and the fraction of respired CO_2 that diffuses to the atmosphere (E_{CO2}/R_S). Because most studies applying the MBA have been performed in saplings or small trees the second modelling exercise assesses how stem diameter affect estimates of R_S and E_{CO2}.

TReSpire consists of two submodels. Submodel A simulates stem hydraulic behaviour to disentangle water- and growth-related variations in stem diameter (Steppe *et al.*, 2006; Steppe *et al.*, 2015a). For this, cell turgor pressure is simulated to separate growing from non-growing metabolism, i.e., R_g and R_m. Subsequently, submodel B estimates R_S based on the GMRP, also

considering CO_2 solubility and diffusivity (Hölttä & Kolari, 2009), stem allometry and nitrogen content to close a double mass balance (McGuire & Teskey, 2004) in the xylem and the outer tissues (cambium, phloem and bark). Data required to run and calibrate TReSpire are sap flow rate, stem diameter variation, soil and xylem water potential, stem temperature, and E_{CO2}. See supporting information for further details on the model and relevant equations to these two exercises (see Material S2 available as Supplementary Data).

Modelling exercise 1: Sap pH

For both modelling exercises, we use data and calibrated parameters for a maple tree shown in Salomón *et al.* (2019a), which is freely available in an open repository (doi: 10.17632/9c9w7mvy9d.1.). Sap pH variability was defined by its mean (constant for all scenarios according to the measured value of 6.12) and a variable standard deviation (SD) of 0.5, 0.75, 1, and 2 pH units (Fig. 1a). The 95th percentile of the four sap pH distributions (6.94, 7.35, 7.76 and 9.39) correspond to a theoretical sap [CO_2^*] of 13, 26, 47 and 89 mmol L^{-1} (Fig. 1b). In other words, a pH increase of 0.82, 1.12, 1.64 and 3.27 units resulted in a 2.8-, 5.5-, 10.1- and 19.1- fold increase in sap [CO_2^*] relative to a pH of 6.12, for which sap [CO_2^*] was 4.6 mmol L^{-1} (see eqns. in Material S2 available as Supplementary Data). Uncertainty in sap pH and sap [CO_2^*] further propagated to E_{CO2}/R_S estimates, as the corresponding fraction of respired CO_2 diffusing to the atmosphere decreased to 0.81, 0.77, 0.68 and 0.40 (Fig. 1c), respectively, which are ratios progressively lower than the E_{CO2}/R_S median of 0.87 at 6.12 pH. This uncertainty analysis highlights the discrepancy between E_{CO2} and R_S and their dependency on sap pH. It illustrates how higher CO_2 solubility in xylem sap increases the contribution of storage and transport CO_2 fluxes to stem respiration ($\Delta S/R_S$ and F_T/R_S) to the detriment of the contribution of radial CO_2 diffusion (E_{CO2}/R_S).

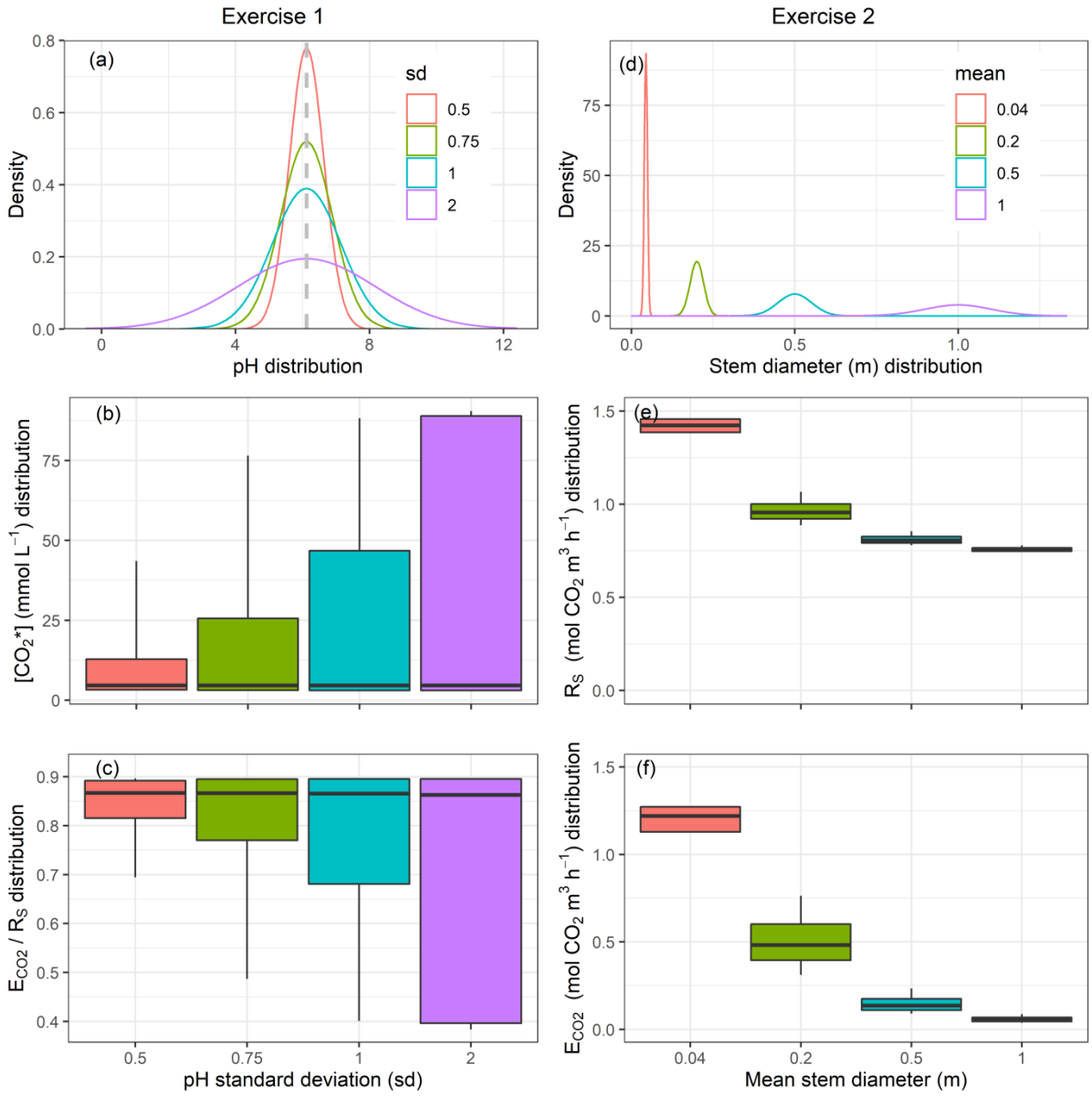

Figure 1 Two modelling exercises to illustrate how sap pH affects estimates of sap $[CO_2]$ in the liquid phase ($[CO_2^*]$) and the contribution of stem CO_2 efflux to stem respiration (E_{CO2}/R_S) (left-hand side panels; a-c) and how stem size affects estimates of E_{CO2} and R_S (right-hand side panels; d-f). We simulated four scenarios in which a normal distribution of sap pH is evaluated by bootstrapping techniques to assess how uncertainty in sap pH propagates throughout the model. Uncertainty distributions are estimated over 1000 evaluations and averaged over the 5-day modelling period. Centerlines, box limits, and whiskers represent the median, 5th and 95th percentiles, and extremes, respectively.

Modelling exercise 2: Stem diameter

The normal distribution of the stem diameter was defined by the mean of progressively larger stems (0.044, 0.2, 0.5 and 1 m, with the first value being the measured diameter of the monitored maple tree) and a standard deviation equal to 10% of the mean value (Fig. 1d). Assuming equal respiratory traits (Y_G, R_{20_N} and Q_{10}) and that the whole stem section is maintained alive and respiring (there is no heartwood), median values of R_S on a volume basis progressively decreased with stem diameter from 1.4 to 0.8 mol CO_2 m^{-3} h^{-1} (Fig. 1e). Such reduction attributable to stem allometry is explained by the higher portion of xylem to outer tissues of larger stems, determined by the non-linear relationship between stem diameter and thickness of the outer tissues (see Supplementary Material 2). The xylem is metabolically less active than the outer tissues due to the N-dependency of respiratory processes and the lower N measured in the xylem relative to the outer tissues (1.5 and 6.3 mg N g dry $mass^{-1}$, respectively). Median values of E_{CO2} on a volume basis decreased with stem diameter to a larger extent, from 1.2 to 0.1 mol CO_2 m^{-3} h^{-1} when comparing stem diameters of 0.04 and 1 m (Fig. 1f). The length of the diffusive pathway from the CO_2 production site to the atmosphere largely explains this E_{CO2} reduction, as according to Fick's law, diffusion is inversely proportional to the diffusion length (see eqns. in Supplementary Material 2). Note that this modelling exercise provides mechanistic support to observations in yellow-poplar trees, for which E_{CO2}/R_S decreased from 0.86 to 0.46 with increasing stem diameter from 0.16 to 0.6 m (Fan *et al.*, 2017).

Research agenda

Various processes can affect the accuracy of R_S estimates and upscaling procedures. In the following, we identify seven key research challenges concerned with these processes that should be addressed via observational studies, manipulative experiments and modelling approaches. Note that the enumerated items in the research agenda refer to the numbering shown in Fig. 2.

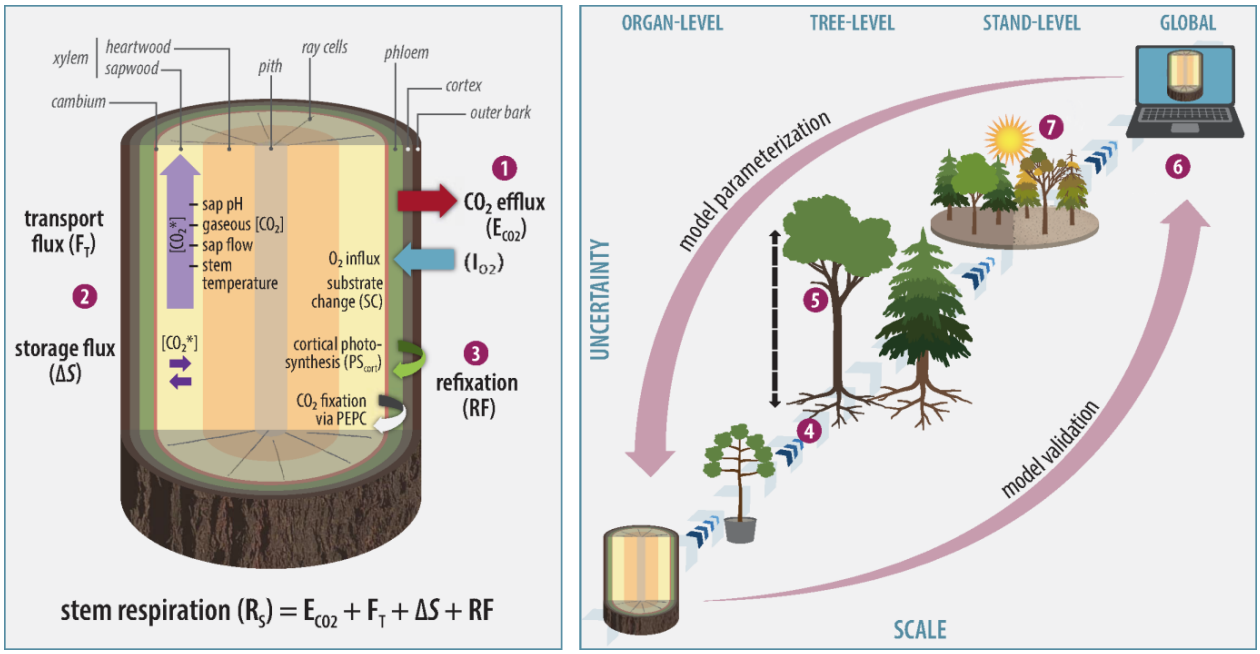

Figure 2 Research needs to improve estimates of stem respiration (R_S) and upscaling procedures. Numbers in red circles refer to specific items in the research agenda. Left: Tree stem section highlighting respiratory fluxes accounted for by the formula $R_S = E_{CO2} + F_T + \Delta S + RF$ (extended Mass Balance Approach) and I_{O2} measurements as an additional proxy for R_S. ❶Combination of MBA with oxygen-based techniques might help to better elucidate the fate of respired CO_2. ❷Accurate measurements of sap pH are key for quantifying the dissolved inorganic carbon (DIC) in the sap solution ($[CO_2^*]$) since pH determines the equilibrium between gaseous CO_2 and total DIC. ❸Refixation (RF) of respired CO_2 via cortical photosynthesis (PS_{cort}) or phosphoenolpyruvate carboxylase (PEPC) enzyme can cause differences between E_{CO2} and actual R_S of underlying tissues. Right: Upscaling from tissue-level measurements to forest stands and above. The upscaling procedure involves ❹comparing processes in saplings and mature trees and, ❺scaling to the whole-tree level. ❻The upscaling ladder can be implemented in stem to stand-level respiration models, progressively improved by 'ground-truthing' with observational and experimental data (red arrows). ❼Environmental factors should be accounted for in R_S studies. Measuring both fluxes (E_{CO2}, I_{O2}) allow conclusions about respiratory metabolism (substrate change, SC) and can be useful to evaluate tree's resilience to environmental stress. Uncertainty increases with observational scale and knowledge gaps (methodology, process-based understanding) from fine to large scales.

1. Closing the C mass balance

Research challenge: We still lack a complete understanding of the fate of CO_2 in tree stems, making estimates of R_S from E_{CO2} measurements highly uncertain. Alternative and complementary approaches to quantify R_S, like simultaneous measurements of I_{O2} and E_{CO2}, can help disentangle the different post-respiratory processes involved in CO_2 removal from the production site.

Hypothesis/Expectation: Mass balance approach (MBA) and oxygen-based methods (ARQ) can be complementary under the assumption that CO_2-removal processes like F_T or PEPC fixation are the key drivers for the imbalance between E_{CO2} and actual R_S. Measuring I_{O2} (O_2 less soluble) in combination with E_{CO2} would allow us to quantify the magnitude of the different contributors to R_S, helping to interpret each other (see Table 3).

Method:

- Measure variables required to apply the MBA and ARQ (E_{CO2}, I_{O2}, xylem CO_2, sap pH, sap flow, stem temperature) simultaneously

Table 3 Overview of relevant variables (E_{CO2} = CO_2 efflux, F_T = transport flux, ΔS = storage flux, RF = local refixation, either PS_{cort} or PEPC) to estimate stem respiration more accurately ($R_S = E_{CO2} + F_T + \Delta S + RF$). O_2 influx (I_{O2}) can be an additional proxy for R_S. However, residual uncertainties remain.

Variables	Approach to directly measure each variable	Residual uncertainties
E_{CO2}	cuvette or chamber (transparent or opaque)	PS_{cort} for transparent chambers, and axial CO_2 diffusivity due to light-induced gradients in xylem CO_2, unknown PEPC activity and substrate use (or SC)
F_T	(a) sap flow (b) gaseous xylem [CO_2] (c) stem temperature (d) xylem sap pH	sap pH from branches (not stem), drift in [CO_2] readings ascribed to potential stem wound closure, unknown PEPC activity and substrate use (or SC)
ΔS	[CO_2^*]	sap pH from branches, drift in [CO_2] readings ascribed to potential stem wound closure

2. Uncertainty in transport flux: Sap pH stem measurements

Research challenge: Given the high impact of pH on the calculation of $[CO_2^*]$ and F_T, uncertainties in pH measurement can result in substantial errors in R_S budgets. Accurate and continuous measurements of stem sap pH *in situ* are urgently needed, for which no suitable method is currently available due to technical constraints. Instead, sap pH measurements of distant canopy twigs are commonly used as a (constant) proxy for stem sap pH.

Hypothesis/Expectation: Advanced technologies that could account for spatial and temporal variability of sap pH (daily, seasonal, species-specific and environmentally dependent) would decrease errors in R_S budgets. See modelling exercise 1 in section 2.

Method:

- Use technologies from other disciplines like gastric probes from medical applications or microdialysis (passive diffusion principle, technique in neuroscience) to achieve continuous measurements of xylem sap of trees *in vivo* (e.g., Jeřábek *et al.*, 2020)
- Calibrate probes in the expected range with pH buffer solutions
- Technical difficulties: ensuring constant contact with xylem sap, be aware of wound reaction of wood and air embolism when placing probes into the xylem and avoid contamination with cellular constituents by damaging living cells in the parenchymatic tissue

3. Refixation of respired CO_2

Cortical photosynthesis (PS_{cort})

Research challenge: Cortical photosynthesis (PS_{cort}) has commonly been measured in green twigs, branches, saplings or young tree stems, not in mature trees. Uncertainties, therefore, remain about the effect of stem age, diameter, bark thickness and optical properties of the outer bark along the vertical stem gradient on the photosynthetic potential of mature woody tissues and its influence on R_S estimates.

Hypothesis/Expectation: PS_{cort} is higher in the outer bark of younger stems, decreases with stem depth (Wittmann & Pfanz, 2018), increases with stem height, but decreases with canopy depth in older branches (Cernusak & Marshall, 2000). This is due to higher light transmission of thinner outer bark and a steep light gradient from the stem surface to the pith. Increasing stem age also reduces light transmission through the bark (Aschan & Pfanz, 2003).

Method:

- Measure chlorophyll fluorescence of stems *in vivo* and of stem cross-sections to assess photochemical activity (photosystem II activity) of the woody tissue
- Measure optical properties of the outer bark (periderm) and inner bark (cortex) (e.g., photosynthetic pigment content) (Wittmann & Pfanz, 2016)

PEPC-mediated refixation

Research challenge: The non-photosynthetic CO_2 fixation catalysed by PEPC has not been well studied so far, therefore, the magnitude of CO_2 PEPC-mediated refixation remains speculative.

Hypothesis/Expectation: Imbalances between actual R_S and measured E_{CO2} might be related to PEPC fixation and PEPC might drive sub-daily variation in ARQ.

Method:

- Perform tracer studies with ^{13}C-labelled CO_2 to track the label in the malate pool within the stem and in root exudates via compound-specific isotope analysis, tracing of the label in the E_{CO2} further up the transpiration stream or using C-14 as another potential tracer
- Perform enzymatic assays (e.g., adapted from the protocol of Bénard & Gibon (2016)) to quantify PEPC capacity
- Analyze PEPC fixation products (organic and amino acids) with time and along the stem (see Schill *et al.*, 1996)

4. Scaling carbon flux dynamics from small to large trees

Research challenge: Most studies applying the MBA have been performed in saplings or small trees for methodological simplicity. However, the movement and fate of respired CO_2 likely depend on stem size (Fan *et al.*, 2017), and this methodological bias could distort our perspective of CO_2 fluxes within the xylem.

Hypothesis/Expectation: Xylem CO_2 diffusion is limited in thicker stems due to the long radial CO_2 diffusive pathway. The relative contribution of E_{CO2} to R_S is expected to decrease with stem diameter, while F_T increases with larger stem sapwood area due to the higher amount of CO_2 dissolved in sap and is transported upwards (see modelling exercise 2). If more CO_2 is transported away from the measurement site, stem ARQ ratios will decrease. Stem age likely reduce C refixation via PS_{cort} (see research challenge 3). PEPC-mediated refixation might be comparable between saplings and mature trees.

Method:

- Assess E_{CO2}, I_{O2}, F_T and RF under comparable environmental conditions for saplings and mature trees, with a marked size contrast

5. Fate of dissolved and re-fixed carbon: Scaling to the whole-tree level

Research challenge: Our process-based understanding of gas exchange at the stem-level has not yet been expanded to the whole tree-level. The drivers to R_S and ARQ among different organs (stem, branches, leaves, and roots) might change with their morphological, anatomical or physiological traits.

Hypothesis/Expectation: If we assume that up to 30% of CO_2 is not emitted locally (Hilman *et al.*, 2019), import and emission of CO_2 in branches originating from respiration in stem tissues may cause local ARQ to increase in upper tree parts (enhanced diffusion of xylem-transported CO_2 in thinner stems/branches) and *vice versa*.

Method:

- Measure sap [CO_2^*] and ARQ along woody tissues in stems and branches

Apply different tracer approaches to advance our understanding of the fate of CO_2 along the soil-plant-atmosphere continuum, like:

- Inject ^{13}C tracer as dissolved ^{13}C-carbonate (Powers & Marshall, 2011) or $^{13}CO_2$ (Bloemen *et al.*, 2015) into the xylem or fed as ^{13}C labelled sugar into the phloem (Gessler *et al.*, 1998) to serve as a respiratory substrate in basipetal locations
- Determine (above the phloem or xylem feeding location), $^{13}CO_2$ efflux and ^{13}C assimilated into different organic compounds (c.f. Joseph *et al.*, 2020), allowing a quantitative assessment of the fate of CO_2
- Use online measurements of the xylem CO_2 ^{13}C (and ^{18}O) isotopologues composition and flux with an adapted online system (Gessler *et al.*, 2022) where the probe design and the laser spectrometer need to target CO_2 instead of water
- Use Cavity Ring-Down Laser Spectroscopy (CRDS) for real-time measurements of ^{13}C-CO_2 (Salomón *et al.*, 2021a)

6. Scaling from trees to stands and from stands to larger spatial scales

Research challenge: Leaf and stem respiration are unlikely to be regulated by the same mechanisms, hereby stem respiration models need to be decoupled from the source-driven perspective (e.g., Fatichi *et al.*, 2014; Schiestl-Aalto *et al.*, 2015; Salomón *et al.*, 2019a). It remains

unclear, if plant respiration is modulated by respiratory substrate supply (source-driven) or by plant demand of metabolic products (sink-driven) (Schiestl-Aalto *et al.*, 2015; Collalti *et al.*, 2020). Refinements of modelling routines are required by decoupling leaf and woody tissue respiration for the upscaling of R_S to larger spatial scales.

Hypothesis/Expectation: The respiratory metabolism of (non-photosynthetic) woody stem tissues, where Rubisco is mainly absent, might substantially differ from that in foliar tissues. Implementing algorithms that consider the partially sink-driven nature of woody tissue respiration (Salomón *et al.*, 2022), its differential thermal acclimation (Smith *et al.*, 2019), and the physical properties of sapwood and bark will improve estimates of whole plant respiration, which constitutes one the largest sources of uncertainty in net primary production in global models (Dietze, 2014).

Method:

- Compile a global database of stem respiratory traits such as basal respiration rates at a standard temperature (R_b), the temperature sensitivity of respiration (Q_{10}), respiratory construction costs (Y_G), CO_2 diffusion rates in compliance with the global database of leaf (dark) respiratory traits (GlobResp; Atkin *et al.*, 2015) and the global database of soil respiration (Bond-Lamberty & Thomson, 2010)
- The analysis of the collected dataset could inform about stem respiratory regulation and acclimation along broad gradients of climatic conditions, potentially improving estimates of whole plant respiration in large-scale models
- Test processes already described in mechanistic models of woody tissue respiration (Hölttä & Kolari, 2009; Schiestl-Aalto *et al.*, 2015; Salomón *et al.*, 2019a) for the incorporation of refined algorithms in large-scale models

7. Changes in respiratory metabolism during environmental stress

Research challenge: When investigating responses of tree C budgets to ongoing global warming and climate extremes, the dynamics of respiratory metabolism and reserve use is an overlooked process critical to buffer stressful periods.

Hypothesis/Expectation: Under heat and drought, leaf photosynthesis is limited following stomatal closure, and trees heavily rely on NSC storage compounds (including starch, sugars or lipids). Trees use their C reserve pools and switch from pure carbohydrate metabolism to alternative (or older) respiratory substrates to cope with severe stress (e.g., ARQ ~ 0.7 and $\delta^{13}CO_2$ ~-33‰ would give a hint towards lipid metabolism; see Fischer *et al.,* 2015 in climate-controlled chambers).

Method:

- Asses ARQ and the ^{13}C natural abundance of stem released CO_2 under gradients of heat and drought stress to gain information on respiratory substrate use
- Assess $^{14}CO_2$ to determine the age of the respiratory substrate

Conclusion

In this *Insight* article we provide an updated view on R_S estimates and their uncertainties. Different perspectives on plant respiration can complement each other when combined and help to better elucidate the fate of respired CO_2. Hereby, combining CO_2 efflux with O_2 influx measurements are of particular interest to disentangle post-respiratory processes. We underscore the need to integrate theory and field observational data to better understand the respiratory physiology in woody tissues. Great progress has been achieved in R_S modelling by getting independent of assumptions inferred from leaf-level studies. An improved upscaling of R_S from the tree to the ecosystem-level is necessary to evaluate the magnitude of R_S to the total C balance of forest ecosystems.

Conflict of Interest

None declared.

Funding

T.E.E.G. received funding by German Research Foundation (GR1881/5-1). R.L.S. received funding from the Spanish Ministry of Science, Innovation and Universities (Juan de la Cierva Programme, grant IJC2018-036123-I). K.S. received funding from the Research Foundation Flanders (FWO) under research programme G.0941.15N.

Acknowledgement

We are grateful to Annett Boerner for producing Figure 2.

Abbreviations

Symbol	Explanation
ARQ	Apparent respiratory quotient
$[CO_2]$	Gaseous $[CO_2]$
$[CO_2^*]$	Dissolved inorganic carbon (DIC); comprises of dissolved CO_2, carbonic acid (H_2CO_3), bicarbonate (HCO_{3-}) and carbonate (CO_3^{2-})
E_{CO2}	CO_2 efflux to the atmosphere
F_T	Transport flux; transport of dissolved respired C in the xylem sap
GMRP	Growth and maintenance respiration paradigm
MBA	Mass balance Approach
I_{O2}	O_2 influx
PEPC	Phosphoenolpyruvatcarboxylase; enzyme for CO_2 fixation
PS_{cort}	Cortical photosynthesis
R_d	Dark leaf respiration
R_g	Growth respiration
R_m	Maintenance respiration
ΔS	Storage flux; change in the storage of dissolved C in the stem section
V_{cmax}	Maximum carboxylation capacity of enzyme Rubisco

CHAPTER 2

Low-cost chamber design for simultaneous CO_2 and O_2 flux measurements between tree stems and the atmosphere

Juliane Helm[1,2], Henrik Hartmann[1], Martin Göbel[1], Boaz Hilman[1], David Herrera-Ramírez[1], Jan Muhr[1,3]

[1]Max Planck Institute for Biogeochemistry, Department of Biogeochemical Processes, Hans-Knöll-Str.10, 07743 Jena, Germany

[2]Department of Environmental Sciences–Botany, Basel University, Schönbeinstr. 6, Basel CH-4056, Switzerland

[3]Department of Bioclimatology, Georg-August University Göttingen, Büsgenweg 2, 37077 Göttingen, Germany

Published in Tree Physiology (2021). Volume 41, Issue 9, September 2021, Pages 1767–1780, https://doi.org/10.1093/treephys/tpab022.

Abstract

Tree stem CO_2 efflux is an important component of ecosystem carbon fluxes and has been the focus of many studies. While CO_2 efflux can easily be measured, a growing number of studies have shown that it is not identical with actual *in situ* respiration. Complementing measurements of CO_2 flux with simultaneous measurements of O_2 flux provides an additional proxy for respiration, and the combination of both fluxes can potentially help getting closer to actual measures of respiratory fluxes. To date, however, the technical challenge to measure relatively small changes in O_2 concentration against its high atmospheric background has prevented routine O_2 measurements in field applications.

Here we present a new and low-cost field-tested device for autonomous real-time and quasi-continuous long-term measurements of stem respiration by combining CO_2 (NDIR based) and O_2 (quenching based) sensors in a tree stem chamber. Our device operates as a cyclic closed system and measures changes in both CO_2 and O_2 concentration within the chamber over time. The device is battery-powered with a >1 week power independence and data acquisition is conveniently achieved by an internal logger. Results from both field and laboratory tests document that our sensors provide reproducible measurements of CO_2 and O_2 exchange fluxes under varying environmental conditions.

Keywords

carbon dioxide consumption, chamber-based measurements, CO_2 efflux, low-cost sensors, O_2 influx, oxygen production, respiratory fluxes

Introduction

Stem CO_2 efflux is an important part of the carbon (C) balance of forest ecosystems, as it accounts for 5–42% of the total ecosystem respiratory fluxes in forests (Lavigne *et al.*, 1997; Damesin *et al.*, 2002; Chambers *et al.*, 2004; Ryan *et al.*, 2009; Yang *et al.*, 2016). It is typically measured by using chambers of various designs and measurement principles (e.g., Xu *et al.*, 2000; Pumpanen *et al.*, 2004; Maier & Clinton, 2006; Saveyn *et al.*, 2008a; Etzold *et al.*, 2013; Hilman & Angert, 2016; Katayama *et al.*, 2016; Brändle & Kunert, 2019) and then often assumed equal, or at least proportional, to the rate of actual respiration in the underlying tissues. This assumption neglects the fact that local CO_2 emission is the combination of respiratory CO_2 production and a number of post-respiratory processes (Teskey *et al.*, 2008; Trumbore *et al.*, 2013). Key processes are the transport of dissolved CO_2 in the xylem both away from or towards the site of measurement (McGuire & Teskey, 2004; Teskey & McGuire, 2007; Teskey *et al.*, 2008; Bloemen *et al.*, 2013), photosynthetic re-assimilation in chloroplasts of sub-corticular cells (Pfanz *et al.*, 2002; Teskey *et al.*, 2008; Ávila *et al.*, 2014; Cernusak & Cheesman, 2015; De Roo *et al.*, 2020c), non-photosynthetic refixation by parenchyma cells within the xylem, cambium and phloem via the enzyme phosphoenolpyruvate carboxylase (PEPC) (Gessler *et al.*, 2009; Hilman *et al.*, 2019) or axial diffusion of CO_2 in the gas phase (De Roo *et al.*, 2019). All these processes can be highly variable over time and may differ between plant organs. Thus, while chambers can provide accurate flux measurements, these fluxes can temporarily differ significantly from local stem respiration rates.

Aerobic respiration does not only produce CO_2, but also results in an anti-correlated uptake of O_2, as O_2 is consumed as the electron acceptor at the end of the mitochondrial electron transport chain to form H_2O. To date, stem O_2 uptake rates have rarely been measured because the high background of O_2 in ambient air (20.95 vol.% or 209 500 ppm) makes the detection of O_2 concentration changes in stem chambers (typically a few hundred ppm over tens of minutes in many chambers) technically challenging. Differential fuel-cell analyzers (e.g., Stephens *et al.*, 2007; Battle *et al.*, 2019) are able to detect very small changes in atmospheric O_2 (down to several ppm), but require costly infrastructure and high maintenance for application in the field, and usually have a very limited application radius around the position of the analyzer. This can be overcome by laboratory measurements of discrete flask samples from the field, which allow for decentralized measurements over wider areas. Still requiring typically costly analyzers, this approach is usually limited by the number of flasks and the required processing time of the samples and thus typically results in low temporal resolution (Seibt *et al.*, 2004; Hilman *et al.*, 2019). Hilman and Angert (2016) presented an intermediate approach ("direct discrete method"): They used low-cost chambers that were

installed independent of each other on several trees and O_2 measurements were carried out with a portable optical fiber system. While this approach allows measurements over a wider area and immediate results this method cannot easily be automated and requires manual measurements, thereby again limiting the temporal and spatial resolution. Cavity-enhanced Raman multi-gas spectrometry (CERS) has been used to measure quasi-continuous fluxes of O_2 in pine (*Pinus sylvestris* L.) branches (Keiner *et al.*, 2013; Keiner *et al.*, 2014; Fischer *et al.*, 2015), however, due to the high sensitivity of the CERS to changes in temperature and air pressure, the methodology is not easily applicable under field conditions.

Like with CO_2, O_2 fluxes are affected by processes other than respiration. For example, O_2 can also be transported to or from the site of respiration by xylem water. However, since O_2 is ~30 times less soluble in water than CO_2 (Dejours, 1981) this effect is considerably smaller. Stem photosynthesis is usually considered to play a minor role in stems of older trees (Wittmann & Pfanz, 2008; Rosell *et al.*, 2015; Tarvainen *et al.*, 2018), but would result in a release of O_2 and an anti-correlated CO_2 consumption. The only O_2-exclusive metabolic processes we are aware of is lignification (Amthor, 2003) resulting in O_2 consumption. While the actual amount of O_2 consumption by lignification is unknown, it seems unlikely to result in large changes of O_2 concentration in mature trees. Differences between actual respiration and measured fluxes therefore have to be expected for both gases.

The ratio of CO_2 release to O_2 uptake (respiratory quotient, RQ) depends on the stoichiometry of the respiratory substrate. For example, the stoichiometric RQ for complete oxidation is ~1 for carbohydrates, ~0.8 for amino acids, and ~0.7 for lipids. Thus, the measured RQ has been used to identify respiratory substrates (Stiles & Leach, 1933; Lambers *et al.*, 2008). Plant respiration is commonly assumed to be dominated by carbohydrate catabolism, but shifts to lower RQ and $\delta^{13}C$ of respired CO_2 have been used to infer a switch to lipid respiration for plants under stress and carbon starvation (Tcherkez *et al.*, 2003; Fischer *et al.*, 2015). The simultaneous measurements of CO_2 and O_2 fluxes therefore provide a more robust estimate of actual respiration rates as well as information on the stoichiometry of the respired substrate. The much smaller solubility of O_2 provides the potential to assess the influence of post-respiratory processes on CO_2 in the stem (Angert & Sherer, 2011; Angert *et al.*, 2012; Trumbore *et al.*, 2013; Hilman & Angert, 2016; Hilman *et al.*, 2019).

Our aim was to develop and test a portable, weatherproof, low-cost and fully autonomous stem chamber design that allows simultaneous *in situ* measurements of CO_2 and O_2 fluxes from tree stems. The data presented here demonstrate the reliability and robustness of the individual sensors as well as the complete chamber design and is based on various laboratory tests and field

measurements. Our new tool can improve our understanding of respiratory fluxes in tree stems. Given its low cost, it allows large-scale assessments of ecosystem carbon fluxes with sufficient replication and the use of O_2 sensors in addition to CO_2 sensors represents a substantial improvement for assessing the importance of tree physiological factors in ecosystem carbon fluxes.

Methods

Gas sensors

In the final version of our chambers, we measured CO_2 concentration with the COZIR non-dispersive infrared (NDIR) absorption sensor (Gas Sensing Solution GSS, UK), O_2 concentration with the LuminOx Optical fluorescence quenching sensor (sealed, LOX-02-S; SST Sensing Ltd, UK), and H2O concentration with a high precision humidity sensor (Digital Humidity Sensor SHT-85 (RH/T), Sensirion, ZH, Switzerland). Measurements of H_2O concentration are necessary for the correction of O_2 measurements (see '*Correction of measurement data (O_2) for the dilution effect of changing H_2O and CO_2 concentrations'*). Initially, we instead used the relative humidity sensor integrated in the COZIR. However, detailed laboratory tests revealed significant mismatches between known and measured humidity and a very slow reaction time for the COZIR built-in sensor. Therefore, we switched to the more accurate and rapidly responding SHT-85 sensor, using the manufacturer's calibration (detailed humidity test results from the laboratory and field can be found in S1 and S2 available as Supplementary Data at Tree Physiology Online).

The COZIR has a CO_2 measurement frequency of 2 Hz and includes a temperature (°C) and relative humidity (%) sensor. Using the internal filter feature, we set the sensor to report running means of the last 50 measurements or 25 s. We do this to reduce high frequency noise and smooth the CO_2 readings, though this leads to an overall slower response times to concentration changes (details see GSS Sensor User's Manual, 2015). The COZIR sensor allows for one-point calibration (see '*Multiple sensor calibration and testing unit'*).

The LuminOx O_2 sensor measures the partial pressure of O_2 (ppO_2; mbar), the total pressure (pO_2; mbar) and temperature (TO_2; °C). The O_2 sensors do not allow for changing the manufacturer-supplied calibration parameters unique to each sensor, which are determined by exposing the sensor to different oxygen concentrations, temperatures and barometric pressures in an environmental chamber. Device specifications are provided in the datasheet of the supplier (see also Table 1).

Table 1 Specifications of COZIR-AH-1 and LuminOx sealed optical oxygen sensor.

	COZIR Ambient sensor AH-1	**LuminOx Sealed Optical Oxygen sensor**
Mechanism principle	non-dispersive infrared (NDIR)	fluorescence quenching
Accuracy/resolution	±0.005% (= 50 ppm +/- 3%)	0.1%
Operating temperature	0°C – 50°C	-30°C – 60°C
Relative humidity	0 to 95%	0 to 99%
Measurement range	0 – 10.000ppm	0 – 25%
Sensor output	CO_2 (ppm) temperature (°C) relative humidity (%)	ppO_2 O_2 (%) barometric pressure (mbar) temperature (°C)
Manuals	*http://www.*CO_2*meters.com/Documentation/Manuals/Manual-GSS-Sensors.pdf*	*https://www.sstsensing.com/wp-content/uploads/2017/07/DS0030rev13_LuminOx.pdf*

The SHT-85 humidity sensor allows measurements in the range of 0–100% RH with an accuracy of ±1.5% RH (Sensirion Datasheet, Digital Humidity Sensor SHT-85 (RH/T)).

Chamber design and measurement principle

We designed a modular measurement system (Fig. 1; see S3 available as Supplementary Data at Tree Physiology Online) consisting of 1) the chamber module for creating a gas tight measurement headspace on the stem surface, 2) a waterproof housing for the CO_2 and O_2 sensors mounted on top of the chamber, 3) a separate housing for a pump, and 4) a waterproof transport-case containing the power supply and an Arduino© logging and control unit. Our device operates as a closed-cycle system, alternating between incubation periods for measuring CO_2/-O_2 concentration changes over time, and periods for flushing the chamber headspace with ambient air.

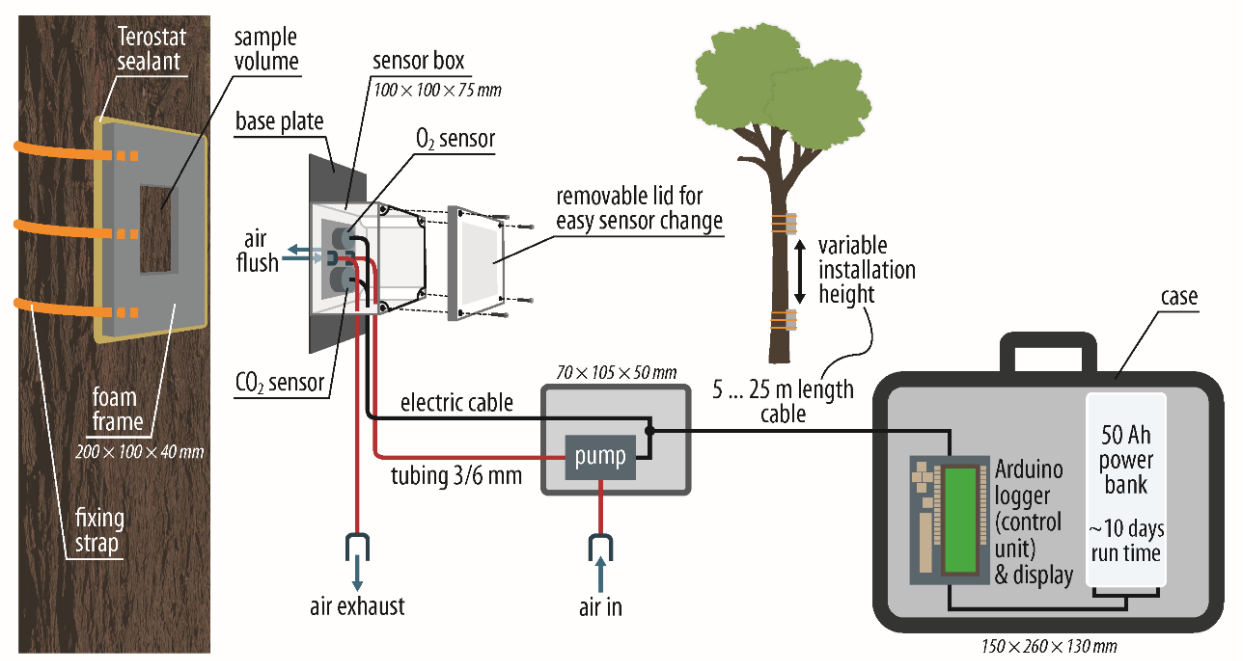

Figure 1 Custom-made modular stem gas exchange system featuring a CO_2 and an O_2 sensor for repeated cyclic measurements of changes in gas concentration over time within a closed dynamic stem chamber installed on the tree stem. A pump automatically flushes the chamber headspace in between measurement cycles. The device is battery powered with up to 10 days operating time. An Arduino® controls switching between measurement and flushing mode and logs the data on a SD card.

The chamber module is made of a 5 mm thick polyethylene high-density sheeting, and is 10 cm wide and 20 cm long, mounted on a 4 cm thick closed-porous cell foam (EPDM, ethylene propylene diene monomer rubber). The foam is placed between the plate and the tree stem prior to fixing the chamber module with three ratchet straps. If required for an air-tight fit, the bark underneath the foam can be smoothed with sandpaper or an angle grinder, but this requires extreme caution to avoid any damage to the underlying cambium and phloem. Putty butyl sealant (Teroson RB IX, Henkel, Düsseldorf, DE) is then applied around the edges of the foam to cover potential small leaks associated with remaining bark irregularities. Installed chambers are tested for leaks by blowing high CO_2 air around the edges while monitoring the headspace CO_2 concentration. Leaks are closed with putty and by refastening the straps until repeated tests show no further leaks. Because chamber headspace volume varies with stem geometry and ratchet strap tension from ca. 75 to 112 cm^3, it is measured for each installation by filling the headspace (*in situ*) with water from a calibrated syringe. To do so we use two syringe needles (inserted from the top of the chamber, between bark and foam, to reach the headspace volume), one for injecting the water, the other to vent air from the chamber until water droplets appear. Sensors should be removed during headspace measurement.

The CO_2, O_2 and H_2O sensors are placed inside a waterproof (IP66 standard) housing (acrylonitrile-butadiene-styrene copolymers; dimensions: 10 cm L x 10 cm W x 7.5 cm H) with a removable lid. For easier handling, the sensor box is permanently welded to the base plate (polyethylene high-density) of the chamber module. The sensors are placed over drill holes on 1 cm thick EPDM rubber rings, allowing gas diffusion from the chamber headspace into the sensors. The O_2 sensor has a sealed sensor base (LOX-02-S) to guarantee that gas from the chamber headspace cannot leak through the sensor into the ambient air. For the CO_2 sensor such a design is currently not available, so we seal the sensor base by applying hot glue around the electronic pins. The polyethylene plate and the sensor box are fully covered with adhesive aluminium foil to prevent heating from sun exposure. We further reduce potential temperature variations by installing the chambers on the side of the tree receiving the least direct sunlight during the day (i.e. north in the northern hemisphere). The air inlet and outlet of the chamber are connected to the pump via metric tubing (PVC tubing, RS Components GmbH, DE) with a diameter of 6 mm (outer) x 3 mm (inner). The sensors (CO_2, O_2 and H_2O) are connected to a 5V power bank (52,800 mAh, Li-ion type, MP-50000, XTPower, Seattle, Washington, USA) in a separate waterproof transport-case (72601 Outdoor Dry Box, Dyntronic GmbH, DE), allowing the system to remain operational unattended for up to 10 consecutive days. The chamber operation and data logging are controlled by a custom-made Arduino® (Arduino Mega 2560 Rev3, Arduino S.r.L.) device (see S4 available as Supplementary Data at Tree Physiology Online). The Arduino processor-based device enables us to program the measurement time interval, incubation time, duration of chamber headspace flushing, and to define a CO_2 concentration threshold in which chamber flushing is desired. Our measurement approach relies on the ability to accurately measure concentration change rather than absolute concentrations, hence we focus here on the rates of change of both gases over time. For a component list of the stem chamber (main parts) see S5 available as Supplementary Data at Tree Physiology Online.

Multiple sensor calibration and testing unit

We built a multiple sensor calibration and testing unit, consisting of a gas-tight chamber with a volume of 1945 ml featuring two valves for flushing and a series of slots for simultaneous operation of up to 10 LuminOx and 10 COZIR sensors (see S3 available as Supplementary Data at Tree Physiology Online). All 20 sensors are connected to a computer via multiple USB HUBs.

For calibration of the COZIR sensors, we used one reference gas of known CO_2 concentration (approx. half of the maximum sensor range, here referred to as “span” gas). First, we flushed the calibration unit for 10 min at 2 l min^{-1} with span gas, then closed it and let the reading stabilize (SD <=30 ppm for CO_2 and <=0.01% for O_2 for at least 10 measurements) before the respective

calibration parameter was adjusted according to the span gas concentration (program: Microsoft Visual Basic). The calibration program allows reading and logging of data, provides access to the filter setting of the COZIRs and for defining stabilization criteria, and (when readings stabilize) sensors can be calibrated to known gas standard. The COZIR sensors allow to automatically store the new calibration parameters internally.

Direct calibration of the LuminOx sensors was not possible since there is no option to adjust their internal calibration parameters. We therefore conducted indirect calibration by comparing the sensors measurement to known O_2 concentrations of gas mixtures being measured. The focus was on accurately measuring changes of the O_2 concentration rather than the absolute concentration since concentration changes over time are the parameter the chamber flux measurements are based upon. We placed the LuminOx sensors in the calibration unit end exposed them to synthetic air with an O_2 concentration of approx. 20.95% O_2. We diluted the headspace concentration by injection of 30 ml pure N_2 into one port of the unit while extracting 30 ml of the unit's air on the opposite side to keep pressure in the chamber constant. We recorded the measurement after equilibration (i.e. SD<=0.01% for at least 10 measurements) and repeated the dilution several times. Since we only have an approximate O_2 concentration of the synthetic air cylinder this does not allow for a typical calibration against known concentrations, but the procedure does allow a relative concentration since the change of concentration between subsequent dilution steps is well defined and reproducible.

Testing of the sensors under laboratory and field conditions

We performed the following tests to validate accuracy and linearity of the COZIR and LuminOX sensors: Measurements of a range of known concentrations (CO_2, O_2) under a) standard laboratory conditions, b) under varying temperatures, c) at increasing time intervals since last calibration (sensor drift), d) measuring the headspace over germinating wheat seeds as a biological model system of carbohydrate catabolism (with an expected ratio of CO_2 production:O_2 consumption of 1), e) direct comparison of the COZIR sensor with another widely used commercially available CO_2 sensor (GMP252, Vaisala GmbH, Helsinki, Finland) under field conditions, and finally f) a field application test of the complete chamber setup.

Measurements of known gas concentrations under standard laboratory conditions

As a reference point, sensor readings were tested against a range of known concentrations. Sensors were mounted in the calibration and testing unit which was subsequently flushed with known gas concentrations. For the COZIR sensor, we used calibrated reference gas bottles (Westfalen AG, Münster, DE) with CO_2 concentrations of 420, 2944, or 6000 ppm. For O_2, we followed the same

procedure as described in '*Multiple sensor calibration and testing unit'*. We performed three dilution steps (20.95%, 20.68%, 20.41%, 20.16%).

Measurements of known gas concentrations: Effect of temperature changes and sensor drift over time

For extended field application it is important to test whether temperature changes or sensor drift over time affect the gas measurements. All tests were performed using 10 CO_2 and/or 10 O_2 sensors. For the temperature test, the equipment (including the reference gas bottles) was set up in a phytochamber where we could control ambient temperature. Tests for the COZIR and LuminOx sensors were done separately. Tests started by adjusting the phytochamber temperature to either 5, 10, 20, or 25°C (for COZIR sensors) or 5, 15, or 25°C (for LuminOx sensors), followed by a period for equilibration of all materials and gas cylinders. We then followed the same procedure as explained in '*Measurements of known gas concentrations under standard laboratory conditions'* (repeated for the different temperature levels).

Sensor drift was determined by repeatedly testing field installed sensors over a period of three weeks without re-calibration, each time measuring known gas concentrations (CO_2: 420 ppm, 1430 ppm, 2944 ppm and 6020 ppm; O_2: 20.95%, 20.68%, 20.41%). The sensors used in this drift test were installed and recorded data in the field between successive tests. They were tested in the lab 14, 18 and 22 days after initial installation and then re-installed in the field without re-calibration.

Incubation of germinating wheat seeds

We tested sensor performance by measuring the CO_2 emission and O_2 uptake of germinating wheat seeds. While absolute fluxes in this setup are unknown, the ratio of CO_2 production to O_2 consumption (respiratory quotient, RQ) is expected to be 1 since wheat seed exclusively use carbohydrates as respiratory substrates (Stiles & Leach, 1933; Lambers *et al.*, 2008). Wheat seeds were soaked in water overnight and placed in the calibration and testing unit (laboratory conditions, 25°C). Headspace concentrations were measured for 80 min (n = 10 for COZIR and LuminOx sensors respectively). Corrections for the dilution effect on O_2 (by CO_2 and H_2O) were implemented.

Sensor comparison under field conditions: COZIR vs. Vaisala GMP252

COZIR measurements were compared to a non-dispersive infrared (NDIR) CO_2-sensor (GMP252, Vaisala GmbH, Helsinki, Finland), frequently used for xylem CO_2 measurements inside the stem (Saveyn *et al.*, 2008b; Cerasoli *et al.*, 2009; Bloemen *et al.*, 2014; Salomón *et al.*, 2016; Fan *et al.*,

2017). Vaisala GMP252 has a measurement range of 0–10.000 ppm CO_2 with accurate ppm-level CO_2 measurements (device specifications are provided in the datasheet of the supplier: Vaisala GMP252 Carbon Dioxide Probe). We designed a special version of our chamber system for simultaneous measurements of both the COZIR and the Vaisala GMP252 sensor in the same chamber under field conditions. Three such chambers were installed at three positions on the same tree (*Prunus avium* L., mean stem circumference: 105 cm) and measured CO_2 efflux for one week in September 2019 (14^{th}–20^{th}) in Jena, Thuringia, Germany.

Field application test

Parallel to our sensor test in the laboratory we tested several chambers under field conditions. These field tests (see '*CO_2 and O_2 flux measurements in the field'*) were conducted in the Thuringian Forest; Germany (Oberschönau, 50°71'N, 10°6'E) at three mature poplar trees at 1.3 m stem height during July 2019 (stem circumference: 95.5 cm to 131.5 cm; ~70 yr old). During this stage, relative humidity was still measured with the integrated COZIR RH sensor that later was replaced by the more accurate SHT-85. Corrections for the dilution effect on O_2 (by CO_2 and H_2O) were implemented.

Correction of measurement data (O_2) for the dilution effect of changing H_2O and CO_2 concentrations

Oxygen as a non-trace gas, is sensitive to concentration changes of any other gas (Keeling *et al.*, 1998). Measured apparent O_2 concentrations thus have to be corrected for changes in CO_2, H_2O, and even for changes in O_2 itself (self-dilution) (Keeling *et al.*, 1998; Bugbee & Blonquist, 2006). We would like to clarify that these corrections have nothing to do with a cross-interference of other gases on the sensor signal, and we are not aware of any cross-interference issues in the sensors we used.

Previous publications usually linked the correction with simultaneously expressing the O_2 concentration changes relative to an arbitrarily defined reference concentration in per meg (= per million), thus following the original method as described by Keeling *et al.* (1998). This conversion undeniably has clear advantages when aiming at reporting and comparing measurements of absolute atmospheric O_2 concentrations and their changes over time. However, considering the focus and target group of our new application, we decided to go for a more intuitive approach that does not require the reader to get acquainted with the per meg scale. Since we are interested in simultaneous concentration changes of CO_2, O_2 and H_2O during separate incubation cycles we refrained from expressing all concentrations relative to a fixed standard, and rather decided to express all

concentrations as relative to the starting concentration ($[CO_2]_{t=0}$, $[O_2]_{t=0}$, $[H_2O]_{t=0}$) during a measurement cycle. The measured apparent change in the O_2 concentration (δO_2, $_{app}$) at any given time during a measurement cycle is correcting for the effect of any observed changes in the concentration of CO_2 and H_2O relative to the starting concentration (δCO_2 and δH_2O). These corrections are proportional to the mole fraction of O_2 in the gas mixture, i.e. $X_{O2, t=0}$, which equals the apparent O_2 concentration in ppm divided by 10^6.

$$\delta O_{2,corr}[ppm] = \frac{\delta O_{2,app}[ppm] + \delta CO_2[ppm] \times X_{O_2\,t=0} + \delta H_2O[ppm] \times X_{O_2\,t=0}}{1 - X_{O_2\,t=0}} \quad [1]$$

For a description of the original approach described by Keeling *et al.* (1998) (extended by a H_2O correction) see S6 available as Supplementary Data at Tree Physiology Online. Please note that the sensors we used do not directly measure the concentration of water in ppm, they rather measure the relative humidity. To convert relative humidity into an absolute H_2O concentration we first calculated the saturation water vapor pressure (es, hPa) as a function of the chamber temperature T (°C) with the Clausius-Clapeyron relation (Bugbee & Blonquist, 2006):

$$\text{es (hPa)} = 6.11 \text{ x } \exp\frac{(17.502 \text{ x T})}{(\text{T} + 240.97)} \quad [2]$$

Since relative humidity is 100% at saturation vapor pressure, the ambient partial pressure of H_2O (ea, in hPa) can be calculated as a function of the current relative humidity:

$$\text{ea} = \text{es x RH} \quad [3]$$

The current concentration of H_2O thus equals the ratio of ea to the total atmospheric pressure of all air inside the chamber (P), which we report in ppm here:

$$H_2O \text{ (ppm)} = \frac{\text{ea}}{\text{P x } 10^6} \quad [4]$$

Flux calculation and Apparent Respiratory Quotient

The CO_2 and O_2 fluxes (F, μmol m^{-2} s^{-1}) were calculated according to the following equation:

$$F = \frac{\Delta C}{\Delta t} \text{ x } \frac{V}{A} \text{ x} \frac{P}{R \text{ x } T} \quad [5]$$

where $\Delta C/\Delta t$ (hereafter referred to as slope) is the change in concentration of gas C (in ppm) over time t (s^{-1}) for CO_2 and O_2 respectively. V is the volume of the chamber (m^3), P the barometric pressure (kPa), R the molar gas constant (0.008314 m^3 kPa K^{-1} mol^{-1}), T the temperature (K) and A the stem surface area (0.0028 m^2). P and T are recorded from the sensors. We assumed linearity in the first 20 min of measurement (time is required to measure changes in the O_2 and CO_2 concentration of at least 1000 ppm, 0.1%) and therefore used the slope of the linear regression to calculate CO_2 (increasing concentration) and O_2 (decreasing concentration) change over time. The negative slope of O_2 is always given as absolute value. Only measurements with correlation coefficient (R^2) > 0.96 for both O_2 and CO_2 were used. Lower correlation coefficients were discarded. For field data the first 5 min of each measurement cycle (user-defined) were discarded after we noticed this data is noisy, probably due to pressure fluctuations after the pumping period. The sensors' readings were extracted every 10 s.

The ratio of CO_2 efflux and O_2 influx results in the Apparent Respiratory Quotient (Angert & Scherer, 2011; ARQ; equation 6) as we don't measure the actual RQ of respiring cells, but the stem equivalent of RQ.

$$ARQ = \frac{CO_2 \text{ production}}{O_2 \text{ consumption}} \quad [6]$$

Statistical analysis

Data from temperature and drift tests were analyzed by regression analysis. As shown in equation 5, flux rates for the chambers were calculated from concentration changes over time. Thus, sensors have to reliably measure concentration changes. We estimated how much the slope of a linear regression of measured concentration vs. known concentration was affected by temperature, or time (drift). We examined the slope of the regression, where slope of 1 represents perfect agreement, slope <1 means the sensors underestimating the true concentration change and vice versa. Slopes measured by individual sensors (n = 10) were tested for temperature and time effects. For the wheat

seed respiration test, linear regressions and comparisons among slopes of CO_2 increase and O_2 decrease over time was performed, too. For normally distributed data, one-way ANOVA was used for comparison among slopes. Correlation between COZIR and Vaisala GMP252 was evaluated by Pearson's correlation coefficient. Data from CO_2 and O_2 flux measurements in the field were combined to 4h mean for further analysis. All statistical analyses were conducted in R (R Development Core Team, 2019).

Results

Measurements of known gas concentrations

Measurements of known CO_2 concentrations by the COZIR sensors showed good accuracy and precision (Fig. 2A). Using 10 sensors, the linear regression for measured vs. known concentration had a slope of almost unity (0.99) and variability between the individual sensors was very small as reflected in the R^2 of 1.0.

For the LuminOx sensors (Fig. 2B), measurements of known O_2 concentrations also resulted in a slope for the linear regression close to 1 (0.98), indicating that the sensors can reliably detect relative concentration changes over the tested range. However, the variability between individual sensors in terms of absolute concentration measurements was far greater than for the COZIR sensors, with individual sensors being off by almost ±0.5%. This results in a low R^2 of the regression of only 0.68.

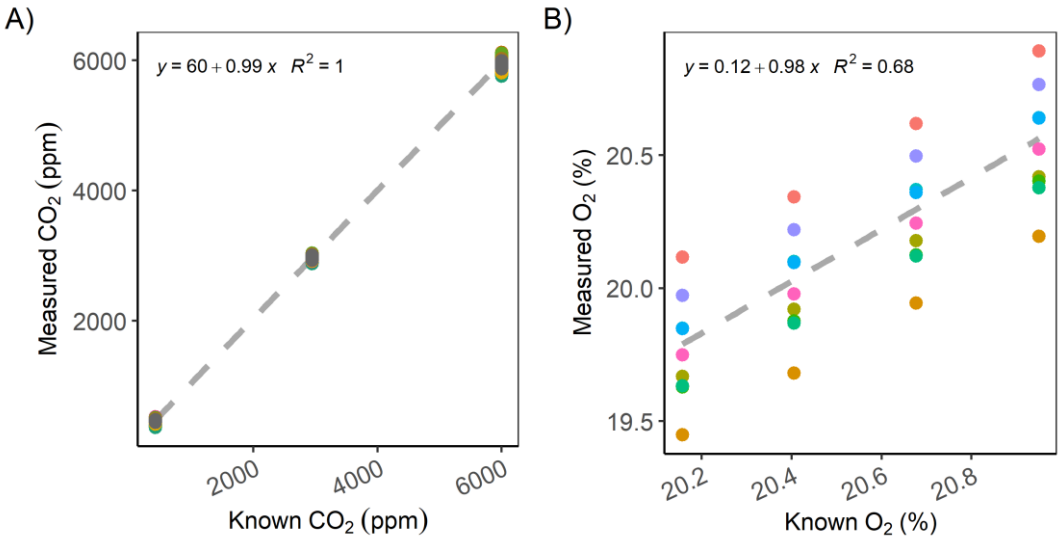

Figure 2 Measurements of known gas concentrations in the calibration and testing unit (25°C) for (A) CO_2 (CO_2 concentrations of 420, 2944 or 6020 ppm) by COZIR sensors (n = 10) and (B) O_2 (in %, dilution

from 20.95 to 20.16%) by LuminOx sensors (n = 10). Colors depict different sensor ID. The dashed line represents the linear regression.

Measurements of known gas concentrations as affected by temperature changes, and sensor drift over time

Changes in temperature did affect O_2 but not CO_2 measurements. For CO_2 measurements, linear regression parameters of measured vs. known concentrations show no statistically significant effect of temperature with mean slopes (±SD) of 0.96±0.05, 0.97±0.03, 0.99±0.01 and 0.97±0.02 at 5, 10, 20 and 25°C, respectively (Table 2). For O_2, differences in temperature were highly significant with mean slopes (±SD) of 0.81±0.06, 0.86±0.03, and 0.97±0.02 at 5, 15, and 25°C, respectively (Table 2). The sensors themselves do not differ significantly (ANOVA, COZIR: $F = 0.12$, $p = 0.73$; Luminox: $F = 0.43$, $p = 0.52$). Based on these findings, we formulate the following temperature correction for the O_2 sensors:

$$SC(O_2) = -0.010 \text{ x T (in °C)} + 1.30 \quad [7]$$

where SC is the slope correction factor that should be multiplied with the measured slope in stem chamber incubation in temperature T. As fluxes were estimated based on slope changes over time, only a slope correction was considered.

Time elapsed since last calibration had an effect on CO_2 measurements when exceeding 22 days, i.e. sensor drift affected the CO_2 sensors after ca. 3 weeks (Table 2). Shorter time intervals (14 and 18 days) showed no significant effect on CO_2 measurements. Mean slopes (±SD) from linear regression parameters of measured vs. known CO_2 concentrations were 0.97±0.05, 0.96±0.05, and 0.95±0.04 after 14, 18, and 22 days of field operation, respectively. We found no effects of sensor drift over time for the O_2 sensors, with mean slopes (±SD) of 1.02±0.10, 1.03±0.10, and 1.03±0.08 after 14,18, and 22 days of field operation, respectively. The sensors themselves do not differ significantly (ANOVA, COZIR: $F = 1.06$, $p = 0.44$; Luminox: $F = 1.36$, $p = 0.28$).

Table 1 Rate of change (slope) for different temperature levels and sensor drift over time (Mean±SD). Analysis of variances (ANOVA) for temperature and drift effect on COZIR and LuminOx reading (n = 10) is shown. Significant results are shown in bold.

		COZIR-AH1		**LuminOx**	
Effect (Temperature/duration)		Mean slope ± SD	ANOVA (*F*, *p*)	Mean slope ± SD	ANOVA (*F*, *p*)
Temperature (°C)	5	0.96 ± 0.05		0.81 ± 0.06	
	10	0.97 ± 0.03	F = 0.21,	-	**F = 80.31,**
	15	-	0.65	0.86 ± 0.03	**<0.001**
	20	0.99 ± 0.01		-	
	25	0.97 ± 0.02		0.97 ± 0.02	
Drift (d)	14	0.97 ± 0.05	F = 2.78,	1.02 ± 0.10	F = 0.10,
	18	0.96 ± 0.05	0.055	1.03 ± 0.10	0.96
	21	0.95 ± 0.04		1.03 ± 0.08	

Incubation of germinating wheat seeds

Over the 80 min incubation period of germinating wheat seeds, the 10 CO_2 sensors reported a mean (±SD) increase of the CO_2 concentration of 5625 ppm±302 ppm, while the 10 O_2 sensors reported a mean decrease of the O_2 concentration of 5800 ppm±300 ppm, i.e. concentration changes over time were anti-correlated and not significantly different with regard to absolute changes (CO_2: slope = 1.27±0.02, R^2 = 0.98; O_2: slope = -1.27±0.05, R^2 = 0.85, Fig. 3), resulting in an RQ value (±SD) of 1.00±0.03.

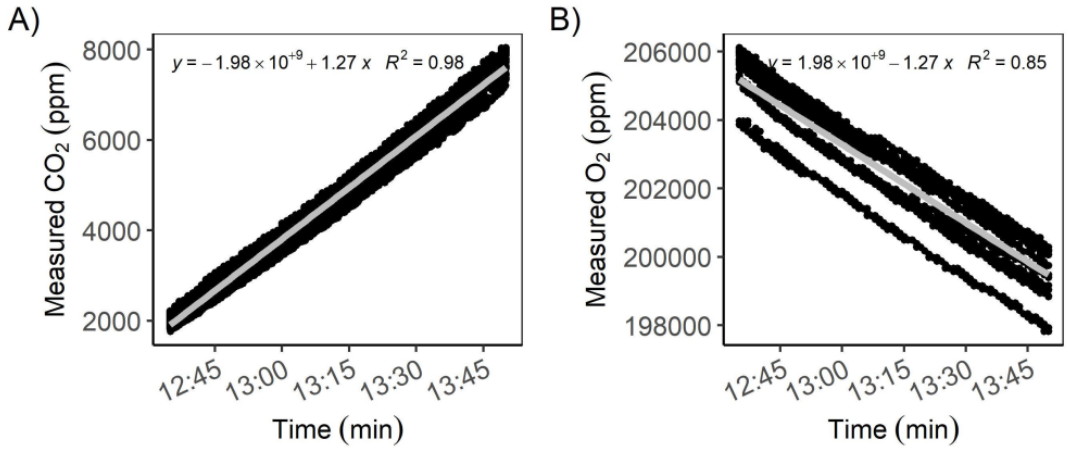

Figure 3 Wheat seed respiration within the calibration and testing unit (25–27°C) over 80 min. (A) Increase of CO_2 (ppm) over time and (B) decrease of O_2 (ppm) is shown (n = 10 for CO_2 and O_2, respectively). Linear regression was used to determine the rate of change.

Comparison of CO_2 measurements between COZIR and Vaisala sensors

We found a significant correlation between simultaneous measurements of COZIR and Vaisala GMP252 (Pearson correlation coefficient, R = 0.95; $p < 0.001$; Fig. 4). However, efflux rates

measured with the COZIR sensor were consistently lower than rates measured with the Vaisala (up to 11%).

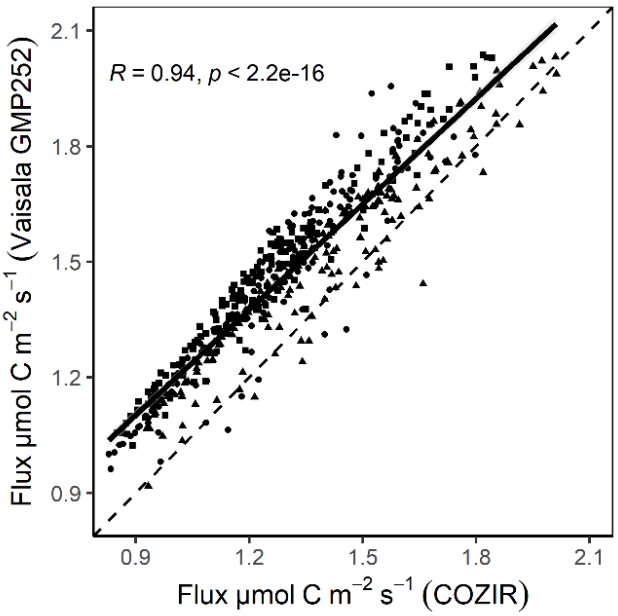

Figure 4 Scatter plot showing the calculated CO_2 fluxes (µmol m^{-2} s^{-1}) measured with Vaisala GMP252 and COZIR at one *P. avium* L. tree in Jena, Germany, in September 2019 (1-week field data pooled; shape depicts data from three chamber devices). Pearson's correlation of the relationship was tested. The black solid line shows the trend line and the dashed line is the 1:1 line.

CO_2 and O_2 flux measurements in the field

During a typical measurement cycle (Fig. 5A, B), CO_2 rapidly increases from atmospheric levels (~400 ppm) to ~6000 ppm (depending on season and time of day) within a 45 min period while the net O_2 decrease is ~0.7%. Following a typical cycle, it takes ~15 min flushing period (starting at 20:40 in Fig. 5) to reach initial concentrations again. For analysis, we focus on the initial 20 min of measurement (beginning 5 min after pumping stopped), for which we assume linearity. In our example, over the 20 min period we observed changes in the O_2 and CO_2 concentration of 4000 ppm and 0.4% respectively (Fig. 5C, D). Relative humidity can vary up to ~8% over the 20 min time interval (change of 1560 ppm at standard condition of 20°C, 945 hPa).

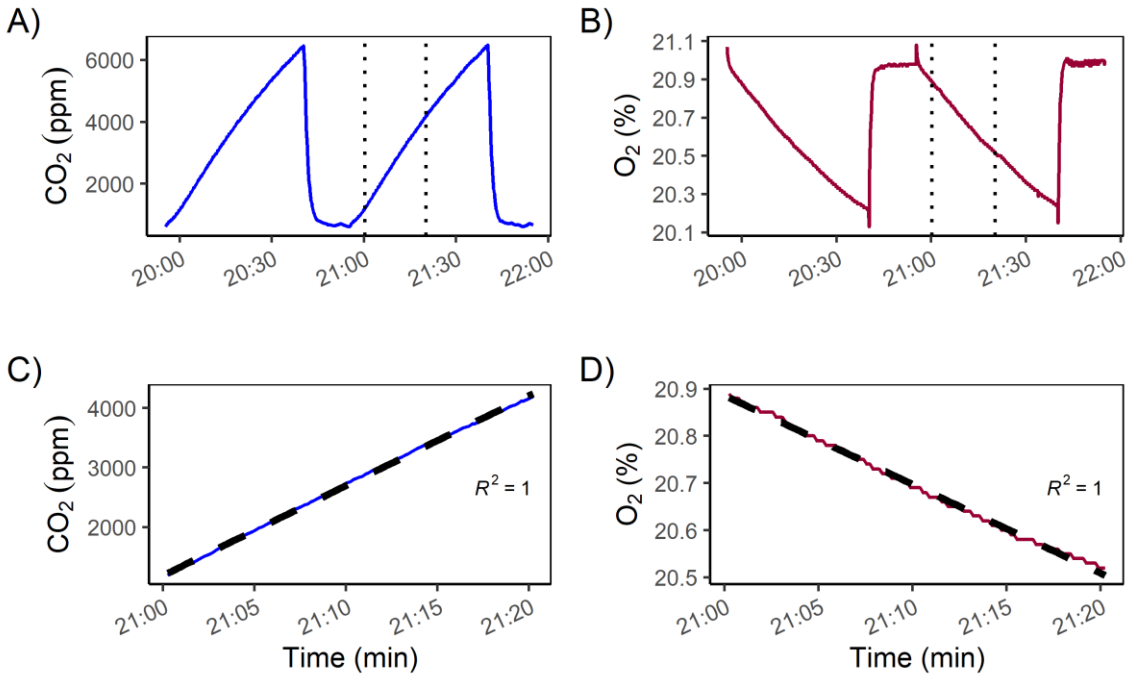

Figure 5 Raw data output of one chamber device installed at one *P. avium* L. tree in Jena, Germany, in September 2019. (A) Increase of CO_2 and (B) decrease of O_2 is shown for two consecutive measurement cycles (each cycle: 45 min). Sharp changes in concentration at the end of each cycle reflect flushing the system with ambient air. Dashed lines show 20-min time interval for flux calculation; (C) The 20-min time interval of CO_2 increases with linear fit (dashed line) and (D) 20-min time interval of O_2 decrease with linear fit (dashed line). The flushing period and the following 5 min were discarded, before the linear fit was applied.

Calculated fluxes (4h mean) from the field application test on three poplar trees are presented in Fig. 6. Two correction steps for O_2 fluxes were implemented: correction 1) dilution effect on O_2 (CO_2 and H_2O) and correction 2) temperature effect on LuminOx readings. Dilution correction (including self-dilution) results in an increase of the mean daily fluxes by 5.6%±2.20% (Fig. 6A), and the subsequent temperature correction from LuminOx readings as determined by our laboratory test results in an increase of the fluxes (daily mean increase of 12.7%±4.5%; Fig. 6A). Over the two weeks measurement period CO_2 efflux is lower than O_2 influx (Fig. 6B), this would result in daily mean ARQ of 0.63±0.06.

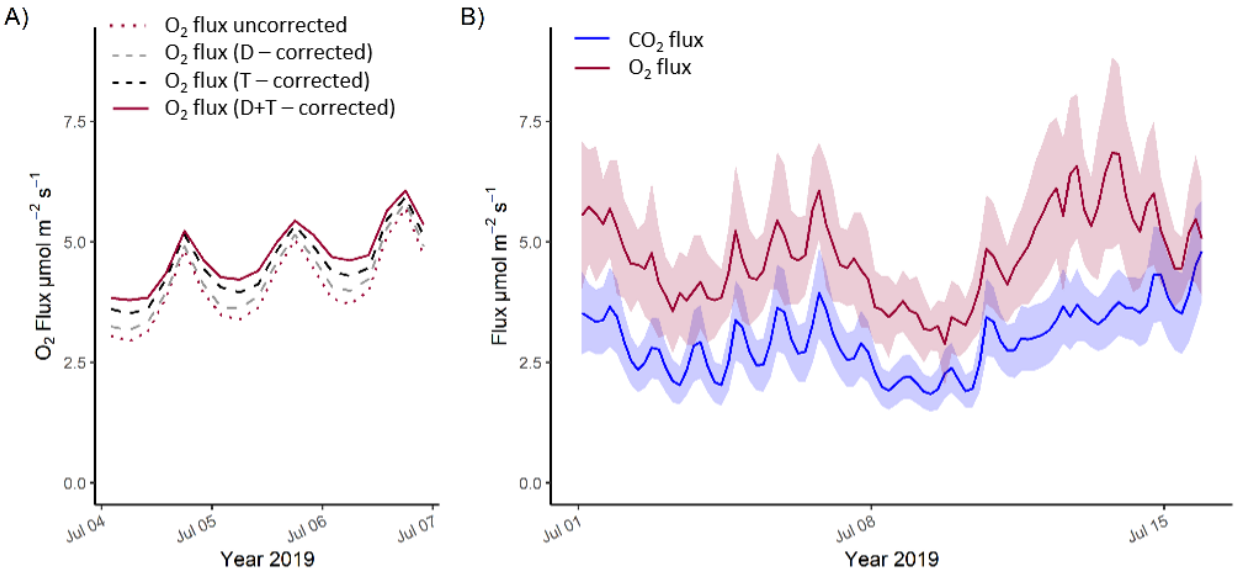

Figure 6 Field data of three mature poplar trees with (A) calculated O_2 fluxes (4-h mean) according to Eq. (5) over 3 days in July 2019 (Thuringia, Germany, n = 3). Uncorrected data and corrected data for O_2 are shown. After the correction for dilution effect (correction 1; see Eq. 1), temperature correction (correction 2; see Eq. 7) was applied. (B) Calculated CO_2 (blue) and corrected O_2 fluxes (red) according to Eq. (5) over 14 days in July 2019 (Thuringia, Germany, n = 3±SD).

Discussion

In our study we were able to show that the combination of three low-cost sensors (CO_2, O_2, H_2O) allows reliable and quasi-continuous measurements of CO_2 and O_2 stem gas exchange under field conditions. Being affordable, highly mobile, and independent of additional infrastructure like local power supply or external logging devices makes our setup highly attractive for application in remote ecosystems or for measuring many individuals and/or widely dispersed trees simultaneously.

Technical aspects and sensor performance

The sensors installed in our chamber design produced robust measurements. Obviously, such low-cost devices have caveats that one has to be aware of. Our chambers followed a non-steady state incubation design, aiming to measure concentration changes of several thousand ppm; therefore we only tested the sensors' performance of measuring relatively big changes of concentration. Especially for the O_2 sensors, measurements of known concentrations revealed high variability between sensors and - for individual sensors - a significant offset between measured and known concentrations, making accurate measurements of absolute concentrations questionable. Accuracy for O_2 measurements in terms of absolute values is 20 times lower than for CO_2 (see sensor specifications in Table 1).

For the COZIR sensors, one important limitation was the effect of sensor drift over time (Table 2). According to our findings, the sensors can be operated without loss of precision for a maximum of 18 days before a new calibration is required. Since calibration has to be done in the laboratory, it is recommended to keep additional calibrated sensors in stock for rapid exchange in the field. Especially when planning to operate a high number of chambers simultaneously, one should consider manufacturing a multi-sensor calibration unit similar to ours for efficient re-calibration.

Direct comparison of the COZIR sensor to the more expensive Vaisala GMP252 showed an offset between the two sensor types, with the COZIR measuring on average 11% smaller fluxes than the Vaisala (Fig. 4). Since this comparison was performed under field conditions with unknown concentrations, it is impossible for us to conclude which of the sensor types has the better accuracy. We did not test or re-calibrate the Vaisala in the lab, instead we relied on the manufacturer calibration. The COZIR sensors, on the other hand, were calibrated and thoroughly tested under various laboratory conditions, but calibration was done in dry air, so it is possible that humidity affected the measurements under field conditions. However, the respiration measurements of germinating wheat seeds matched expectations (see below), which indicates that the COZIR works reliably under a realistic humidity range of typical field measurements (50–85%). Assuming that the differences between the Vaisala and the COZIR sensor were due to measurement errors of the COZIR sensor, we would have to consider correction of the field test by up to 11%, thus reducing the observed imbalance between measured O_2 and CO_2 fluxes. We would like to point out, however, that this offset is smaller than the observed differences in the field application test.

Field tests in a tropical rainforest (Tanguro ranch, Matogroso, Brazil) indicated complete sensor failure at relative humidity levels between 95–100%. One possible solution for tropical applications of stem chambers can be to use humidity traps as shown by Brecheisen *et al.* (2019) for a field-portable soil gas analyzer. Brändle and Kunert (2019) presented a stem chamber design with an implemented low-cost CO_2 sensor type MH-Z14A (Winsen Electronics Technology Co., Ltd, Zhengzhou, China). They found good agreement of their device with a portable infrared gas analyzer (Li-8 100; Li-COR Inc., Lincoln, NE, USA) under tropical rainforest conditions at high temperature and high humidity. However, their chamber design was still limited to CO_2 measurements.

We found two problems that were specific to the LuminOx sensors. First, changes in temperature did affect LuminOx sensor reading. At lower temperatures (5–15°C), O_2 fluxes based on sensor readings significantly underestimated actual O_2 fluxes and required a temperature correction (equation 7). Our data indicated that the effect of temperature on sensor readings can differ between individual sensors. In our approach we used the average correction determined by measuring 10

individual sensors, but correction parameters for individual sensors deviated from the mean by as much as ±8% (see S7 available as Supplementary Data at Tree Physiology Online). In order to avoid this deviation, correction functions for each sensor individually can be applied. We only tested sensor performance between 5–25°C, so it remains uncertain how the sensors behave at temperatures outside of this temperature range. Second, the fact that the sensor does not support adjustment of the manufacturer calibration parameters makes working with this sensor less convenient. However, since we observed no critical sensor drift as with the COZIR sensor this issue was less of a problem, but it should still be kept in mind when considering using this sensor. In addition to the abovementioned temperature correction, the O_2 sensors also require a dilution correction to compensate for apparent changes in O_2 concentration resulting from concentration changes of other gases (mainly CO_2 and H_2O). Please note that this is not a correction resulting from technical issues of the sensors, but is a general requirement when measuring concentrations of non-trace gases like oxygen. In the dilution correction, O_2 self-dilution outweighed the dilution by other gases (CO_2 and H_2O), resulting in an increase of ~6% (two-week average) for calculated O_2 fluxes after correction. In our application, we used the relative humidity sensor SHT-85 successfully as this sensor responded quickly (within seconds) to changes in relative humidity whereas the integrated COZIR RH sensor often underestimate actual humidity levels in the chambers as their response time is very slow to the increasing humidity (see S1 and S2 available as Supplementary Data at Tree Physiology Online).

To evaluate actual sensor performance under realistic conditions we measured respiration of germinating wheat seeds. This test allowed testing the sensors over a wider range of concentration changes and within a realistic humidity range. Wheat seeds are a suitable biological model system for this purpose as their carbohydrate-based respiration during the initial germination implies equal CO_2 and O_2 fluxes. Results from these wheat seed measurements confirmed that the sensors can reproduce expected values and work under field-humidity levels (Fig. 3). The test also underlined the shortcomings of the low-cost sensors with respect to absolute concentration measurements: While the sensors showed identical concentration changes (slopes) during the incubation, absolute concentration measurements at any given time were subject to major offset biases, especially for the O_2 sensors (see also Fig. 2).

To ensure gas tightness, we decided to seal our chambers by means of closed-porous cell foam. The area of the tree stem covered by foam was relatively large compared to the chamber headspace area. Gas exchange for any live tissue underneath the area covered by the foam has to occur via an alternative surface, and some of it will occur via the chamber headspace surface. As a rule of thumb, one may assume that roughly half of the area covered by the foam should be considered as

effectively being part of the chamber area. In any case, assuming that the resulting effect is identical for CO_2 and O_2 we postulate that the area covered by foam has no impact on the gas exchange ratio or the ARQ.

Beyond CO_2: Potential application of simultaneous CO_2 and O_2 flux measurements in ecosystem and ecophysiological research

The combination of simultaneous CO_2 and O_2 measurements in one chamber design allows addressing new additional research questions. It could be used for the detection of respiratory substrate shifts during stress by calculating the ratio of CO_2 efflux to O_2 influx like demonstrated by Fischer *et al.* (2015) in a greenhouse experiment using Raman Spectroscopy. Embedded in the correct experimental design it could also help to quantify actual rates of local *in situ* respiration by disentangling respiratory CO_2 production and O_2 consumption from the effect of other post-respiratory processes (see Hilman *et al.*, 2019 for a detailed discussion). Using simultaneous measurements of CO_2 and O_2 fluxes in multiple tree species, they observed a significant mismatch in the amount of CO_2 emitted vs. the amount of O_2 consumed, which they interpreted as the effect of a variety of whole-tree processes on locally measured CO_2 concentrations, like non-photosynthetic refixation or stem xylem transport of CO_2 away from (e.g., to canopy) and to (e.g., from roots) the site of measurement. Data from our initial field test also indicates mismatches between CO_2 and O_2 fluxes (Fig. 6B), which could be further explored in future experiments. Experimental approaches may include, for example, simultaneous CO_2 and O_2 measurements at different stem heights and in the canopy to quantify the effect of vertical gas transport. Combining flux measurements with ^{13}C isotope labeling of stem tissue in the dark could help to quantify the postulated non-photosynthetic CO_2 uptake in tree stems due to PEPC activity. With slight modifications, our chamber design may also be useful for measuring other ecosystem components like soil, root, branch or leaf fluxes.

Furthermore, data provided by our device can serve as important input and calibration variables for mechanistic models of tree and stem functioning. For instance, Salomón *et al.* (2019a) developed TreSpire, a process-based model which couples carbon and water fluxes at the organ (stem) level. Implementation of combined CO_2 and O_2 data can provide crucial information to constrain the model parameter space. In this way, key parameters used to estimate overall tree respiration at large spatial scales - growth respiration coefficient, respiration sensitivity to temperature (Q10) and basal maintenance respiration (Atkin *et al.*, 2017) - could be accurately estimated. Such insights are much needed to improve model predictions and advance our understanding of stem respiration, for which currently measurements of CO_2 efflux at breast height are commonly used as estimates for whole-

tree respiration, even though stem CO_2 efflux does not reflect respiration rates of underlying tissues (Darenova *et al.*, 2018; Salomón *et al.*, 2019a).

Conclusion

We present a versatile low-cost chamber setup for measuring CO_2 and O_2 fluxes between tree stems and the atmosphere. Adaptation of the general setup to other applications (e.g. soil or branch measurements) should technically be relatively easy. We showed that low-cost sensors are prone to drift over time and/or require temperature correction. Our data also show that O_2 sensors require dilution correction to get accurate O_2 data that are not biased from concentration changes of other gases (CO_2 and H_2O). Using both CO_2 and O_2 measurements in the correct experimental design provides additional information on tree physical and physiological processes like xylem CO_2 transport, post respiratory enzymatic fixation of CO_2 and subcortical photosynthetic uptake of respired CO_2.

Conflict of interest

None declared.

Acknowledgements

Funding was provided by German-Israeli-Foundation for Scientific Research and Development for support under grant no.1334 and Max Planck Society. JH acknowledges the continuous support of the International Max Planck Research School for Global Biogeochemical Cycles. JM received funding from the European Research Council under the European Union's Horizon 2020 research and innovation programme (grant agreement no. 682512 - OXYFLUX). Explicit thanks go to Prof. Schulze for the accessibility of the field site for various tests and Annett Börner for graphical support (Fig. 1). We also thank anonymous reviewers for their constructive comments and suggestions. The authors thanked Olaf Kolle, Frank Voigt and Bernd Schlöffel for technical support and Savoyane Lambert, Nadine Hempel and Agnes Fastnacht for field assistance.

CHAPTER 3

Differences between tree stem CO_2 efflux and O_2 influx rates cannot be explained by internal CO_2 transport or storage in large beech trees

Juliane Helm[1,2], Roberto L. Salomón[3], Boaz Hilman[1], Jan Muhr[1,4], Alexander Knohl[5], Kathy Steppe[6], Yves Gibon[7], Cédric Cassan[7], Henrik Hartmann[1,8]

[1]Department of Biogeochemical Processes, Max Planck Institute for Biogeochemistry, Jena, Germany

[2]Department of Environmental Sciences–Botany, Basel University, Basel, Switzerland

[3]Department of Natural Systems and Resources, Technical University of Madrid (UPM), Madrid, Spain

[4]Laboratory for Radioisotopes, Georg-August University Göttingen, Göttingen, Germany

[5]Department of Bioclimatology, Faculty of Forest Sciences and Forest Ecology, Georg-August University Göttingen, Göttingen, Germany

[6]Department of Plants and Crops, Laboratory of Plant Ecology, Faculty of Bioscience Engineering, Gent University, Gent, Belgium

[7]UMR 1332 Biologie du Fruit et Pathologie, INRAE, University of Bordeaux, Villenave d'Ornon, France

[8]Institute for Forest Protection, Federal Research Centre for Cultivated Plants, Quedlinburg, Germany

Published in Plant, Cell and Environment (2023). Volume 46, Issue 9, September 2023, Pages 2680-2693, https://doi.org/10.1111/pce.14614.

Abstract

Tree stem respiration (R_s) is a substantial component of the forest carbon balance. The mass balance uses stem CO_2 efflux and internal xylem fluxes to sum up R_S, while the oxygen-based method assumes O_2 influx as a proxy of R_S. So far, both approaches have yielded inconsistent results regarding the fate of respired CO_2 in tree stems, a major challenge for quantifying forest carbon dynamics. We collected a data set of CO_2 efflux, O_2 influx, xylem CO_2 concentration, sap flow, sap pH, stem temperature, nonstructural carbohydrates concentration, and potential phosphoenolpyruvate carboxylase (PEPC) capacity on mature beech trees to identify the sources of differences between both approaches. The ratio of CO_2 efflux to O_2 influx was consistently below unity (0.7) along a 3-m vertical gradient, but internal fluxes did not bridge the gap between influx and efflux, nor did we find evidence for changes in respiratory substrate use. PEPC capacity was comparable with that previously reported in green current-year twigs. Although we could not reconcile differences between approaches, results shed light on the uncertain fate of CO_2 respired by parenchyma cells across the sapwood. Unexpected high values of PEPC capacity highlight its potential relevance as a mechanism of local CO_2 removal which merits further research.

Keywords

carbon dioxide transport, CO_2/O_2 ratio, mature trees, oxygen consumption, temperate forest, vertical stem gradient

Introduction

Tree stem respiration (R_S) is an important component of the forest carbon (C) budget and is estimated to account for 5–42% of total ecosystem respiration (Campioli *et al.*, 2016; Salomón *et al.*, 2017; Yang *et al.,* 2016). Respiration rate is usually extrapolated to the whole stem from CO_2 efflux measurement at breast height. Even though direct measurements of CO_2 efflux are easy to conduct, various processes can decouple CO_2 efflux from R_S, resulting in mismatches of up to 45% (Hilman *et al.,* 2019; Teskey & McGuire, 2007): (1) Dissolution of CO_2 in xylem water (Teskey & McGuire, 2007; Aubrey & Teskey, 2009; Bloemen *et al.*, 2013), (2) axial CO_2 diffusivity (De Roo *et al.*, 2019), (3) non-phototrophic CO_2 refixation via the enzymes carbonic anhydrase and phosphoenolpyruvate carboxylase (PEPC) (Berveiller & Damesin, 2008), or (4) photosynthetic CO_2 refixation via woody tissue photosynthesis (e.g., Ávila *et al.*, 2014; De Roo *et al.*, 2020c, Pfanz *et al.*, 2002; Steppe *et al.*, 2015a). Even if we could accurately estimate R_S at a given stem point, upscaling R_S to the whole tree level in mature stands is questionable as the relative contribution of abovementioned processes might vary with stem height (Ceschia *et al.*, 2002).

Two main measurement approaches have been applied to estimate R_S. The carbon-based mass balance approach (McGuire & Teskey, 2004) not only considers CO_2 efflux (E_{CO2}), but also takes into account the dissolution of CO_2 in the xylem (accounting for its equilibrium species H_2CO_3, HCO_3^- and CO_3^{2-}; hereafter CO_2^*), its vertical transport through the xylem sap (F_T) and the CO_2 storage flux (ΔS), as the accumulation or depletion of CO_2 in the xylem sap over time, to achieve a more precise estimation of R_S on a volume basis (μmol m^{-3} s^{-1}):

$$R_S = E_{CO2} + F_T + \Delta S \qquad [1]$$

Most studies applying the mass balance approach examined the contribution of CO_2 efflux, CO_2 transport and CO_2 storage to R_s in small trees or saplings (e.g., McGuire & Teskey, 2004; Salomón *et al.*, 2018; Saveyn *et al.*, 2008c) due to the easiness of constructing custom-made stem cuvettes surrounding the whole stem. However, applying findings from small trees to interpret CO_2 efflux in mature trees could be hampered by the long radial diffusive pathway in thick stems, which could result in significantly limited CO_2 diffusion rates (Steppe *et al.*, 2007). This assumption is supported by findings in yellow poplar, where the relative contribution of CO_2 efflux to R_S decreased with stem diameter (up to 60 cm), while CO_2 transport increased with stem size, as could be expected by larger sapwood conductive area, transpiration rates, and potential for CO_2 removal from the point of production (Fan *et al.*, 2017).

Many studies have relied primarily on CO_2 efflux (and CO_2 transport) to estimate R_S; nevertheless, aerobic respiration involves oxygen (O_2) consumption, and the influx of O_2 from the atmosphere into the stem (I_{O2}) can also serve as a proxy for R_S. The second measurement approach to estimate Rs is based on simultaneous measurements of O_2 influx and CO_2 efflux. Given the much lower water solubility of O_2 compared to CO_2 (Dejours, 1981), dissolution effects and vertical transport should play a potentially negligible role for O_2. Boosted by technological improvements to register small O_2 fluctuations in an atmosphere with a large O_2 background, emerging interest arises in the coupled measurement of CO_2 efflux and O_2 influx at the stem surface (Angert & Sherer, 2011; Hilman & Angert, 2016). The ratio of CO_2 efflux to O_2 influx is called the respiratory quotient (RQ) at the cell level. The cell-level RQ allows exploring the substrate of respiratory metabolism. In trees, non-structural carbohydrates (NSC) are assumed to be the primary respiratory substrate, theoretically resulting in a RQ of ~ 1. More O_2 is needed for the breakdown of lipids compared to carbohydrates, resulting in RQ ~ 0.7 (Masiello *et al.*, 2008). Organic acids catabolism would yield RQ above one because of the greater O_2 content of those molecules being oxidized (Masiello *et al.*, 2008). At the organ level, as the stem in this case, the ratio of CO_2 efflux to O_2 influx at the surface is named the apparent respiratory quotient (ARQ) (Angert & Sherer, 2011):

$$ARQ = \frac{E_{CO2}}{I_{O2}} \quad [2]$$

Therefore, simultaneous measurements of both gases allow for the assessment of potential shifts in respiratory substrate over time and under environmental stresses (Fischer *et al.*, 2015). Furthermore, the ARQ ratio can be affected by postrespiratory processes (Trumbore *et al.*, 2013), providing information about the role of CO_2 dissolution and transport on R_S estimates, as CO_2 is highly soluble in xylem sap, while O_2 is less soluble. Hereby, assuming NSC as respiratory substrate, RQ would be ~1, and so would ARQ as long as CO_2 transport and storage were negligible, as CO_2 efflux versus O_2 influx equalize. However, Hilman *et al.* (2019) showed the inability of sap flow (and hence CO_2 transport) to account for the variability in the ARQ of *Q. ilex* trees. Authors suggested CO_2 refixation via the enzyme PEPC as the primary cause of ARQs below the unit, a mechanism of local CO_2 removal commonly overlooked in R_S research. However, the role of PEPC capacity in mature stems is still speculative as it has mainly been investigated in C4 plants and only in leaves and young green twigs of C3 plants (Berveiller & Damesin, 2008).

It is essential to reconcile insights gained through the mass balance approach and oxygen-based measurement methods, which disagree on the primary factor causing the mismatch between R_S and CO_2 efflux, either CO_2 transport through the xylem and storage or PEPC-mediated CO_2 fixation, respectively. Note that both approaches commonly use opaque stem cuvettes or chambers, precluding photosynthetic reassimilation of locally respired CO_2 (see De Roo *et al.*, 2020). Mathematically, as a first approximation assuming R_S and O_2 influx are equivalent, the mass balance approach could be formulated as follows:

$$ARD = I_{O2} - E_{CO2} = R_S - E_{CO2} = F_T + \Delta S \quad [3]$$

Where the apparent respiratory difference (ARD), as an alternative metric to interpret the mismatch of CO_2 and O_2 fluxes in absolute terms, should equal the amount of locally respired CO_2 transported and stored if CO_2 refixation (either photosynthetic or nonphotosynthetic) is neglected. If this assumption is valid, carbon- and oxygen-based methods could be indistinguishably applied to estimate R_S. If not, it would be necessary to revisit underlying assumptions from both approaches to constrain the interpretation of each other and provide a more comprehensive perspective on the fate of respired CO_2 not emitted locally to the atmosphere. This is precisely the main challenge in research on metabolism of woody tissue respiration. A direct comparison of both approaches is lacking so far. By combining both approaches at the same individuals and under the same conditions, it would be possible to assess whether discrepancies observed so far vanish or whether assumptions should be revisited.

To do so, we continuously monitored the vertical and temporal variability in CO_2 efflux, O_2 influx and xylem [CO_2] along a 3-m stem gradient in beech trees (*Fagus sylvatica* L.) during 1.5 summer months. Importantly, the study was performed in large mature trees, in which the contribution of CO_2 transport to R_S is expected to be higher (Fan *et al.*, 2017), thereby enhancing the potential discrepancies between carbon- and oxygen-based approaches. Required additional variables to estimate the abovementioned respiration-related variables, like stem temperature, sap flow rate, and twig sap pH were also measured. Additionally, NSC concentrations and PEPC capacity from stem discs of the outermost tissues were discretely measured to evaluate potential shifts in substrate stoichiometry and the role of PEPC fixation on respiratory fluxes, respectively. We addressed the following hypothesis: When concurrently applying the carbon- and oxygen-based approaches in the same trees, xylem CO_2 transport and storage can close the gap between O_2 influx and CO_2 efflux (i.e., the ARD = 0). Alternatively, the fraction of missing CO_2 not explained by xylem CO_2 transport

and storage could be attributed to CO_2 refixation via PEPC capacity if significant in large mature stems.

Material and Methods

Site description and experimental set-up

The experiment was conducted in a managed pure 130-year-old beech stand at ~100 m distance to the Fluxnet tower site Leinefelde (DE-Lnf, https://doi.org/10.18140/FLX/1440150) in the forest district of Heiligenstadt near the city of Leinefelde (51°20′N, 10°22′E; altitude 450 m a.s.l; Thuringia; central Germany). The mean annual air temperature and precipitation are 8.3±0.7 ºC and 601±154 mm (Tamrakar *et al.*, 2018). We measured four even-sized mature beech trees with a tree height of ca. 38 m and stem diameter at breast height (DBH) of 0.38 and 0.54 m (Table 1) during July and August 2019 (Days of year [DOY] 185-226).

Table 1 Diameter at breast height (DBH) and sapwood depth of the four beech trees.

Tree	Diameter (cm)	Sapwood depth (cm)
1	41	12.5
2	45	13.5
3	54	16.5
4	38	12.0

Stem CO_2 efflux, O_2 influx and xylem [CO_2])

Stem CO_2 efflux and O_2 influx at the stem surface were measured hourly on every tree at three stem heights (1, 2.5, and 4 m) following the approach described in Helm *et al.* (2021). Briefly, we installed a custom-made chamber in each stem location that consisted of (i) a closed-porous cell foam and a base plate of 20 cm length, 10 cm width, and 4 cm height, (ii) a waterproof housing for the CO_2 and O_2 sensors with a removable lid for easy exchange of the sensors, and (iii) a transport-case containing an air pump, an Arduino® unit for data logging and 5 V power bank battery for power supply (800 mAh, Li-ion type, MP-50000, XTPower, Seattle, WA, USA). See Supporting Information: Figures S1 and S2 for a schematic overview and a photograph of the set-up. Chambers were installed on the north side of the trees, and chambers were covered with aluminium foil to avoid direct solar radiation and impede local cortical photosynthesis. Chambers were attached against the tree stem using three ratchet straps. The measurement principle is based on a closed system with measurement cycles of 45 min followed by 15 min to flush the chamber's headspace

with ambient air. To monitor [CO_2] increase and [O_2] decrease within the chamber headspace, a non-dispersive infrared (NDIR) absorption sensor (COZIR; Gas Sensing Solution GSS) and an optical fluorescence quenching sensor (LuminOx sealed, LOX-02-S; SST Sensing Ltd) were used, respectively. The relative humidity sensor integrated within the COZIR device was used to account for the dilution effect of changing H_2O and CO_2 concentrations and correct O_2 measurements (for further details see Helm *et al.,* 2021). Sensors were changed after three weeks to limit reading drift (Helm *et al.*, 2021). E_{CO2} and I_{O2} on a surface basis (μmol m^{-2} s^{-1}) were calculated from the linear CO_2 increase and O_2 decrease of the first 20-min time interval (of the 45 min measurement cycle excluding 3 min after flushing) following Equation 4:

$$E_{CO2} \; or \; I_{O2} = \frac{\Delta C}{\Delta t} \; x \; \frac{V}{A} \; x \; \frac{P}{R \; x \; T} \qquad [4]$$

where $\Delta C/\Delta t$ is the change in gas concentration over time (ppm s^{-1}) for CO_2 or O_2, V is the chamber headspace volume (m^3) determined by water displacement, A is the stem surface (m^2), P is the barometric pressure (kPa), R is the molar gas constant (m^3 kPa K^{-1} mol^{-1}), and T is the temperature (K) obtained from the COZIR sensor. From CO_2 efflux and O_2 influx time series, the ARQ and ARD were calculated following Equations (2) and (3).

The concentration of xylem [CO_2] in the gas phase (%) was measured with NDIR CO_2 sensors (GMP221 and GMP251; Vaisala Inc.) calibrated before installation using reference gases at known [CO_2] of 0, 5, 10 and 15%. For each sensor, we drilled a hole of 40 mm deep and 25 mm wide into the stem and pushed the probe (length: 96 mm) halfway within the hole (~20 mm), leaving a closed headspace in the xylem tissues beyond the cambium layer. Synthetic rubber sealant (Teroson RB IX; Henkel) was used for isolation from the atmospheric gas. Four sensors were installed in each tree along the vertical profile monitored with stem chambers at 1, 2.35, 2.65 and 4 m. We initially envisaged applying the mass balance approach in the 30-cm-length stem segment between 2.35 and 2.65 m probes. Nevertheless, we eventually decided to average the xylem [CO_2] time series from these two probes to survey longer (and more representative) stem segments, from 1 to 2.5 m (lower stem) and from 2.5 to 4 m (upper stem) (Supporting Information: Figure S1). Probes were placed ca. 10 cm from each chamber on the northwest side of the trees. Readings of the 16 sensors were recorded every 5 min with a datalogger (CR1000x; Campbell Scientific) for the whole experiment period.

Xylem CO_2 transport and storage

The amount of CO_2 transported upwards through the xylem and stored within the xylem was estimated in the lower and upper stem segments. The concentration of dissolved CO_2 in xylem sap ($[CO_2^*]$, mol CO_2 l^{-1}) was calculated using temperature-dependent Henry's Law coefficients (Levy *et al.*, 1999; McGuire & Teskey, 2002), assuming equilibrium between CO_2 in the gaseous and liquid phases. For this, xylem $[CO_2]$ in the gas phase, xylem sap pH, and stem temperature must be known. To monitor sap pH, xylem sap was collected from twigs of low branches of monitored trees ($n = 3$, as one tree was inaccessible for sampling) using a Scholander pressure chamber at four sampling dates (DOYs 204, 212, 218 and 226). Sap samples were quickly placed in Eppendorf tubes and a cold box for transportation to the laboratory and then stored in a refrigerator until measurement. Xylem sap pH was measured using a pH meter (Five Easy; Mettler Toledo) with a microelectrode (InLab®, Ultra-Micro-ISM; Mettler Toledo). Preliminary tests confirmed that sap pH did not significantly vary over the sample storage period. Stem temperature (T_{stem}, °C) was continuously measured and recorded with a datalogger (CR1000x; Campbell Scientific) every 5 min using thermocouples inserted at 2 cm depth next to each stem chamber.

Once sap $[CO_2^*]$ was known, CO_2 transport (F_T, µmol CO_2 m^{-3} s^{-1}) for both lower and upper stem segments were estimated according to:

$$F_T = \left(\frac{SF}{v}\right) x\, \Delta[CO_2{}^*] \qquad [5]$$

where SF is the sap flow rate (l s^{-1}), v is the sapwood volume (m^3), and $\Delta[CO_2^*]$ is the difference in sap $[CO_2^*]$ above and below the corresponding stem segment (µmol l^{-1}). The sap flow rate was estimated as the product of sap flux density (l cm^{-2} h^{-1}) and sapwood area (cm^{-2}) using the Sap Flow Tool software (Plant AnalytiX). Sap flux density was monitored using sap flow meters SFM1 (ICT International Pty Ltd.) operated by the heat ratio method (Burgess *et al.*, 2001), assuming a stem water content of 400 l m^{-3} (Gartner *et al.*, 2004). Sap flow probes were installed at breast height on the north side of the trees, and measurements were recorded every 15 min.

A staining method was applied to determine the sapwood area; upon extraction of one wood core per tree at breast height on the northwest side of the tree (until the pith), a blue dye (E131) was injected into the hole, and a second core was extracted one cm above the first one after 1 h. Sapwood depth was determined by the length of the stained region of the core and assuming a cylindrical shape for both heartwood and sapwood (Table 1, Goldstein *et al.*, 1998).

The stem CO_2 storage flux (ΔS) was estimated as a function of the time derivative of $[CO_2^*]$ in the xylem; that is, the rate of accumulation and depletion of dissolved CO_2 for both lower and upper stem segments according to:

$$\Delta S = \frac{\mathrm{d}[CO_2^*]}{\mathrm{dt}} \times WC \quad [6]$$

Soil water content and shoot water potential

Soil water content (%) was continuously measured at the meteorological flux tower with one sensor (ML-2x; DeltaT) inserted at 16 cm depth, 100 m away from our instrumented trees, with a temporal resolution of 10 min. Shoot water potential (MPa) was measured around solar midday (as for sap pH sampling) at four sampling dates (DOYs 204, 212, 218, and 226) using the Scholander pressure chamber.

PEPC capacity and NSC in woody tissues

We took one stem disc (one cm-length, bark to xylem) at three stem heights (1, 2.5, and 4 m) on the south side of each monitored tree on 14 August (DOY 226). Samples were immediately frozen in liquid nitrogen to stop the metabolic activity and transported to the laboratory. Stem discs were stored at -80°C before grinding into a fine powder in liquid nitrogen with a mortar and pestle. 20 mg of woody tissue material was used for the discontinuous assay performed in a 96-well microplate (Bénard & Gibon, 2016). Briefly, aliquots were extracted by shaking with an extraction buffer. After centrifugation (7 min, 3000 g, 4°C), extracts were diluted and incubated for 20 min. The reaction was stopped with HCl. The sealed microplate was then incubated at 95°C for 10 min to destroy NADH. After cooling down, each well was neutralized with NaOH and Tricine-KOH pH 9.0 to adjust the pH to 9.0. The absorbance was read at 570 nm (30°C) until rates were stabilized. Reaction rates ($mOD.min^{-1}$) were used to calculate the amount of NAD^+ formed during the first step of the assay. All pipetting steps were performed using a 96-head robot (Hamilton Star), and absorbances were measured in a filter-based microplate reader (SAFAS MP96). For further details, see Supporting Information: Methods S1 and Bénard and Gibon (2016).

We measured soluble sugars and starch in stem cores from the instrumented trees following the Landhäusser *et al.* (2018) protocol. One stem core per height (1, 2.5, 4 m, south-side) was collected on 4 July (DOY 185) and 14 August (DOY 226) for NSC measurements. Samples were stored in cooling bags for transportation and then oven dried at 60°C for 72 h. Stem cores were cut into two 2-cm long sections starting at the cambium (wood depth: 0–2 cm and 2–4 cm) and ground into a fine powder (ball mill, MM 400, Retsch). We extracted the soluble sugars glucose, fructose,

sucrose, and starch from each sample. Briefly, ~30 mg of dry plant powder was extracted with 80% ethanol. Supernatants were analysed by a High-Performance Liquid Chromatography coupled to a Pulsed Amperometric Detection (HPLC-PAD) for soluble sugar determination. We enzymatically converted the starch from the remaining pellet to glucose, using α-amylase amyloglucosidase. Glucose hydrolysate was measured by the HPLC.

Data analysis

Statistical analyses were performed using R software (R Development Core Team, 2019). CO_2 efflux and O_2 influx data were discarded when the R^2 of the linear fit for CO_2 and O_2 readings were below 0.96 to ensure good data quality. For gap filling, we used the *pad* function in *padr* package. To test whether the average daily values of CO_2 efflux, O_2 influx and xylem [CO_2] varied with stem height, linear mixed models were adjusted using the *lme* function in *nlme* package (Pinheiro *et al.*, 2017), considering height as a fixed factor and tree as a random factor including an autocorrelation structure to account for repeated measurements. To test whether PEPC capacity varied with stem height, and sap pH among sampling dates, linear mixed models were adjusted likewise, considering the tree as a random factor. The normality of residuals was checked visually. When significant, differences among heights were tested post hoc with Tukey contrasts using the *emmeans* function (*emmeans* package). Consistency between carbon- and oxygen-based measurements was tested by evaluating the relationship between R_S ($E_{CO2} + F_T + \Delta S$) and O_2 influx, and between CO_2 internal fluxes ($F_T + \Delta S$) and ARD, with mixed models considering tree a random factor. Potential deviances from the 1:1 relationship would indicate a lack of consistency between methodological approaches, hence the need to revisit the underlying assumptions of Equation (3). The conditional and marginal R^2 (Nakagawa & Schielzeth, 2013) of these models was further estimated (*r2_nakagawa* in the *performance* library) to further evaluate the degree of agreement between approaches. Finally, sap flow, sap [CO_2^*] and the ARD were normalized to their daily maxima, and sub-daily patterns were compared to evaluate the potential of xylem transport to remove locally respired CO_2 on a sub-daily basis.

Results

Stem temperature, soil water content, sap flow rate and shoot water potential

The mean stem temperature during the experiment was 17.7°C, with minimum values of 10°C during early July and peaking at the end of July with values close to 30°C (Fig. 1a). Volumetric soil water content at 16 cm depth was lowest end of July, reaching minimum values of 15.7 vol% and maximum values of 19.0 vol% afterwards following summer rains (Fig. 1b). Sap flow rate showed

a typical sub-daily pattern with maximum rates of 30 l h^{-1} during sunny and warm days (Fig. 1c). Shoot midday Ψ (shoot water potential) was close to -1.4 MPa on most measurement days, except the one following rains when it relaxed up to -0.5 MPa (Fig. 1c).

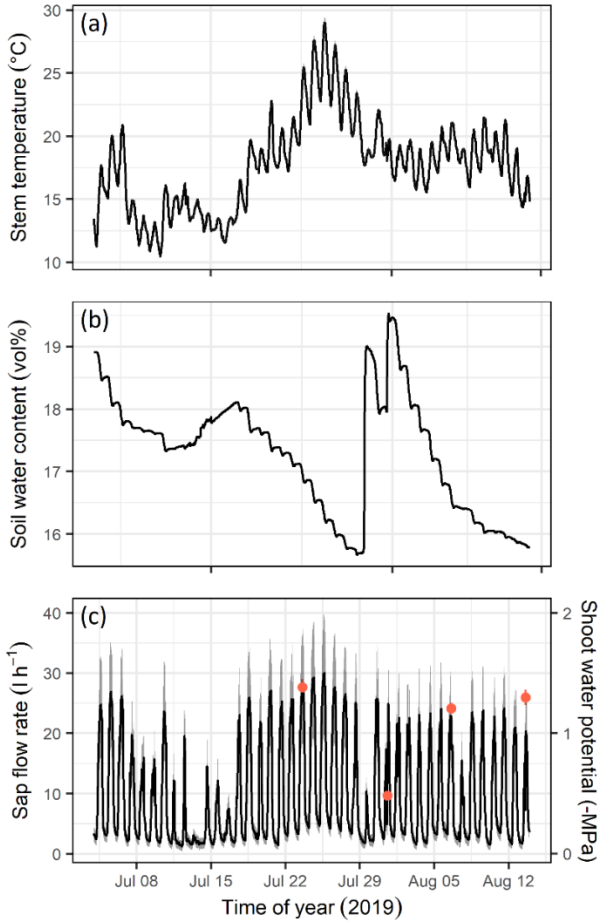

Figure 1 (a) One-hour average of stem temperature, (b) volumetric soil water content, and (c) sap flow rate (lines) with shoot water potential (orange dots) from 4 July to 14 August 2019. Shading in (c) indicates average ±1 SE across the beech trees (n = 4).

Gas exchange and internal [CO_2] at different stem heights

The vertical position did not affect CO_2 efflux and O_2 influx (p = 0.69 and 0.71, respectively). Mean daily CO_2 efflux (±SE) was 2.9±0.6, 2.7±0.4 and 2.3±0.6 µmol m^{-2} s^{-1} at 1, 2.5, and 4 m stem height, respectively (Fig. 2a). Mean daily O_2 influx was 4.1±0.7, 3.9±0.5 and 3.3±0.6 µmol m^{-2} s^{-1}, respectively (Fig. 2b). O_2 influx was consistently higher than CO_2 efflux along the vertical gradient (p < 0.001), resulting in mean daily ARQ of 0.71±0.04, 0.69±0.04 and 0.69±0.06 at 1, 2.5 and 4 m stem height, respectively (Fig. 2c). Xylem [CO_2] ranged from ca. 5.9 to 12.4%, with no significant effect of height over the whole surveyed period (Fig. 2d; p = 0.11). However, when considering the last third of the experiment (1 - 14 August), stem height did affect xylem [CO_2] (p = 0.03), with

values being lower at 1 m compared to 2.5 m height. Sap pH ranged between 6.48 and 7.41 over the measurement period (Fig. 2d), and differences in sap pH among trees ($p = 0.17$) or dates ($p = 0.21$) were not significant. Stem temperature had a strong effect on xylem [CO_2] ($p < 0.001$), CO_2 efflux and O_2 influx ($p < 0.01$). Likewise, respiratory fluxes had maximum values during the afternoon, following sub-daily thermal dynamics.

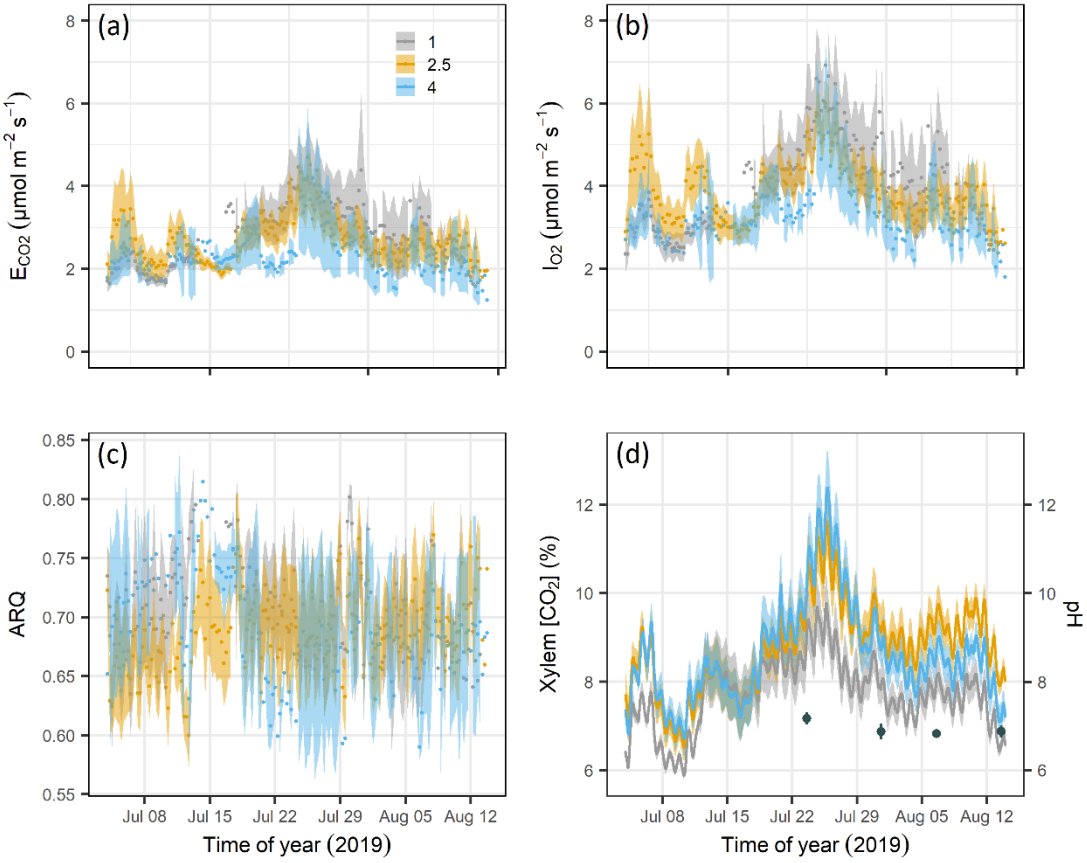

Figure 2 (a) CO_2 efflux (E_{CO2}), (b) O_2 influx (I_{O2}), (c) the apparent respiratory quotient (ARQ; E_{CO2}/I_{O2}) and (d) internal xylem [CO_2] at 1, 2.5 and 4 m height from 4 July to 14 August 2019. Sap pH (d, black dots) was measured from twigs (n = 3).

PEPC capacity and non-structural carbohydrates at different stem heights

Stem height had no significant effect on PEPC capacity in the outermost stem section ($p = 0.23$) and did not differ among trees ($p = 0.93$). Mean PEPC capacity was 760.5±201.6, 661.25±60.2 and 547.25±77.4 nmol min^{-1} gFW^{-1} at 1, 2.5 and 4 m, respectively.

Stem height did not affect soluble sugar and starch concentrations ($p = 0.37$ and 0.40, respectively) (Fig. 3). Sapwood depth did affect NSC; both soluble sugar and starch concentrations were higher near the cambium (0–2 cm) than deeper into the sapwood (2–4 cm) ($p < 0.05$). Soluble sugar and

starch concentrations were higher on the second sampling date in August (DOY 226) for the 0–2 cm depth ($p < 0.001$, $p < 0.01$ for soluble sugar and starch, respectively), while they remained constant deeper into the cambium ($p = 0.1$, $p = 0.6$ for soluble sugar and starch, respectively).

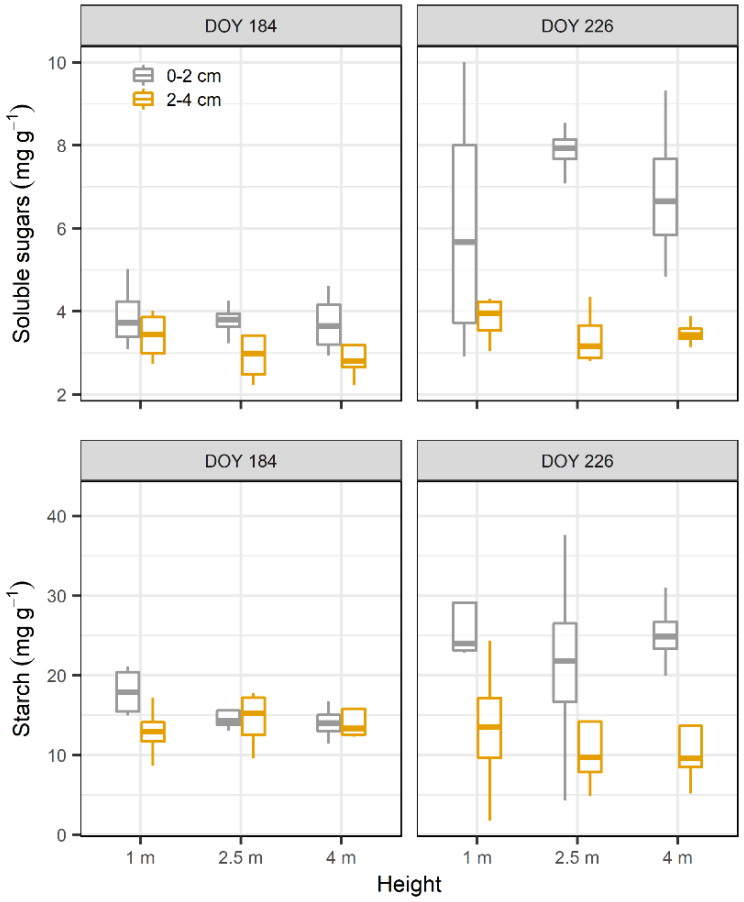

Figure 3 Starch and soluble sugar concentration (mg g DW^{-1}) in stem xylem tissues of beech trees at three stem heights, two wood depths, and two sampling dates ($n = 4$). Box whisker plots present the median, lower (25^{th}), and upper (75^{th}) percentiles, minimum and maximum values. Colors denote different sapwood depths.

Comparison of carbon- and oxygen-based estimates of R_S

We applied the mass balance approach on the lower (1 m–2.5 m) and upper (2.5 m–4 m) stem segments to estimate R_S and its contributors for comparison with the oxygen-based approach (Fig. 4). In the lower stem segment, there was a positive vertical gradient in sap [CO_2^*], and CO_2 transport was, therefore, positive. Averaged across days and trees, the contribution of CO_2 efflux to R_S was 64.6±14.5%, and the remaining fraction was attributed to CO_2 transport (35.8±14.3%), as CO_2 storage was negligible (-0.4±0.2%).

The R_S daily average (as the sum of E_{CO2}, F_T and ΔS) was greater than O_2 influx, but on a sub-daily basis, R_S exceeded O_2 influx only during daytime. During night-time, R_S equaled CO_2 efflux, and both were lower than O_2 influx.

The upper stem showed a different pattern where the vertical gradient in sap [CO_2^*] approached zero and even became negative for the last two weeks of our study. As a consequence, the relative contributions of CO_2 transport (-1.2±2.2%) and CO_2 storage (0.0±2.2%) to R_S were negligible, and apparently all the respired CO_2 diffused to the atmosphere (E_{CO2} = 101.1±22.9%). In this stem section both CO_2 efflux and R_S were on average lower than O_2 influx. Notably, the shift from positive towards negative CO_2 transport flux followed the peak in temperature and transpiration at the end of July.

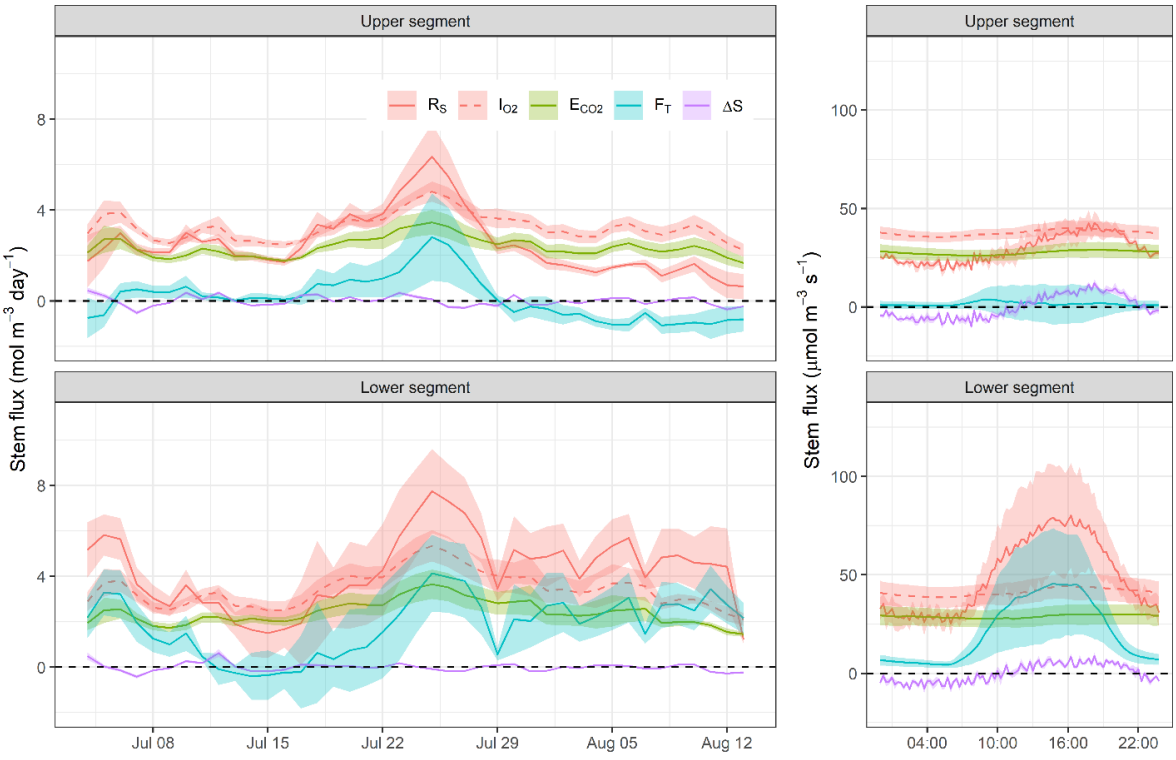

Figure 4 Seasonal (left-hand-side panels) and sub-daily (right-hand-side panels) variation in carbon- and oxygen-based estimates of stem respiration (R_S and O_2 influx [I_{O2}], respectively) in the lower (from 1 to 2.5 m) and upper (from 2.5 to 4 m) stem segments of four mature beech trees. Carbon-based R_S is calculated as the sum of CO_2 efflux to the atmosphere (E_{CO2}), CO_2 transport through the xylem (F_T) and CO_2 storage (ΔS). Mean values ±SE are shown with continuous lines and shaded areas.

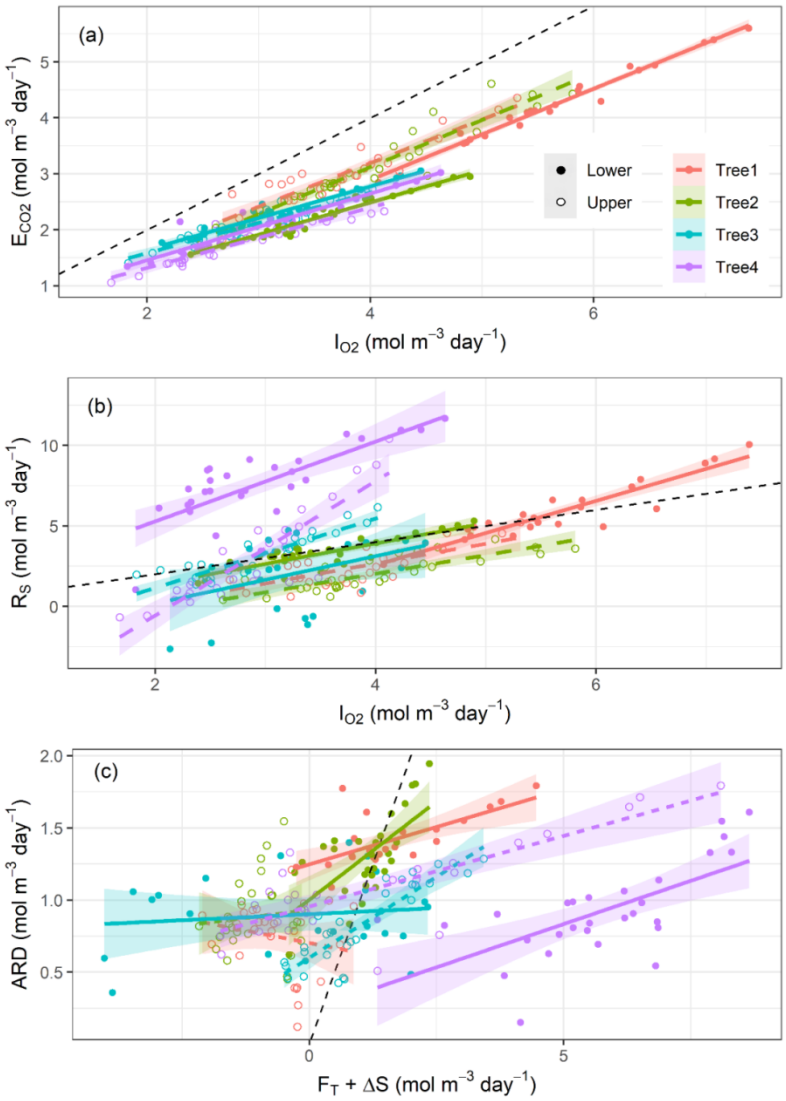

Figure 5 (a) Relationship between daily stem CO_2 efflux (E_{CO2}) and O_2 influx (I_{O2}) denoting apparent respiratory quotients below the unit. (b) The relationship between carbon-based estimates of stem respiration (R_S) and O_2 influx illustrates the deviation from the 1:1 line and, thus, discrepancies between measurement approaches. (c) The relationship between the apparent respiratory difference (ARD) and internal CO_2 transport and storage ($F_T + \Delta S$) indicates the limited potential of internal CO_2 transport and storage to predict the difference between CO_2 efflux and O_2 influx. Measurements were performed in four mature beech trees (shown by different colors) in the lower (from 1 to 2.5 m) and upper (from 2.5 to 4 m) stem segments (shown by different point and line types). Dashed black lines show the 1:1 relation.

Daily values of stem CO_2 efflux and O_2 influx showed good agreement (Fig. 5a) with a slope of 0.65±0.02 ($p < 0.0001$), a significant intercept of 0.23±0.11 ($p < 0.05$), and conditional and marginal R^2 of 0.87 and 0.86, respectively. When this relation was forced through the origin (the intercept is zero), the slope increased to 0.69±0.02, which is in better agreement with the mean ARQ of 0.70. Nevertheless, carbon- and oxygen-based estimates of R_S showed poor consistency.

Although R_S and O_2 influx were positively related (Fig. 5b), the deviation of the mean slope from unity was significant (1.57±0.18; $p < 0.0001$), as well as its intercept (-2.08±1.01; $p < 0.05$). The model conditional and marginal R^2 were 0.52 and 0.31, respectively. The slope of the relation between ARD and CO_2 internal fluxes ($F_T + \Delta S$) (Fig. 5c) was almost 0 (0.056±0.012; $p < 0.0001$), and its intercept was again significant (0.84±0.09; $p < 0.0001$), denoting the limited potential of CO_2 transport and storage to bridge the gap between CO_2 efflux and O_2 influx. The conditional and marginal R^2 of this model were 0.21 and 0.13, respectively. Stem location did not affect the intercept of any of these relations ($p > 0.1$), according to the lack of consistency in vertical gradients of respiratory-related variables.

To further evaluate the potential of the transpiration stream to transport respired CO_2 away from its point of production, we evaluate the sub-daily patterns of ARD, sap flow and sap [CO_2^*] (as a proxy of CO_2 solubility). For the comparison, we normalized the values of each of the variables to their corresponding daily maxima (Fig. 6). Compared with sap flow dynamics, the ARD showed a relatively stable pattern over the 24-h period. It was higher during the daytime, with night-time reductions of ca. 30%-35% relative to the daily maxima. By contrast, sap flow showed night-time reductions of ca. 85%-90% relative to the daily maxima, denoting sub-daily decoupling between CO_2 transport and the ARD. Sub-daily variation in sap [CO_2^*] was minimal, with the highest values observed during night-time and limited reductions during daytime (< 2%) according to the inverse relation between solubility and temperature.

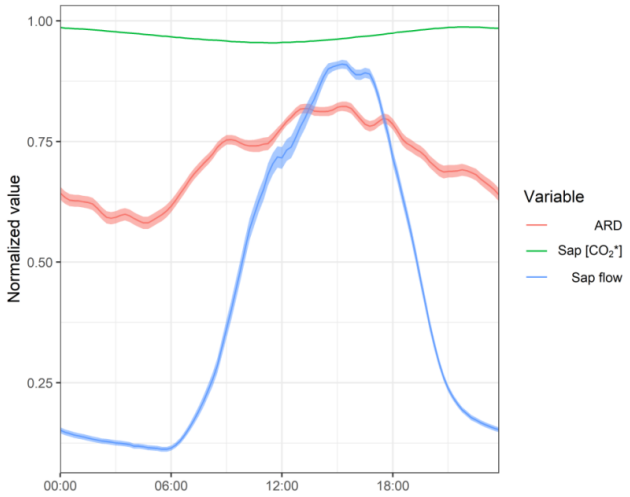

Figure 6 Subdaily variation in normalized values to the daily maxima of the apparent respiratory difference (ARD, as the difference between stem O_2 influx and CO_2 efflux), sap flow, and sap [CO_2] in the liquid phase ([CO_2^*]). The night-time reduction in ARD was limited compared to sap flow, indicating a limited role of the transpiration stream in filling the gap between CO_2 efflux and O_2 influx. Subdaily patterns were averaged across four beech trees and two stem locations (lower and upper) over the experimental period.

Discussion

Factors contributing to a mismatch between E_{CO2} and I_{O2}

We combined a carbon-based mass balance approach and an oxygen-based method to estimate R_S and reconcile apparent discrepancies regarding the fate of respired CO_2 not locally emitted to the atmosphere. O_2 influx was consistently higher than CO_2 efflux across trees, locations and time, with ARQs fluctuating around 0.7 (Fig. 2c and 5a), as similarly observed in several species applying the same methodological approach (Angert *et al.,* 2012; Hilman & Angert, 2016; Hilman *et al.,* 2019). Assuming the beech trees use carbohydrates for respiration, the measured ARQ suggests that 30% of the respired CO_2 is retained in the stem. Figure 7 summarises potential sources of discrepancy between CO_2 efflux and O_2 influx. The ARD could be attributed to an underestimation of the respiratory activity by CO_2 efflux measurements, an overestimation by O_2 influx, or a combination of both. In any case, we must be cautious about the specific methodological issues related to the measurement of the numerous variables monitored here (i.e., CO_2 efflux, O_2 influx, xylem [CO_2], sap flow, and sap pH), which might affect the magnitude of the mismatch between measurement approaches (see below).

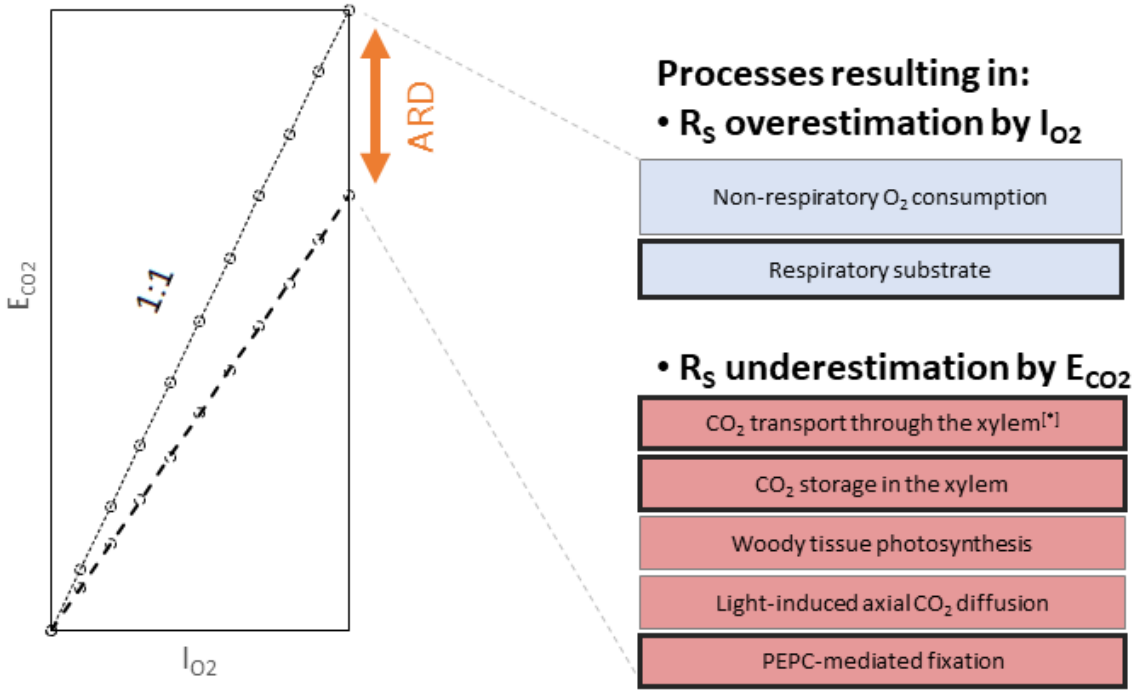

Figure 7 Overview of the potential factors contributing to the apparent respiratory difference (ARD), here observed as the difference between stem CO_2 efflux (E_{CO2}) and O_2 influx (I_{O2}) measurements (cf. Fig. 5a). Our results suggest that CO_2 transport and PEPC-mediated fixation of CO_2 may be the main causes for the deviance from the 1:1 line. Nonrespiratory consumption of O_2 and respiratory substrate change can lead to overestimating stem respiration (R_S) by O_2 influx measurements. By contrast, R_S underestimation by CO_2 efflux measurements can be driven by CO_2 transport through the xylem (although, if coming from below, it can also lead to R_S overestimation [*]), CO_2 storage in xylem sap, woody tissue photosynthesis (here avoided by using opaque stem chambers), light-induced axial CO_2 diffusion above or below the stem chamber, and PEPC-mediated fixation. Investigated processes within this study are shown with a black frame.

No apparent vertical patterns in stem CO_2 efflux, O_2 influx and xylem [CO_2] were observed along a 3-m-long stem segment (Fig. 2), likely because of the modest vertical gradient in 38-m-tall beech trees. The temporal variability of CO_2 efflux, O_2 influx and xylem [CO_2] showed that temperature was the dominant environmental driver controlling R_S, as similarly observed before (e.g., Acosta *et al.,* 2008; Lavigne *et al.,* 1996; Maier *et al.,* 2010; Rodríguez-Calcerrada *et al.,* 2014; Ryan *et al.,* 1995). Interestingly, during and after the peak in temperature and respiratory fluxes at the end of July, xylem [CO_2] did increase along the lower stem segment (from 1 to 2.5 m height) but remained relatively stable between along the upper stem (from 2.5 to 4 m height). This observed difference in the vertical gradient of xylem [CO_2] led to contrasting contributions of CO_2 transport to R_S in the lower and upper stem segment, as discussed below. The lack of a significant relation of both CO_2 efflux and O_2 influx with soil water content denotes that the mild drought did not limit respiratory

metabolism to a large extent. Interestingly, ARQ remained relatively stable over the 1.5 summer months, where a temperature peak (30°C) occurred, suggesting similar sensitivity to temperature of CO_2 efflux and O_2 influx.

CO_2 internal fluxes cannot explain differences between stem O_2 influx and CO_2 efflux

Higher O_2 influx than CO_2 efflux could result from the higher solubility of CO_2 in xylem sap (30 fold) compared with O_2 (Dejours, 1981), hence the possibility of CO_2 dissolving in the sap solution and being transported upwards or stored. If true, this would be evident in our mature beech trees, whose large sapwood conducting area provides room for potentially high transport and storage of respired CO_2 (Fan *et al.,* 2017). We found a nonneglectable contribution of CO_2 transport to R_S, up to 1/3 in the lower stem segment, highlighting the potentially significant role of CO_2 xylem transport in diverting root-respired CO_2 from soil measurements (Aubrey & Teskey, 2021). Nevertheless, we found two lines of evidence refuting our hypothesis, as CO_2 internal fluxes could not bridge the gap between stem O_2 influx and CO_2 efflux.

First, the relation between O_2 influx and R_S diverged from the 1:1 line (Fig. 5b), as indicated by a slope different from the unit and a significant intercept. Furthermore, the marginal $R^2 = 0.31$ of this relation denotes that stem O_2 influx accounted for less than one-third of the variability in the carbon-based estimate of R_S. Identical reasoning applies to the comparison between CO_2 internal fluxes ($F_T + \Delta S$) and ARD (Fig. 5c), with a marginal R^2 of 0.13, further supporting the limited potential of xylem CO_2 transport and storage to predict the ARD. Second, if the ARD could be primarily ascribed to xylem CO_2 transport, ARD and sap flow sub-daily variability should follow similar patterns (Bowman *et al.*, 2005; McGuire & Teskey, 2004; McGuire *et al.*, 2007). However, the sub-daily variation in ARD was limited compared to sap flow (Fig. 6). Specifically, ARD maintained values above 50% of the daily maxima during night-time, when sap flow was reduced to a much larger extent, down to 10%–15% of the daily maxima. Moreover, sap [CO_2^*] on a sub-daily basis was remarkably stable, with minimal reductions during daytime ascribed to temperature-driven reductions in CO_2 solubility, partly offset by the daytime increase in respiratory activity and xylem [CO_2]. Therefore, CO_2 solubility in sap could not significantly affect the strength of CO_2 transport as a mechanism to remove respired CO_2 from its production site. Taken together, subdaily patterns of ARD, sap flow and sap [CO_2^*] thus provide further evidence of the limited role of the transpiration stream in filling the gap between CO_2 efflux and O_2 influx in this study. This observation agrees with Hilman *et al.* (2019), showing the inability of sap flow to account for the variability in ARD of *Q. ilex* trees.

Nevertheless, we must be cautious about the specific methodological issues related to the measurement of sap flow and sap pH and their corresponding propagation errors. For instance, sap flow measured with the heat pulse methods often underestimates the actual sap flow, on average, by 35% (Steppe *et al.*, 2010). Considering a proportional underestimation of CO_2 transport, its contribution to R_S would also increase in parallel, affecting the difference between R_S and O_2 influx differently among individuals and heights. Sap pH, especially above 6.5, is another critical factor for calculating CO_2 transport, as the solubility of CO_2 increases exponentially with pH. Here, we applied a constant pH value across daily and subdaily temporal scales and assumed similar pH between twig sap and stem sap. However, these assumptions can lead to further CO_2 transport misestimation (Aubrey *et al.,* 2011; Erda *et al.,* 2014, Salomón *et al.,* 2016) and deviances between carbon-based estimates of R_S and O_2 influx. Moreover, if parenchyma cells were damaged upon sap extraction, the sample might be contaminated, resulting in an overestimation of the pH values (Tarvainen *et al.*, 2023) and hence CO_2 transport. Another source of uncertainty in ARQ estimation is the relative humidity correction applied to estimate O_2 influx. The relative humidity sensor integrated into the [CO_2] sensor has a slow response time, as shown in Helm et al. (2021). Assuming an underestimation of humidity levels in the measurement chamber by, for example, 5%, the dilution correction required for O_2 estimation would increase the ARQ by ~0.001.

Regardless of these potential measurement uncertainties, we did not succeed in reconciling differences between the two approaches which highlights a crucial methodological difference. The carbon-based approach estimates R_S based on fluxes measured at the stem surface and internal fluxes measured in the xylem, while the oxygen-based approach relies on O_2 influx at the stem surface. Therefore, the disagreement between approaches might be related to the fact that (i) CO_2 efflux and O_2 influx likely reflect respiration in the outermost tissues of the stem (bark, phloem, cambium and outer xylem), and that (ii) respiration of the inner sapwood in large trees cannot be appropriately detected by measurements taken at the surface. According to Fick´s law of diffusion, the rate of gas (CO_2 or O_2) diffusion is inversely related to the length of the diffusive pathway (Nobel, 2009) and, therefore, such decoupling likely increases in large-sized trees. Here, in the mature beech trees with a sapwood depth between 12 and 16.5 cm, the diffusion of respired CO_2 by inner living cells is much slower than in seedlings and saplings, wherein each respiring cell is located nearer to the bark-atmosphere interface. Decoupling between internal respiratory fluxes and fluxes from the stem surface can be exacerbated by the high water content of the cambium layer (De Schepper *et al.*, 2012), acting as a major diffusion barrier according to the slow gas diffusivity in water (ca. 10^4 times lower than in air; Nobel 2009).

PEPC-mediated CO_2 fixation as a relevant driver of the systematic mismatch between CO_2 efflux and O_2 influx

Higher O_2 influx than CO_2 efflux could be explained by CO_2 refixation via PEPC, which hinders CO_2 from being locally emitted. We measured PEPC capacity of 656 nmol min^{-1} g FW^{-1}, equivalent to 22 nmol s^{-1} g DW^{-1} (assuming stem water content of 50%). For comparison, the PEPC capacity in current-year twigs of beech trees was 13 nmol s^{-1} g DW^{-1} (Hilman *et al.*, 2019, recalculated from Berveiller & Damesin 2008), and 17 nmol s^{-1} g DW^{-1} in *Pinus sylvestris* (Hilman *et al.,* 2019, recalculated from Ivanov *et al.*, 2006). Therefore, the capacity of CO_2 refixation via PEPC measured here was comparable with that observed in younger, greener twigs. In nonphotosynthetic tissue, PEPC is involved in anaplerotic reactions, compensating for the depletion of C skeletons consumed by the tricarboxylic acid cycle towards other pathways (synthesis of amino acids) or even other organs (export of malate and citrate via the xylem stream). Part of the phosphoenolpyruvate (PEP) produced by glycolysis may be converted to oxaloacetate and further to malate, with a zero net balance of ATP and NADH during the fixation of two molecules of CO_2.Given the low ARQ values observed here, the resulting malate may not be locally oxidized, but further metabolized to produce, for example, citrate or amino acids.

Evidence shows that malate concentration increases in the stem of *Acer platanoides* trees moving upwards (Schill *et al.,* 1996). Transported malate can increase the malate pool in leaves (Gessler *et al.,* 2009), where it could be metabolized via malic enzymes releasing CO_2, thus favouring carboxylation via Rubisco (Hibberd & Quick 2002). Alternatively, the products can be transported downwards via the phloem (Hoffland *et al.*, 1992; Shane *et al.*, 2004; Touraine *et al.,* 1992), followed by excretion in the rhizosphere as root exudates. Alternatively or additionally, PEPC could be involved in pH regulation (Caburatan & Park, 2021), the latter having appeared stable despite fluctuations in xylem CO_2 (see e.g. Erda *et al.,* 2014). Extrapolating PEPC capacity on a volume basis for comparison with CO_2 efflux or O_2 influx (as in Fig. 4) resulted in unrealistically high rates of PEPC fixation (up to two orders of magnitude higher than R_S estimates). First, enzyme activity measured in vitro under saturating substrate usually exceeds the in vivo flux (Junker *et al.*, 2007). Second, PEPC capacity likely decreases with xylem depth (Höll, 1974), and PEPC samples were uniquely taken from the outermost stem tissues. Nevertheless, the high values of PEPC capacity on a volume basis suggest that even low PEPC capacity could be significant for the stem C budget and could help explain the discrepancy between CO_2 efflux and O_2 influx.

Other potential C sinks

Another potential missing C sink in R_S budgets is the CO_2 photosynthetic refixation occurring in chloroplast-containing cells located in peripheral woody tissues (Ávila *et al.*, 2014; De Roo *et al.*, 2020c; Teskey *et al.*, 2008), which can reduce stem CO_2 emissions by half, as observed in young poplar trees (De Roo *et al.*, 2020c). However, local photosynthetic fixation can be safely discarded within our experimental set-up, as opaque stem chambers were used to measure CO_2 efflux, precluding photosynthetic light reactions. Nevertheless, we cannot discard the possibility of axial diffusion of CO_2 in the gas phase ascribed to distant woody tissue photosynthesis (De Roo *et al.*, 2019; Saveyn *et al.*, 2008a). In this line, light-driven photosynthesis above and below the (opaque) stem chamber can develop light-induced vertical [CO_2] gradients, leading to CO_2 axial diffusion in the gas phase that has been observed to reduce CO_2 efflux by 22% in oak stems (De Roo *et al.*, 2019). Furthermore, we cannot rule out the possibility of O_2 influx measurements overestimating stem respiratory activity. We must critically note that O_2 influx measurements should be considered as additional information that helps disentangle CO_2 sinks and sources, but not as an equivalent to R_S as uncertainties remain. First, a shift in the respiratory substrate from NSCs to lipids or proteins, with a lower oxidation state, requires a higher amount of O_2 for respiratory reduction, hence increasing the ARD (and reducing the ARQ; Fischer *et al.*, 2015; Hanf *et al.*, 2015). However, our study extended over 6 weeks during the summer season and measured NSC concentrations at different heights and depths did not indicate a seasonal NSC depletion that would alter the respiratory substrate (Fig. 3). Moreover, beech is not known to store lipids (Hoch *et al.*, 2003), further suggesting the limited role of substrate change on the ARD. Secondly, nonrespiratory O_2 uptake by O_2-consuming enzymes, like oxidases and hydroxylases (Sweetlove *et al.*, 2013) that are not involved in respiratory metabolism may increase O_2 influx while CO_2 efflux remains constant (Kruse & Adams, 2008; O'Leary *et al.,* 2019; Tcherkez *et al.,* 2012). Thirdly, high growth rates related to cell wall deposition, likely occurring at the end of the growing season, may also lead to a nonrespiratory increase in O_2 consumption, as observed in *Pinus radiata* (Kruse & Adams, 2008).

Conclusion and outlook

Carbon- and oxygen-based methods to estimate R_S yield inconsistent results when simultaneously applied to the same individuals under the same conditions. We found a consistent ratio between CO_2 efflux and O_2 influx close to 0.7, which cannot be primarily explained by internal fluxes (xylem CO_2 transport and storage) and might be linked to alternative sinks of respired CO_2 (PEPC fixation and axial CO_2 diffusion) and non-respiratory O_2 consumption. Remarkably, the high PEPC capacity

measured here in mature tree stems, comparable with that observed in current-year greener twigs, points towards PEPC-mediated CO_2 fixation as a relevant driver of the systematic mismatch between CO_2 efflux and O_2 influx. We encourage further research combining CO_2 efflux and O_2 influx readings in parallel with measurements of potential respiration and PEPC capacity at different sapwood depths, as this would help to assess the contribution of inner and outer tissues to total R_S and how they relate to fluxes at the stem surface. Ideally, incorporating O_2 consumption and biochemical-level knowledge (such as PEPC fixation) into plant mechanistic models could help to more accurately estimate R_S and better constrain larger-scale C models.

Conflict of interest

None declared.

Acknowledgements

The authors thank Martin Göbel, Edgar Tunsch, Frank Tiedemann, Dietmar Fellert for technical support, Savoyane Lambert, Nadine Hempel, David Herrera Ramírez for field assistance and Iris Kuhlmann, Anett Enke and Christin Leschik for laboratory support. Thanks to Philip Deman for his help in calibrating the xylem [CO_2] probes. We thank Christian Markwitz for soil water content data. JH acknowledges the continuous support of the International Max Planck Research School for Biogeochemical Cycles. We thank the administration of the forestry district Heiligenstadt for the opportunity for research in their forest area. Finally, we are also very grateful to Prof. Aubrey and one anonymous reviewer for their valuable comments.

Funding

J.M. and A.K. acknowledge funding by the European Research Council under the European Union's Horizon 2020 research and innovation programme (grant agreement no. 682512 - OXYFLUX). RLS acknowledge funding from the Research Foundation Flanders (FWO) and the Marie Skłodowska-Curie research programme (grant no. 665501).

Abbreviations

Symbol	Explanation
ARD	Apparent respiratory difference, as O_2 influx – CO_2 efflux
ARQ	Apparent respiratory quotient, as CO_2 efflux/O_2 influx
$[CO_2]$	$[CO_2]$ in the gas phase
$[CO_2^*]$	Dissolved inorganic carbon comprises of dissolved CO_2, carbonic acid (H_2CO_3), bicarbonate (HCO_3^-) and carbonate (CO_3^{2-})
E_{CO2}	Stem CO_2 efflux to the atmosphere (stem surface)
F_T	Transport of dissolved respired C in the xylem sap
I_{O2}	Stem O_2 influx (stem surface)
PEPC	Phosphoenolpyruvatcarboxylase; enzyme for CO_2 fixation
R_S	Stem respiration
ΔS	Storage flux, as the temporal change in dissolved CO_2 in the sap

CHAPTER 4

Carbon dynamics in long-term starving poplar trees – the importance of older carbohydrates and a shift to lipids during survival

Juliane Helm[1,2], Jan Muhr[1,3], Boaz Hilman[1], Ansgar Kahmen[2], Ernst-Detlef Schulze[1], Susan Trumbore[1], David Herrera-Ramírez[1], Henrik Hartmann[1,4]

[1]Department of Biogeochemical Processes, Max Planck Institute for Biogeochemistry Hans-Knöll-Str.10, 07743 Jena, Germany

[2]Department of Environmental Sciences–Botany, Basel University, Schönbeinstr. 6, Basel CH-4056, Switzerland

[3]Department of Forest Botany and Tree Physiology, Laboratory for Radioisotopes, Georg-August University, Büsgenweg 2, 37077 Göttingen, Germany

[4]Institute for Forest Protection, Federal Research Centre for Cultivated Plants, Erwin-Baur-Str. 27, 06484 Quedlinburg, Germany

Published in Tree Physiology (2023). 1-13.

Abstract

Carbon (C) assimilation can be severely impaired during periods of environmental stress like drought or defoliation, making trees heavily dependent on the use of C reserve pools for survival; yet, dynamics of reserve use during periods of reduced C supply are still poorly understood. We used stem girdling in mature poplar trees (*Populus tremula* L. hybrids), a lipid-storing species, to permanently interrupt phloem C transport and induced C shortage in the isolated stem section below the girdle and monitored metabolic activity during three campaigns in the growing seasons of 2018, 2019, and 2021. We measured respiratory fluxes (CO_2 and O_2), NSC concentration, the respiratory substrate (based on isotopic analysis and CO_2/O_2 ratio) and the age of the respiratory substrate (based on radiocarbon analysis). Our study shows that poplar trees can survive long periods of reduced C supply from the canopy by switching in metabolism from recent carbohydrates to older storage pools with a potential mixture of respiratory substrates, including lipids. This mechanism of stress resilience can explain why tree decline may take many years until death occurs.

Keywords

bomb radiocarbon ^{14}C, carbon allocation, CO_2 efflux, ^{13}C of respired CO_2, non-structural carbohydrates, O_2 influx, stem respiration, tree girdling

Introduction

Trees require sufficient carbon (C) to build up new biomass (including reproductive structures), fuel respiration, use C for defense and allocate C to storage pools (Chapin *et al.*, 1990; Lambers & Poorter, 1992; Sala *et al.*, 2012). When the C supply from assimilation exceeds demand, trees can store substantial amounts of non-structural carbon (NSC). Those reserves may be used to maintain tree functions (e.g., respiration, osmoregulation, repair, biosynthesis of defense compounds) when supply is reduced below requirements, like during periods of harsh environmental conditions (e.g., Regier *et al.*, 2009; Hartmann *et al.*, 2013; Hartmann & Trumbore, 2016). Carbon storage compounds, including starch, sugars or lipids provide an essential buffer against C shortage and play an essential role in tree's resilience capability (Hartmann & Trumbore, 2016). Large NSC storage pools can be beneficial for the recovery of a tree after stress (e.g., insect herbivore defoliation, drought, fire) (Sala *et al.*, 2010; Dietze *et al.*, 2014; Piper & Paula, 2020). The dynamics of reserve use and their availability during periods of reduced C supply in mature trees, over the short- and long term, are still poorly understood (Gessler & Treydte, 2016; Hartmann & Trumbore, 2016). For a more comprehensive understanding of C storage and remobilization dynamics in trees, studies over several years are needed to improve predictions of tree and forest resilience over time (McDowell, 2011; Rosas *et al.*, 2013; Gessler & Treydte, 2016).

In order to gain insights into C reserve use under stressful conditions, one can artificially produce a lack of photo-assimilate supply via stem girdling. When removing a circumferential band of bark, phloem and cambium of a tree, the C supply from the canopy to the lower stem section is interrupted, and only upward water transport through the xylem is maintained. The stem section below the girdle is isolated from the rest of the tree above and is forced to use C reserves from within the stem or from the root system to maintain metabolic activity beneath the girdle. To date, empirical evidence supporting substrate shifts in trees is scarce, but see Fischer *et al.* (2015) and Wiley *et al.* (2019). It is still unclear whether and to what degree all types of reserve compounds, including sugars, starch, and lipids, can be used as respiratory substrate when C supply is limited. Plant lipid metabolism is far less studied due to methodological challenges in quantifying neutral lipids (Fischer & Höll, 1991; Hoch *et al.*, 2003; Fischer *et al.*, 2015), but progress has been made (see Grimberg *et al.,* 2018; Herrera-Ramírez *et al.,* 2021).

The simultaneous measurement of CO_2 and O_2 enables to calculate the ratio of CO_2/-O_2, that provides an excellent indicator for the respiratory substrate identity (cellular level: Respiratory Quotient (RQ)). Respiratory substrates differ in their stoichiometric ratios of C:O:H and in their degree of oxidation. Thus, during respiration, quantities of O_2 required as electron acceptor vary

depending on the respiratory substrate. During the break-down of carbohydrates, one molecule of O_2 is consumed for each molecule of CO_2 released, resulting in RQ ~ 1, while for the break-down of lipids more oxygen is needed, resulting in RQ ~ 0.7. While RQ refers to the respiratory processes in the strict sense (i.e. measured at the mitochondrion), the apparent respiratory quotient (ARQ, Angert & Sherer 2011) may imply post-respiratory processes also (see Trumbore *et al.*, 2013 for a summary), and this is the case when measured away from the mitochondrion, e.g. at the tree stem. More precisely, highly soluble CO_2 can be transported away from the respiration site (e.g., Teskey & McGuire, 2002; McGuire & Teskey, 2004) or refixation mechanisms during the day (stem photosynthesis) (e.g., Pfanz *et al.*, 2002; Wittmann *et al.*, 2006) or during the night (phosphoenolpyruvatcarboxylase; PEPC hereafter) can fix CO_2 locally and therefore reduce the CO_2 efflux (E_{CO2}) to the atmosphere, leading to ARQ values below 1 (Angert *et al.*, 2012; Hilman & Angert, 2016). However, the potential role of fixation via PEPC has been investigated mainly in leaves and young green twigs of C3 plants (Berveiller & Damesin, 2008), but might be relevant as a mechanism of local CO_2 removal, as shown for mature beech trees (Helm *et al.,* 2023).

Sugars, starch, and lipids can also be distinguished by their C isotope signal of respired CO_2 ($\delta^{13}C$) (Gleixner *et al.*, 1993; Cernusak *et al.*, 2003; Bowling *et al.*, 2008; Brüggemann *et al.*, 2011). Former studies showed that 2-yr old oak saplings shifted substrate for respiration from recently fixed carbohydrates to starch reserves (below the girdle) after girdling (Maunoury-Danger *et al.*, 2010), deduced from a $\delta^{13}C$ enrichment of CO_2 respired by stems (Brugnoli *et al.*, 1988; Tcherkez *et al.*, 2004). In young *Pinus sylvestris* trees, reducing C assimilation by experimental shading triggered a shift from carbohydrate-dominated respiration to almost pure lipid-based respiration, indicated by lower $\delta^{13}CO_2$, as well as lower RQ (Fischer *et al.*, 2015). The $\delta^{13}C$ signal can also reflect environmental conditions (stomatal closure to avoid water loss), as e.g., a change towards a more enriched $\delta^{13}C$ signal could be explained by expected changes in photosynthetic discrimination (Farquhar *et al.*, 1989; Högberg *et al.*, 1995).

To enhance our understanding of NSC dynamics in trees, it is important to know how long these C reserves can be stored and how fast they can be used. The bomb-radiocarbon (^{14}C) approach allows determining the mean age of C assimilated by a plant, and thus can be used to estimate the age of substrates used for respiration by calculating the amount of time elapsed between fixation and use, and the time trees take to tap into their long-term reserves (Levin *et al.*, 2010; Trumbore *et al.*, 2016). Amazonian tree stems below the girdle mobilized ~5 yr old C for respiration within one month of girdling, and of decade-old C about 1 yr post-girdling (Muhr *et al.*, 2018). NSC age of stump sprouts (*Acer rubrum*) regenerated following harvesting was maximum 17 years (Carbone

et al., 2013) and maximum 16 yr old C was used for new fine root growth after hurricane damage in a seasonally dry tropical forest (Vargas *et al.*, 2009).

In our study, we investigated responses of mature poplar trees (*Populus tremula* L. hybrids) to reduced C supply to stem sections. This species is a very common and fast-growing tree species that is known to store, besides sugars and starch, substantial amounts of lipids (Hoch *et al.*, 2003). We acknowledge here the potential effect of root grafting during starvation, as C transfer between trees has been reported in mature poplar trees (DesRochers & Lieffers, 2001; Fraser *et al.*, 2006; Jelínková *et al.*, 2009) and could compensate for the lack of photo-assimilates. We investigated how reduced C supply of recent photo-assimilates via girdling affects respiratory substrate use and mobilization of storage pools in the isolated stem section. In particular, we tested the following hypotheses (Fig. 1):

H1. After the disruption of the supply of photo-assimilates, poplar trees initially mobilize NSCs (decrease in NSC concentration), increasingly digging into older C reserves (increase in $\Delta^{14}C$).

H2. Lipids contribute to metabolism maintenance during starvation, indicated by progressive mobilization and metabolization of lipids as starvation proceeds (decline in ARQ ratios, lower $\delta^{13}CO_2$ signal).

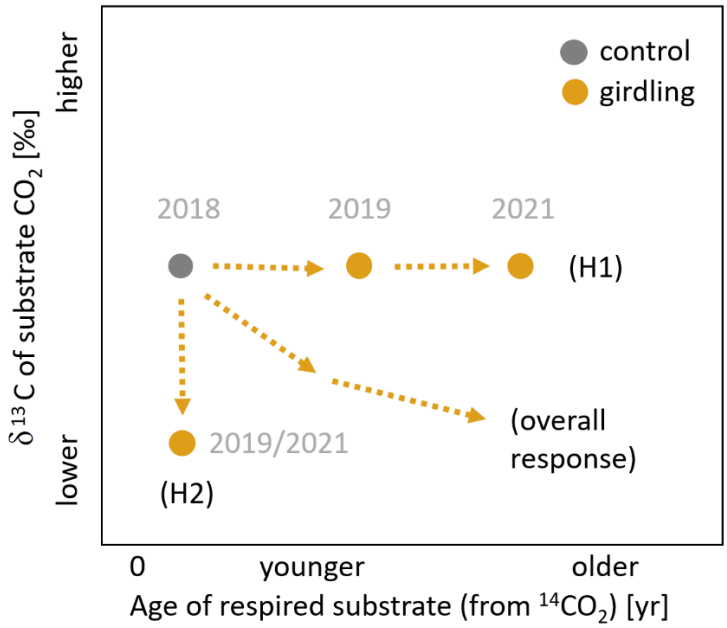

Figure 1 Graphical representation of the expected 3-year pattern of C reserve mobilization in mature poplar trees after girdling. Two hypotheses related to C reserve use (H1) and substrate identity (H2) are presented together with the expected overall response.

Material and Methods

Study site and girdling treatment

The study site is located in the Thuringian forest, Germany (50°42′50′′N, 10°36′13′′E, site elevation 616 m a.s.l, north slope). Mean annual temperature is ~7°C and mean annual precipitation is 800 to 1200 mm (Bouriaud *et al.*, 2016). Soil was formed on volcanic bedrock. Our measurements were carried out in the growing season (May to September) of 2018 and 2019. We included a short measurement campaign in 2021 as most of the girdled trees were still alive (with a reduced canopy leaf area) after 3 yr. Meteorological information was available from a weather station nearby, however not directly at the north slope. Annual precipitation was 360 mm (2018), 510 mm (2019) and 626 mm (2021), respectively (Fig. 2). Average annual temperature at our site was 8°C (2018), 9.2°C (2019) and 7.7°C (2021), respectively (Fig. 2). In 2018 and 2019, extreme summer drought affected central Europe (Bastos *et al.*, 2021). In 2018 we selected 12 mature poplar trees (*Populus tremula* hybrids, approx. 60 yr-old) in minimum 3 m to maximum 18 m distance to the neighboring tree, that were free of obvious signs of injury or disease, with easily accessible stems and stem diameter at breast height (DBH) between 29 cm and 42 cm (Table S1 available as Supplementary data at *Tree Physiology* Online). Those trees were growing on terraces that were formerly used for agriculture, afterwards became grassland and then forest. On 4 July 2018 (DOY 185), 6 of the 12 trees were randomly chosen and girdled by carefully removing a ~ 4-cm-wide circumferential band of bark, cambium and phloem at approx. 1.5 m height above ground (Picture S2 available as Supplementary data at *Tree Physiology* Online). All stem measurements were made below the girdle (for girdled trees). For an overview of the different measurements and the timing of sampling see Table S2 available as Supplementary data at *Tree Physiology* Online. As we could not see any signs of wound repair/cambium regrowth at the girdling band, nor any sprouting over the time of measurements, we assume continuous interruption of the phloem transport pathway over the 3 yr.

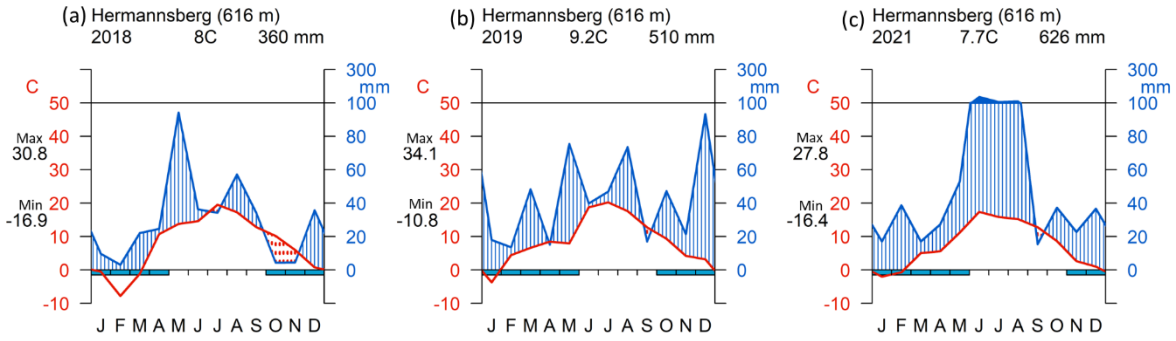

Figure 2 Walter Lieth climate diagram of the study site Hermannsberg (Germany) in (a) 2018, (b) 2019 and (c) 2021. Average annual temperature (°C) and annual precipitation (mm) are shown. Max: mean of the maximum temperatures of the warmest month. Min: mean of the minimum temperatures of the coldest month.

Stem CO_2 efflux and O_2 influx measurements

We installed automated measurement chambers for quantifying stem CO_2 efflux (E_{CO2}) and O_2 influx (I_{O2}) (Helm *et al.*, 2021). The highly autonomous low-cost chamber-based measurement device was installed at a height of approx. 1.3 m, i.e. below the girdling on the girdled trees (Picture S2 available as Supplementary data at *Tree Physiology* Online). In 2018, chambers were installed on all trees and measurements were conducted from 5th of May to 20th of September. Due to limited capacity, in 2019, chambers were installed on three control and three girdled trees from 2nd of June to 2nd of September. In 2021, chambers were installed on four control and four girdled trees from 2nd of July to 3rd of August. Chambers were installed on the north side of the trees and were covered with reflective foil to prevent heating from direct solar radiation. For details about the chamber set-up and sensor specifications see Helm *et al.* (2021). Configuration settings are based on a repeated closed chamber-mode with 45-min measurement cycles (CO_2 and O_2 values were recorded every 10 sec), followed by a 15-min flushing period of the chamber headspace to reach ambient air concentrations before a new measurement cycle with measurements of CO_2/-O_2 headspace concentrations starts. As a general requirement, O_2 as a non-trace gas needs to be corrected for the dilution effect of changing H_2O and CO_2 concentrations (Helm *et al.*, 2021), therefore we used the relative humidity sensor integrated in the COZIR non-dispersive infrared (NDIR) absorption sensor (Gas Sensing Solution GSS, Cumbernauld, UK) for the correction. Relative humidity was converted to [H_2O] using the Magnus formula (see Helm *et al.*, 2021).

Measurements of CO_2/-O_2 headspace concentrations over time are subsequently used to calculate CO_2 and O_2 fluxes. To this end, the linear increase of CO_2 and decrease of dilution corrected O_2

concentrations of the first 20-min were used, after removing the first 5-min period following flushing to avoid the influence of pressure fluctuations:

$$\text{Flux} = \frac{\Delta C}{\Delta t} \text{x} \frac{V}{A} \text{x} \frac{P}{R \text{x} T} \quad [1]$$

Where $\Delta C/\Delta t$ is the change in gas concentration over time (ppm s^{-1}) for CO_2 and O_2 (absolute value), respectively, V is the volume of the chamber (m^3), A is the stem surface (0.0028 m^2), P is the barometric pressure (kPa), R is the molar gas constant (0.008314 m^3 kPa K^{-1} mol^{-1}) and T the temperature (Kelvin). Volumes of the stem chambers ranged from 70 to 105 cm^3 and were determined after installation by injecting water with a calibrated syringe into the chamber headspace. To allow air-bleeding from headspace we inserted two syringe needles into the chamber headspace; one to inject water, the other to vent air from the chamber (Table S1 available as Supplementary data at *Tree Physiology* Online).

Sensor calibration

In 2018, CO_2 sensors initially were calibrated every six weeks. Upon noticing substantial sensor drift beyond 3 weeks since calibration (Helm *et al.*, 2021) we excluded all data recorded more than 3 weeks since last calibration, and from 2019 on, sensors were calibrated every ~3 weeks. For O_2 sensors, electronic storing of calibrated parameters was not possible, therefore stability/validity has been checked regularly by evaluating possible drift (predefined limit of the slope: 1±0.03) using different reference gas concentrations (Westfalen AG, Münster, Germany). For more in-depth information about the calibration procedure and calibration unit see (Helm *et al.*, 2021).

Sap flow rate

Sap flux density (l cm^{-2} h^{-1}) was monitored during the growing season 2018 (May to September), only. We measured the sap flow with Sap Flow Meter *SFM1* sensors from *ICT* International installed below the glass flask chamber at approx. 0.5 m stem height. Sap flux density was recorded every 20-min and converted to sap flow rate (l h^{-1}) by using the software Sap Flow Tool (ICT International, University Ghent). Sapwood depth was assumed to be 50% of the xylem radius.

Non-structural carbohydrate analysis

The effect of girdling on storage reserves in the sapwood was evaluated by seasonal NSC measurements of stem cores. In 2018 we sampled twice a year, before the girdling (DOY 172) and 90 days after the girdling (DOY 262). In 2019 and 2021 we sampled once a year (DOY 147 and

DOY 195). Stem cores from all 12 trees were immediately placed in a cooler (0–5°C) for transport to the laboratory, where they were dried for 72 h at 60°C within 4 h after the core collection in the field. Cores were sanded with sand paper to facilitate identification of annual rings under a light microscope (Stemi 2000-C, Carl Zeiss Microscopy GmbH, Göttingen, Germany). Defining the outermost (most recent) annual ring as ring 1, we then cut the cores into pieces consisting of rings 1–6 (without bark) and 7–14. Wood material was ground to a fine powder in a ball mill. Aliquots of 30 mg homogenized wood material were analyzed for concentrations of sugars (glucose, fructose, sucrose) and starch according to protocols S1 and S2 from Landhäusser *et al.* (2018). In short, ethanol (80% v/v) was used as solvent for sugar extraction. After vortexing for 1 min, incubating at 90°C for 10 min and centrifuging at 13,000*g* for 1 min, supernatants were analyzed by a High-Performance Liquid Chromatography coupled to a Pulsed Amperometric Detection (HPLC-PAD). Concentrations are expressed in glucose equivalents per dry wood mass. Starch was extracted from the remaining pellet from soluble sugar extraction using two digestive enzymes: alpha-amylase and amyloglucosidase (Sigma-Aldrich). The glucose hydrolysate was measured by HPLC-PAD.

^{14}C and ^{13}C signatures of respired CO_2

We repeatedly collected gas flask samples for $\delta^{13}CO_2$ and $\Delta^{14}CO_2$ measurements by means of additional stem chambers that were installed in close proximity below the respiration chamber (Picture S2 available as Supplementary data at *Tree Physiology* Online). A glass flask chamber consisted of polypropylene plate equipped with three connectors for sampling flasks and a foam frame (2.4 cm thick; ^{14}C neutral material) placed between the stem and the plate to ensure airtight sealing. Chambers for sampling isotopes were installed temporarily for sampling campaigns using 4 rachet straps for fastening the chamber on the stem. Three flasks were connected to the chamber and opened. Each of these incubation periods lasted approx. 1 week to ensure sufficient amounts of CO_2 for ^{13}C and ^{14}C analysis and establishment of steady state conditions. Then, flask inlets were closed and glass flasks removed from the stem. The sampling flasks were custom-built, made of glass and with a volume of 115ml. Glass flasks were evacuated prior to sampling and inlets were equipped with a Louwers O-ring high-vacuum valve (Louwers H.V. glass valves, Louwers Glass and Ceramic Technologies, Hapert, Netherlands) (Muhr *et al.*, 2018). We conducted three pre-girdling samplings. Following girdling, sampling took place at approx. monthly intervals from July to October in the same year, from June to September in 2019 and from July to September in 2021. Leaks in the field or problems during extractions repeatedly resulted in smaller number of replicates than intended (n = 6 for control and girdling each) (Table S3, S4 and S5 available as Supplementary

data at *Tree Physiology* Online). Flask samples were brought to the laboratory at the MPI-BGC in Jena for analysis.

For $\Delta^{14}C$ of CO_2, gas samples (~0.5 mg of C) were cryogenically purified, graphitized and analyzed with an accelerator mass spectrometer (Steinhof *et al.*, 2017; Muhr *et al.*, 2018). Radiocarbon data are reported as $\Delta^{14}C$ (‰), i.e. the per mil deviation from the ^{14}C to ^{12}C ratio of oxalic acid standard in 1950. Accounting for any mass-dependent fractionation effects, $\Delta^{14}C$ is corrected to a $\delta^{13}C$ value of -25‰ (Stuiver & Polach, 1977). Detailed calculation can be found in Trumbore *et al.* (2016). The $\Delta^{14}C$ of any given sample can be used for estimating the ´age´ of respired CO_2 by calculating the difference to the atmospheric $\Delta^{14}C$ of the study site at the time of sampling. The local atmospheric $\Delta^{14}C$ record between 1993–2019 was estimated previously by Hua *et al.* (2022) (northern hemisphere zone 1) and Hilman *et al.* (2021). We added to this record an estimation for 2021 atmospheric $\Delta^{14}CO_2$ by analyzing a local annual plant, which is assumed to fix majority of its C from the 2021 growing season atmospheric CO_2 (Figure S5 available as Supplementary data at *Tree Physiology* Online, adapted from Hilman *et al.* (2021)). Samples with $\Delta^{14}C$ values clearly below atmospheric $\Delta^{14}C$ (< 5‰) were discarded, as those samples might reflect influence of CO_2 from local fossil sources.

We used the following formula to estimate the mean age of respired CO_2 (yr) according to Hilman *et al.* (2021):

$$Mean\ Age = \frac{\Delta 14C_{sample} - \Delta 14C_{atmosphere}}{4.7‰/year} \quad [2]$$

$\Delta^{14}C_{sample}$ is the measured value from the gas sample, $\Delta^{14}C_{atmosphere}$ is the signature of the current atmospheric CO_2, and 4.7‰ is the mean annual decline in atmospheric $\Delta^{14}C$. The estimate for the atmospheric $\Delta^{14}C$ during the growing seasons was +2.3‰ (2018), -2.4‰ (2019) and -5.4‰ (2021), respectively.

For $\delta^{13}CO_2$ measurement two aliquots (50 µl) from each gas sample were analyzed with an isotope ratio mass spectrometer (Delta+ XL; Thermo Fisher Scientific, Bremen, Germany) coupled to a modified gas bench with a Conflow III and GC (Thermo Fisher Scientific). $\delta^{13}CO_2$ samples were analyzed against a laboratory air standard on the Vienna Pee Dee Belemnite scale realized by the Jena Reference Air Set-06 (JRAS-06) (Wendeberg *et al.*, 2013). The values obtained were corrected using the Davidson equation (Davidson, 1995) to account for fractionation effects:

$$\frac{C_s(\delta_s - 4.4) - C_a\,(\delta_a - 4.4)}{1.0044\,(C_s - C_a)} \qquad [3]$$

where C_s is the CO_2 concentration of respired CO_2 in the flask (ppm), δ_s (‰) is the isotopic composition of respired CO_2 (‰), C_a is the ambient air concentration of CO_2 (assumed 400 ppm) and δ_a is the isotopic composition of ambient air (assumed -9‰).

Besides $\delta^{13}C$ of respired CO_2, we measured $\delta^{13}C$ also for soluble sugars and neutral lipids following a modified protocol (Bligh & Dyer, 1959; White *et al.*, 1979) and liquid chromatography (Schwab *et al.*, 2019). Increment cores from all 12 trees were extracted at breast height using a standard 5.15 mm diameter increment borer (Haglöf Company Group, Sweden) in 2021 (DOY 236, ring 1-14). Wood material was ground to a fine powder in a ball mill (MM 400, Retsch, Haan, Germany) and in a next step phase-separated: water-soluble C was analyzed as proxy for soluble sugars and C extractable in methanol:chloroform solution (total lipids) was transferred to silica gel column. The lipids that eluted by chloroform were regarded as "neutral" and analyzed (further details see Method S1 available as Supplementary data at *Tree Physiology* Online). Aliquots from the extractions were put into tin cups, dried and afterwards the measurement was performed with a Finnigan MAT DeltaPlus XL EA-IRMS (ThermoFinnigan GmbH, Bremen, Germany), coupled to an autosampler (Koppenaal *et al.*, 1991).

Quantification of neutral lipids in stem-woods

For the visualization and quantification of lipids, we took stem cores in 2021 (DOY 147) from 3 randomly selected trees from each treatment. To quantify neutral lipids in the stem wood, we used a histological method based on the protocols proposed by Mehlem *et al.* (2013) and Herrera-Ramírez *et al.* (2021). We took histological slides (of 30 µm thick) from the first 3 cm, from bark to pith. The slices were washed with distilled water and then placed in a petri box. Wood histological slices were stained with Oil Red O (ORO) to visualize neutral lipids. ORO stock solution was prepared adding 2.5 g of ORO to 400 ml of 99% (vol/vol) isopropyl alcohol and mixing the solution for 2 h at room temperature. ORO working solution was prepared by adding 1.5 parts of ORO stock solution to one part of distilled water, shaking it for 5 min, letting it stand for 10 min at room temperature and filtering it through a 45 µm filter to remove the precipitates. ORO working solution was added into the petri box until completely covering the wood slices. We closed the petri box to avoid drying and precipitating of the ORO solution, and let the sample incubate for 20 min at room temperature. Then, we rinsed the samples with running distilled water

for ca. 15 min, changing water every 5 min. The histological slices were mounted on glass slides using water as a mounting medium, and placed under a coverslip. We took pictures of each histological slice within one hour after mounting them on the glass slide. After that time water started to dry out and the ORO solution started to precipitate. Panoramic photos of the wood slides were taking using an optical digital microscope with large depth of field (Keyence, VHX-6000, USA) at x500 magnification.

We used the pictures to quantify the percentage of the aerial surface covered by neutral lipid droplets using ImageJ (Schneider *et al.*, 2012). We quantified the percentage of lipid coverages in small regions of interest (ROIs) of 0.25 mm^2 randomly generated by the automatic script used for Image J (Anexx 1). We divided the images in sections corresponding to 3 mm of wood counted from bark to pith and in each 3 mm wood section we measured 50 ROIs, leading to a total of 500 ROIs along the 3 cm of wood. We estimated the percentage of the aerial surfaced covered by neutral lipids in the wood as the average between all the measured ROIs along the wood sample.

Potential PEPC capacity in woody tissue

For PEPC capacity measurements, we collected stem cores from all 12 trees in August 2019 (DOY 236). Cores were immediately frozen in liquid nitrogen in order to avoid any further metabolic activity, transported to the laboratory and stored at a -80°C freezer. We cut the first 2 cm of stem material (bark to xylem) and ground the wood to a fine powder with a mortar and pestle in liquid nitrogen. A discontinuous assay was performed following the steps of Bénard and Gibon (2016) in order to quantify potential PEPC activity. We used 20 mg of woody tissue material. All pipetting steps were performed using a 96-head robot (Hamilton Star). Aliquots, together with 500 µL of extraction buffer, were shaken for extraction. Extracts were centrifuged for 7 min (3000 g, 4°C) before the extracts were diluted by a factor of 2000 (w/v). NAD^+ standards were prepared in the before mentioned extraction buffer (ranging from 0 to 1 nmol per well). Afterwards, those standards and the diluted extracts were incubated for 20 min in a 20 µl medium (100 mM Tricine-KOH pH 8.0, 20 mM $MgCl_2$, 1 $unit.ml^{-1}$ malate dehydrogenase, 10 mM $NaHCO_3$, 0.1 mM NADH, 1% w/v polyvinylpyrrolidone, phosphoenolpyruvate 0 (blanks) or 2 mM (maximal activity)). In order to stop the reaction 0.5 M HCl (20 µl) was used. In order to destroy NADH, the 96-well microplate was sealed and incubated for 10 min at 95°C. In a next step, the microplate had to acclimate to room temperature, and a neutralization step with NaOH 0.5M (20 µl) and 0.2 M Tricine-KOH followed to adjust the pH to 9.0. Together with 6 $units.ml^{-1}$ alcohol dehydrogenase, 100 mM Tricine-KOH pH 9.0, 4 mM EDTA, 0.1 mM PES, 0.6 mM MTT, and 500 mM ethanol, NAD+ was quantified. The absorbance at 570 nm was measured at 30°C in a filter-based microplate reader (SAFAS

MP96). To calculate the amount of NAD^+ formed during the first step of the assay, the reaction rates ($mOD.min^{-1}$) were used. For further details see Bénard and Gibon (2016).

Statistics

All analyses were performed using R software (R Development Core Team, 2019). We used R package *climatol* for Walther lieth climate graph. We used *pad* function from the *padr* package for linear interpolation of the flux data to fill flux data gaps short than 2h. Flux data were discarded if R^2 of the slope of the linear regression < 0.96 and relative humidity > 99% (after filtering 2018: 89%; 2019: 81%; 2021: 65% used). The ARQ ratio was calculated as the slope of changing CO_2 concentration over time divided by the negative slope of changing O_2 concentration over time (slope CO_2/-slope O_2). For ARQ values we applied an outlier removal function, accepting only ARQs between 25% quantile – 1.5*Inter Quartil Range (IQR) and 75% quantile + 1.5*IQR. Data were averaged over 6h time intervals (net efflux of CO_2 (E_{CO2}), net influx of O_2 (I_{O2}) and ARQ) for raw data plotting. We computed daily mean values only when data for the whole 24h period exist.

We used the *lme* function (nlme package; Pinheiro *et al.*, 2017) to perform linear mixed-effect models. We analyzed if treatment influenced E_{CO2} and I_{O2}, ARQ, NSC, $\delta^{13}CO_2$ and $\Delta^{14}CO_2$ month-wise (in 2018 three-week-average). Treatment was considered as a fixed factor, while tree and if applicable sensor ID, to account for the effect of different sensors being installed on trees across years, were considered as random factors. An autocorrelation structure was included into the models to account for temporal correlation. The model's normality of residuals was checked visually (quantile-quantile (Q-Q) plots). All results were expressed as mean ± standard deviation (SD).

Results

CO_2 efflux, O_2 influx and ARQ

E_{CO2} and I_{O2} during the pre-girdling period did not differ between treatments ($p = 0.48$ and $p = 0.53$, for E_{CO2} and I_{O2}, respectively, Fig. 3). After the girdling event in 2018, a significant difference was observed in E_{CO2} between treatments for the measurement period in August ($p < 0.01$). One year after girdling, control and girdled trees differed significantly ($p = 0.03$ and $p = 0.02$, for E_{CO2} and I_{O2} respectively) with a marked decline of E_{CO2} and I_{O2} in girdled trees. However, in 2019 fluxes in control trees were also ca. 40% lower than in 2018. Daily maximum values of 6.7 (control) and 2.4 (girdling) μmol m^{-2} s^{-1} were recorded for E_{CO2}, while for I_{O2} daily maximum values reached 9.7 (control) and 2.9 (girdling) μmol m^{-2} s^{-1} in 2019. In 2021, differences between treatments increased ($p < 0.001$, $p < 0.0001$ for E_{CO2} and I_{O2}). Control fluxes were twice as high as in 2019, roughly the

same as in 2018. Differences between E_{CO2} and I_{O2} were significantly different in all 3 yr ($p < 0.001$).

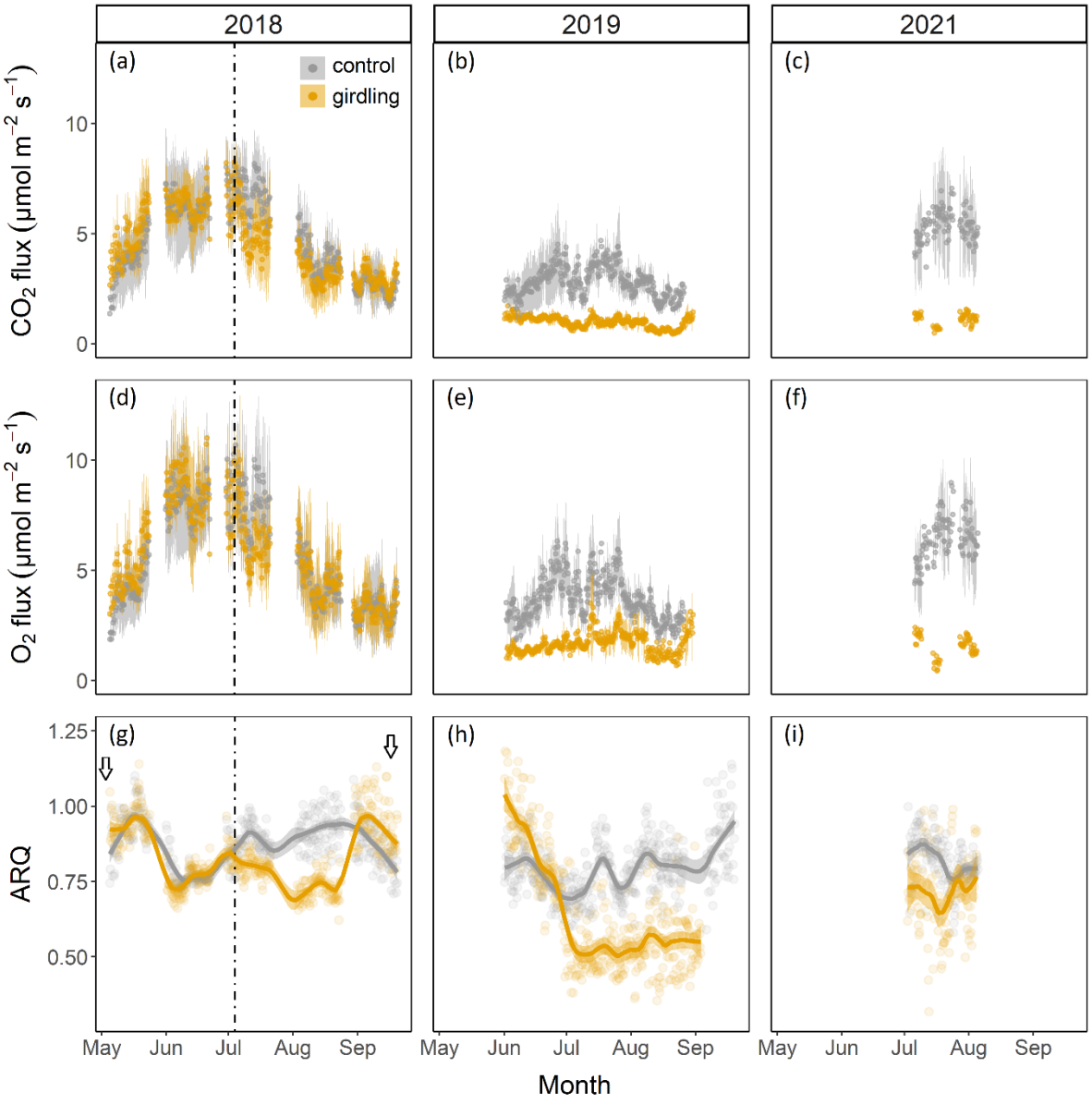

Figure 3 Upper panels: (a-c) CO_2 efflux (E_{CO2}) measurements (6 h mean±SD) in 2018, 2019 and 2021 (a-c). Middle panels: (d-f) O_2 influx (I_{O2}) measurements (6 h mean±SD, absolute values) in 2018, 2019 and 2021 (d-f). Lower panels: (g-i) ratio of CO_2 efflux to O_2 influx (ARQ) in 2018, 21019 and 2021 with LOESS smooth (span = 0.4). Arrows indicate budburst before May and leaf-fall in September. The time of girdling is indicated by the vertical dashed line. All values are 6 h mean±SD ($n = 12$ (2018), $n = 6$ (2019), $n = 8$ (2021)).

Before the girdling, the ratio of E_{CO2} to I_{O2} influx did not differ between treatments ($p = 0.4$) with daily mean ARQ values (±SD) of 0.85±0.1 (control) versus 0.84±0.1 (intended girdling; Fig. 3).

After the girdling event in 2018, daily ARQ values of the two treatments in August differed significantly ($p = 0.02$) with daily mean ARQ values of 0.93±0.03 (control) versus 0.72±0.02 (girdled). In 2019, a treatment effect was visible in mean ARQ values ($p < 0.01$), with 0.77±0.1 (control) versus 0.63±0.2 (girdling) from July until the end of August. In June 2019, ARQ was higher in girdled than in control trees. In summer 2021, mean ARQ values did not differ significantly ($p = 0.4$) with 0.84±0.1 (control) versus 0.78±0.2 (girdling).

Sap flow rate and ARQ in 2018

Sap flow rate (l h^{-1}) clearly decreased after the girdling event (Figure S1 available as Supplementary data at *Tree Physiology* Online). When looking at daily patterns of ARQ in 2018, the ratio was significantly higher during the night (~8pm to ~4am; 0.93 for control, 0.83 for girdling) compared to daytime (~8am to ~4pm; 0.85 for control and 0.79 for girdling), when sap flow rate is maximal (Fig. 4). Negative correlation was found between ARQ and sap flow rates (Pearson correlation, $r^2 = -0.57$, $p < 0.01$ for both control and girdling).

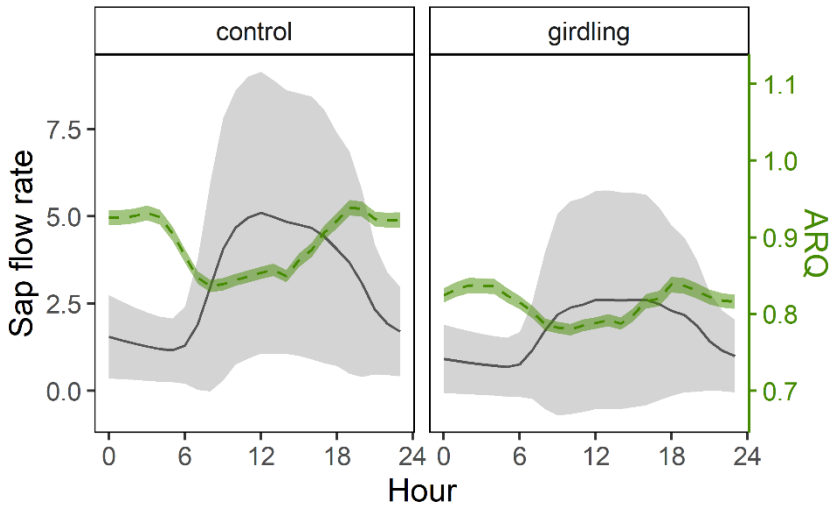

Figure 4 Subdaily values of ARQ and sap flow rate (±SD) for control and girdled trees, respectively (data pooled from 5 July to 30 September 2018).

Non-structural carbohydrates and neutral lipids

Pre-girdling sampling of the outer stem segment (0–6 yr) showed no differences in soluble sugar concentration of the xylem (glucose, fructose, sucrose; mg g^{-1}) ($p = 0.3$) and starch concentration (mg g^{-1}) between treatments ($p = 1.0$; Fig. 5). In 2018 and 2019, starch concentration was lower than 2 mg g^{-1}, independent from treatment. Soluble sugar concentration increased from 1.0 to 5.1 mg g^{-1} after the growing season (09/2018) in control trees. Finally, in 2021, soluble sugar

concentration and starch concentration varied significantly between treatments ($p < 0.001$ and $p < 0.001$, respectively) with mean soluble sugar concentration of 17.5±3.5 mg g^{-1} and mean starch concentration of 11.0±3.0 mg g^{-1} for control trees, while for girdled trees soluble sugar concentration and starch concentration remained low (3.6±4.2 and 1.4±2.2 mg g^{-1}, respectively). The concentrations of soluble sugars and starch in the second stem segment to a maximum depth of ring 14 did not show significant differences in concentrations in all 3 yr (Figure S2 available as Supplementary data at *Tree Physiology* Online).

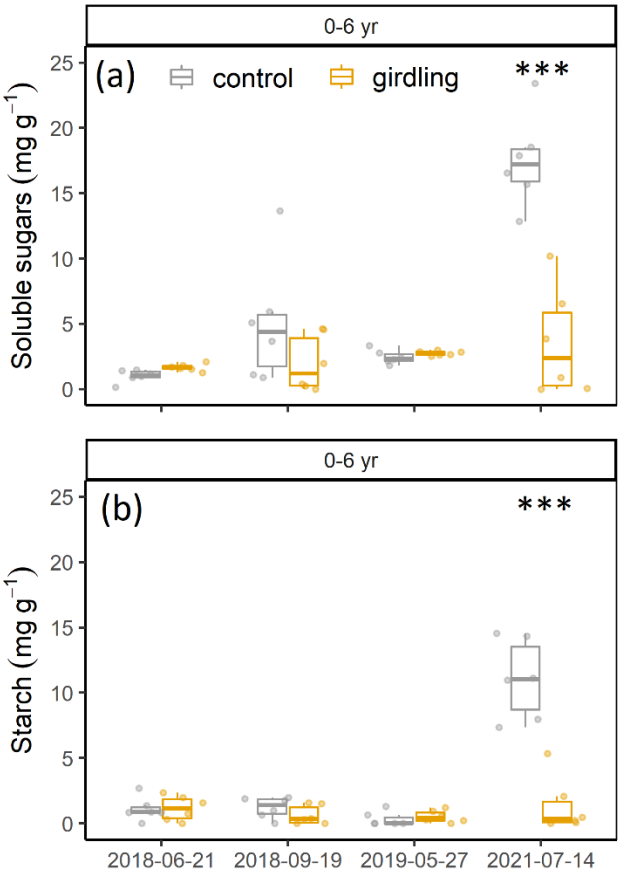

Figure 5 (a) Soluble sugar (glucose, fructose, sucrose) concentration (mg g^{-1}) and (b) starch concentration (mg g^{-1}) before girdling (21 June 2018) and three time points after girdling, extracted from stem cores to a depth of ring 6. Box whisker plots present the median, lower (25^{th}) and upper (75^{th}) percentiles, minimum and maximum values.

Neutral lipids, analyzed in 2021, were 0.76±0.1 and 0.56±0.2% area in control and girdled trees, respectively without a notable treatment effect (Wilcoxon test, $p = 0.4$) and high variability in girdled trees (for individual trees, Table S6 available as Supplementary data at *Tree Physiology* Online). For visualization of histological slices see Picture S3 available as Supplementary data at *Tree Physiology* Online.

^{14}C-based estimates of respired CO_2 age and ^{13}C signature of stem-respired CO_2

Mean age of respired CO_2 from the pre-girdling sampling was 1.4 yr±1.1 (control) versus 1.5 yr±1.3 (girdling) (Fig. 6). For the control trees, C age reached its highest value of 4.0 yr±1.2 in October 2018, after leaves had senesced. By contrast, C age from girdled trees increased up to 15.1±11.8 in 2021. In 2018 and 2019, C age between control and girdled trees was significantly different for certain time points with mean differences of all sampling dates in 2019 of 3.5 yr and 2021 of 7.5 yr (for individual trees, see Table S4 and S5 available as Supplementary data at *Tree Physiology* Online).

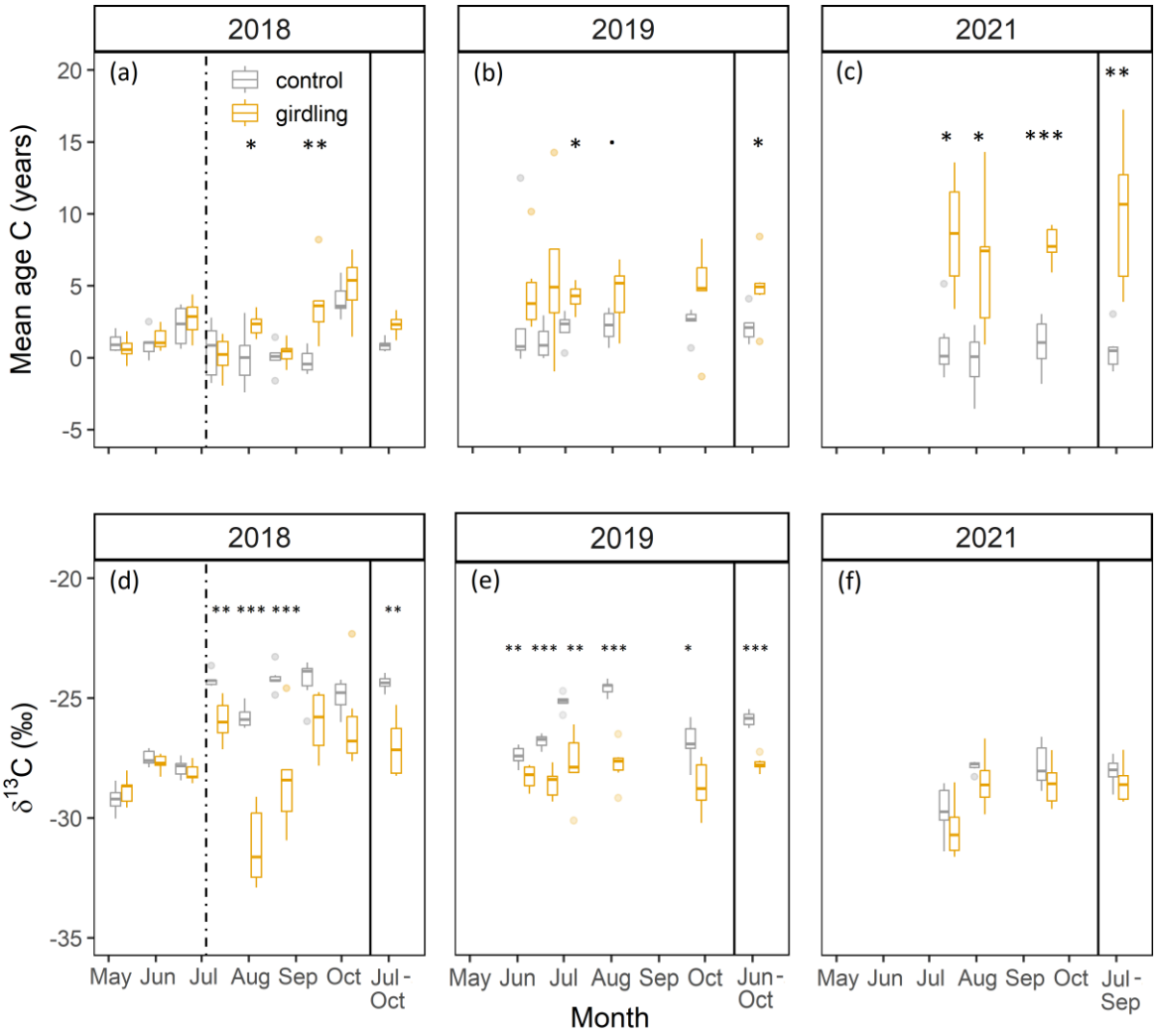

Figure 6 (a-c) Calculated mean age of carbon (^{14}C) of the chamber incubation gas samples of control and girdled poplar trees in (a) 2018, (b) 2019 and (c) 2021. Carbon ages were calculated based on Equ. (2). (d-f) $\delta^{13}C$ of CO_2 of the chamber incubation gas samples of control (n = 6) and girdled (n = 6) poplar trees in (d) 2018, (e) 2019 and (f) 2021. $\delta^{13}C$ was corrected using Equ. (3). The time of girdling is indicated by the vertical dashed line. Asteriks on top represent the statistical differences between the treatments. Box whisker plots present the median, lower (25th) and upper (75th) percentiles, minimum and maximum values.

$\delta^{13}C$ of CO_2 (‰), from the pre-girdling sampling was -28.2‰±0.9 (control) versus -28.2‰±0.8 (girdling) (Fig. 6). One month after the girdling event, mean $\delta^{13}C$ of the collected CO_2 was -25.8‰±0.5 (control) versus -31.2‰±1.6 (girdling). Significant differences between control and girdled trees did occur on specific dates in July and August 2018 and over the whole measurement campaign in 2019. In 2021, mean $\delta^{13}CO_2$ for the three sampling dates was -28.5‰±1.2 (control) versus -29.2‰±1.4 (girdling) without a notable treatment effect ($p = 0.15$). As a general pattern, post-girdling $\delta^{13}CO_2$ values of girdled trees were always lower than $\delta^{13}CO_2$ values of control trees (for individual trees, Table S3 available as Supplementary data at *Tree Physiology* Online), even though in 2021 difference was marginal.

The obtained $\delta^{13}C$ values (±SD) of putative substrates in 2021 were -31.14‰±0.6 (n = 12) in neutral lipids and -27.11‰±0.9 (n = 12) in soluble sugars, without a treatment effect.

Potential PEPC activity in woody tissue

At the end of the growing season in 2019, *in vitro* PEPC activity (±SD) was 568.2±149.2 and 267.3±94.7 nmol g FW min for control and girdled trees, respectively with a notable treatment effect (t-test, $p < 0.001$) (for individual trees see Table S7 available as Supplementary data at *Tree Physiology* Online).

Discussion

Our 3-yr experimental study indicates that the use of a mixture of respiratory substrates with a late contribution of increasingly older reserves provides a mechanism of tree resilience to strong reduction in C supply in poplar trees. Our data suggest that lipid metabolism, indicated by changes in ^{13}C of respired CO_2 (Fig. 7), may allow poplar trees to ride out periods of C starvation, yet, further dedicated studies on lipid metabolism will be helpful. Tree decline may take much longer than the duration of our study, as most of the trees were still alive after the 3-yr starvation manipulation.

Significant differences in carbohydrate pools between treatments developed only over time

In our experiment, we combined short- and longer-term responses of poplar trees to a girdling treatment. We could not confirm an initial decrease in NSC concentration (H1) as concentration in both treatments was very low (starch < 2 mg g^{-1}) in 2018 (Fig. 5). Girdled trees apparently downregulated their metabolism in concern with sugar supply, as suggested by the strong reduction in respiration rates in 2019 (Fig. 3). The downregulation of respiration and growth can be a strategy to maintain certain NSC concentrations in aboveground organs in order to ensure tree survival

(Huang *et al.*, 2019). Reduced growth respiration may explain why sugar concentrations initially remained stable. Girdled trees ceased growth after the girdling event (Figure S3 and Method S2 available as Supplementary data at *Tree Physiology* Online), in accordance with other studies reporting cessation of stem growth below the girdle (Maunoury-Danger *et al.*, 2010; De Schepper & Steppe, 2011; Oberhuber *et al.*, 2017) and reduced growth in chilled mature red maple trees below the phloem restriction (Rademacher *et al.*, 2022). Transport of NSC from neighbouring trees via root grafts has been shown to be critical for survival of root suckers in poplar trees (DesRochers & Lieffers, 2001; Jelínková *et al.*, 2009), however, net exchange between trees usually is very low (Klein *et al.*, 2016) and may not explain why girdled trees were able to maintain NSC concentrations. In other studies on C limitation, no complete depletion of starch reserves had been observed (e.g., Hoch, 2015; Weber *et al.*, 2019) and NSC concentrations of drought-stressed *Picea abies*, also strongly C limited, did not differ to control trees in aboveground organs, whereas only starch reserves in roots strongly declined under drought (Hartmann *et al.*, 2013). However, with regard to stem girdling, various studies showed that NSC concentrations usually decrease below the girdle and/or in the roots, with a concomitant accumulation of NSC above the girdle (Jordan & Habib, 1996; Maunoury-Danger *et al.*, 2010; Regier *et al.*, 2010; De Schepper & Steppe, 2011; Mei *et al.*, 2015).

In our study, significant differences in carbohydrate pools between treatments developed only over time. In 2021, control trees showed significantly greater carbohydrate concentrations with a 5- to 10-fold increase in starch and soluble sugar respectively, potentially because climate conditions had normalized, after the 2018 and 2019 dry years (see below). Surprisingly, concentrations of soluble sugars in two of the 6 girdled trees increased in 2021. We hypothesize a remobilization of NSCs from deeper stem layers or from the roots to the section below the girdle in the stem. Overall NSC concentrations in girdled trees were more or less stable and remained at a low level over the 3 years, despite the lack of new photo-assimilate provision. Some of the observed differences between 2018/2019 and 2021 may be due to seasonal variation of NSCs, as sampling dates differed somewhat between years. Concentrations typically decrease after bud break and then increase in the late growing season (Hoch *et al.*, 2003; Richardson *et al.*, 2013; Scartazza *et al.*, 2013; Martínez-Vilalta *et al.*, 2016), however, seasonal variability of NSCs has been shown to be only 10% in stem sapwood of deciduous trees (Hoch *et al.*, 2003), much less than in our study. Also, as our stem cores were not microwaved, this may have resulted in loss of NSCs to respiration during the initial stage of oven drying (Landhäusser *et al.*, 2018).

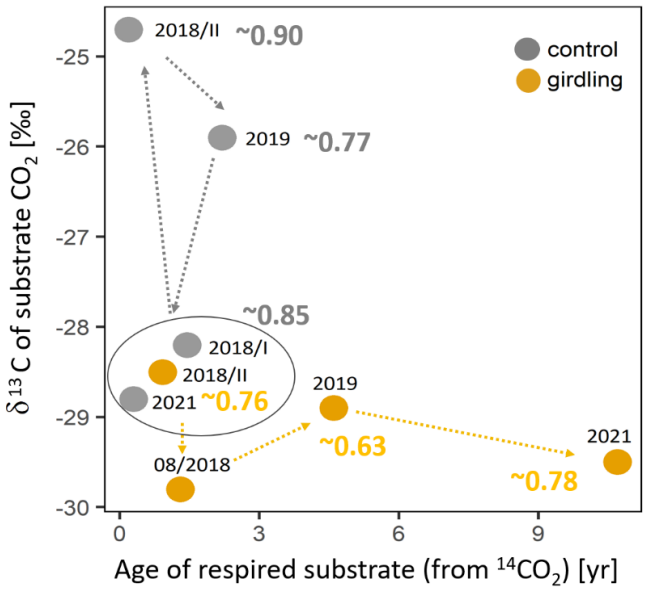

Figure 7 Schematic overview summarizing our results about substrate identity and C mean age. 2018/I refers to pre-girdling and 2018/II refers to post-girdling in 2018. Mean values for the time period June–August (if data available) are shown to avoid seasonal effects. Numbers in bold refer to mean ARQ values. Control trees use fresh photosynthesis product over the study period. After the girdling in 2018 and 2019, the $\delta^{13}CO_2$ signal is more enriched, which is possible due to drought effects of those years, while 2021 is comparable with the pre-girdling measurement. ARQ values of ≤0.85 might be explained by a mixture of respiratory substrates, including carbohydrates and lipids. However, ARQ values cannot be seen as a substrate-use indicator alone, as (post-) respiratory processes can affect this ratio (see further explanations in 'The contribution of lipids during starvation'). In girdled trees, we observed a lower $\delta^{13}CO_2$ signal in August 2018 as trees start to use lipids for respiration. After this initial decline, $\delta^{13}CO_2$ signal and ARQ values points towards the use of a mixture of respiratory substrates (COH and lipids). A progressive increase in the mean age of C was observed.

Slow mobilization of older carbohydrate storage pools 3-yr after girdling

In accordance with our hypothesis (H1), poplar trees accessed older C pools once the supply of fresh assimilates was disrupted. In a girdling study in the Amazon rainforest, trees that were presumably older than 100 yr used ~ 6 yr old C, already two months after stem girdling (Muhr *et al.,* 2018) while our ^{14}C data indicated a delayed use of older C reserves (Fig. 6). Girdled trees respired slightly older C than control trees starting in late summer 2018, except for the date in October, when leaf shedding was almost complete and both treatments used older stored C. In girdled trees, the age of respired CO_2 increased up to a maximum of 15 years (average 2021: 7.5 yrs). These values were in accord with previous studies showing maximum C age of 14 yr after girdling of tropical trees (Muhr *et al.*, 2018) and decade old stored C in temperate trees (Richardson

et al., 2013). Control trees relied mostly on recent photo-assimilates throughout the 3-yr period (Fig. 7). But, mixing of young and old NSCs for stem respiration was also reported in undisturbed mature oak trees (Trumbore *et al.*, 2015).

The contribution of lipids during starvation

We found evidence supporting our second hypothesis (H2), that poplar trees mobilize and metabolize lipids after starvation via girdling. In August 2018, $\delta^{13}CO_2$ values close to -30‰ (Fig. 6 and 7) indicate that a substantial amount of CO_2 originates from lipid catabolism ($\delta^{13}C$ of neutral lipids ~-32‰, data not shown) but see also 4.4. We found substantial average differences between treatments in $\delta^{13}CO_2$ (2.5‰), starting already within one month after girdling, indicating that control and girdled trees did not use the same respiratory C source mixture. For control trees, we assume that poplar use a mixture of carbohydrates and lipids supporting respiration (Fig. 7; mean ARQ: ~ 0.85, mean $\delta^{13}CO_2$ ~-28.5‰), similar to what have been found in *Pinus sylvestris* (Fischer *et al.*, 2015). In general, we observed high seasonal variations in control trees (e.g., -29.22‰ (05/2018) to -24.17‰ (08/2018); Table S3 available as Supplementary data at *Tree Physiology* Online), most likely with increased values during stem growth (Damesin & Lelarge, 2003) and seasonal variations due to phenological changes (e.g., leaf growth, senescence) (Seibt *et al.*, 2008). The observed decline in ARQ values after the girdling treatment in autumn 2018 was followed by a more drastic decline in ARQ values during the summer months in 2019 (~ 0.63, Fig. 3 and 7), indicating the contribution of lipids to maintain metabolism during starvation. During shading-induced starvation, Fischer *et al.* (2015) found evidence for lipid metabolism, with ARQ ratios ~ 0.7 in *Pinus sylvestris* trees. In May/June (2018, 2019) we observed highest ARQ, which could indicate the use of carbohydrates caused by mobilization of reserves. The treatment effect in ARQ and $\delta^{13}CO_2$ decreased then towards the end of the seasons, likely because remobilization of storage decreased at the onset of dormancy. Despite the high soluble sugar and starch concentrations observed in control trees in 2021, we found no clear difference in $\delta^{13}CO_2$ or ARQ in that year. By contrast, we observed with the histological staining method (Table S6 available as Supplementary data at *Tree Physiology* Online) the depletion of lipids in one of the girdled trees in 2021, but dedicated studies to address lipid distribution in stem wood would be necessary to fully understand lipid metabolism in stems under C limitation.

ARQ is an useful indicator for respiratory substrate use, but a variety of other processes, like stem photosynthesis, CO_2 transport in the sap, or CO_2 refixation, can lead to lower than 1 ARQ values (see Trumbore et al., 2013 for a summary). In our study, we can neglect stem photosynthesis because we used opaque chambers. Stem photosynthesis around the chamber could generate a

gradient of CO_2, and cause axial diffusion of CO_2 from the chamber to the illuminated parts, affecting ARQ (De Roo *et al.*, 2019). Also, high solubility of CO_2 in the xylem sap may facilitate import to or export from the site of measurement (Teskey & McGuire, 2007; Aubrey & Teskey, 2009; Bloemen *et al.*, 2013). Considering that sap flow was reduced in girdled trees in 2018 (Figure S1 available as Supplementary data at *Tree Physiology* Online), indicating a limited amount of upward transport, we would expect a correlation between sap flow and absolute deviation of ARQ from unity. Refixation of CO_2 via the enzyme phosphoenolpyruvatecarboxylase (PEPC) might remove CO_2 locally, but we found ~ 50% reduced PEPC activity in girdled trees the year after girdling (Table S7 available as Supplementary data at *Tree Physiology* Online), which suggests a limiting role of pepc-mediated C fixation in lowering ARQ values.

Potential effect of the exceptional 2018-2019 drought

Our study coincided with the exceptionally dry and hot summers in 2018 and 2019 in Central Europe, during which C supply may have been impaired also in control trees from reduced C assimilation. A tree ring analysis showed ~50% reduced tree ring width in 2019, but also in 2020, which can be seen as a legacy effect of drought (e.g., Miller *et al.*, 2023) (Figure S3 available as Supplementary data at *Tree Physiology* Online). While in 2018, trees either were still able to cope with the dry and hot conditions, or were simply not yet severely affected by the 2018 summer drought at the north slope where our study was located. E_{CO2} and I_{O2} were reduced by ~40% in 2019 compared to 2018 in control trees, which could potentially be explained by the drought effect in 2019. Similar results (50% decline in E_{CO2}) were observed in *Quercus ilex* when soil predawn water potential decreased (Rodríguez-Calcerrada *et al.*, 2014). Drought-induced decline in stomatal conductance would also lead to increased $\delta^{13}C$ values of CO_2 (due to changes in photosynthetic discrimination; Farquhar *et al.*, 1989; Högberg *et al.*, 1995), as most likely observed in 2018 and 2019. Compared to wetter years, an increase in $\delta^{13}CO_2$ of control trees might also be due to starch hydrolysis, as an alternative and more enriched C source that causes a shift towards a more enriched CO_2 pool (Maunoury-Danger *et al.*, 2010). In 2021, control trees showed no longer an enriched $\delta^{13}C$, possibly because fresh C no longer had a drought signal in $\delta^{13}C$. Overall, we critically note that we did not assess tree water relations, and that we lack evidence of how severe the drought stress was**.**

Outlook

Storage use provides a buffer and enables long-term survival under periods when C supply from the canopy is not given. Insights about how long trees can store and access reserve compounds, in

response to changes in source-sink relationships, are highly needed to improve our understanding of tree resilience under ongoing climate change. Several studies have highlighted shortcomings in the representation of tree stress responses and resilience, mediated by C storage, in vegetation models (Ogle & Pacala, 2009; DeSoto *et al.*, 2020; Peltier & Ogle, 2020; Hartmann *et al.*, 2022). The common assumption that assimilated C via photosynthesis is directly respired to the atmosphere needs to be updated for model improvement (Sierra *et al.*, 2022) as it is contradictory to our study results and previous empirical evidence (Vargas *et al.*, 2009; Carbone *et al.*, 2013; Muhr *et al.*, 2013; Muhr *et al.*, 2018). Combining empirical studies on remobilization and metabolization of C with C dynamic models may help improve predictions and constrain model parameters (Sierra *et al.*, 2022).

Acknowledgements

We want to thank Savoyane Lambert, Agnes Fastnacht, Nadine Hempel and Sophie von Fromm for the support in the field; Martin Göbel, Reimo Leppert, Bernd Schlöffel, Frank Voigt, Martin Strube for the technical support; Iris Kuhlmann, Anett Enke, Janin Naumann, Christin Leschick, Sonja Rosenlöcher, Stephanie Strahl for the support in the laboratory. We thank Christine Römermann for the possibility to use the optical digital microscope. We thank Heiko Moossen and Petra Linke for $\delta^{13}C$ analysis; Axel Steinhof and the Jena ^{14}C laboratory for ^{14}C analysis. We thank Olaf Kolle for technical support (sensor calibration) and for providing the meteorological data from the site. We thank Gerd Gleixner for helpful input, Yves Gibon for helpful comments and edits about PEPC fixation and Cédric Cassan for PEPC analysis. Reviews by three anonymous reviewers were very helpful in improving this paper.

Funding

This study was funded by the Max Planck Society and the European Research Council (Horizon 2020 Research and Innovation Programme, grant agreement 695101, 14Constraint.

General discussion and outlook

This doctoral thesis was motivated by the need to improve our understanding of carbon (C) dynamics in mature trees. Our mechanistic understanding of the respiratory processes at the stem-level is limited which hinders accurate stem respiration (R_S) estimates (e.g., Meir *et al.*, 2017; Teskey *et al.*, 2017). Large amounts of C can also be stored within the stem wood. It is of great importance to understand how mature trees utilize stored C reserves to survive under stress (e.g., Regier *et al.*, 2009; Hartmann & Trumbore, 2016). I addressed three current challenges within this thesis: i) to develop a field-robust method for simultaneous measurements of CO_2 efflux and O_2 influx at the stem-surface to better constrain local respiration, ii) to elucidate the fate of respired CO_2 by simultaneously measuring CO_2 (internal and at the stem-surface) and O_2 fluxes (at the stem-surface) in the same trees, and iii) to explore whether stressed trees shift respiration supply from carbohydrates to alternative storage compounds to ensure survival under reduced C supply.

Simultaneous CO_2 and O_2 flux measurements between tree stems and the atmosphere revealed discrepancy between both gases

Respiration is a sensitive process that changes rapidly with environmental and physiological variations. Hence, developing the first quasi-continuous measurement system for simultaneous CO_2 and O_2 fluxes to better constrain respiratory processes (**Chapter 2**) was the basis for all subsequent experimental approaches that I performed as part of my dissertation. Having a highly mobile, easy-to-use and quasi-autonomous system available allowed me to provide new insights into seasonal, diurnal and along-stem variations in respiratory fluxes.

By comparing both gases (CO_2 and O_2), I showed that between 10 and 30% of CO_2 was not locally emitted but was retained in the stem of mature trees (**Chapter 2-4** (control trees)). Further, I observed a greater difference between CO_2 efflux and O_2 influx during the day (**Chapter 3, 4**), indicating that high sap flow might facilitated the transport of respired CO_2 away from its point of production This clearly showed that efflux-based methods (especially during day-time) underestimate the true respiration rate at the stem-level. I will discuss the sources for the CO_2

retention and its implications in more detail in the next sections when synthesizing the main findings of the two experimental studies (**Chapter 3, 4)**.

CO_2 mass balance approach and oxygen-based approach: The mismatch between CO_2 efflux and O_2 influx cannot be primarily explained by internal fluxes, but is also linked to an alternative sink of respired CO_2

Understanding missing C sinks in respiration budgets is essential to improve predictions of respiratory C loss under changing climate conditions (Carey *et al.,* 1997; Huntingford *et al.,* 2017). However, the fate of respired CO_2 in tree stems remains inconclusive, and the combined use of different measurement approaches could help to shed light on this line. The novelty of the field study in **Chapter 3** was the concurrent application of the CO_2 mass balance approach (MBA) and the simultaneous measurement of O_2 (oxygen-based approach) in the same individuals to mechanistically understand CO_2 production and movement across the stem.

In the beech trees surveyed here in July and August 2019, 30% of the respired CO_2 was retained in the stem. This is based on the assumption that trees use carbohydrates for respiration. We hypothesized that xylem CO_2 transport and storage could explain the mismatch between CO_2 and O_2 due to the lower solubility of O_2 in the xylem sap compared to CO_2. However, in contrast to our expectation, internal fluxes (xylem CO_2 transport and storage) could only partially explain the difference between CO_2 efflux and O_2 influx. Our results indicated that measurements at the stem surface, conducted with chamber-based methods, most likely reflect respiration in the outermost tissues of the stem (bark, phloem, cambium and outer xylem) but poorly reflect the respiratory activity in the inner sapwood in mature trees. Moreover, in this thesis, I provided novel evidence for an alternative sink of respired CO_2. PEPC (phosphoenolpyruvatcarboxylase)- mediated CO_2 fixation can be a relevant driver of the mismatch between CO_2 efflux and O_2 influx in mature trees. We measured high PEPC-capacity in the outer stem tissues, similar to values from green current-year twigs (Berveiller & Damesin, 2008). This observation implies that PEPC fixation can be a relevant mechanism of local CO_2 removal that needs to be considered to complete the stem C balance.

Poplar trees are well buffered against multi-year C shortage by using a mixture of respiratory substrates and taping into older C reserves in the long term

Predicting tree survival under environmental stress requires a better understanding of the dynamics of respiratory metabolism and C reserve use. However, the availability and usage of such C

reserves in field-grown mature trees is still very limited (e.g., Gessler & Treydte, 2016; Hartmann & Trumbore, 2016).

We manipulated the access to new photo-assimilates by girdling mature poplar trees. Hereby, phloem C transport to the lower stem was permanently interrupted, forcing trees to rely on C reserves (**Chapter 4**). I combined a unique dataset of long-term (i.e. two and a half growing seasons) isotopic measurements of respired CO_2 ($^{14}CO_2$ and $^{13}CO_2$) and apparent respiratory quotient (ARQ) to infer the respiratory substrates and the age of the respired C. Remarkably, some of the trees in our study were still alive 4 years after girdling. Long-term survival of the trees was possible by downregulating metabolism and mobilizing up to 15-yr-old C to sustain respiration in the long term. The age of respired CO_2 was in accordance with decade-old C reserve use after girdling of tropical trees (Muhr *et al.,* 2018). As a consequence of reduced photo-assimilates, ARQ, as an useful tracer to identify respiratory substrates, suggested the contribution of storage lipids to respiration. This has been shown in previous work for young *Pinus sylvestris* trees under experimental shading in a greenhouse study (Fischer *et al.*, 2015; Hanf *et al.*, 2015). The results of the $\delta^{13}CO_2$ signal indicated that poplar trees use lipids for respiration one month after girdling. After this initial decline in $\delta^{13}CO_2$, our results suggested the use of a mixture of respiratory substrates (carbohydrates and lipids). The observed change in metabolism from recent carbohydrates to older storage pools with a mixture of carbohydrates and lipids can explain why the decline of tree vigor may take many years until death occurs. Multi-year field experiments can greatly enhance our mechanistic understanding of storage dynamics inside stems of mature trees. Our findings imply that in species that store C not only in the form of carbohydrates but also in the form of lipids, these currently overlooked alternative compounds must be considered as potential reserves that allows trees to survive for several years under C-limiting conditions.

Conclusion and Outlook

The results obtained within this thesis have important implications for our understanding of respiratory processes and the role of stems in C metabolism of trees. Respiration is a key factor to determining if a forest ecosystem acts as net C sink or source (Valentini *et al.*, 2000). Current CO_2-efflux based estimates most likely underestimate the contribution of R_S to ecosystem respiration. Integrating O_2 and CO_2 measurements can better constrain local respiration and accounting for the mismatch will improve current estimates of R_S. The need to analyze internal C fluxes and C-refixation mechanisms is imperative for quantifying 'real' R_S, and further research into O_2-consuming processes should additionally be considered. The ability of mature trees to use

alternative substrates for respiration and to remobilize older C storage pools adds an important contribution to our understanding of tree resilience to changing climate conditions.

Despite the novel insights on R_S, their underlying regulatory factors and the important role of C reserves in tree's resilience capability, new questions and challenges arise that need to be addressed in future research. Many opportunities for prospective explorations of the complex nature of CO_2 inside tree stems are summarized in the review article (**Chapter 1**). I would like to call special attention to the following points: (1) sap pH measurement in the stem, (2) scaling respiratory processes from stems to the ecosystem, (3) implementing empirical datasets into stem respiration modelling and (4) recycling and storage of C during drought. I will discuss each of these suggestions in detail in the following sections.

Continuous measurements of xylem sap pH in the stem

One urgent task for future work is to develop a reliable method for *in situ* pH measurements in the stem that can be included as a standard procedure for R_S measurement protocols. Sap pH, especially above 6–6.5 (e.g., Levy *et al.*, 1999; Erda *et al.*, 2014), is a critical factor for calculating the transport and storage of CO_2 (from the MBA), as the solubility of CO_2 increases exponentially with pH. Sap pH is currently measured from twigs far away from the site of CO_2 measurements at the stem (**Chapter 1, 3**) and potential discrepancies between twigs and stem may become greater in mature trees. Another open question is the temporal variability (short- and long-term) of stem pH values, and whether twig sampling can reflect those changes (Erda *et al.,* 2014). Unfortunately, a first attempt from our group to achieve continuous measurements of xylem sap pH of trees *in situ*, using gastric probes from medical applications, was not successful. Quantifying the magnitude of CO_2 transport within the xylem is essential to estimate total respiration rate (based on the MBA). New technical innovations (**Chapter 1**) would bring us closer to overcome technical difficulties and solving this fundamental issue.

Linking stem respiratory processes across scales: from stems to trees to ecosystems

Along a stem gradient

Due to limited accessibility of elevated regions of the stem and canopy, R_S has been measured almost exclusively at breast height. To estimate whole R_S, studies typically upscale breast height measurements. This overlooks within-tree variation. For example, an underestimation of annual tree-scale CO_2 efflux by up to 17% was observed when comparing modelled versus observed effluxes along the stem of spruce trees (1.3, 10 and 18 m; Tarvainen *et al.*, 2014). In **Chapter 3**, I found no apparent vertical pattern in stem CO_2 efflux and O_2 influx along a 3-m-long stem segment.

This is probably due to the modest vertical gradient (3 m) in 38 m tall beech trees. It is still largely unknown how fluxes will change along the entire stem gradient of large trees. Following up on the work in **Chapter 3**, more infrastructure is needed e.g. by the use of a canopy crane to tackle this challenge. Future studies should incorporate chamber-based measurements and internal CO_2 flux measurements, with morphological, anatomical or physiological traits influencing the diffusivity, solubility, and transport of respired CO_2 (e.g., sapwood density, bark thickness, stem temperature) along the whole stem gradient. Further research should also consider sapwood depth gradients to asses the contribution of inner and outer tissue respiration to total R_S. Investigating within-tree variation is necessary to avoid miscalculation of the entire tree R_S (**Chapter 1**).

Whole-tree level ARQ and implication for the ecosystem-level

Future work should expand to the entire tree-level ARQ. I measured lower than unity ARQ values in two deciduous tree species and during different time of the year (**Chapter 2-4**). If the local ARQ below one is explained by a net export of locally respired CO_2, we have to assume that other tree compartments (foliage, branches, roots) experience a net import of CO_2, resulting in an ARQ above one. In this regard, future research can profit from our general chamber setup (**Chapter 2**), as the current device can be used for flux measurements in other tree compartments, such as root, branch or leaf, with only minor modifications.

One may ask whether our findings have implications at the ecosystem scale. The O_2:CO_2 ratio of the global terrestrial biosphere is around ~1 (1.04; Worrall et al., 2013), therefore we can assume a CO_2:O_2 ratio (ARQ) of 1 with narrow variability at the ecosystem-level. Emissions that are not detected at one location or in one plant compartment should end up at another plant compartment (Meir *et al.,* 2017). The overall ecosystem ARQ will not be affected, but measurements in different plant compartments and different forest components are still required to understand tree and forest respiratory processes.

Our results showed a clear retention of respired CO_2 in the stem of poplar and beech trees under normal environmental conditions, when measuring CO_2 and O_2 in parallel. This leads to the conclusion that the contribution of R_S to the forest C balance may be larger than previously estimated (from CO_2 efflux measurements). The same has been shown for belowground respiration. Neglecting internal CO_2 flux from tree roots through the stem resulted in underestimation of total belowground respiration (18% in *Quercus* species; up to 50% in *Populus deltoides*) (Aubrey & Teskey 2009; Bloemen *et al.*, 2014; Salomón *et al.*, 2015). A comprehensive understanding of the pathways of CO_2 within forest ecosystems is crucial to improve predictions of respiration and ultimately of the forest C balance under future climate change scenarios.

On the need to implement empirical datasets into stem respiration modelling

Plant respiration estimates are commonly based on temperature-dependent equations or calculated as a fixed fraction of the difference between gross primary production (GPP) and whole-plant maintenance respiration (Atkin *et al.,* 2017; Fatichi *et al.,* 2019; for details see also **Chapter 1**). Additional factors like substrate availability, water status or oxygen concentration within woody tissues are commonly ignored by large-scale models, as well as the fact that GPP changes with stand age and across biomes (e.g., DeLucia *et al.*, 2007; Piao *et al.*, 2010). Recent modeling efforts have been made by developing a process-based model of R_S that couples water and carbon fluxes at the stem-level (e.g., Salomón *et al.*, 2019a). However, we are still far from implementing mechanistic insights into large-scale models. The quotation from Gifford (2003): "Plant respiratory regulation is too complex for a mechanistic representation in current terrestrial productivity models for carbon accounting and global change research" is still relevant today. For future research, I underscore the need to implement empirical datasets collected globally across broad gradients of environmental conditions into R_S modeling routines, as has been done for the leaf (Atkin *et al.*, 2015; Heskel *et al.*, 2016). Empirical data of combined CO_2 and O_2 measurements, as provided by our stem-chamber device, can serve as important input and calibration variables for mechanistic models of tree respiration and stem functioning. Such efforts are much needed to improve model predictions and further advance our mechanistic understanding of R_S.

Recycling and storage of C during drought

Ongoing climate change has triggered a growing interest in drought-induced tree mortality during the past ~15 years (McDowell *et al.*, 2008; Allen *et al.*, 2010) with a particular interest in unravelling the C dynamics during drought (e.g., Sala *et al.*, 2012; Adams *et al.*, 2013; Piper & Fajardo, 2016). Especially after the recent drought events and increased tree mortality in central Europe in 2018 and 2019, there is a need to better understand the regulation and functioning of tree C dynamics. This understanding is crucial to predict tree resilience under changing climate conditions. I want to highlight two aspects aligned with this thesis that are of interest for future research: i) the recycling of internal C and ii) further insights into lipid storage pools.

Internal recycling/refixation of CO_2

Recycling of respired CO_2 within woody tissues may be conducive in periods of drought stress. When photosynthetic activity in leaves is limited due to stomatal closure, C fixation by photosynthetic bark can prevent the risk of C starvation and increase drought tolerance. Cortical photosynthesis can provide local sugars and compensate for the reduced long-distance sugar

transport from the leaves to woody tissue (Bloemen *et al.,* 2016; De Baerdemaeker *et al.,* 2017; De Roo *et al.,* 2020). Further research e.g., by light exclusion treatments of the stem and manipulations of temperature, atmospheric CO_2 concentration, and water availability can help to further unravel the role of cortical photosynthesis with respect to varying climate conditions.

Additionally, the internal tree C from PEPC fixation might become progressively important under C-limiting conditions. Enhanced PEPC activity in the roots of young girdled beech trees could provide additional C when supply is restricted (Clausing *et al.,* 2021). Contrary to our expectations, we found reduced PEPC capacity in girdled trees 1-yr after girdling, denoting a limiting role in compensating for reduced C supply (**Chapter 4**). Nevertheless, broader consideration of this mechanism to maintain the C status (under, e.g. a lack of new photo-assimilates from the canopy) in different tree species and along sapwood depth gradients is needed before concluding about the relevance of this C recycling mechanism in a changing climate.

Further insights into lipid storage pools

In tree species that store C in the form of carbohydrates and lipids (Sinnott, 1918; Höll, 1997; Hoch *et al.*, 2002; Hoch *et al.*, 2003), progress can be made in quantifying and localizing neutral lipids in the wood. The quantification of lipids remains challenging, but histological staining methods (Grimberg *et al.*, 2018; Herrera-Ramírez *et al.,* 2021) in combination with imaging analysis can facilitate broader implementation in future studies about C storage pools in trees (**Chapter 4**). Interestingly, lipid storage correlated with lower mortality rates in tropical trees (Herrera-Ramírez *et al.*, 2021), and this might suggest that lipid-storing tree species may be more resilient to future drought events. The staining method can bring new insights into where and how much lipids are stored, and therefore could give valuable insights into lipid metabolism in mature trees. In addition, a similar method for analyzing the spatial distribution of starch has recently been presented (Herrera-Ramírez *et al.*, 2021). With further in-depth investigations, considering different tree species, seasonal sampling, and the radial distribution from the bark towards the pith, those techniques offer a great potential to assess lipid and starch storage strategies in trees which would help to predict tree survival under constraining conditions.

Overall, this thesis dealed with C dynamics at the stem-level. With ongoing climate warming, understanding the factors determining C losses and the dynamics of C storage in trees is fundamental to understand how forest ecosystems respond to climate change and trees ensure survival. However, further studies about tree C dynamics under drought need to be coupled with other mechanisms such as changes in tree water relations, xylem dysfunction, or phloem transport

failure (e.g., McDowell, 2011; Sevanto *et al.*, 2014; Hartmann, 2015; Dannoura *et al.,* 2019) in order to better understand drought impacts on forests. The combination of water and C relations provide a good framework for understanding the complex physiological causes of tree mortality (Hartmann *et al.*, 2018; Hajek *et al.*, 2022). Field experiments, greenhouse studies, and observations during naturally occurring drought events should be complemented by a close collaboration between modelers and experimentalists to improve projections of forest mortality under future climate change scenarios. This is a much needed and demanding task going forward (e.g., Anderegg *et al.*, 2015; Trumbore *et al.*, 2015a; Hartmann *et al.*, 2018).

Bibliography

Abadie C, Tcherkez G. 2019. In vivo phosphoenolpyruvate carboxylase activity is controlled by CO2 and O2 mole fractions and represents a major flux at high photorespiration rates. *New Phytologist* **221**(4): 1843-1852.

Abson DJ, Von Wehrden H, Baumgärtner S, Fischer J, Hanspach J, Härdtle W, Heinrichs H, Klein A, Lang D, Martens P. 2014. Ecosystem services as a boundary object for sustainability. *Ecological Economics* **103**: 29-37.

Acosta M, Pavelka M, Pokorný R, Janouš D, Marek MV. 2008. Seasonal variation in CO2 efflux of stems and branches of Norway spruce trees. *Annals of botany* **101**(3): 469-477.

Adams HD, Germino MJ, Breshears DD, Barron-Gafford GA, Guardiola-Claramonte M, Zou CB, Huxman TE. 2013. Nonstructural leaf carbohydrate dynamics of *Pinus edulis* during drought-induced tree mortality reveal role for carbon metabolism in mortality mechanism. *New Phytologist* **197**(4): 1142-1151.

Adams HD, Macalady AK, Breshears DD, Allen CD, Stephenson NL, Saleska SR, Huxman TE, McDowell Ng. 2010. Climate-induced tree mortality: Earth system consequences. *Eos, Transactions American Geophysical Union* **91**(17): 153-154.

Adams HD, Zeppel MJ, Anderegg WR, Hartmann H, Landhäusser SM, Tissue DT, Huxman TE, Hudson PJ, Franz TE, Allen CD. 2017. A multi-species synthesis of physiological mechanisms in drought-induced tree mortality. *Nature ecology & evolution* **1**(9): 1285-1291.

Allan RP, Hawkins E, Bellouin N, Collins B. 2021. *IPCC, 2021: Summary for Policymakers.* Global Warming of 1.5°C. An IPCC Special Report on the Impacts of Global Warming of 1.5°C above Pre-Industrial Levels and Related Global Greenhouse Gas Emission Pathways, in the Context of Strengthening the Global Res, IPCC. Geneva. Switzerland. 2018.

Allen CD, Breshears DD, McDowell NG. 2015. On underestimation of global vulnerability to tree mortality and forest die-off from hotter drought in the Anthropocene. *Ecosphere* **6**(8): 1-55.

Allen CD, Macalady AK, Chenchouni H, Bachelet D, McDowell N, Vennetier M, Kitzberger T, Rigling A, Breshears DD, Hogg ET. 2010. A global overview of drought and heat-induced tree mortality reveals emerging climate change risks for forests. *Forest Ecology and Management* **259**(4): 660-684.

Amthor JS. 2003. Efficiency of lignin biosynthesis: a quantitative analysis. *Annals of botany* **91**(6): 673-695.

Amthor JS 1995. Higher plant respiration and its relationships to photosynthesis. *Ecophysiology of photosynthesis*: Springer, 71-101.

Amthor JS. 1989. Crop growth and maintenance respiration. *In: Respiration and crop productivity.* Springer. New York. NY. pp 69-104.

Anderegg WR, Hicke JA, Fisher RA, Allen CD, Aukema J, Bentz B, Hood S, Lichstein JW, Macalady AK, McDowell N. 2015. Tree mortality from drought, insects, and their interactions in a changing climate. *New Phytologist* **208**(3): 674-683.

Anderegg WR, Kane JM, Anderegg LD. 2013. Consequences of widespread tree mortality triggered by drought and temperature stress. *Nature climate change* **3**(1): 30-36.

Angert A, Muhr J, Negron Juarez R, Alegria Muñoz W, Kraemer G, Ramirez Santillan J, Barkan E, Mazeh S, Chambers J, Trumbore SE. 2012. Internal respiration of Amazon tree stems greatly exceeds external CO2 efflux. *Biogeosciences* **9**(12): 4979-4991.

Angert A, Sherer Y. 2011. Determining the relationship between tree-stem respiration and CO2 efflux by δO2/Ar measurements. *Rapid Communications in Mass Spectrometry* **25**(12): 1752-1756.

Araújo WL, Tohge T, Ishizaki K, Leaver CJ, Fernie AR. 2011. Protein degradation–an alternative respiratory substrate for stressed plants. *Trends in plant science* **16**(9): 489-498.

Aschan G, Pfanz H. 2003. Non-foliar photosynthesis–a strategy of additional carbon acquisition. *Flora-Morphology, Distribution, Functional Ecology of Plants* **198**(2): 81-97.

Aschan G, Wittmann C, Pfanz H. 2001. Age-dependent bark photosynthesis of aspen twigs. *Trees* **15**(7): 431-437.

Atkin OK, Bahar NH, Bloomfield KJ, Griffin KL, Heskel MA, Huntingford C, Torre AMdl, Turnbull MH 2017. Leaf respiration in terrestrial biosphere models. *Plant respiration: Metabolic fluxes and carbon balance*: Springer, 107-142.

Atkin OK, Bloomfield KJ, Reich PB, Tjoelker MG, Asner GP, Bonal D, Bönisch G, Bradford MG, Cernusak LA, Cosio EG. 2015. Global variability in leaf respiration in relation to climate, plant functional types and leaf traits. *New Phytologist* **206**(2): 614-636.

Atkin OK, Bruhn D, Hurry VM, Tjoelker MG. 2005. Evans Review No. 2: The hot and the cold: unravelling the variable response of plant respiration to temperature. *Functional Plant Biology* **32**(2): 87-105.

Aubrey DP, Boyles JG, Krysinsky LS, Teskey RO. 2011. Spatial and temporal patterns of xylem sap pH derived from stems and twigs of *Populus deltoides* L. *Environmental and Experimental Botany* **71**(3): 376-381.

Aubrey DP, Teskey RO. 2009. Root-derived CO2 efflux via xylem stream rivals soil CO2 efflux. *New Phytologist* **184**(1): 35-40.

Ávila E, Herrera A, Tezara W. 2014. Contribution of stem CO2 fixation to whole-plant carbon balance in nonsucculent species. *Photosynthetica* **52**(1): 3-15.

Baldocchi DD. 2020. How eddy covariance flux measurements have contributed to our understanding of Global Change Biology. *Global change biology* **26**(1): 242-260.

Barker Plotkin A, Blumstein M, Laflower D, Pasquarella VJ, Chandler JL, Elkinton JS, Thompson JR. 2021. Defoliated trees die below a critical threshold of stored carbon. *Functional Ecology* **35**(10): 2156-2167.

Bastos A, Orth R, Reichstein M, Ciais P, Viovy N, Zaehle S, Anthoni P, Arneth A, Gentine P, Joetzjer E. 2021. Vulnerability of European ecosystems to two compound dry and hot summers in 2018 and 2019. *Earth System Dynamics* **12**(4): 1015-1035.

Battle MO, Munger JW, Conley M, Sofen E, Perry R, Hart R, Davis Z, Scheckman J, Woogerd J, Graeter K. 2019. Atmospheric measurements of the terrestrial O2: CO2 exchange ratio of a midlatitude forest. *Atmospheric Chemistry and Physics* **19**(13): 8687-8701.

Beech E, Rivers M, Oldfield S, Smith P. 2017. GlobalTreeSearch: The first complete global database of tree species and country distributions. *Journal of Sustainable Forestry* **36**(5): 454-489.

Bénard C, Gibon Y. 2016. Measurement of enzyme activities and optimization of continuous and discontinuous assays. *Current Protocols in Plant Biology* **1**(2): 247-262.

Berveiller D, Damesin C. 2008. Carbon assimilation by tree stems: potential involvement of phosphoenolpyruvate carboxylase. *Trees* **22**(2): 149-157.

Berveiller D, Vidal J, Degrouard J, Ambard-Bretteville F, Pierre JN, Jaillard D, Damesin C. 2007. Tree stem phosphoenolpyruvate carboxylase (PEPC): lack of biochemical and localization evidence for a C4-like photosynthesis system. *New Phytologist* **176**(4): 775-781.

Bloemen J, Agneessens L, Van Meulebroek L, Aubrey DP, McGuire MA, Teskey RO, Steppe K. 2014. Stem girdling affects the quantity of CO2 transported in xylem as well as CO2 efflux from soil. *New Phytologist* **201**(3): 897-907.

Bloemen J, Bauweraerts I, De Vos F, Vanhove C, Vandenberghe S, Boeckx P, Steppe K. 2015. Fate of xylem-transported 11C-and 13C-labeled CO2 in leaves of poplar. *Physiologia plantarum* **153**(4): 555-564.

Bloemen J, McGuire MA, Aubrey DP, Teskey RO, Steppe K. 2013. Transport of root-respired CO2 via the transpiration stream affects aboveground carbon assimilation and CO2 efflux in trees. *New Phytologist* **197**(2): 555-565.

Bloemen J, Vergeynst LL, Overlaet-Michiels L, Steppe K. 2016. How important is woody tissue photosynthesis in poplar during drought stress? *Trees* **30**(1): 63-72.

BMEL. 2021. Ergebnisse der Waldzustandserhebung 2020; Bonn, Germany, 72p.

Bollmark L, Sennerby-Forsse L, Ericsson T. 1999. Seasonal dynamics and effects of nitrogen supply rate on nitrogen and carbohydrate reserves in cutting-derived Salix viminalis plants. *Canadian Journal of Forest Research* **29**(1): 85-94.

Bonan GB. 2008. Forests and climate change: forcings, feedbacks, and the climate benefits of forests. *Science* **320**(5882): 1444-1449.

Bond-Lamberty B, Thomson A. 2010. A global database of soil respiration data. *Biogeosciences* **7**(6): 1915-1926.

Bouriaud O, Marin G, Bouriaud L, Hessenmöller D, Schulze E-D. 2016. Romanian legal management rules limit wood production in Norway spruce and beech forests. *Forest ecosystems* **3**(1): 1-11.

Bowling DR, Pataki DE, Randerson JT. 2008. Carbon isotopes in terrestrial ecosystem pools and CO2 fluxes. *New Phytologist* **178**(1): 24-40.

Bowman WP, Barbour MM, Turnbull MH, Tissue DT, Whitehead D, Griffin KL. 2005. Sap flow rates and sapwood density are critical factors in within-and between-tree variation in CO2 efflux from stems of mature *Dacrydium cupressinum* trees. *New Phytologist* **167**(3): 815-828.

Boysen-Jensen P. 1933. Respiration I stamme og grene af traer. *Svenska Skogsvardsforeningens Tidskrift* **31**: 239-241.

Brändle J, Kunert N. 2019. A new automated stem CO2 efflux chamber based on industrial ultra-low-cost sensors. *Tree Physiology* **39**(12): 1975-1983.

Brecheisen ZS, Cook CW, Heine PR, Ryang J, Richter Dd. 2019. Development and deployment of a field-portable soil O2 and CO2 gas analyzer and sampler. *PloS one* **14**(8): e0220176.

Brüggemann N, Gessler A, Kayler Z, Keel S, Badeck F, Barthel M, Boeckx P, Buchmann N, Brugnoli E, Esperschütz J. 2011. Carbon allocation and carbon isotope fluxes in the plant-soil-atmosphere continuum: a review. *Biogeosciences* **8**(11): 3457-3489.

Brugnoli E, Hubick KT, von Caemmerer S, Wong SC, Farquhar GD. 1988. Correlation between the carbon isotope discrimination in leaf starch and sugars of C3 plants and the ratio of intercellular and atmospheric partial pressures of carbon dioxide. *Plant Physiology* **88**(4): 1418-1424.

Brunetti C, Gori A, Marino G, Latini P, Sobolev AP, Nardini A, Haworth M, Giovannelli A, Capitani D, Loreto F. 2019. Dynamic changes in ABA content in water-stressed Populus nigra: effects on carbon fixation and soluble carbohydrates. *Annals of botany* **124**(4): 627-643.

Bugbee B, Blonquist M. 2006. Absolute and relative gas concentration: understanding oxygen in air. *February* **27**: 1-9.

Burgess SS, Adams MA, Turner NC, Beverly CR, Ong CK, Khan AA, Bleby TM. 2001. An improved heat pulse method to measure low and reverse rates of sap flow in woody plants. *Tree Physiology* **21**(9): 589-598.

Butler JN 1991. Carbon dioxide equilibria and their applications. Lewis Publishers, Chelsea, Michigan. 259 p.

Bužková R, Acosta M, Dařenová E, Pokorný R, Pavelka M. 2015. Environmental factors influencing the relationship between stem CO2 efflux and sap flow. *Trees* **29**(2): 333-343.

Caburatan L, Park J. 2021. Differential Expression, Tissue-Specific Distribution, and Posttranslational Controls of Phosphoenolpyruvate Carboxylase. *Plants* **10**(9): 1887.

Campioli M, Malhi Y, Vicca S, Luyssaert S, Papale D, Peñuelas J, Reichstein M, Migliavacca M, Arain M, Janssens IA. 2016. Evaluating the convergence between eddy-covariance and biometric methods for assessing carbon budgets of forests. *Nature Communications* **7**(1): 1-12.

Cannell M, Thornley J. 2000. Modelling the components of plant respiration: some guiding principles. *Annals of botany* **85**(1): 45-54.

Carbone MS, Czimczik CI, Keenan TF, Murakami PF, Pederson N, Schaberg PG, Xu X, Richardson AD. 2013. Age, allocation and availability of nonstructural carbon in mature red maple trees. *New Phytologist* **200**(4): 1145-1155.

Carey EV, Callaway RM, DeLucia EH. 1997. Stem respiration of ponderosa pines grown in contrasting climates: implications for global climate change. *Oecologia* **111**: 19-25.

Cavaleri MA, Oberbauer SF, Ryan MG. 2006. Wood CO2 efflux in a primary tropical rain forest. *Global Change Biology* **12**(12): 2442-2458.

Cerasoli S, McGuire M, Faria J, Mourato M, Schmidt M, Pereira J, Chaves MM, Teskey R. 2009. CO2 efflux, CO2 concentration and photosynthetic refixation in stems of Eucalyptus globulus (Labill.). *Journal of Experimental Botany* **60**(1): 99-105.

Cernusak LA, Marshall J. 2000. Photosynthetic refixation in branches of Western White Pine. *Functional Ecology* **14**(3): 300-311.

Cernusak LA, Cheesman AW. 2015. The benefits of recycling: how photosynthetic bark can increase drought tolerance. *New Phytologist* **208**(4): 995-997.

Cernusak LA, Wong SC, Farquhar GD. 2003. Oxygen isotope composition of phloem sap in relation to leaf water in Ricinus communis. *Functional Plant Biology* **30**(10): 1059-1070.

Ceschia É, Damesin C, Lebaube S, Pontailler J-Y, Dufrêne É. 2002. Spatial and seasonal variations in stem respiration of beech trees (*Fagus sylvatica*). *Annals of Forest Science* **59**(8): 801-812.

Chambers JQ, Tribuzy ES, Toledo LC, Crispim BF, Higuchi N, Santos Jd, Araújo AC, Kruijt B, Nobre AD, Trumbore SE. 2004. Respiration from a tropical forest ecosystem: partitioning of sources and low carbon use efficiency. *Ecological Applications* **14**(sp4): 72-88.

Chapin FS, Schulze E-D, Mooney HA. 1990. The ecology and economics of storage in plants. *Annual review of ecology and systematics*: 423-447.

Chapin FS, Woodwell GM, Randerson JT, Rastetter EB, Lovett GM, Baldocchi DD, Clark DA, Harmon ME, Schimel DS, Valentini R. 2006. Reconciling carbon-cycle concepts, terminology, and methods. *Ecosystems* **9**: 1041-1050.

Chollet R, Vidal J, O'Leary MH. 1996. Phosphoenolpyruvate carboxylase: a ubiquitous, highly regulated enzyme in plants. *Australian Review of Plant Physiology and Plant Molecular Biology* **47**(1): 273-298.

Clausing S, Pena R, Song B, Müller K, Mayer-Gruner P, Marhan S, Grafe M, Schulz S, Krüger J, Lang F. 2021. Carbohydrate depletion in roots impedes phosphorus nutrition in young forest trees. *New Phytologist* **229**(5): 2611-2624.

Collalti A, Tjoelker MG, Hoch G, Mäkelä A, Guidolotti G, Heskel M, Petit G, Ryan MG, Battipaglia G, Matteucci G. 2020. Plant respiration: controlled by photosynthesis or biomass? *Global Change Biology* **26**(3): 1739-1753.

D'Andrea E, Rezaie N, Battistelli A, Gavrichkova O, Kuhlmann I, Matteucci G, Moscatello S, Proietti S, Scartazza A, Trumbore S. 2019. Winter's bite: beech trees survive complete defoliation due to spring late-frost damage by mobilizing old C reserves. *New Phytologist* **224**(2): 625-631.

Dannoura M, Epron D, Desalme D, Massonnet C, Tsuji S, Plain C, Priault P, Gérant D. 2019. The impact of prolonged drought on phloem anatomy and phloem transport in young beech trees. *Tree Physiology* **39**(2): 201-210.

Damesin C. 2003. Respiration and photosynthesis characteristics of current-year stems of *Fagus sylvatica*: from the seasonal pattern to an annual balance. *New Phytologist* **158**(3): 465-475.

Damesin C, Ceschia E, Le Goff N, Ottorini JM, Dufrêne E. 2002. Stem and branch respiration of beech: from tree measurements to estimations at the stand level. *New Phytologist* **153**(1): 159-172.

Damesin C, Lelarge C. 2003. Carbon isotope composition of current-year shoots from *Fagus sylvatica* in relation to growth, respiration and use of reserves. *Plant, cell & environment* **26**(2): 207-219.

Darenova E, Acosta M, Pokorny R, Pavelka M. 2018. Variability in temperature dependence of stem CO2 efflux from Norway spruce trees. *Tree Physiology* **38**(9): 1333-1344.

Davidson GR. 1995. The stable isotopic composition and measurement of carbon in soil CO2. *Geochimica et Cosmochimica Acta* **59**(12): 2485-2489.

De Baerdemaeker NJ, Salomón RL, De Roo L, Steppe K. 2017. Sugars from woody tissue photosynthesis reduce xylem vulnerability to cavitation. *New Phytologist* **216**(3): 720-727.

De Guzman ME, Santiago LS, Schnitzer SA, Álvarez-Cansino L. 2017. Trade-offs between water transport capacity and drought resistance in neotropical canopy liana and tree species. *Tree physiology* **37**(10): 1404-1414.

De Roo L, Bloemen J, Dupon Y, Salomón RL, Steppe K. 2019. Axial diffusion of respired CO2 confounds stem respiration estimates during the dormant season. *Annals of Forest Science* **76**(2): 1-11.

De Roo L, Lauriks F, Salomón RL, Oleksyn J, Steppe K. 2020a. Woody tissue photosynthesis increases radial stem growth of young poplar trees under ambient atmospheric CO2 but its contribution ceases under elevated CO2. *Tree Physiology* **40**(11): 1572-1582.

De Roo L, Salomón RL, Oleksyn J, Steppe K. 2020b. Woody tissue photosynthesis delays drought stress in *Populus tremula* trees and maintains starch reserves in branch xylem tissues. *New Phytologist* **228**(1): 70-81.

De Roo L, Salomón RL, Steppe K. 2020c. Woody tissue photosynthesis reduces stem CO2 efflux by half and remains unaffected by drought stress in young *Populus tremula* trees. *Plant, cell & environment* **43**(4): 981-991.

De Schepper V, Van Dusschoten D, Copini P, Jahnke S, Steppe K. 2012. MRI links stem water content to stem diameter variations in transpiring trees. *Journal of Experimental Botany* **63**(7): 2645-2653.

De Vries FP, Brunsting A, Van Laar H. 1974. Products, requirements and efficiency of biosynthesis a quantitative approach. *Journal of theoretical Biology* **45**(2): 339-377.

Dejours P. 1981. Control of respiration. *Principles of comparative respiratory physiology* **28**: 185-220.

del Hierro AM, Kronberger W, Hietz P, Offenthaler I, Richter H. 2002. A new method to determine the oxygen concentration inside the sapwood of trees. *Journal of Experimental Botany* **53**(368): 559-563.

DeLucia EH, Drake JE, Thomas RB, Gonzalez-Meler M. 2007. Forest carbon use efficiency: is respiration a constant fraction of gross primary production? *Global Change Biology* **13**(6): 1157-1167.

DeSoto L, Cailleret M, Sterck F, Jansen S, Kramer K, Robert EM, Aakala T, Amoroso MM, Bigler C, Camarero JJ. 2020. Low growth resilience to drought is related to future mortality risk in trees. *Nature Communications* **11**(1): 1-9.

DesRochers A, Lieffers VJ. 2001. The coarse-root system of mature *Populus tremuloides* in declining stands in Alberta, Canada. *Journal of Vegetation Science* **12**(3): 355-360.

Dietze MC. 2014. Gaps in knowledge and data driving uncertainty in models of photosynthesis. *Photosynthesis research* **119**(1): 3-14.

Dietze MC, Sala A, Carbone MS, Czimczik CI, Mantooth JA, Richardson AD, Vargas R. 2014. Nonstructural carbon in woody plants. *Annual review of plant biology* **65**(1): 667-687.

Doubnerová V, Ryšlavá H. 2011. What can enzymes of C4 photosynthesis do for C3 plants under stress? *Plant Science* **180**(4): 575-583.

Engqvist MK, Kuhn A, Wienstroer J, Weber K, Jansen EE, Jakobs C, Weber AP, Maurino VG. 2011. Plant D-2-hydroxyglutarate dehydrogenase participates in the catabolism of lysine especially during senescence. *Journal of Biological Chemistry* **286**(13): 11382-11390.

Erda FG, Bloemen J, Steppe K. 2014. Quantifying the impact of daily and seasonal variation in sap p H on xylem dissolved inorganic carbon estimates in plum trees. *Plant Biology* **16**(1): 43-48.

Etzold S, Zweifel R, Ruehr NK, Eugster W, Buchmann N. 2013. Long-term stem CO2 concentration measurements in Norway spruce in relation to biotic and abiotic factors. *New Phytologist* **197**(4): 1173-1184.

Fan H, McGuire MA, Teskey RO. 2017. Effects of stem size on stem respiration and its flux components in yellow-poplar (*Liriodendron tulipifera* L.) trees. *Tree Physiology* **37**(11): 1536-1545.

FAO. 2015. Global forest resources assessment 2015. Desk Reference. *Food and agriculture organization of the United Nations.* Rome. Italy.

Farquhar GD, Ehleringer JR, Hubick KT. 1989. Carbon isotope discrimination and photosynthesis. *Annual review of plant physiology and plant molecular biology* **40**(1): 503-537.

Farquhar GD, von Caemmerer Sv, Berry JA. 1980. A biochemical model of photosynthetic CO2 assimilation in leaves of C3 species. *Planta* **149**(1): 78-90.

Fatichi S, Leuzinger S, Körner C. 2014. Moving beyond photosynthesis: from carbon source to sink-driven vegetation modeling. *New Phytologist* **201**(4): 1086-1095.

Fatichi S, Pappas C, Zscheischler J, Leuzinger S. 2019. Modelling carbon sources and sinks in terrestrial vegetation. *New Phytologist* **221**(2): 652-668.

Fischer C, Höll W. 1991. Food reserves of Scots pine (*Pinus sylvestris* L.). *Trees* **5**(4): 187-195.

Fischer S, Hanf S, Frosch T, Gleixner G, Popp J, Trumbore S, Hartmann H. 2015. Pinus sylvestris switches respiration substrates under shading but not during drought. *New Phytologist* **207**(3): 542-550.

Flo V, Martinez-Vilalta J, Steppe K, Schuldt B, Poyatos R. 2019. A synthesis of bias and uncertainty in sap flow methods. *Agricultural and Forest Meteorology* **271**: 362-374.

Fraser EC, Lieffers VJ, Landhäusser SM. 2006. Carbohydrate transfer through root grafts to support shaded trees. *Tree Physiology* **26**(8): 1019-1023.

Friedlingstein P, O'Sullivan M, Jones MW, Andrew RM, Gregor L, Hauck J, Le Quéré C, Luijkx IT, Olsen A, Peters GP. 2022. Global carbon budget 2022. *Earth System Science Data* **14**(11): 4811-4900.

Friedlingstein P, O'sullivan M, Jones MW, Andrew RM, Hauck J, Olsen A, Peters GP, Peters W, Pongratz J, Sitch S. 2020. Global carbon budget 2020. *Earth System Science Data* **12**(4): 3269-3340.

Gartner BL, Moore JR, Gardiner BA. 2004. Gas in stems: abundance and potential consequences for tree biomechanics. *Tree Physiology* **24**(11): 1239-1250.

Gärtner H, Nievergelt D. 2010. The core-microtome: a new tool for surface preparation on cores and time series analysis of varying cell parameters. *Dendrochronologia* **28**(2): 85-92.

Gessler A, Bächli L, Rouholahnejad Freund E, Treydte K, Schaub M, Haeni M, Weiler M, Seeger S, Marshall J, Hug C. 2022. Drought reduces water uptake in beech from the drying topsoil, but no compensatory uptake occurs from deeper soil layers. *New Phytologist* **233**(1): 194-206.

Gessler A, Brandes E, Keitel C, Boda S, Kayler ZE, Granier A, Barbour M, Farquhar GD, Treydte K. 2013. The oxygen isotope enrichment of leaf-exported assimilates–does it always reflect lamina leaf water enrichment? *New Phytologist* **200**(1): 144-157.

Gessler A, Schultze M, Schrempp S, Rennenberg H. 1998. Interaction of phloem-translocated amino compounds with nitrate net uptake by the roots of beech (*Fagus sylvatica*) seedlings. *Journal of Experimental Botany* **49**(326): 1529-1537.

Gessler A, Tcherkez G, Karyanto O, Keitel C, Ferrio JP, Ghashghaie J, Kreuzwieser J, Farquhar GD. 2009. On the metabolic origin of the carbon isotope composition of CO2 evolved from darkened light-acclimated leaves in *Ricinus communis*. *New Phytologist* **181**(2): 374-386.

Gessler A, Treydte K. 2016. The fate and age of carbon–insights into the storage and remobilization dynamics in trees. *New Phytologist* **209**(4): 1338-1340.

Gifford RM. 2003. Plant respiration in productivity models: conceptualisation, representation and issues for global terrestrial carbon-cycle research. *Functional Plant Biology* **30**(2): 171-186.

Glavac V, Koenies H, Ebben U. 1990. Seasonal variations in mineral concentrations in the trunk xylem sap of beech (*Fagus sylvatica* L.) in a 42-year-old beech forest stand. *New Phytologist* **116**(1): 47-54.

Gleixner G, Danier H-J, Werner RA, Schmidt H-L. 1993. Correlations between the 13C content of primary and secondary plant products in different cell compartments and that in decomposing basidiomycetes. *Plant Physiology* **102**(4): 1287-1290.

Goldstein G, Andrade J, Meinzer F, Holbrook N, Cavelier J, Jackson P, Celis A. 1998. Stem water storage and diurnal patterns of water use in tropical forest canopy trees. *Plant, cell & environment* **21**(4): 397-406.

González-González BD, Rozas V, García-González I. 2014. Earlywood vessels of the sub-Mediterranean oak *Quercus pyrenaica* have greater plasticity and sensitivity than those of the temperate Q. petraea at the Atlantic–Mediterranean boundary. *Trees* **28**(1): 237-252.

Gowik U, Westhoff P. 2011. The path from C3 to C4 photosynthesis. *Plant Physiology* **155**(1): 56-63.

Grimberg Å, Lager I, Street NR, Robinson KM, Marttila S, Mähler N, Ingvarsson PK, Bhalerao RP. 2018. Storage lipid accumulation is controlled by photoperiodic signal acting via regulators of growth cessation and dormancy in hybrid aspen. *New Phytologist* **219**(2): 619-630.

Hajek P, Link RM, Nock CA, Bauhus J, Gebauer T, Gessler A, Kovach K, Messier C, Paquette A, Saurer M. 2022. Mutually inclusive mechanisms of drought-induced tree mortality. *Global Change Biology* **28**(10): 3365-3378.

Hanf S, Fischer S, Hartmann H, Keiner R, Trumbore S, Popp J, Frosch T. 2015. Online investigation of respiratory quotients in *Pinus sylvestris* and Picea abies during drought and shading by means of cavity-enhanced Raman multi-gas spectrometry. *Analyst* **140**(13): 4473-4481.

Hartmann H. 2015. Carbon starvation during drought-induced tree mortality–are we chasing a myth? *Journal of Plant Hydraulics* **2**: e005.

Hartmann H, Bastos A, Das AJ, Esquivel-Muelbert A, Hammond WM, Martínez-Vilalta J, McDowell NG, Powers JS, Pugh TA, Ruthrof KX. 2022. Climate change risks to global forest health: emergence of unexpected events of elevated tree mortality worldwide. *Annual review of plant biology* **73**(1): 673-702.

Hartmann H, Moura CF, Anderegg WR, Ruehr NK, Salmon Y, Allen CD, Arndt SK, Breshears DD, Davi H, Galbraith D. 2018. Research frontiers for improving our understanding of drought-induced tree and forest mortality. *New Phytologist* **218**(1): 15-28.

Hartmann H, Trumbore S. 2016. Understanding the roles of nonstructural carbohydrates in forest trees–from what we can measure to what we want to know. *New Phytologist* **211**(2): 386-403.

Hartmann H, Ziegler W, Trumbore S. 2013. Lethal drought leads to reduction in nonstructural carbohydrates in Norway spruce tree roots but not in the canopy. *Functional Ecology* **27**(2): 413-427.

Helm J, Hartmann H, Göbel M, Hilman B, Herrera DA, Muhr J. 2021. Low-cost chamber design for simultaneous CO2 and O2 flux measurements between tree stems and the atmosphere. *Tree Physiology* **41**(9): 1767-1780.

Helm J, Salomón RL, Hilman B, Muhr J, Knohl A, Steppe K, Gibon Y, Cassan C, Hartmann H. 2023. Differences between tree stem CO2 efflux and O2 influx rates cannot be explained by internal CO2 transport or storage in large beech trees. *Plant, Cell & Environment* **46**(9):2680-2693.

Herrera-Ramírez D, Sierra CA, Römermann C, Muhr J, Trumbore S, Silvério D, Brando PM, Hartmann H. 2021. Starch and lipid storage strategies in tropical trees relate to growth and mortality. *New Phytologist* **230**(1): 139-154.

Heskel MA, O'sullivan OS, Reich PB, Tjoelker MG, Weerasinghe LK, Penillard A, Egerton JJ, Creek D, Bloomfield KJ, Xiang J. 2016. Convergence in the temperature response of leaf respiration across biomes and plant functional types. *Proceedings of the National Academy of Sciences* **113**(14): 3832-3837.

Hibberd JM, Quick WP. 2002. Characteristics of C4 photosynthesis in stems and petioles of C3 flowering plants. *Nature* **415**(6870): 451-454.

Hildebrandt TM, Nesi AN, Araújo WL, Braun H-P. 2015. Amino acid catabolism in plants. *Molecular plant* **8**(11): 1563-1579.

Hilman B, Angert A. 2016. Measuring the ratio of CO2 efflux to O2 influx in tree stem respiration. *Tree Physiology* **36**(11): 1422-1431.

Hilman B, Muhr J, Helm J, Kuhlmann I, Schulze ED, Trumbore S. 2021. The size and the age of the metabolically active carbon in tree roots. *Plant, Cell & Environment* **44**(8): 2522-2535.

Hilman B, Muhr J, Trumbore SE, Kunert N, Carbone MS, Yuval P, Wright SJ, Moreno G, Pérez-Priego O, Migliavacca M. 2019. Comparison of CO2 and O2 fluxes demonstrate retention of respired CO2 in tree stems from a range of tree species. *Biogeosciences* **16**(1): 177-191.

Hilman B, Weiner T, Haran T, Masiello CA, Gao X, Angert A. 2022. The Apparent Respiratory Quotient of Soils and Tree Stems and the processes that control it. *Journal of Geophysical Research: Biogeosciences* **127**(3): e2021JG006676.

Hoch G. 2015. Carbon reserves as indicators for carbon limitation in trees. In: U Lüttge. W. Beyschlag. eds. Progress in botany. Cham. Switzerland: Springer International. pp 321–346

Hoch G, Popp M, Körner C. 2002. Altitudinal increase of mobile carbon pools in *Pinus cembra* suggests sink limitation of growth at the Swiss treeline. *Oikos* **98**(3): 361-374.

Hoch G, Richter A, Körner C. 2003. Non-structural carbon compounds in temperate forest trees. *Plant, cell & environment* **26**(7): 1067-1081.

Hoffland E, van den Boogaard R, Nelemans J, FINDENEGG G. 1992. Biosynthesis and root exudation of citric and malic acids in phosphate-starved rape plants. *New Phytologist* **122**(4): 675-680.

Högberg P, Johnnisson C, Högberg M, Högbom L, Näsholm T, Hällgren J-E. 1995. Measurements of abundances of 15N and 13C as tools in retrospective studies of N balances and water stress in forests: A discussion of preliminary results. *Plant and soil* **168**(1): 125-133.

Höll W. 1974. Dark CO2 fixation by cell-free preparations of the wood of *Robinia pseudoacacia*. *Canadian Journal of Botany* **52**(4): 727-734.

Höll W. 1997. Storage and mobilization of carbohydrates and lipids. *Trees–Contribution to modern tree physiology. Leiden, The Netherlands: Backhuys Publishers*: 197-211.

Hölttä T, Kolari P. 2009. Interpretation of stem CO2 efflux measurements. *Tree Physiology* **29**(11): 1447-1456.

Houghton R. 2007. Balancing the global carbon budget. *Annu. Rev. Earth Planet. Sci.* **35**: 313-347.

Hua Q, Turnbull JC, Santos GM, Rakowski AZ, Ancapichún S, De Pol-Holz R, Hammer S, Lehman SJ, Levin I, Miller JB. 2022. Atmospheric radiocarbon for the period 1950–2019. *Radiocarbon* **64**(4): 723-745.

Huang J, Hammerbacher A, Weinhold A, Reichelt M, Gleixner G, Behrendt T, Van Dam NM, Sala A, Gershenzon J, Trumbore S. 2019. Eyes on the future–evidence for trade-offs between growth, storage and defense in Norway spruce. *New Phytologist* **222**(1): 144-158.

Hunt S. 2003. Measurements of photosynthesis and respiration in plants. *Physiologia plantarum* **117**(3): 314-325.

Huntingford C, Atkin OK, Martinez-De La Torre A, Mercado LM, Heskel MA, Harper AB, Bloomfield KJ, O'sullivan OS, Reich PB, Wythers KR. 2017. Implications of improved representations of plant respiration in a changing climate. *Nature Communications* **8**(1): 1602.

Ivanov AG, Krol M, Sveshnikov D, Malmberg G, Gardeström P, Hurry V, Öquist G, Huner NP. 2006. Characterization of the photosynthetic apparatus in cortical bark chlorenchyma of Scots pine. *planta* **223**(6): 1165-1177.

Jelínková H, Tremblay F, DesRochers A. 2009. Molecular and dendrochronological analysis of natural root grafting in *Populus tremuloides* (Salicaceae). *American Journal of Botany* **96**(8): 1500-1505.

Jeřábek J, Rinderer M, Gessler A, Weiler M. 2020. Xylem sap phosphorus sampling using microdialysis—a non-destructive high sampling frequency method tested under laboratory and field conditions. *Tree Physiology* **40**(11): 1623-1638.

Joseph J, Gao D, Backes B, Bloch C, Brunner I, Gleixner G, Haeni M, Hartmann H, Hoch G, Hug C. 2020. Rhizosphere activity in an old-growth forest reacts rapidly to changes in soil moisture and shapes whole-tree carbon allocation. *Proceedings of the National Academy of Sciences* **117**(40): 24885-24892.

Junker BH, Lonien J, Heady LE, Rogers A, Schwender J. 2007. Parallel determination of enzyme activities and in vivo fluxes in Brassica napus embryos grown on organic or inorganic nitrogen source. *Phytochemistry* **68**(16-18): 2232-2242.

Kader AA, Saltveit ME. 2002. Respiration and gas exchange. *In: Bartz JA, Brecht JK. (eds) Postharvest physiology and pathology of vegetables.* Marcel Dekker. New York. NY. pp 7-29.

Katayama A, Kume T, Ohashi M, Matsumoto K, Nakagawa M, Saito T, Kumagai To, Otsuki K. 2016. Characteristics of wood CO2 efflux in a Bornean tropical rainforest. *Agricultural and Forest Meteorology* **220**: 190-199.

Keeling RF. 1988. Measuring correlations between atmospheric oxygen and carbon dioxide mole fractions: A preliminary study in urban air. *Journal Of Atmospheric Chemistry* **7**: 153-176.

Keeling RF, Manning AC, McEvoy EM, Shertz SR. 1998. Methods for measuring changes in atmospheric O2 concentration and their application in southern hemisphere air. *Journal of Geophysical Research: Atmospheres* **103**(D3): 3381-3397.

Keeling RF, Najjar RP, Bender ML, Tans PP. 1993. What atmospheric oxygen measurements can tell us about the global carbon cycle. *Global Biogeochemical Cycles* **7**(1): 37-67.

Keeling RF, Shertz SR. 1992. Seasonal and interannual variations in atmospheric oxygen and implications for the global carbon cycle. *Nature* **358**(6389): 723-727.

Keiner R, Frosch T, Hanf S, Rusznyak A, Akob DM, Küsel K, Popp Jr. 2013. Raman Spectroscopy An Innovative and Versatile Tool To Follow the Respirational Activity and Carbonate Biomineralization of Important Cave Bacteria. *Analytical chemistry* **85**(18): 8708-8714.

Keiner R, Frosch T, Massad T, Trumbore S, Popp J. 2014. Enhanced Raman multigas sensing–a novel tool for control and analysis of 13 CO2 labeling experiments in environmental research. *Analyst* **139**(16): 3879-3884.

King AW, Gunderson CA, Post WM, Weston DJ, Wullschleger SD. 2006. Plant respiration in a warmer world. *Science* **312**(5773): 536-537.

Koppenaal R, Tschaplinski T, Colombo S. 1991. Carbohydrate accumulation and turgor maintenance in seedling shoots and roots of two boreal conifers subjected to water stress. *Canadian Journal of Botany* **69**(11): 2522-2528.

Kozlowski T. 1992. Carbohydrate sources and sinks in woody plants. *The botanical review* **58**: 107-222.

Kruse J, Adams MA. 2008. Integrating two physiological approaches helps relate respiration to growth of *Pinus radiata*. *New Phytologist* **180**(4): 841-852.

Lambers H, Chapin FS III, Pons TL. 2008. Respiration. *In: Lambers H, Chapin FS III, Pons TL. (eds) Plant physiological ecology.* Springer. New York. NY. pp 101-150.

Lambers H, Poorter H 1992. Inherent variation in growth rate between higher plants: a search for physiological causes and ecological consequences. *Advances in ecological research* **23**: 187-261.

Landhäusser SM, Chow PS, Dickman LT, Furze ME, Kuhlman I, Schmid S, Wiesenbauer J, Wild B, Gleixner G, Hartmann H. 2018. Standardized protocols and procedures can precisely and accurately quantify non-structural carbohydrates. *Tree Physiology* **38**(12): 1764-1778.

Lavigne M, Franklin S, Hunt Jr E. 1996. Estimating stem maintenance respiration rates of dissimilar balsam fir stands. *Tree Physiology* **16**(8): 687-695.

Lavigne M, Ryan M, Anderson D, Baldocchi D, Crill P, Fitzjarrald D, Goulden M, Gower S, Massheder J, McCaughey J. 1997. Comparing nocturnal eddy covariance measurements to estimates of ecosystem respiration made by scaling chamber measurements at six coniferous boreal sites. *Journal of Geophysical Research: Atmospheres* **102**(D24): 28977-28985.

Le Quéré C, Andrew RM, Friedlingstein P, Sitch S, Hauck J, Pongratz J, Pickers PA, Korsbakken JI, Peters GP, Canadell JG. 2018. Global carbon budget 2018. *Earth System Science Data* **10**(4): 2141-2194.

Levin I, Naegler T, Kromer B, Diehl M, Francey R, Gomez-Pelaez A, Steele P, Wagenbach D, Weller R, Worthy D. 2010. Observations and modelling of the global distribution and long-term trend of atmospheric 14CO2. *Tellus B: Chemical and Physical Meteorology* **62**(1): 26-46.

Levy P, Meir P, Allen S, Jarvis P. 1999. The effect of aqueous transport of CO2 in xylem sap on gas exchange in woody plants. *Tree Physiology* **19**(1): 53-58.

Litton CM, Raich JW, Ryan MG. 2007. Carbon allocation in forest ecosystems. *Global Change Biology* **13**(10): 2089-2109.

Luyssaert S, Inglima I, Jung M, Richardson AD, Reichstein M, Papale D, Piao S, Schulze ED, Wingate L, Matteucci G. 2007. CO2 balance of boreal, temperate, and tropical forests derived from a global database. *Global Change Biology* **13**(12): 2509-2537.

Luyssaert S, Reichstein M, Schulze ED, Janssens IA, Law BE, Papale D, Dragoni D, Goulden ML, Granier A, Kutsch WL. 2009. Toward a consistency cross-check of eddy covariance flux–based and biometric estimates of ecosystem carbon balance. *Global Biogeochemical Cycles* **23**(3).

Maier CA, Clinton BD. 2006. Relationship between stem CO2 efflux, stem sap velocity and xylem CO2 concentration in young loblolly pine trees. *Plant, cell & environment* **29**(8): 1471-1483.

Maier CA, Johnsen KH, Clinton BD, Ludovici KH. 2010. Relationships between stem CO2 efflux, substrate supply, and growth in young loblolly pine trees. *New Phytologist* **185**(2): 502-513.

Manning A, Keeling RF. 2006. Global oceanic and land biotic carbon sinks from the Scripps atmospheric oxygen flask sampling network. *Tellus B: Chemical and Physical Meteorology* **58**(2): 95-116.

Martínez-Vilalta J, Sala A, Asensio D, Galiano L, Hoch G, Palacio S, Piper FI, Lloret F. 2016. Dynamics of non-structural carbohydrates in terrestrial plants: a global synthesis. *Ecological Monographs* **86**(4): 495-516.

Masiello C, Gallagher M, Randerson J, Deco R, Chadwick O. 2008. Evaluating two experimental approaches for measuring ecosystem carbon oxidation state and oxidative ratio. *Journal of Geophysical Research: Biogeosciences* **113**(G3).

Maunoury-Danger F, Fresneau C, Eglin T, Berveiller D, Francois C, Lelarge-Trouverie C, Damesin C. 2010. Impact of carbohydrate supply on stem growth, wood and respired CO2 δ13C: assessment by experimental girdling. *Tree Physiology* **30**(7): 818-830.

McDowell N, Pockman WT, Allen CD, Breshears DD, Cobb N, Kolb T, Plaut J, Sperry J, West A, Williams DG. 2008. Mechanisms of plant survival and mortality during drought: why do some plants survive while others succumb to drought? *New Phytologist* **178**(4): 719-739.

McDowell NG. 2011. Mechanisms linking drought, hydraulics, carbon metabolism, and vegetation mortality. *Plant Physiology* **155**(3): 1051-1059.

McGuire M, Cerasoli S, Teskey R. 2007. CO2 fluxes and respiration of branch segments of sycamore (*Platanus occidentalis* L.) examined at different sap velocities, branch diameters, and temperatures. *Journal of Experimental Botany* **58**(8): 2159-2168.

McGuire M, Teskey R. 2002. Microelectrode technique for in situ measurement of carbon dioxide concentrations in xylem sap of trees. *Tree Physiology* **22**(11): 807-811.

McGuire M, Teskey R. 2004. Estimating stem respiration in trees by a mass balance approach that accounts for internal and external fluxes of CO2. *Tree Physiology* **24**(5): 571-578.

Mehlem A, Hagberg CE, Muhl L, Eriksson U, Falkevall A. 2013. Imaging of neutral lipids by oil red O for analyzing the metabolic status in health and disease. *Nature protocols* **8**(6): 1149-1154.

Meir P, Mencuccini M, Coughlin SI. 2020. Respiration in wood: integrating across tissues, functions and scales. *New Phytologist* **225**(5): 1824-1827.

Meir P, Shenkin A, Disney M, Rowland L, Malhi Y, Herold M, da Costa AC. 2017. Plant structure-function relationships and woody tissue respiration: upscaling to forests from laser-derived measurements. *Plant respiration: Metabolic fluxes and carbon balance*: 89-105.

Miller TW, Stangler DF, Larysch E, Honer H, Puhlmann H, Schindler D, Jung C, Seifert T, Rigling A, Kahle H-P. 2023. Later growth onsets or reduced growth rates: What characterises legacy effects at the tree-ring level in conifers after the severe 2018 drought? *Science of The Total Environment* **854**: 158703.

Morris H, Plavcová L, Cvecko P, Fichtler E, Gillingham MA, Martínez-Cabrera HI, McGlinn DJ, Wheeler E, Zheng J, Ziemińska K. 2016. A global analysis of parenchyma tissue fractions in secondary xylem of seed plants. *New Phytologist* **209**(4): 1553-1565.

Muhr J, Angert A, Negrón-Juárez RI, Muñoz WA, Kraemer G, Chambers JQ, Trumbore SE. 2013. Carbon dioxide emitted from live stems of tropical trees is several years old. *Tree Physiology* **33**(7): 743-752.

Muhr J, Messier C, Delagrange S, Trumbore S, Xu X, Hartmann H. 2016. How fresh is maple syrup? Sugar maple trees mobilize carbon stored several years previously during early springtime sap-ascent. *New Phytologist* **209**(4): 1410-1416.

Muhr J, Trumbore S, Higuchi N, Kunert N. 2018. Living on borrowed time–Amazonian trees use decade-old storage carbon to survive for months after complete stem girdling. *New Phytologist* **220**(1): 111-120.

Myers N. 1997. The world's forests and their ecosystem services. *Nature's Services: societal dependence on natural ecosystems*: 215-235.

Nakagawa S, Schielzeth H. 2013. A general and simple method for obtaining R2 from generalized linear mixed-effects models. *Methods in ecology and evolution* **4**(2): 133-142.

Nimmo HG. 2008. Control of phosphoenolpyruvate carboxylase in plants. *In: Plaxtonm WC and McManus MT (eds) Control of primary metabolism in plants.* Annual Plant Reviews. Blackwell Publishing. Oxford. pp 219-233.

Nobel PS. 2009. *Physicochemical & environmental plant physiology* (4th ed). Academic press/Elsevier. San Diego. CA.

Oberhuber W, Gruber A, Lethaus G, Winkler A, Wieser G 2017. Stem girdling indicates prioritized carbon allocation to the root system at the expense of radial stem growth in Norway spruce under drought conditions. *Environmental and Experimental Botany* **138**(4):109–118.

O'Leary B, Park J, Plaxton WC. 2011. The remarkable diversity of plant PEPC (phosphoenolpyruvate carboxylase): recent insights into the physiological functions and post-translational controls of non-photosynthetic PEPCs. *Biochemical Journal* **436**(1): 15-34.

O'Leary BM, Asao S, Millar AH, Atkin OK. 2019. Core principles which explain variation in respiration across biological scales. *New Phytologist* **222**(2): 670-686.

Ogle K, Pacala SW. 2009. A modeling framework for inferring tree growth and allocation from physiological, morphological and allometric traits. *Tree Physiology* **29**(4): 587-605.

Pan Y, Birdsey RA, Phillips OL, Jackson RB. 2013. The structure, distribution, and biomass of the world's forests. *Annual Review of Ecology, Evolution, and Systematics. 44 (1): 593-622.* **44**(1): 593-622.

Park Williams A, Allen CD, Macalady AK, Griffin D, Woodhouse CA, Meko DM, Swetnam TW, Rauscher SA, Seager R, Grissino-Mayer HD. 2013. Temperature as a potent driver of regional forest drought stress and tree mortality. *Nature climate change* **3**(3): 292-297.

Patonnier M, Peltier J, Marigo G. 1999. Drought-induced increase in xylem malate and mannitol concentrations and closure of *Fraxinus excelsior* L. stomata. *Journal of Experimental Botany* **50**(336): 1223-1229.

Peltier DM, Ogle K. 2020. Tree growth sensitivity to climate is temporally variable. *Ecology letters* **23**(11): 1561-1572.

Petit RJ, Hampe A. 2006. Some evolutionary consequences of being a tree. *Annual review of ecology, evolution, and systematics*: 187-214.

Pfanz H, Aschan G 2001. The existence of bark and stem photosynthesis in woody plants and its significance for the overall carbon gain. An eco-physiological and ecological approach. *Progress in botany*: Springer, 477-510.

Pfanz H, Aschan G, Langenfeld-Heyser R, Wittmann C, Loose M. 2002. Ecology and ecophysiology of tree stems: corticular and wood photosynthesis. *Naturwissenschaften* **89**(4): 147-162.

Piao S, Luyssaert S, Ciais P, Janssens IA, Chen A, Cao C, Fang J, Friedlingstein P, Luo Y, Wang S. 2010. Forest annual carbon cost: A global-scale analysis of autotrophic respiration. *Ecology* **91**(3): 652-661.

Pinheiro J, Bates D, DebRoy S, Sarkar D, Heisterkamp S, Van Willigen B, Maintainer R. 2017. Package 'nlme'. *Linear and nonlinear mixed effects models. version* **3**:274. Available at https://cran.r-project.org/web/packages/nlme/nlme.pdf.

Piper FI, Fajardo A. 2016. Carbon dynamics of *Acer pseudoplatanus* seedlings under drought and complete darkness. *Tree physiology* **36**(11): 1400-1408.

Piper FI, Paula S. 2020. The role of nonstructural carbohydrates storage in forest resilience under climate change. *Current Forestry Reports* **6**(1): 1-13.

Plaxton WC, Podestá FE. 2006. The functional organization and control of plant respiration. *Critical Reviews in Plant Sciences* **25**(2): 159-198.

Poorter H, Niklas KJ, Reich PB, Oleksyn J, Poot P, Mommer L. 2012. Biomass allocation to leaves, stems and roots: meta-analyses of interspecific variation and environmental control. *New Phytologist* **193**(1): 30-50.

Powers EM, Marshall JD. 2011. Pulse labeling of dissolved 13C-carbonate into tree xylem: developing a new method to determine the fate of recently fixed photosynthate. *Rapid Communications in Mass Spectrometry* **25**(1): 33-40.

Pruyn ML, Gartner BL, Harmon ME. 2002. Within-stem variation of respiration in *Pseudotsuga menziesii* (Douglas-fir) trees. *New Phytologist* **154**(2): 359-372.

Pruyn ML, Gartner BL, Harmon ME. 2005. Storage versus substrate limitation to bole respiratory potential in two coniferous tree species of contrasting sapwood width. *Journal of Experimental Botany* **56**(420): 2637-2649.

Pumpanen J, Kolari P, Ilvesniemi H, Minkkinen K, Vesala T, Niinistö S, Lohila A, Larmola T, Morero M, Pihlatie M. 2004. Comparison of different chamber techniques for measuring soil CO2 efflux. *Agricultural and Forest Meteorology* **123**(3-4): 159-176.

R Development Core Team. 2019. R: A language and environment for statistical computing. R Foundation for Statistical Computing, Vienna, Austria.

Rademacher T, Fonti P, LeMoine JM, Fonti MV, Bowles F, Chen Y, Eckes-Shephard AH, Friend AD, Richardson AD (2022). Insights into source/sink controls on wood formation and photosynthesis from a stem chilling experiment in mature red maple. New Phytology **236**(4):1296–1309.

Regier N, Streb S, Zeeman SC, Frey B (2010). Seasonal changes in starch and sugar content of poplar (*Populus deltoides × deltoides × nigra* cv. Dorskamp) and the impact of stem girdling on carbohydrate allocation to roots. *Tree Physiology* **30**(8):979–987

Regier N, Streb S, Cocozza C, Schaub M, Cherubini P, Zeeman SC, Frey B. 2009. Drought tolerance of two black poplar (*Populus nigra* L.) clones: contribution of carbohydrates and oxidative stress defence. *Plant, cell & environment* **32**(12): 1724-1736.

Reich PB, Tjoelker MG, Pregitzer KS, Wright IJ, Oleksyn J, Machado JL. 2008. Scaling of respiration to nitrogen in leaves, stems and roots of higher land plants. *Ecology letters* **11**(8): 793-801.

Richardson AD, Carbone MS, Keenan TF, Czimczik CI, Hollinger DY, Murakami P, Schaberg PG, Xu X. 2013. Seasonal dynamics and age of stemwood nonstructural carbohydrates in temperate forest trees. *New Phytologist* **197**(3): 850-861.

Rodríguez-Calcerrada J, Martin-StPaul NK, Lempereur M, Ourcival J-M, del Rey MdC, Joffre R, Rambal S. 2014. Stem CO2 efflux and its contribution to ecosystem CO2 efflux decrease with drought in a Mediterranean forest stand. *Agricultural and Forest Meteorology* **195**: 61-72.

Rosas T, Galiano L, Ogaya R, Peñuelas J, Martínez-Vilalta J. 2013. Dynamics of non-structural carbohydrates in three Mediterranean woody species following long-term experimental drought. *Frontiers in plant science* **4**: 400.

Rosell JA, Castorena M, Laws CA, Westoby M. 2015. Bark ecology of twigs vs. main stems: functional traits across eighty-five species of angiosperms. *Oecologia* **178**(4): 1033-1043.

Ryan MG. 1991. Effects of climate change on plant respiration. *Ecological Applications* **1**(2): 157-167.

Ryan MG, Cavaleri MA, Almeida AC, Penchel R, Senock RS, Luiz Stape J. 2009. Wood CO2 efflux and foliar respiration for Eucalyptus in Hawaii and Brazil. *Tree Physiology* **29**(10): 1213-1222.

Ryan MG, Gower ST, Hubbard RM, Waring RH, Gholz HL, Cropper WP, Running SW. 1995. Woody tissue maintenance respiration of four conifers in contrasting climates. *Oecologia* **101**(2): 133-140.

Sala A, Piper F, Hoch G. 2010. Physiological mechanisms of drought-induced tree mortality are far from being resolved. *New phytologist* **186**(2): 274-281.

Sala A, Woodruff DR, Meinzer FC. 2012. Carbon dynamics in trees: feast or famine? *Tree Physiology* **32**(6): 764-775.

Salomón, Valbuena-Carabaña M, Teskey R, McGuire MA, Aubrey D, González-Doncel I, Gil L, Rodríguez-Calcerrada J. 2016. Seasonal and diel variation in xylem CO2 concentration and sap pH in sub-Mediterranean oak stems. *Journal of Experimental Botany* **67**(9): 2817-2827.

Salomón RL, De Roo L, Bodé S, Boeckx P, Steppe K. 2021a. Efflux and assimilation of xylem-transported CO2 in stems and leaves of tree species with different wood anatomy. *Plant, cell & environment* **44**(11): 3494-3508.

Salomón RL, De Roo L, Oleksyn J, De Pauw DJ, Steppe K. 2019a. TReSpire-a biophysical TRee Stem respiration model. *New phytologist* **225**(5): 2214-2230.

Salomón RL, De Roo L, Oleksyn J, Steppe K. 2022. Mechanistic drivers of stem respiration: A modelling exercise across species and seasons. *Plant, cell & environment* **45**(4): 1270-1285.

Salomón RL, De Schepper V, Valbuena-Carabaña M, Gil L, Steppe K. 2018. Daytime depression in temperature-normalised stem CO2 efflux in young poplar trees is dominated by low turgor pressure rather than by internal transport of respired CO2. *New Phytologist* **217**(2): 586-598.

Salomón RL, Rodríguez-Calcerrada J, Staudt M. 2017. Carbon losses from respiration and emission of volatile organic compounds—the overlooked side of tree carbon budgets. *Oaks physiological ecology. Exploring the functional diversity of genus Quercus L.*: 327-359.

Salomón RL, Steppe K, Crous KY, Noh NJ, Ellsworth DS. 2019b. Elevated CO2 does not affect stem CO2 efflux nor stem respiration in a dry Eucalyptus woodland, but it shifts the vertical gradient in xylem [CO2]. *Plant, cell & environment* **42**(7): 2151-2164.

Sauter JJ, van Cleve B. 1994. Storage, mobilization and interrelations of starch, sugars, protein and fat in the ray storage tissue of poplar trees. *Trees* **8**(6): 297-304.

Saveyn A, Steppe K, Lemeur R. 2008a. Report on non-temperature related variations in CO2 efflux rates from young tree stems in the dormant season. *Trees* **22**(2): 165-174.

Saveyn A, Steppe K, Lemeur R. 2008b. Spatial variability of xylem sap flow in mature beech (*Fagus sylvatica*) and its diurnal dynamics in relation to microclimate. *Botany* **86**(12): 1440-1448.

Saveyn A, Steppe K, McGuire MA, Lemeur R, Teskey RO. 2008c. Stem respiration and carbon dioxide efflux of young *Populus deltoides* trees in relation to temperature and xylem carbon dioxide concentration. *Oecologia* **154**(4): 637-649.

Saveyn A, Steppe K, Ubierna N, Dawson TE. 2010. Woody tissue photosynthesis and its contribution to trunk growth and bud development in young plants. *Plant, cell & environment* **33**(11): 1949-1958.

Scartazza A, Moscatello S, Matteucci G, Battistelli A, Brugnoli E. 2013. Seasonal and inter-annual dynamics of growth, non-structural carbohydrates and C stable isotopes in a Mediterranean beech forest. *Tree Physiology* **33**(7): 730-742.

Schiestl-Aalto P, Kulmala L, Mäkinen H, Nikinmaa E, Mäkelä A. 2015. CASSIA–a dynamic model for predicting intra-annual sink demand and interannual growth variation in Scots pine. *New Phytologist* **206**(2): 647-659.

Schiestl-Aalto P, Ryhti K, Mäkelä A, Peltoniemi M, Bäck J, Kulmala L. 2019. Analysis of the NSC storage dynamics in tree organs reveals the allocation to belowground symbionts in the framework of whole tree carbon balance. *Frontiers in Forests and Global Change* **2**: 17.

Schill V, Hartung W, Orthen B, Weisenseel MH. 1996. The xylem sap of maple (*Acer platanoides*) trees—sap obtained by a novel method shows changes with season and height. *Journal of Experimental Botany* **47**(1): 123-133.

Schimel DS. 1995. Terrestrial ecosystems and the carbon cycle. *Global change biology* **1**(1): 77-91.

Schneider CA, Rasband WS, Eliceiri KW. 2012. NIH Image to ImageJ: 25 years of image analysis. *Nature methods* **9**(7): 671-675.

Schuldt B, Buras A, Arend M, Vitasse Y, Beierkuhnlein C, Damm A, Gharun M, Grams TE, Hauck M, Hajek P. 2020. A first assessment of the impact of the extreme 2018 summer drought on Central European forests. *Basic and Applied Ecology* **45**: 86-103.

Schwab VF, Nowak ME, Trumbore SE *et al.* 2019. Isolation of individual saturated fatty acid methyl esters derived from groundwater phospholipids by preparative high-pressure liquid chromatography for compound-specific radiocarbon analyses. *Water Resources Research* **55**(3):2521-2531.

Seibt U, Brand W, Heimann M, Lloyd J, Severinghaus J, Wingate L. 2004. Observations of O2: CO2 exchange ratios during ecosystem gas exchange. *Global Biogeochemical Cycles* **18**(4).

Seibt U, Rajabi A, Griffiths H, Berry JA 2008. Carbon isotopes and water use efficiency: sense and sensitivity. *Oecologia* **155**(3):441–454.

Sevanto S, Mcdowell NG, Dickman LT, Pangle R, Pockman WT. 2014. How do trees die? A test of the hydraulic failure and carbon starvation hypotheses. *Plant, cell & environment* **37**(1): 153-161.

Shane MW, Cramer MD, Funayama-Noguchi S, Cawthray GR, Millar AH, Day DA, Lambers H. 2004. Developmental physiology of cluster-root carboxylate synthesis and exudation in harsh hakea. Expression of phosphoenolpyruvatecarboxylase and the alternative oxidase. *Plant Physiology* **135**(1): 549-560.

Sierra CA, Ceballos-Núñez V, Hartmann H, Herrera-Ramírez D, Metzler H. 2022. Ideas and perspectives: Allocation of carbon from net primary production in models is inconsistent with observations of the age of respired carbon. *Biogeosciences* **19**(16): 3727-3738.

Sinnott EW. 1918. Factors determining character and distribution of food reserve in woody plants. *Botanical Gazette* **66**(2): 162-175.

Smith NG, Dukes JS. 2013. Plant respiration and photosynthesis in global-scale models: incorporating acclimation to temperature and CO2. *Global Change Biology* **19**(1): 45-63.

Smith NG, Li G, Dukes JS. 2019. Short-term thermal acclimation of dark respiration is greater in non-photosynthetic than in photosynthetic tissues. *AoB Plants* **11**(6): plz064.

Spicer R, Holbrook N. 2005. Within-stem oxygen concentration and sap flow in four temperate tree species: does long-lived xylem parenchyma experience hypoxia? *Plant, cell & environment* **28**(2): 192-201.

Spicer R, Holbrook NM. 2007. Effects of carbon dioxide and oxygen on sapwood respiration in five temperate tree species. *Journal of Experimental Botany* **58**(6): 1313-1320.

Sprugel D. 1991. Measuring woody-tissue respiration and photosynthesis. *Techniques and approaches in forest tree ecophysiology*: 329-355.

Steinhof A, Altenburg M, Machts H. 2017. Sample preparation at the Jena 14C laboratory. *Radiocarbon* **59**(3): 815-830.

Stephens BB, Bakwin PS, Tans PP, Teclaw RM, Baumann DD. 2007. Application of a differential fuel-cell analyzer for measuring atmospheric oxygen variations. *Journal of atmospheric and oceanic technology* **24**(1): 82-94.

Steppe K, De Pauw DJ, Doody TM, Teskey RO. 2010. A comparison of sap flux density using thermal dissipation, heat pulse velocity and heat field deformation methods. *Agricultural and Forest Meteorology* **150**(7-8): 1046-1056.

Steppe K, De Pauw DJ, Lemeur R, Vanrolleghem PA. 2006. A mathematical model linking tree sap flow dynamics to daily stem diameter fluctuations and radial stem growth. *Tree Physiology* **26**(3): 257-273.

Steppe K, Saveyn A, McGuire MA, Lemeur R, Teskey RO. 2007. Resistance to radial CO2 diffusion contributes to between-tree variation in CO2 efflux of Populus deltoides stems. *Functional Plant Biology* **34**(9): 785-792.

Steppe K, Sterck F, Deslauriers A. 2015a. Diel growth dynamics in tree stems: linking anatomy and ecophysiology. *Trends in plant science* **20**(6): 335-343.

Steppe K, Vandegehuchte MW, Tognetti R, Mencuccini M. 2015b. Sap flow as a key trait in the understanding of plant hydraulic functioning. *Tree Physiology* **35**(4): 341-345.

Stiles W, Leach WE. 1933. Researches on plant respiration. II.—Variations in the respiratory quotient during germination of seeds with different food reserves. *Proceedings of the Royal Society of London. Series B, Containing Papers of a Biological Character* **113**(784): 405-428.

Strain BR, Johnson PL. 1963. Corticular photosynthesis and growth in Populus tremuloides. *Ecology* **44**(3): 581-584.

Stuiver M, Polach HA. 1977. Discussion reporting of 14C data. *Radiocarbon* **19**(3): 355-363.

Stutz SS, Anderson J. 2021. Inside out: Measuring the effect of wood anatomy on the efflux and assimilation of xylem-transported CO2. *Plant Cell Environ* **44**: 3490-3493.

Sweetlove LJ, Williams TC, Cheung CM, Ratcliffe RG. 2013. Modelling metabolic CO2 evolution–a fresh perspective on respiration. *Plant, cell & environment* **36**(9): 1631-1640.

Tamrakar R, Rayment MB, Moyano F, Mund M, Knohl A. 2018. Implications of structural diversity for seasonal and annual carbon dioxide fluxes in two temperate deciduous forests. *Agricultural and Forest Meteorology* **263**: 465-476.

Tarvainen L, Henriksson N, Näsholm T, Marshall JD. 2023. Among-species variation in sap pH affects the xylem CO2 transport potential in trees. *New Phytologist*.

Tarvainen L, Räntfors M, Wallin G. 2014. Vertical gradients and seasonal variation in stem CO2 efflux within a Norway spruce stand. *Tree Physiology* **34**(5): 488-502.

Tarvainen L, Wallin G, Lim H, Linder S, Oren R, Ottosson Löfvenius M, Räntfors M, Tor-Ngern P, Marshall J. 2018. Photosynthetic refixation varies along the stem and reduces CO2 efflux in mature boreal *Pinus sylvestris* trees. *Tree Physiology* **38**(4): 558-569.

Tarvainen L, Wallin G, Linder S, Näsholm T, Oren R, Ottosson Löfvenius M, Räntfors M, Tor-Ngern P, Marshall JD. 2021. Limited vertical CO2 transport in stems of mature boreal *Pinus sylvestris* trees. *Tree Physiology* **41**(1): 63-75.

Tcherkez G, Boex-Fontvieille E, Mahé A, Hodges M. 2012. Respiratory carbon fluxes in leaves. *Current opinion in plant biology* **15**(3): 308-314.

Tcherkez G, Farquhar G, Badeck F, Ghashghaie J. 2004. Theoretical considerations about carbon isotope distribution in glucose of C3 plants. *Functional Plant Biology* **31**(9): 857-877.

Tcherkez G, Ghashghaie J. 2017. *Plant Respiration: Metabolic Fluxes and Carbon Balance*: Springer.

Tcherkez G, Nogués S, Bleton J, Cornic G, Badeck F, Ghashghaie J. 2003. Metabolic origin of carbon isotope composition of leaf dark-respired CO2 in French bean. *Plant Physiology* **131**(1): 237-244.

Teskey R, McGuire M. 2002. Carbon dioxide transport inxylem causes errors in estimation of rates of respiration in stemsand branches of trees. *Plant, cell & environment* **25**(11): 1571-1577.

Teskey R, McGuire M. 2007. Measurement of stem respiration of sycamore (Platanus occidentalis L.) trees involves internal and external fluxes of CO2 and possible transport of CO2 from roots. *Plant, cell & environment* **30**(5): 570-579.

Teskey RO, McGuire MA, Bloemen J, Aubrey DP, Steppe K. 2017. Respiration and CO2 fluxes in trees. *Plant respiration: Metabolic fluxes and carbon balance*: 181-207.

Teskey RO, Saveyn A, Steppe K, McGuire MA. 2008. Origin, fate and significance of CO2 in tree stems. *New Phytologist* **177**(1): 17-32.

Thornley J. 1970. Respiration, growth and maintenance in plants. *Nature* **227**(5255): 304-305.

Tohjima Y, Mukai H, Machida T, Hoshina Y, Nakaoka S-I. 2019. Global carbon budgets estimated from atmospheric O2/N2 and CO2 observations in the western Pacific region over a 15-year period. *Atmospheric Chemistry and Physics* **19**(14): 9269-9285.

Touraine B, Muller B, Grignon C. 1992. Effect of phloem-translocated malate on NO3− uptake by roots of intact soybean plants. *Plant Physiology* **99**(3): 1118-1123.

Trumbore S. 2006. Carbon respired by terrestrial ecosystems–recent progress and challenges. *Global change biology* **12**(2): 141-153.

Trumbore S, Brando P, Hartmann H. 2015a. Forest health and global change. *Science* **349**(6250): 814-818.

Trumbore S, Czimczik CI, Sierra CA, Muhr J, Xu X. 2015b. Non-structural carbon dynamics and allocation relate to growth rate and leaf habit in California oaks. *Tree Physiology* **35**(11): 1206-1222.

Trumbore SE, Angert A, Kunert N, Muhr J, Chambers JQ. 2013. What's the flux? Unraveling how CO2 fluxes from trees reflect underlying physiological processes. *New Phytologist* **197**(2): 353-355.

Trumbore SE, Sierra C, Hicks Pries C. 2016. Radiocarbon nomenclature, theory, models, and interpretation: Measuring age, determining cycling rates, and tracing source pools. *In: Schuur EAG, Druffel ERM, Trumbore SE (eds) Radiocarbon and global change.* Springer. Cham. pp 45-82.

Valentini R, Matteucci G, Dolman A, Schulze E-D, Rebmann C, Moors E, Granier A, Gross P, Jensen N, Pilegaard K. 2000. Respiration as the main determinant of carbon balance in European forests. *Nature* **404**(6780): 861-865.

Vandegehuchte MW, Bloemen J, Vergeynst LL, Steppe K. 2015. Woody tissue photosynthesis in trees: salve on the wounds of drought? *New Phytologist* **208**(4): 998-1002.

Vandegehuchte MW, Steppe K. 2013. Sap-flux density measurement methods: working principles and applicability. *Functional Plant Biology* **40**(10): 1088-1088.

Vargas R, Trumbore SE, Allen MF. 2009. Evidence of old carbon used to grow new fine roots in a tropical forest. *New Phytologist* **182**(3): 710-718.

Vick J, Young D. 2009. Corticular photosynthesis: a mechanism to enhance shrub expansion in coastal environments. *Photosynthetica* **47**(1): 26-32.

Vogel JS, Southon JR, Nelson DE, Brown TA 1984. Performance of catalytically condensed carbon for use in accelerator mass spectrometry. *Nuclear Instruments and Methods in Physics Research Section B* **5**(2):289–293.

Wang H, Atkin OK, Keenan TF, Smith NG, Wright IJ, Bloomfield KJ, Kattge J, Reich PB, Prentice IC. 2020. Acclimation of leaf respiration consistent with optimal photosynthetic capacity. *Global Change Biology* **26**(4): 2573-2583.

Wang X, Mao Z, McGuire M, Teskey R. 2019. Stem radial CO2 conductance affects stem respiratory CO2 fluxes in ash and birch trees. *Journal of Forestry Research* **30**(1): 21-29.

Waring R, Whitehead D, Jarvis P. 1979. The contribution of stored water to transpiration in Scots pine. *Plant, cell & environment* **2**(4): 309-317.

Weber R, Gessler A, Hoch G 2019. High carbon storage in carbon-limited trees. *New Phytology* **222**(1):171–182.

Wendeberg M, Richter J, Rothe M, Brand WA 2013. Jena Reference Air Set (JRAS): a multi-point scale anchor for isotope measurements of CO2 in air. *Atmospheric Measurement Techniques* **6**(3):817–822.

Werner C, Gessler A. 2011. Diel variations in the carbon isotope composition of respired CO2 and associated carbon sources: a review of dynamics and mechanisms. *Biogeosciences* **8**(9): 2437-2459.

White D, Davis W, Nickels J, King J, Bobbie R 1979. Determination of the sedimentary microbial biomass by extractible lipid phosphate. *Oecologia* **40**(1):51–62.

Wiley E, King CM, Landhäusser SM 2019. Identifying the relevant carbohydrate storage pools available for remobilization in aspen roots. *Tree Physiology* **39**(7):1109–1120.

Wittmann C, Pfanz H. 2008. General trait relationships in stems: a study on the performance and interrelationships of several functional and structural parameters involved in corticular photosynthesis. *Physiologia plantarum* **134**(4): 636-648.

Wittmann C, Pfanz H. 2014. Bark and woody tissue photosynthesis: a means to avoid hypoxia or anoxia in developing stem tissues. *Functional Plant Biology* **41**(9): 940-953.

Wittmann C, Pfanz H. 2016. The optical, absorptive and chlorophyll fluorescence properties of young stems of five woody species. *Environmental and Experimental Botany* **121**: 83-93.

Wittmann C, Pfanz H. 2018. More than just CO2-recycling: corticular photosynthesis as a mechanism to reduce the risk of an energy crisis induced by low oxygen. *New Phytologist* **219**(2): 551-564.

Wittmann C, Pfanz H, Loreto F, Centritto M, Pietrini F, Alessio G. 2006. Stem CO2 release under illumination: corticular photosynthesis, photorespiration or inhibition of mitochondrial respiration? *Plant, cell & environment* **29**(6): 1149-1158.

Woodwell G, Botkin D 1973. Metabolism of terrestrial ecosystems by gas exchange techniques: the Brookhaven approach. *Analysis of temperate forest ecosystems*: Springer, 73-85.

Worrall F, Clay GD, Masiello CA, Mynheer G. 2013. Estimating the oxidative ratio of the global terrestrial biosphere carbon. *Biogeochemistry* **115**: 23-32.

Xu M, DeBiase TA, Qi Y. 2000. A simple technique to measure stem respiration using a horizontally oriented soil chamber. *Canadian Journal of Forest Research* **30**(10): 1555-1560.

Yang J, He Y, Aubrey DP, Zhuang Q, Teskey RO. 2016. Global patterns and predictors of stem CO2 efflux in forest ecosystems. *Global Change Biology* **22**(4): 1433-1444.

Zohner CM, Rockinger A, Renner SS. 2019. Increased autumn productivity permits temperate trees to compensate for spring frost damage. *New Phytologist* **221**(2): 789-795.

Acknowledgements

I would like to thank all the people that guided me on my way. My biggest thanks go to Prof. Henrik Hartmann. I would like to thank you for your support over the last years and for all your immediate feedback on the manuscripts presented here, or revisions of conference abstracts, and feedback to talks and posters.

I would like to thank Prof. Ansgar Kahmen for co-supervising this thesis and supporting me with scientific advice. I enjoyed my short stays in Basel with the Physiological Plant Allocation Group. Prof. John Marshall is thanked for agreeing to do the external review of this thesis and for his interest in the topic.

A special thanks go to Dr. Jan Muhr for his constant advice, long days in the field, expertise about sensors, gas bottles, calibration procedures and the initial idea and set-up of the respiration chambers on which all the chapters of this thesis are based on.

I would like to thank Prof. Susan Trumbore for the constant support over the years, the interest in my work, the field days at 'Hermannsberg' and critical feedback on the manuscripts.

Thank you, Dr. Boaz Hilman, for your expertise in the topic, your various comments to all my manuscripts and your company to numerous field trips.

I sincerely thank Prof. Ernst-Detlef Schulze for giving us the opportunity to work at the beautiful forest site 'Hermannsberg', and for constructive feedback.

For assistance with experimental, laboratory and field work, I would like to thank first of all Iris Kuhlmann, who always supported me in the lab. Thanks for your time (especially your time dedicated to the PEPC assay) and expertise in the lab. The same is true for Martin Göbel, he took care of all the technical aspects of this thesis, especially the respiration chambers, and without his practical expertise and all his efforts the realization of our experiments would have been impossible. Thanks for that, Martin.

Thanks to Olaf Kolle for technical expertise on the calibration unit of the respiration chambers. I thank Savoyane Lambert, Agnes Fastnacht and Nadine Hempel for the enjoyable field trips to the forest. It was always fun with you. Thanks to Anett Enke for HPLC measurements, to Axel Steinhof, Heike Machts and Melanie Altenburg for the radiocarbon measurements and to Heiko Moossen and Petra Linke for $\delta^{13}C$ analysis. Further, thanks to the mechanic and electronic

workshops (Frank Voigt, Bernd Schlöffel, Reimo Leppert, Martin Strube) at our institute for always having the right tool for me, and all the technical help.
Thanks also to Kerstin Lohse for administrative guidance, for all the paper work that had to be done.
Thanks to Prof. Kathy Steppe and her Plant Ecology Group for hosting me in Ghent during parts of my research stay. Thanks Kathy for your expertise in many of those chapters, as co-author or editor. At the same time, I am very grateful that Dr. Roberto Salomón approached the Plant Allocation Group for a stay at our institute. The resulting collaboration had greatly improved this thesis, I learnt a lot from you Roberto. Graçias!
I thank the Hiwis Christin and Stephanie for their great help in the laboratory and in the field.
Special thanks go to Steffi for the nice guidance throughout the IMPRS program, but also the lunch breaks, evenings or time with the kids.
I thank my office mates in B1.003 and my colleges of the BGP department. Thanks to Sophie, Linda, Shane, David, Melanie, Lucia, Jianbei, Antonios and Kasun. I really enjoyed the time with you during lunch and coffee breaks, during hiking, bouldering and bar evenings, it was a pleasure meeting you all.
I would like to thank my parents for their support during my studies and during the four years of my PhD project. Last but not least, I have to give a big thanks to Christoph. Thanks for all your support, especially for all the afternoons and weekends with Oskar the last months!

Supplementary Data

CHAPTER 1 – Supplementary data

Material S1 Henry's Law

Dissolved inorganic carbon in the xylem ($[CO_2^*]$) comprises of dissolved CO_2, carbonic acid (H_2CO_3), and the two deprotonated forms, bicarbonate (HCO_3^-) and carbonate (CO_3^{2-}). $[CO_2^*]$ cannot be measured directly, but can be calculated from gaseous $[CO_2]$, xylem sap temperature and sap pH. The partial pressure of CO_2 in air (pCO_2), Henry's constant for CO_2 (K_H) and dissociation constants for bicarbonate and carbonate ions (K_1 and K_2) should be calculated as parts of Henry's formula (McGuire & Teskey, 2002):

$$[CO_2^*] = \left(1 + \frac{K_1}{10^{-pHx}} + \frac{K_1 K_2}{(10^{-pHx})^2}\right) K_H pCO_2 \quad [1]$$

$$K_H = 0.0114 + (0.0661 e^{-0.0433T} \quad [2]$$

$$K_1 = (2.5764 \times 10^{-7}) + (3.3742 \times 10^{-7})(1 - e^{-0.0318T}) \quad [3]$$

$$K_2 = (2.3777 \times 10^{-11}) + (9.0041 \times 10^{-13})\, T \quad [4]$$

Where K_1 and K_2 are first and second acidity constants, K_H is Henry's constant. K_H, K_1 and K_2 are temperature-dependent solubility coefficients for CO_2 in water and pCO_2 is the partial pressure of $[CO_2]$. According to those eqs. $[CO_2^*]$ increases with higher PCO_2, lower temperatures, and higher pH values.

Table S1 Summary of published studies on sap pH measurements (measured at least twice during the campaign) with observed seasonal and/or daily trends.

Species	pH value					Measurement location	Daily trends	Seasonal trends from spring to winter	References
	spring	summer	autumn	winter	wet and dry season				
Actinidia chinensis	5.3	6.2	6.2	6.2		shoots	na	spring acidification	(Ferguson *et al.,* 1983)
Populus × canademis "robusta"	5.4	6-7	7.5	7.5		branches	na	spring acidification	(Sauter, 1988)
Fagus sylvatica	6.0	5.6	6.0-6.5	6.0-6.5		lowest trunk parts (42-yr-old)	na	summer acidification	(Glavac *et al.,* 1990)
Fagus sylvatica	~5.8-6.5	~5.8	~6.6-6.8	~6.4		trunk segments (45-yr-old)	na	xylem sap became more acidic from february to april, alkalinisation from spring to autumn	(Rennenberg *et al.,* 1994) Estimated values from height 1.2 - 2.4 m, see Fig.3
Robinia pseudoacacia	5.3	5.4-5.5	NA	5.7-6.0		branches	na	spring/summer acidification	(Fromard *et al.,* 1995)
Ricinus communis	na	na	na	na	6.8 (well-watered); 6.3 (drought stressed)		night decrease (6.0); daytime alkalinisation (6.6)		(Schurr & Schulze, 1995; Schurr & Schulze 1996)
Eucalyptus species, Acacia mimula, Alphitonia excelsa, Planchonia careya, Cochlospermum fraseri, Terminalia ferdinandiana	na	na	na	na	evergreen and semi-decidious species: sap pH increased from the wet to dry season (0.7 pH units) deciduous species: sap pH declined slightly from wet to dry season	branches	no	na	(Thomas & Eamus, 2002)
Juglans regia	5.6	na	6.8	5.3		twigs	na	winter acidification	(Alves *et al.,* 2004)

Species	pH value					Measurement location	Daily trends	Seasonal trends from spring to winter	References
	spring	summer	autumn	winter	wet and dry season				
Populus deltoides	6.94–7.18	na	na	na		twigs, stem cores	No (higher at lower stem during night)	no	(Aubrey *et al.,* 2011)
Prunus domestica	5.29	5.21	na	5.43		branches	no	summer acidification	(Erda *et al.,* 2014)
Quercus pyrenaica	6.18	6.4	6.68	na		twigs	night decrease (6.1); daytime alkalinisation (6.46-6.5)	alkalinisation from spring to autumn	(Salomón *et al.,* 2016)
Pinus cembra, Picea abies, Larix decidua	na	5.8	na	7.3		branches	na	summer acidification	(Losso *et al.,* 2018)
Grapefruit orchard	na	5.9-6.0	na	5.1-5.7				winter acidification	(Paudel *et al.,* 2018)
Populus nigra	5.7-6.0	NA	na	na		cut stems (1-yr-old)	pre-dawn lowest value	na	(Brunetti *et al.,* 2019) note: we report well-watered conditions only

Note: Terminology twigs and branches was maintained from the original studies

Material S2 Equations for modelling exercises 1 and 2.

For a fully detailed explanation of model equations, variables, parameters and corresponding units, see Salomón *et al.* (2019). For an abridged explanation of the model see Salomón *et al.* (2022).

Relevant equations in modelling exercise 1:

According to Henry´s law, sap [CO_2^*] is proportional to the partial pressure of CO_2 in the gas phase in the xylem (pCO_2) (see equation 1, Supplementary Material 1). This equation illustrates how sap [CO_2^*] increases with sap pH. Consequently, higher solubility of CO_2 leads to a higher contribution of the storage flux and the transport flux to stem respiration, and hence, a lower contribution of E_{CO2} to R_S.

Relevant equations in modelling exercise 2:

The higher portion of the xylem to outer tissues with increasing stem size is a consequence of the non-linear relationship between stem diameter (D) and thickness of the outer tissues (d_{OT}). According to Genard *et al.* (2001):

$$d_{OT} = a\,(1 - e^{(-b\,D)})$$

where a and b are allometric parameters. See Fig. S2 in Salomón *et al.* (2019).

Once the dimensions of the xylem and outer tissues are known and assuming here that non-respiring heartwood is absent, maintenance respiration in the xylem (R_{M_XY}) and outer tissues (R_{M_OT}) is estimated according to equations 20 and 21 in Salomón *et al.* (2019) accounting for tissue volume, density, N content and temperature-dependent kinetics:

$$R_{M\_XY} = R_{b\_N}\,[N]_{XY}\,\frac{\rho_{XY}}{M_N}\,Q_{10}^{\frac{T-T_b}{10}}\,\frac{V_{XY}}{V_S}$$

$$R_{M\_OT} = R_{b\_N}\,[N]_{OT}\,\frac{\rho_{OT}}{M_N}\,Q_{10}^{\frac{T-T_b}{10}}\,\frac{V_S-V_{XY}}{V_S}$$

where Rb_N is respiration at basal temperature (Tb, °C) on a Nitrogen molar basis, M_N is the molar mass of N, Q10 is the temperature sensitivity of R_M, T is the stem temperature, and V_{XY} and V_S are the volumes of the xylem and the stem within the monitored segment.

Stem size also plays a role in the CO_2 diffusion process, as radial CO_2 efflux from the xylem to the outer tissues (E_{XY}) and radial CO_2 efflux from the outer tissues to the atmosphere (E_{CO2}) follows Fick´s law of diffusion. According to the geometry of the xylem and outer tissues (equations 27 and 28 in Salomón *et al.* (2019)):

$$E_{XY} = \text{Dif}\ \frac{[CO_2]_{XY} - [CO_2]_{OT}}{\frac{2D_{XY}}{3\pi}}\ \frac{A_{XY}}{V_S}$$

$$E_{CO2} = \text{Dif}\ \frac{[CO_2]_{OT} - [CO_2]_{ATM}}{\frac{d_{OT}}{2}}\ \frac{A_S}{V_S}$$

where Dif is diffusivity, $[CO_2]_{XY}$, $[CO_2]_{OT}$ and $[CO_2]_{ATM}$ are the gaseous $[CO_2]$ in xylem, outer tissues and atmosphere, respectively, D_{XY} is the diameter of the xylem tissue, d_{OT} is the thickness of the outer tissues, and A_{XY} and A_S are the axial surface of xylem and stem within the monitored stem segment, respectively.

Alves G, Ameglio T, Guilliot A, Fleurat-Lessard P, Lacointe A, Sakr S, Petel G, Julien J-L. 2004. Winter variation in xylem sap pH of walnut trees: involvement of plasma membrane H+-ATPase of vessel-associated cells. *Tree Physiology* **24**(1): 99-105.

Aubrey DP, Boyles JG, Krysinsky LS, Teskey RO. 2011. Spatial and temporal patterns of xylem sap pH derived from stems and twigs of *Populus deltoides* L. *Environmental and Experimental Botany* **71**(3): 376-381.

Brunetti C, Gori A, Marino G, Latini P, Sobolev AP, Nardini A, Haworth M, Giovannelli A, Capitani D, Loreto F. 2019. Dynamic changes in ABA content in water-stressed *Populus nigra*: effects on carbon fixation and soluble carbohydrates. *Annals of botany* **124**(4): 627-643.

Erda FG, Bloemen J, Steppe K. 2014. Quantifying the impact of daily and seasonal variation in sap pH on xylem dissolved inorganic carbon estimates in plum trees. *Plant Biology* **16**(1): 43-48.

Ferguson A, Eiseman J, Leonard J. 1983. Xylem sap from *Actinidia chinensis*: seasonal changes in composition. *Annals of botany* **51**(6): 823-833.

Fromard L, Babin V, Fleurat-Lessard P, Fromont J-C, Serrano R, Bonnemain J-L. 1995. Control of vascular sap pH by the vessel-associated cells in woody species (physiological and immunological studies). *Plant Physiology* **108**(3): 913-918.

Genard M, Fishman S, Vercambre G, Huguet J-G, Bussi C, Besset J, Habib R. 2001. A biophysical analysis of stem and root diameter variations in woody plants. *Plant Physiology* **126**(1): 188-202.

Glavac V, Koenies H, Ebben U. 1990. Seasonal variations in mineral concentrations in the trunk xylem sap of beech (*Fagus sylvatica* L.) in a 42-year-old beech forest stand. *New Phytologist* **116**(1): 47-54.

Losso A, Nardini A, Dämon B, Mayr S. 2018. Xylem sap chemistry: seasonal changes in timberline conifers *Pinus cembra*, *Picea abies*, and *Larix decidua*. *Biologia Plantarum* **62**(1): 157-165.

McGuire M, Teskey R. 2002. Microelectrode technique for in situ measurement of carbon dioxide concentrations in xylem sap of trees. *Tree Physiology* **22**(11): 807-811.

Paudel I, Bar-Tal A, Rotbart N, Ephrath J, Cohen S. 2018. Water quality changes seasonal variations in root respiration, xylem CO2, and sap pH in citrus orchards. *Agricultural Water Management* **197**: 147-157.

Rennenberg H, Schupp R, Glavac V, Jochheim H. 1994. Xylem sap composition of beech (*Fagus sylvatica* L.) trees: seasonal changes in the axial distribution of sulfur compounds. *Tree Physiology* **14**(5): 541-548.

Salomón RL, De Roo L, Oleksyn J, De Pauw DJ, Steppe K. 2019. TReSpire-a biophysical TRee Stem respiration model. *New Phytologist* **225**(5): 2214-2230.

Salomón RL, De Roo L, Oleksyn J, Steppe K. 2022. Mechanistic drivers of stem respiration: A modelling exercise across species and seasons. *Plant, cell & environment* **45**(4): 1270-1285.

Salomón RL, Valbuena-Carabaña M, Gil L, McGuire MA, Teskey RO, Aubrey DP, González-Doncel I, Rodríguez-Calcerrada J. 2016. Temporal and spatial patterns of internal and external stem CO2 fluxes in a sub-Mediterranean oak. *Tree Physiology* **36**(11): 1409-1421.

Sauter JJ. 1988. Seasonal changes in the efflux of sugars from parenchyma cells into the apoplast in poplar stems (Populus× canademis "robusta"). *Trees* **2**(4): 242-249.

Schurr U, Schulze ED. 1995. The concentration of xylem sap constituents in root exudate, and in sap from intact, transpiring castor bean plants (*Ricinus communis* L.). *Plant, cell & environment* **18**(4): 409-420.

Schurr U, Schulze ED. 1996. Effects of drought on nutrient and ABA transport in *Ricinus communis*. *Plant, cell & environment* **19**(6): 665-674.

Thomas DS, Eamus D. 2002. Seasonal patterns of xylem sap pH, xylem abscisic acid concentration, leaf water potential and stomatal conductance of six evergreen and deciduous Australian savanna tree species. *Australian Journal of Botany* **50**(2): 229-236.

CHAPTER 2 – Supplementary data

Tree Physiology

Supplemental Information

Article title: Low-cost chamber design for simultaneous CO_2 and O_2 flux measurements between tree stems and the atmosphere

Authors: Juliane Helm, Henrik Hartmann, Martin Göbel, Boaz Hilman, David Herrera, Jan Muhr

The following Supporting Information is available for this article:

Supplementary data S1 and S2

We tested two different humidity sensors in the laboratory- the internal relative humidity sensor integrated in the COZIR sensor, and the SHT-85. Both sensors were exposed to air that was pumped through a dew point generator (DPG, LI-610, LI-COR Biosciences, Bad Homburg, DE) to create known levels of humidity. Our tests showed very fast response and accurate measurements for the SHT-85. The internal humidity sensor of the COZIR, however, reacted much slower to changes and consistently underestimated the humidity. In the beginning and during the field tests we used the COZIR data for dilution corrections, but this will underestimate humidity (S2). For the humidity correction, we recommend using the more accurate alternative.

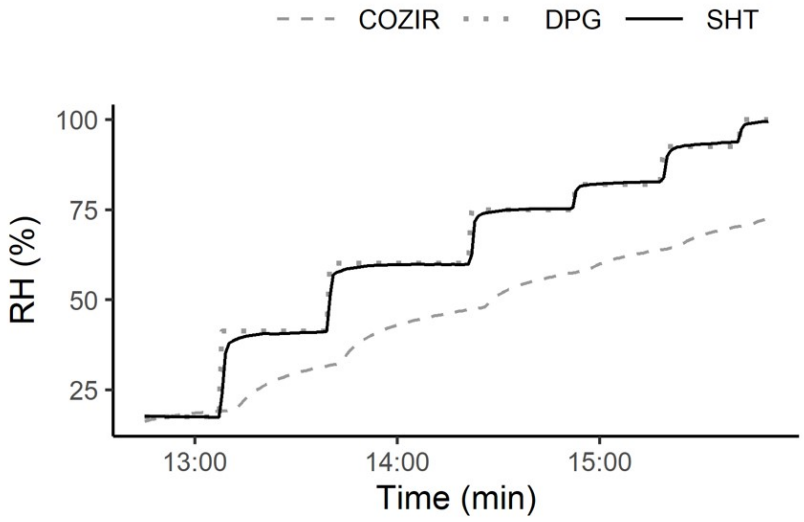

S1 Relative humidity measurements (%) of the external humidity sensor (SHT-85, n = 2) and COZIR sensors (n = 10) over time within the calibration and testing unit in the laboratory. Different humidity levels were set with a Dew Point Generator (DPG, LI-610, LI-COR Biosciences, Bad Homburg, DE).

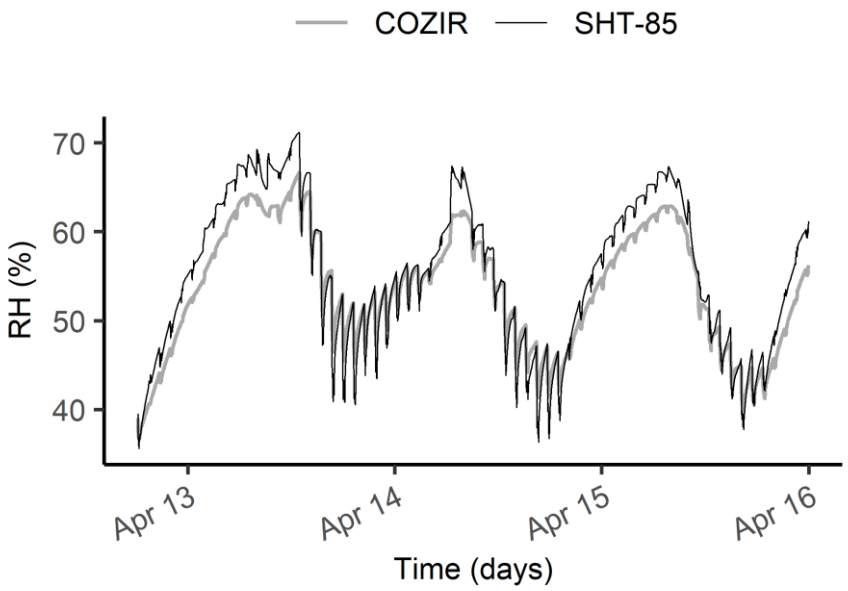

S2 Relative humidity measurements (%) of the external humidity sensor (SHT-85) and COZIR RH sensor within the headspace of the stem chamber over time (n = 3). Three chambers were installed at three positions on the same tree (*Prunus avium* L., mean stem circumference: 105 cm) and measured relative humidity for three days in April 2020 in Jena, Thuringia, Germany.

Supplementary Data S3

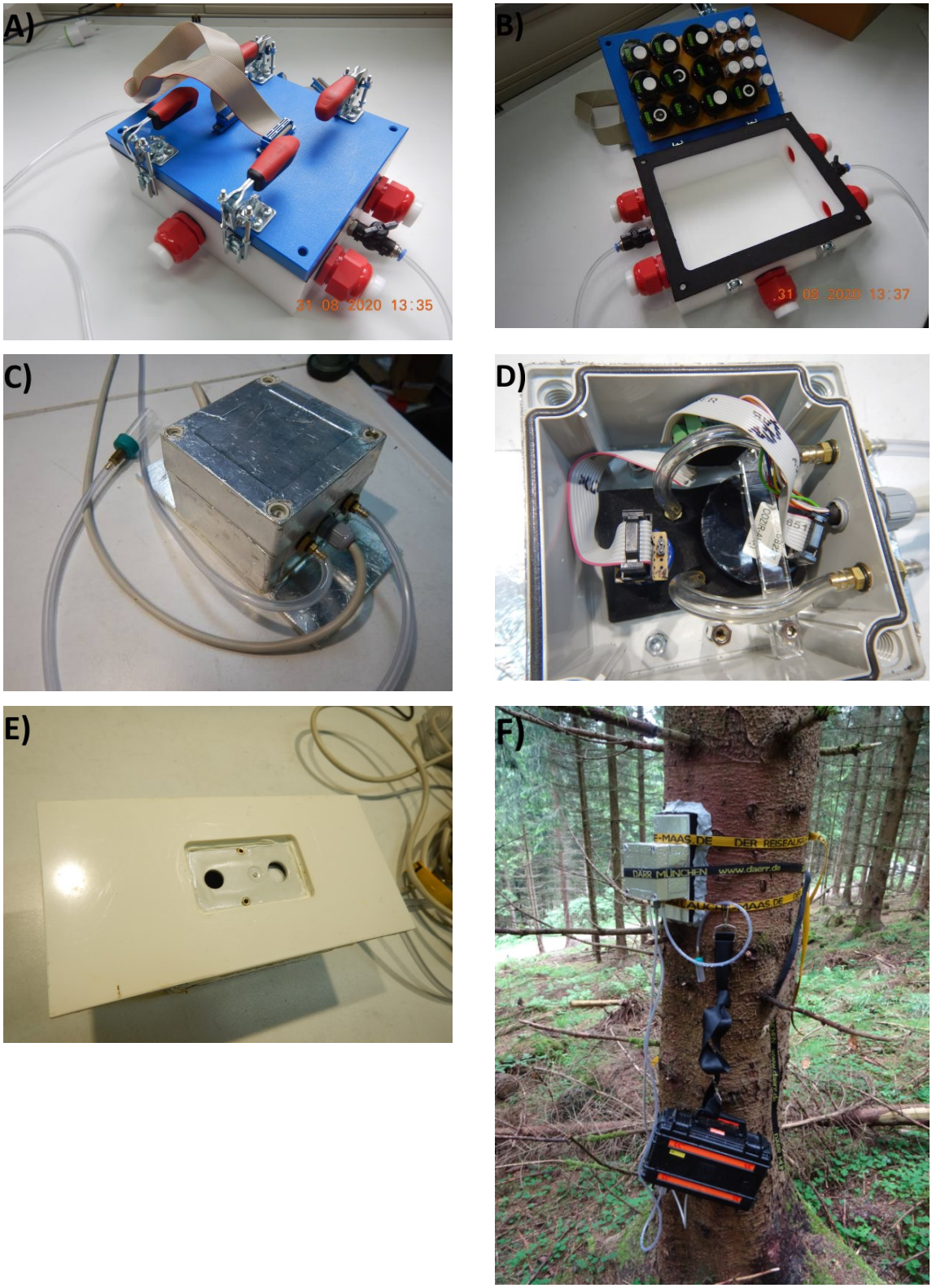

S3 A) and B) Calibration and testing unit for 10 COZIR and 10 LuminOx sensors. C) Sensor box for COZIR and LuminOx sensors covered with aluminium foil, D) COZIR and LuminOx sensors placed inside the waterproof housing. E) Sensor box and base plate of the chamber module and F) Installation in the field with sensor box and waterproof transport-case.

Supplementary Data S4

Details for custom made datalogger: The custom-built data logger comprises an Arduino Mega 2560 R3 with added data logging shield and a 16x2 RGB LCD shield.

The LCD shield displays actual CO_2 and O_2 values and other parameters like time/date, file name and accumulation/flushing times, which can be set using the buttons.

The data logging shield holds the SD memory card for data storage (4 MB, more than one year of operation) and the real-time-clock chip for time-stamping the measurement values. The prototyping area of the shield also holds the MOSFET driver for the 6V pump (NMP015S from KNF, ca. 1 L/min due to running at 5V).

The program (a.k.a. „sketch“) on the arduino has the following structure: On powering up, the last known parameters (pump/flush duration, file number, measurement interval) are loaded from the EEPROM. Both sensors are set into poll mode to not flood the arduino in buffer. The SD card is checked for existing data files and a new one is being created to hold this session's data. After this initialisation, the standard main loop is entered, which runs ad infinitum. The main loop checks if pumping is due or not, then checks and resolves any user input on the LCD shield buttons, then polls both sensors for all data they can possibly measure (O_2: O_2partial pressure, temperature, barometric pressure, O_2 percentage value; CO_2: CO_2 in ppm, temperature, RH). After all data has been received it’s checked for integrity then formatted and saved to the file on the SD card.

Supplementary Data S5

S5 Component list of the stem chamber (main parts).

Component description	Quantity	Supplier	Part number	Unit price [€]
Transport-case	1	Dyntronic-plenty.de	72601-K	25.-
Fibox Grey ABS Enclosure 100mmx100mmx75mm IP67	1	RS	498-4025	8.-
Ratchet straps	3	Various		15.-
Closed cell EPDM foam mat 40mm	1	luxCO$_2$4.de	8470020004 0	2.-
Arduino Mega	1	RS	7154084	35.-.
Arduino Display Shield negative	1	exp-tech.de	EXP-R15-123	30.-
Arduino Datalogger Shield	1	exp-tech.de	EXP-R15-003	1.5.-
Generic SD card (4GB)	1	Various		10.-
Components for circuit board assembly (self-made design)	1			10.-
Battery 50.000mAh*	1	Xtpower.de		150.-
Membrane pump, NMP015S, 6VDC	1	KNF	NMP015B	70.-
CO_2 Sensor 10k ppm	1	GSS Ltd.		90.-
O_2 Sensor 0...25%	1	SST Ltd.		50.-
H_2O Sensor SHT-85	1	RS		23.-

*We used this power bank to achieve up to 12 days of continuous operation. Smaller power banks (20 Ah) are much cheaper (ca. 30 €) and can be more easily acquired, but only allow ca. 4-5 days of continuous operation.

Total [€]: 519.5

Supplementary Data S6

Correction of measurement data (O_2) for the dilution effect of changing H_2O and CO_2 concentrations; Description of the original approach described by Keeling *et al.* (1998); extended by a H_2O correction:

We can convert our measurements of apparent mole fraction to relative changes on the per meg scale while correcting for the diluting effect of changes in the simultaneously measured CO_2 concentration as follows (using the Kozlova *et al.* (2008) modified version of the Stephens *et al.* (2007) equation):

$$\delta(O_2/N_2) = \frac{\delta X_{O_2} + S_{O_2}\left([CO_2]_{sample} - [CO_2]_{reference}\right) + S_{O_2}\left([H_2O]_{sample} - [H_2O]_{reference}\right)}{S_{O_2}(1 - S_{O_2})}$$

where $\delta(O_2/N_2)$ is the change of the O_2/N_2 ratio in per meg, δXO_2 is apparent mole fraction change. i.e. the differences between the measured apparent mole fraction and the arbitrarily defined reference mole fraction (SO_2) of 0.20946, multiplied by 10^6 to express as 'per meg'. $[CO_2]$sample is the measured CO_2 concentration in µmol mol^{-1}, $[CO_2]_{reference}$ is the CO_2 concentration of the reference cylinders that define the zero point on the Scripps O_2 scale (363.29 µmol mol^{-1}). $[H_2O]$sample is given in ppm (conversion from % to ppm, see section 2.5). $[H_2O]_{reference}$ is 0. The addition of 1 µmol of O_2 to 1 µmol of dry air results in a change of 4.77 per meg (Keeling *et al.*, 1998), so for comparison of O_2 and CO_2 fluxes we divided the results by this factor to get O_2 concentrations relative to the reference in ppm equivalents, which we used as the basis for all subsequent O_2 flux calculations.

New mathematical approach (explanation see section 2.5):

$$\delta O_{2,corr}[ppm] = \frac{\delta O_{2,app}[ppm] + \delta CO_2[ppm] \times X_{O_2\,t=0} + \delta H_2O[ppm] \times X_{O_2\,t=0}}{1 - X_{O_2\,t=0}}$$

No significant difference between the two approaches was found for our measurement campaign on three poplar trees (t = 0.0283, p = 0.9776).

General note: The implemented correction function we use within this manuscript for dilution by O_2, CO_2 and H_2O is based on some assumptions that might not always be justified (personal communication Dr. Jelka Braden-Behrens). Among other assumptions, such as constant nitrogen and argon content and a constant O_2 mole fraction relative to CO_2 (and H_2O)-free air, this correction function neglects some second order (mixed) terms (personal communication Dr. Jelka Braden-Behrens). These are basically the same assumptions as those that underlie the often-used CO_2 and O_2 dilution correction (see e.g., Kozlova *et al.*, 2008).

Supplementary Data S7

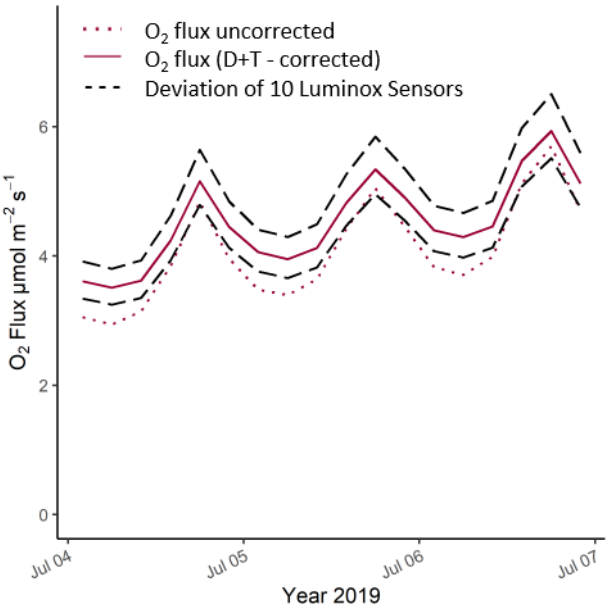

S7 Calculated O_2 fluxes (4h mean) according to eq. [6] over 3 days in July 2019 (Thuringia, Germany, n = 3). Uncorrected data (dotted line) and corrected data (dilution (D-) and temperature (T-) corrected, solid line) for O_2 are shown. Black dashed line represents the extremes of 10 sensors, applying the formulas $SC(O_2) = -0.010\ x\ T\ (in\ °C) + 1.40$ and $SC(O_2) = -0.009\ x\ T\ (in\ °C) + 1.20$.

Keeling RF, Manning AC, McEvoy EM, Shertz SR. 1998. Methods for measuring changes in atmospheric O2 concentration and their application in southern hemisphere air. *Journal of Geophysical Research: Atmospheres* **103**(D3): 3381-3397.

Kozlova EA, Manning AC, Kisilyakhov Y, Seifert T, Heimann M. 2008. Seasonal, synoptic, and diurnal-scale variability of biogeochemical trace gases and O2 from a 300-m tall tower in central Siberia. *Global Biogeochemical Cycles* **22**(4).

Stephens BB, Bakwin PS, Tans PP, Teclaw RM, Baumann DD. 2007. Application of a differential fuel-cell analyzer for measuring atmospheric oxygen variations. *Journal of atmospheric and oceanic technology* **24**(1): 82-94.

CHAPTER 3 – Supplementary data

Plant, Cell and Environment

Supplemental Information

Article title: Differences between tree stem CO_2 efflux and O_2 influx rates cannot be explained by internal CO_2 transport or storage in large beech trees

Authors: Juliane Helm, Roberto L. Salomón; Boaz Hilman, Jan Muhr, Alexander Knohl, Kathy Steppe, Yves Gibon, Cédric Cassan, Henrik Hartmann

The following Supporting Information is available for this article:

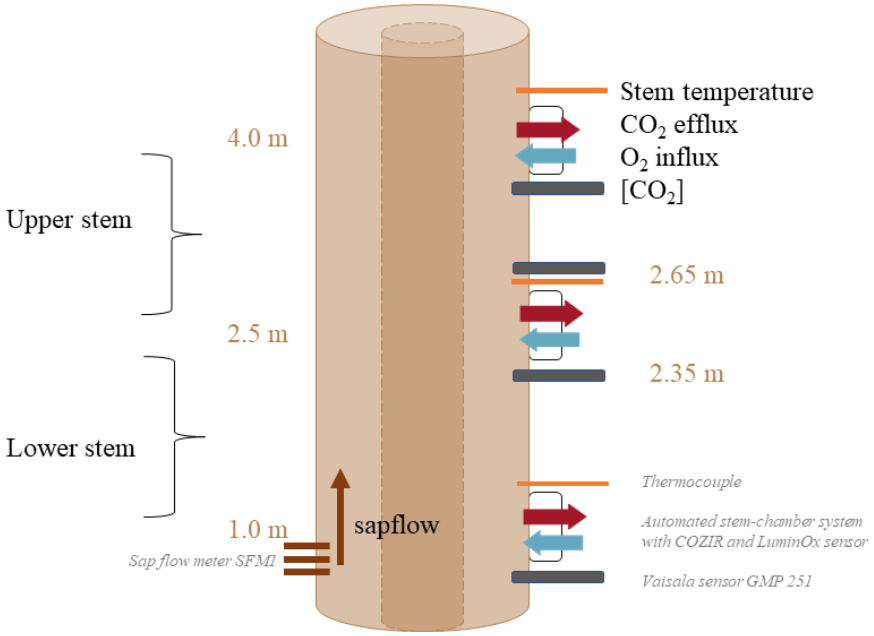

Figure S1 Schematic overview of the experimental set-up and measurement devices installed on the stem at different stem-levels.

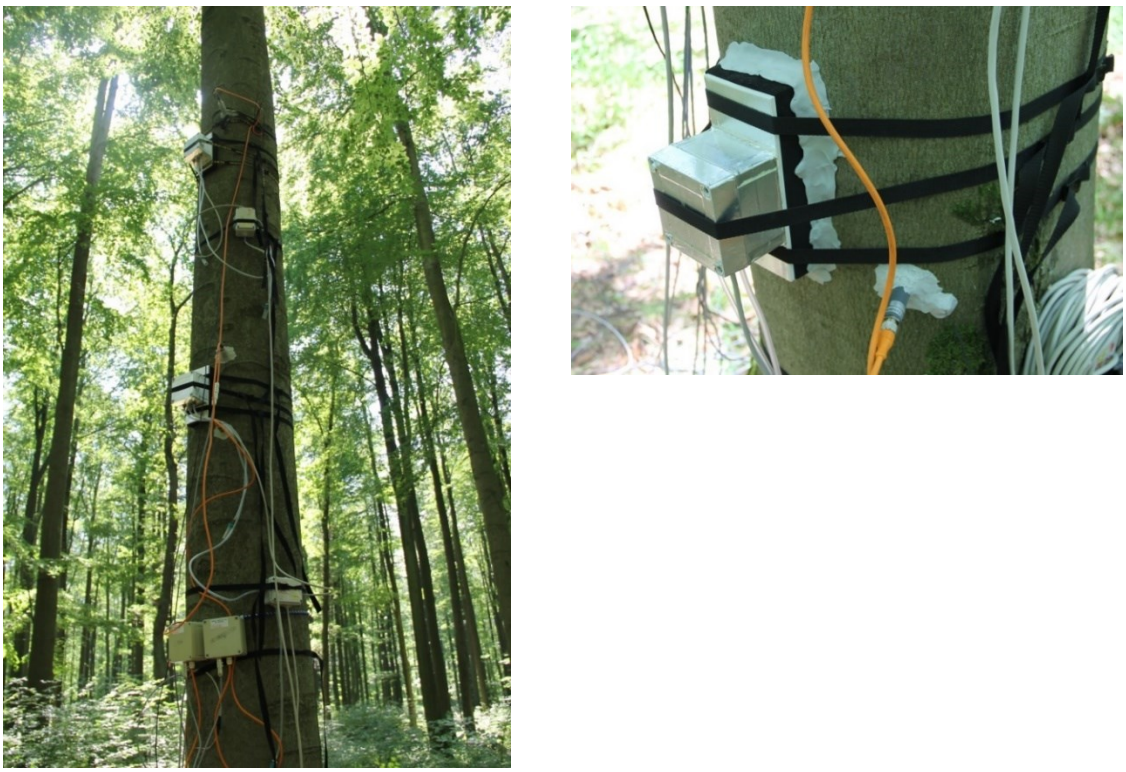

Picture S1 (a) Beech tree with stem chambers (CO_2 efflux, O_2 influx) and Vaisala sensors (internal $[CO_2]$) at different stem heights. (b) Close-up of the equipment with butty butyl sealant for isolation from the atmosphere.

Method S1: Measurement of PEPC capacity

Aliquots were extracted by vigorous shaking with 500 µL of extraction buffer (20% v/v glycerol, 0.25% w/v bovine serum albumin, 1% v/v Triton X-100, 50 mM Hepes-KOH pH 7.5, 10 mM $MgCl_2$, 1 mM EDTA, 1 mM EGTA, 1 mM aminocaproic acid, 1 mM benzamidine, 20 µM leupeptin, 0.5 mM dithiothreitol, 1 mM phenylmethylsulfonylfluoride, 10% w/v polyvinylpolypyrrolidone and 1% w/v polyvinylpyrrolidone). After centrifugation (7 min, 3000 g, 4 °C), extracts were diluted by a factor of 2000 (w/v). Diluted extracts and NAD^+ standards (prepared in the extraction buffer and ranging from 0 to 1 nmol per well) were incubated for 20 min in 20 µl of a medium containing 100 mM Tricine-KOH pH 8.0, 20 mM $MgCl_2$, 1 unit ml^{-1} malate dehydrogenase, 10 mM $NaHCO_3$, 0.1 mM NADH, 1% w/v polyvinylpyrrolidone and phosphoenolpyruvate 0 (blanks) or 2 mM (maximal activity). The reaction was stopped with 20 µl of 0.5 M HCl. The sealed microplate was then incubated at 95 °C for 10 min to destroy NADH. After cooling down, each well was neutralised with 20 µl of NaOH 0.5 M and 0.2 M Tricine-KOH pH 9.0 to adjust the pH to 9.0. NAD^+ was then measured with 6 units ml^{-1} alcohol dehydrogenase, 100 mM Tricine-KOH pH 9.0, 4 mM EDTA, 0.1 mM PES, 0.6 mM MTT, and 500 mM ethanol. The absorbance was read at 570 nm and 30 °C until rates were stabilised. Reaction rates expressed in $mOD.min^{-1}$ were used to calculate the amount of NAD^+ formed during the first step of the assay. All pipetting steps were performed using a 96-head robot (Hamilton Star), and absorbances were measured in a filter-based microplate reader (SAFAS MP96).

CHAPTER 4 – Supplementary data

Tree Physiology

Supplemental Information

Article title: Carbon dynamics in long-term starving poplar trees – the importance of older carbohydrates and a shift to lipids during survival

Authors: Juliane Helm, Jan Muhr, Boaz Hilman, Ansgar Kahmen, Ernst-Detlef Schulze, Susan Trumbore, David Herrera-Ramírez, Henrik Hartmann

The following Supporting Information is available for this article:

Table S1 Diameter at breast height (cm) of the 12 poplar trees (6 control, 6 girdled) in July 2018. Volume of the stem chamber was determined once after installation in each year.

Tree Number	DBH (cm)	Treatment	Volume determination (cm^3)		
			2018	2019	2021
1	36.0	Girdling	92		
2	39.3	Control	101		
3	34.6	Control	105	84	95
4	32.8	Control	96		
5	30.4	Control	98	84	98
6	31.1	Girdling	96		100
7	29.1	Girdling	83		93
8	33.4	Girdling	99	88	90
9	41.9	Control	101	97	87
10	37.1	Girdling	104	85	97
11	34.9	Girdling	99	97	
12	36.3	Control	76		92

Table S2 Overview of measurements taken in all three campaigns 2018, 2019 and 2021 or in individual years, only.

Measurement	Time period	Number of trees (n)
CO_2 efflux, O_2 influx	2018, 2019, 2021	12, 6, 8
NSC	2018 (DOY 172, 262), 2019 (DOY 147), 2021 (DOY 195)	10-12 (when analysis failed)
$\delta^{13}CO_2$, ^{14}C	16 measurement points, for details see Tables S4, S6	10-12 (when analysis failed)
Sap flow	2018	12
PEPC capacity	2019 (DOY 236)	11
Neutral lipids (staining method)	2021 (DOY 147)	6
$\delta^{13}C$ of substrates	2021 (DOY 236)	12

Table S3 Mean $\delta^{13}CO_2$ (±SD) of the chamber incubation gas samples for all trees individually.

Year	Date	DOY	Treatment		Sample Number (n)	
			Control ± SD	Girdled ± SD	Control	Girdled
2018	09.05.2018	129	-29.22 ± 0.6	-28.84 ± 0.6	6	6
	31.05.2018	151	-27.50 ± 0.3	-27.70 ± 0.4	6	6
	21.06.2018	172	-27.90 ± 0.4	-28.11 ± 0.4	6	6
	11.07.2018	192	-24.23 ± 0.3	-25.93 ± 0.9	6	6
	02.08.2018	214	-25.78 ± 0.5	-31.20 ± 1.6	6	6
	22.08.2018	234	-24.17 ± 0.5	-28.40 ± 2.2	6	6
	12.09.2018	255	-24.27 ± 0.9	-26.04 ± 1.5	6	4
	04.10.2018	277	-24.92 ± 0.7	-26.07 ± 2.0	6	6
2019	05.06.2019	156	-27.37 ± 0.4	-28.26 ± 0.5	6	6
	20.06.2019	171	-26.76 ± 0.3	-28.51 ± 0.6	6	6
	04.07.2019	185	-25.09 ± 0.3	-30.92 ± 7.8	6	5
	02.08.2019	214	-24.51 ± 0.3	-27.71 ± 0.9	6	6
	25.09.2019	268	-26.80 ± 0.9	-28.65 ± 1.0	5	6
2021	14.07.2021	195	-29.70 ± 1.1	-30.47 ± 1.2	6	6
	03.08.2021	215	-27.85 ± 0.2	-28.48 ± 1.1	6	6
	16.09.2021	259	-27.81 ± 0.9	-28.57 ± 0.9	6	6

Table S4 Mean $\Delta^{14}C$ (±SD) of the chamber incubation gas samples for all trees individually.

Year	Date	DOY	Treatment		Sample Number (n)	
			Control ± SD	Girdled ± SD	Control	Girdled
2018	09.05.2018	129	7.28 ± 1.2	5.25 ± 1.6	6	6
	31.05.2018	151	6.87 ± 1.8	8.48 ± 1.5	6	6
	21.06.2018	172	12.77 ± 2.7	15.15 ± 2.5	6	6
	11.07.2018	192	4.70 ± 3.7	2.98 ± 2.6	6	6
	02.08.2018	214	2.53 ± 3.8	13.17 ± 1.6	6	6
	22.08.2018	234	2.47 ± 1.9	3.93 ± 1.6	6	6
	12.09.2018	255	1.20 ± 1.6	19.90 ± 4.8	6	6
	04.10.2018	277	21.22 ± 2.3	25.73 ± 4.1	6	6
2019	05.06.2019	156	12.44 ± 11.1	19.42 ± 5.7	5	6
	20.06.2019	171	3.05 ± 3.1	24.80 ± 14.8	4	4
	04.07.2019	185	7.33 ± 2.9	17.40 ± 2.5	4	4
	02.08.2019	214	7.98 ± 2.1	18.38 ± 4.2	6	6
	25.09.2019	268	9.37 ± 1.8	19.55 ± 6.2	6	6
2021	14.07.2021	195	-1.33 ± 4.5	66.98 ± 23.1	6	6
	03.08.2021	215	-6.55 ± 4.1	25.23 ± 9.5	6	6
	16.09.2021	259	-0.92 ± 3.5	31.42 ± 2.8	6	5

Table S5 Mean Age of C (±SD) of the chamber incubation gas samples for all trees individually.

Year	Date	DOY	Treatment		Sample Number (n)	
			Control ± SD	Girdled ± SD	Control	Girdled
2018	09.05.2018	129	1.04 ± 0.6	0.61 ± 0.8	6	6
	31.05.2018	151	0.95 ± 0.9	1.29 ± 0.8	6	6
	21.06.2018	172	2.18 ± 1.4	2.68 ± 1.3	6	6
	11.07.2018	192	0.5 ± 1.9	0.14 ± 1.3	6	6
	02.08.2018	214	0.05 ± 1.9	2.26 ± 0.8	6	6
	22.08.2018	234	0.03± 1.0	0.34 ± 0.8	6	6
	12.09.2018	255	-0.23 ± 0.8	3.67 ± 2.4	6	6
	04.10.2018	277	3.94 ± 1.2	4.88 ± 2.1	6	6
2019	05.06.2019	156	3.09± 5.2	4.55 ± 2.9	5	6
	20.06.2019	171	1.14 ± 1.3	5.67 ± 6.2	4	4
	04.07.2019	185	2.03 ± 1.2	4.13 ± 1.1	4	4
	02.08.2019	214	2.16 ± 1.1	4.13 ± 1.1	6	6
	25.09.2019	268	2.45 ± 0.9	4.57 ± 3.2	6	6
2021	14.07.2021	195	0.85 ± 2.3	15.08 ± 11.8	6	6
	03.08.2021	215	-0.24 ± 2.1	6.38 ± 4.8	6	6
	16.09.2021	259	0.93 ± 1.8	7.7 ± 1.3	6	5

Table S6 Neutral lipid quantification for control and girdled trees in 2021 (sampling, DOY 147). First 3 cm has been analyzed.

Treatment	Tree number	Lipid quantification (% area) (first 3 cm)
Control	3	0.72
	9	0.89
	12	0.67
Girdling	7	0.61
	8	0.75
	10	0.33

Table S7 *In vitro* PEPC activity for control and girdled trees in 2019 (from wood material of the first 2 cm, sampling: DOY 236).

Treatment	Tree number	PEPC activity (nmol/gFW/min^{-1})
Control	2	764.8.0
	3	529.1
	4	417.7
	5	398.0
	9	594.7
	12	705.2
Girdling	1	NA
	6	129.1
	7	257.2
	8	241.1
	10	334.4
	11	374.4

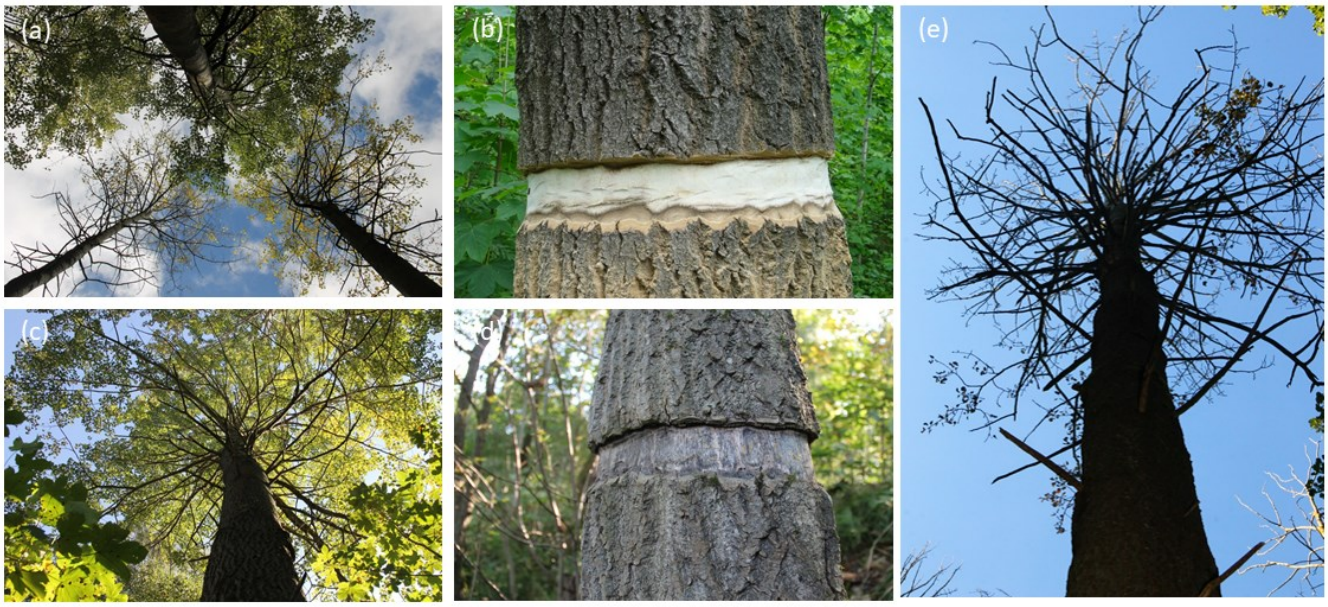

Picture S1 a) Two girdled and one control poplar tree at the study site in September 2018, b) girdling band in 2018, c) control tree in 2021, d) girdling band in 2021 and e) girdled tree in 2021.

Picture S2 Experimental set-up with the respiration chamber below the girdling, the glass flasks for gas sample analysis and Sap Flow Meter SFM1 in 2018.

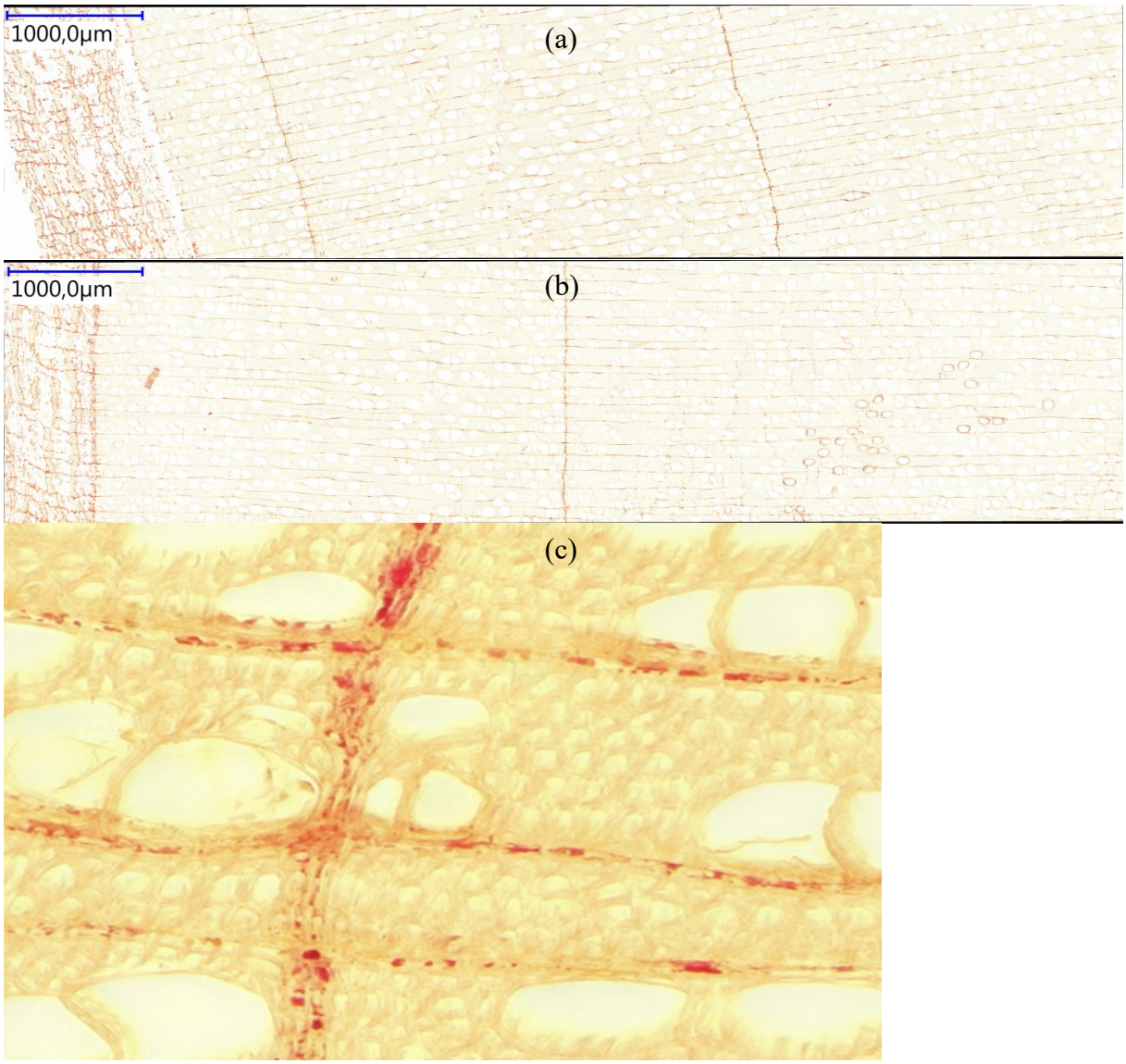

Picture S3 Wood histological slices stained with Oil Red O (ORO) ($C_{26}H_{24}N_4O$). This is a lysochrome (fat-soluble dye) used for staining neutral lipids (i.e. triglycerides, diacylglycerols and cholesterol esters). We visualized neutral lipids in a) a control, b) a girdled tree and c) red lipid droplets in ray parenchyma cells of a control tree.

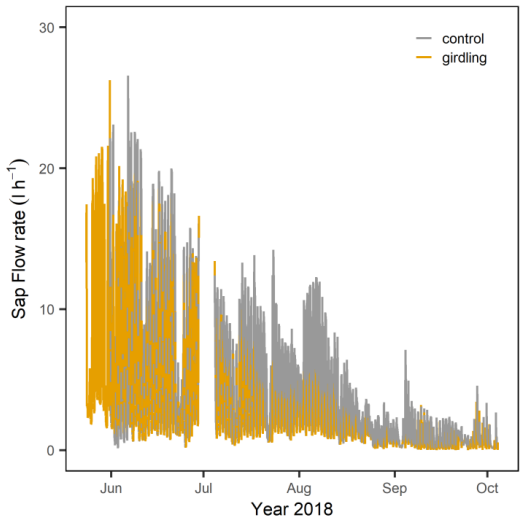

Figure S1 Sap flow rate (l h^{-1}) in 2018 (n = 6 for control (grey) and girdled (yellow) trees, respectively). Girdling event took place 4 July 2018.

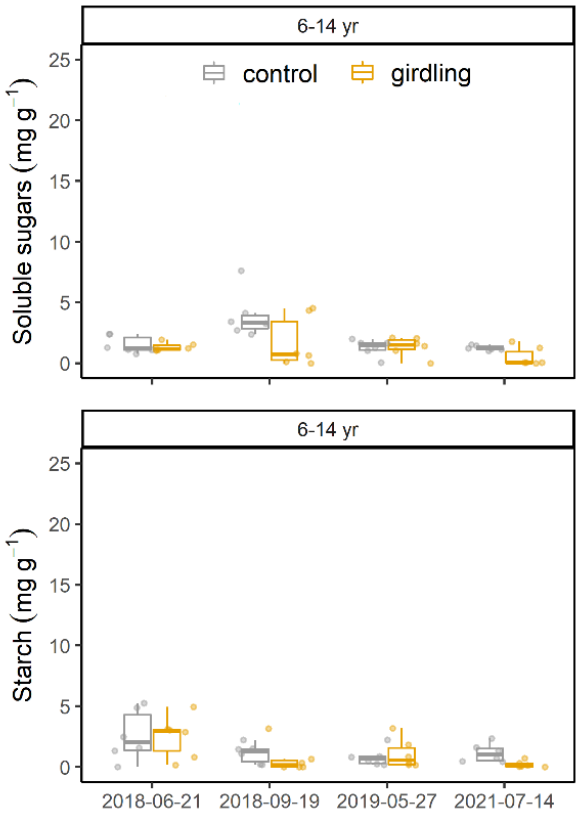

Figure S2 Soluble sugar (glucose, fructose, sucrose) concentration (mg g^{-1}) and starch concentration (mg g^{-1}) before girdling (DOY 172) and three time points after girdling, extracted from stem cores from a depth of ring 6 to 14. Colors denote treatment (n = 6 for control (grey) and girdled (yellow) trees, respectively). Box whisker plots present the median, lower (25^{th}) and upper (75^{th}) percentiles, minimum and maximum values.

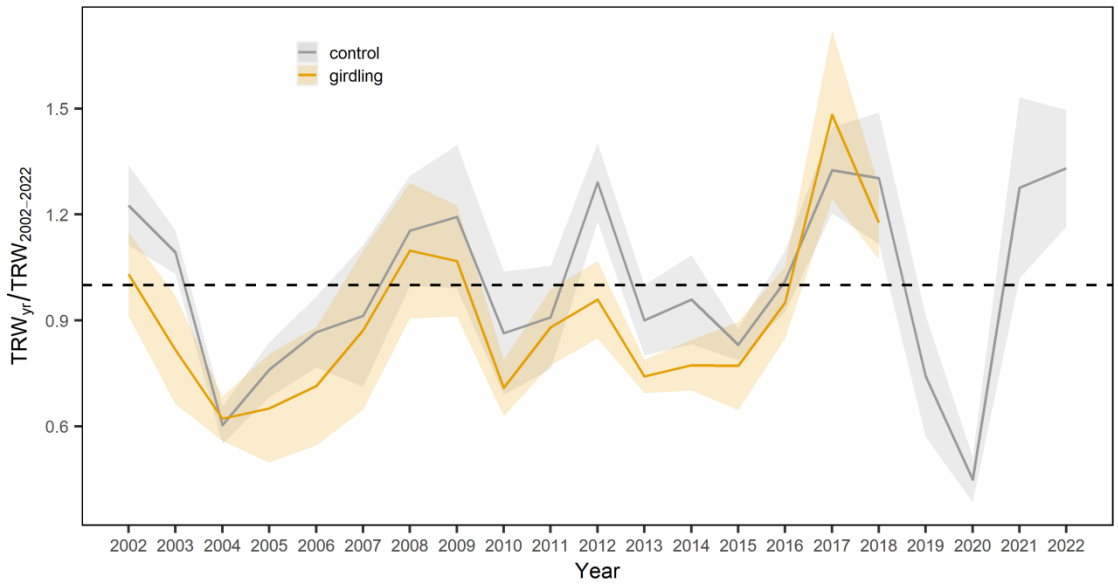

Figure S3 Deviation of tree ring width (TRW) from the 20 yr average ($TRW_{2002-2022}$), analyzed in control trees (grey, n = 6) and girdled trees (yellow, n = 3).

Method S1 Estimation of the $\delta^{13}C$ signatures of sugars and neutral lipids.

To estimate the $\delta^{13}C$ signatures of sugars and neutral lipids we followed a modified protocol (Bligh and Dyer 1959; White et al. 1979) and liquid chromatography (Schwab et al. 2019). We separated stem cores into the two treatments (n = 6, each). We then milled the wood and prepared 100 mg aliquots, sonicated in a mixture of chloroform, methanol and water, and centrifuged at 2000 rpm for 10 min. The upper phase in the solution contains the water and its solutes, e.g. sugars. To exhaust all sugars we re-added water, centrifuged, and collected the water phase two more times. The lower phase that assumed to contain all lipid fractions was dried over sodium sulfate. Then we extracted the neutral-lipids fraction with column chromatography (SPE 6 ml column) of silica gel (Merck silica mesh 230–400, 3 g activated 1 hr at 120 °C) eluted with 18 ml chloroform. Aliquotes from the sugars and neutral lipids solutions were pipetted into tin capsules and analyzed for δ13C in Delta+XL IRMS (Thermo Finnigan, Bremen, Germany).

Bligh EG, Dyer WJ. 1959. A rapid method of total lipid extraction and purification. *Canadian journal of biochemistry and physiology* **37**(8): 911-917.

Schwab VF, Nowak ME, Trumbore SE, Xu X, Gleixner G, Muhr J, Küsel K, Totsche KU. 2019. Isolation of individual saturated fatty acid methyl esters derived from groundwater phospholipids by preparative high-pressure liquid chromatography for compound-specific radiocarbon analyses. *Water Resources Research* **55**(3): 2521-2531.

White D, Davis W, Nickels J, King J, Bobbie R. 1979. Determination of the sedimentary microbial biomass by extractible lipid phosphate. *Oecologia* **40**(1): 51-62.

Method S2 Tree ring width analysis.

In order to quantify radial growth and to better evaluate whether the drought events in 2018 and 2019 impacted our measurements in the control trees, we analyzed variations in tree ring width as an indicator of stress. In 2022, we took increment cores from 3 control trees and 3 girdled trees (west side of the trees). After gluing the cores on wood strips, we cut them with a core-microtome using a cutter blade (Gärtner and Nievergelt 2010). To enhance contrast for analysis of ring boundaries, the cut surface was stained with ink, and covered with white chalk powder to fill vessels of earlywood (González-González et al. 2014). Stem cores were scanned at 2400 dpi. Radial growth measurements and cross-dating were performed using the program CDendro suite software (Cybis Elektronik & Data, Saltsjöbaden, Sweden). Cross-dating was further checked by comparing the tree-ring series to that of non-girdled spruces trees growing near to the site. We calculated the 20-yr average ring width (2002-2022) and compared this calculated average with each individual year for control and girdled trees, respectively.

Gärtner, H. and D. Nievergelt. 2010. The core-microtome: a new tool for surface preparation on cores and time series analysis of varying cell parameters. *Dendrochronologia.* **28**(2):85-92.

González-González, B.D., V. Rozas and I. García-González. 2014. Earlywood vessels of the sub-Mediterranean oak Quercus pyrenaica have greater plasticity and sensitivity than those of the temperate Q. petraea at the Atlantic–Mediterranean boundary. *Trees.* **28**(1):237-252.